Physical and chemical processes affecting atmospheric aerosols in the Western Mediterranean regional background

Michael Cusack, PhD Thesis
Barcelona, 2013

Supervisors:

Dr. Xavier Querol Carceller

Dr. Andrés Alastuey Urós

Institute of Environmental Assessment and Water Research

Tutor:

Dr. Montserrat Sarrà Adroguer

Institute of Environmental Science & Technology (UAB)

Front and back cover photographs courtesy of Alfons Puertas, Secció de Meteorologia, Observatori Fabra

Acknowledgements

I would like to take this opportunity to express how grateful I am to those that have helped me, in one way or another, in my time spent here in Barcelona, both on a personal and professional level, and whose support has contributed immeasurably to the completion of this thesis. I would like to expressly acknowledge the following people:

First and foremost, I extend my sincerest gratitude to my directors Andrés Alastuey and Xavier Querol for affording me the opportunity to work with and learn from them. The journey for me may have been arduous at times, but I always felt secure in the knowledge that I had their full support. Their door was always open, and they always responded with enthusiasm and passion that everyday was an inspiration. The wealth of knowledge they have imparted on me through their guidance, education and patience has inspired in me a desire to continue to learn, to question and never tire of looking for the answers. Whatever the future may hold for me, I go forward with an ambition instilled in me to follow in their footsteps. With sincerity, thank you.

To the Spanish Ministry of Science and Innovation for financing my studies for four years through the fellowship awarded to me from the *Programa de becas predoctorales para formación de personal investigador* (FPI).

To the Institute of Environmental Assessment and Water Research (IDAEA-CSIC) and the Institute of Earth Sciences Jaume Almera (IJA-CSIC) for providing me with such a pleasurable and professional work environment. Thank you to all the management personnel, administration and maintenance for your professionalism, your eagerness to help and your kindness.

To the Universidad Autónoma de Barcelona and the Environmental Science and Technology Institute for their management of the doctorate programme.

From the moment I started working with my colleagues I was welcomed with open arms, for which I am eternally grateful. To Jorge and Noemí, for your professional and personal support, without which I'm not sure I would be here today. You helped me more than you know. To my office mates, all the girls, Anna, Patri, Ioar and Cristina, for the great chat and the many laughs and Spanish lessons! And to Angeliki, Mari Cruz, Marco, Natalia, Oriol, Fulvio, Mar, Tere, Mariola, Manuel, for being the kindest, funniest, most supportive colleagues anyone could ever ask for, it has been an absolute

pleasure to work alongside you. And to those of you who took the time to accompany to Montseny, thank you for your company, your help and the great chats we had on the road.

To the people in the laboratory, Iria, Rebecca, Carmen, Silvia, Silvia, Silvia (!!), Mercé, Patri and Rafa, for your help and your great company during all the digestions. You made every moment spent in the lab a pleasure.

To Jordi and Jesus, thank you sincerely for taking me to Montseny on so many occasions, for your conversation and your assistance. You were always there to help whenever I needed you.

To all the co-authors of my articles comprising this thesis, none of which would have been possible without you. And to everyone who was always there to answer any questions I may have had.

To my friends, my 21st century family, both here, at home and all corners of the world. I couldn't begin to name you all, but you have left an indelible mark that has contributed to the person I am today. Some of you I've known my whole life, some I've only known my time here in Barcelona, but whatever the future may hold I know we will share it together. In a few months I will be leaving Barcelona, but I will take with me the memories and the friendships that I will cherish forever.

To Conor, your emails helped me through some tough times, always made me laugh, never failed to inspire, and reminded me no matter how bad things look, there is always noize. Beth and Natalie, there are no words. Every moment, every laugh, even the tears, was shared with you. For me, you are Barcelona.

And finally, and most definitely not least, I thank my family. For your undying support, even if you never fully understood what it is that I do, but for understanding the importance of it to me. All that I am, all that I have achieved and all that I will ever do, is because of you, and without your love and support could never be worthwhile. I love you and I thank you, for everything. I hope I've made you proud.

"And this, our life, exempt from public haunt, finds tongues in trees, books in the running brooks, sermons in stones, and good in everything"
--William Shakespeare

Index

Abstract

Air pollution is currently an area of study of great interest owing to the health implications of exposure to airborne contaminants and the effects of aerosols on global climate change. Exposure to air pollution has been linked to 380,000 premature deaths annually in the European Union alone. Since the industrial revolution in the 18th century, it has been estimated that the average global temperature has increased 0.8ºC as a direct result of increased anthropogenic emissions. For these reasons, among others, legislation at a national level and Directives at a European level have been introduced in an effort to combat the negative effects associated with air pollution.

In order to accurately characterise long-term trends of aerosols and the influence of synoptic features, regional background measurement sites are employed because they represent pollution levels across a larger area and the influence of transport of pollution is easier to identify.

The Western Mediterranean basin is characterised by complex atmospheric dynamics and meteorological processes which largely govern the fate of atmospheric aerosols after emission. The abrupt topography of the region, the recirculation of air masses, low precipitation, intense solar radiation giving rise to photochemical reactions and increased convective conditions favouring local soil resuspension, make the area considerably different to other regions of Europe. These features combined with the large atmospheric anthropogenic emissions produced along the Mediterranean coast (from numerous urbanised areas, industrial estates, shipping lanes, agriculture, construction, biomass burning, among others), and natural primary aerosol, high secondary particle formation and transformation, and interactions between particles and gaseous pollutants produce a complex aerosol phenomenology in the region.

A detailed study of the physical and chemical processes and sources affecting atmospheric aerosols in Montseny (MSY) in the Western Mediterranean is presented in this work, a region relatively under-studied in Europe. A long term time series of data of $PM_{2.5}$ (particulate matter of diameter less than 2.5 μm) and chemical composition will be analysed with the aim to identify the trends and fluctuations in concentrations, and describe the possible causes for such fluctuations. This work also aims to identify the emission sources of both PM_1 (PM of diameter less than 1 μm) and sub-micron particles, to observe if the sources are similar or related, and to observe the daily and

seasonal changes in the emission sources. As a final objective, an in-depth study of particle number concentration and size distribution will be presented for the first time in the Western Mediterranean regional background, with the aim of identifying seasonality, the modality of particle size distributions, new particle formation processes and possible particle evaporation, a process relatively underreported in literature.

Fine atmospheric particulate matter ($PM_{2.5}$ and PM_1) in the Western Mediterranean regional background is comprised of (in order of concentration) organic matter, sulphate, crustal material, ammonium, nitrate, marine aerosol, elemental carbon and trace elements. Mean concentrations of $PM_{2.5}$ (12.7 μg m^{-3}; 2002-2010) for the site are shown to be higher than other regional background sites in the rest of Spain, Scandinavia and Western Europe, and lower than concentrations in Central Europe (Northern Italy, Austria and Switzerland). Higher concentrations at the site are partially attributed to the influence of anthropogenic emissions from across the region. A strong seasonality for PM concentrations with elevated levels in summer is a consequence of the predominance of organic matter and sulphate. PM concentrations are lowest in winter due to higher precipitation and more frequent Atlantic advection that efficiently remove aerosols. However, lower temperatures give rise to increased nitrate levels as a consequence of the thermal instability of ammonium nitrate.

Trend analysis of long-term time series of $PM_{2.5}$ (2002-2010) for various sites across Spain and Europe show a statistically significant decreasing trend over the past decade. Median reductions across Europe were around 35%, with reductions ranging from 7 to 49%. These reductions are mostly attributed to the effectiveness of pollution abatement strategies employed by member states of the E.U., as enforced by E.U. Directives and IPPC licensing. Variations around this decreasing trend are a result of large-scale meteorology affecting much of the continent of Europe, although a decoupling of the effects of the meteorological conditions between Northern and Southern Europe induces different variations in pollutants. In winter, the North Atlantic Oscillation governs the prevailing weather across the continent, and can govern the frequency of Saharan dust intrusions to the Iberian Peninsula. A more pronounced reduction in certain countries coinciding with the economic recession was also identified, and it is hypothesised that this is a result of reduced anthropogenic emissions as a result of slower economic activity.

Long-term chemical speciation of $PM_{2.5}$ shows that much of the reduction observed in $PM_{2.5}$ is a result of ongoing reductions in sulphate and organic carbon. For these components, the reduction has been gradual and uniform with statistical significance. The reduction in sulphate has likely been a result of the gradual replacement of fuel-oil combustion in power plants in the region with natural gas throughout the past decade. However, nitrate concentrations were relatively constant until the economic crisis and drop significantly from 2008 onwards as a consequence of reduced road traffic and possibly unusual meteorology occurring in the last two winters of measurements. Many anthropogenic trace elements also undergo steep declines, specifically those targeted by Directives such as Pb, As, Cd and Ni.

Source apportionment studies identified six emission sources affecting PM_1, including secondary sulphate, secondary organic aerosol, fuel oil combustion, traffic and biomass burning, industrial and secondary nitrate. Secondary sulphate and secondary organic aerosol concentrations are highest in summer as a result of enhanced photochemistry, and in the case of organic matter, enhanced biogenic and biomass burning emissions and forest fires. Secondary organic aerosol is also elevated during winter as a result of anthropogenic organic emissions accumulating within the stagnant mixing layer during sporadic intense pollution episodes. Fuel oil combustion is identified by the presence of typical fuel-oil combustion tracers V, Ni and Sn. The influence of shipping emissions is indicated by the presence of marine aerosol tracers Mg and Na, and this source shows elevated concentrations in summer when on-shore breezes are more active. A traffic and biomass burning source contributes the majority of elemental carbon at the site (78%), and is also identifiable by typical traffic tracers such as Sn, Sb and organic carbon which is emitted by both traffic and biomass burning. An industrial source is characterised exclusively by trace elements (Pb, As, Cd, Sn, Cu, Zn, Cr, Fe and Mn) and thus contributed little to the mass. Both the industrial source and traffic and biomass burning source are minimum during the vacation periods in summer. The secondary nitrate source is most abundant in winter. The direct influence of anthropogenic activity is highlighted by the reduced concentrations of many sources at weekends, such as the nitrate, industrial, traffic and biomass and fuel oil combustion.

Five sources of sub-micron particles were identified, namely industrial + traffic + biomass burning, new particle formation and growth, secondary sulphate + fuel oil combustion, crustal material and nitrate. The source entitled new particle formation and growth was characterised by high particle concentrations in the ultrafine mode (particles

less than 100 nm in diameter), contributing the majority of particles to this mode, and solar radiation as a result of photochemical nucleation. The other sources typically contribute particles to the accumulation mode, although the industrial + traffic + biomass burning source can contribute particles to the ultrafine mode also. Meteorology is an important influencing factor on particle number concentrations. Nitrate particles are most abundant in winter, especially during sustained episodes of pollution, and under such conditions nucleation mode particles are very low. Similarly, episodes of pollution mostly characterised by sulphate particles during warmer periods also have reduced nucleation mode particles.

Particle number concentrations undergo a similar seasonality to that of PM, with elevated concentrations in the warmer months relative to winter. Daily variability of particles is largely governed by local meteorology, whereby mountain breezes activated in the morning by insolation carry polluted mixing layer air to MSY and increase pollutant and particle levels significantly, most especially in winter. However, in the absence of this breeze, nucleation and lower Aitken mode concentrations are elevated as a result of new particle formation and growth processes in the absence of a high background particle loading. During the warmer months, new particle formation and growth is still an effective source of ultrafine particles even in the presence of high levels of background particles. This is likely a result of enhanced photochemistry and greater levels of condensable organic vapours produced from the photochemical oxidation of secondary organic aerosol precursor gases and biogenic emissions in the warmer months.

The ideal conditions for new particle formation are identified, which include a source of sulphuric acid for forming nucleating clusters and elevated solar radiation for photochemical reactions. In colder months, nucleation typically occurs under clean air conditions, but can also occur under polluted conditions depending on the availability of condensable organic aerosols which contribute to particle growth after nucleation. Reductions in modal diameters, indicating particle shrinkage, can also occur and are attributed to the evaporation of semi-volatile species from the particulate phase to the gas phase. Evaporation appears to be favoured under warm temperatures, high solar radiation, low relative humidity and atmospheric dilution.

Resumen

La contaminación del aire es un área de estudio de gran interés en la actualidad debido a las implicaciones en la salud de la exposición a los contaminantes aéreos y a los efectos de los aerosoles atmosféricos en el clima. La exposición humana a la contaminación atmosférica causa 380,000 muertos prematuros solo en la Unión Europea. Desde la revolución industrial en el siglo XVIII, se ha estimado un aumento de la temperatura media del mundo de 0.8ºC como consecuencia del incremento de emisiones antropogénicas. Por estas razones, se han implantado leyes y directivas a escala nacional y europea para combatir los efectivos negativos asociados a la contaminación del aire.

Para poder identificar tendencias de aerosoles e investigar la influencia de la meteorología a escala sinóptica es necesario utilizar estaciones de fondo regional que son representativas de un área extensa y que permiten discriminar procesos de transporte de contaminantes a larga distancia. La cuenca del Mediterráneo Occidental está caracterizada por una dinámica atmosférica y unos procesos meteorológicos complejos que controlan el comportamiento de los aerosoles atmosféricos después de su emisión. La topografía abrupta de la región, la recirculación de las masas de aire, el bajo volumen de precipitación, la intensa radiación solar que favorece las reacciones fotoquímicas y las condiciones convectivas que incrementan la resuspensión local del suelo, le confieren a esta región unas cualidades propias que la diferencian de otras zonas de Europa. Estas características, combinadas con otros factores como las elevadas tasas de emisiones atmosféricas antropogénicas a lo largo la costa Mediterránea (emisiones urbanas, polígonos industriales, barcos, agricultura, construcción y quema de biomasa, entre otros), las elevadas concentraciones de aerosoles primarios de origen natural, la importancia de los procesos de formación y transformación de partículas secundarias y la interacción entre partículas y contaminantes gaseosos, resultan en una compleja fenomenología de los aerosoles atmosféricos en la región.

En este trabajo se presenta un estudio detallado de los procesos físicos y químicos y las fuentes que afectan a los aerosoles atmosféricos en un emplazamiento de fondo regional situado en el Montseny (MSY) en el Mediterráneo Occidental. El objetivo de esta tesis es identificar y caracterizar los procesos físico-químicos de los aerosoles atmosféricos que tiene lugar en el fondo regional del Mediterráneo Occidental. Se ha

analizado una serie larga de datos de niveles y composición de $PM_{2.5}$ (partículas de diámetro aerodinámico inferior a 2.5 μm) con el fin de identificar tendencias y fluctuaciones en las concentraciones y describir las posibles causas de estas fluctuaciones. Por otra parte se han identificado las fuentes de emisión con impacto en los niveles de concentración en de masa partículas de diámetro aerodinámico inferior a 1 μm (PM_1) y en el número de partículas sub-micrónicas, con objeto de determinar si las fuentes que afectan a estos dos parámetros son similares o están relacionadas y determinar variaciones diarias y estacionales en estas fuentes de emisión. El objetivo final es realizar, por primera vez en el fondo regional del Mediterráneo Occidental, un estudio en detalle de la concentración y distribución según tamaño del número de partículas ultrafinas, que ha permitido identificar la estacionalidad y la moda de la distribución granulométrica de partículas, los procesos de formación de nuevas partículas y posiblemente los procesos de evaporación, estos últimos poco frecuentes en la literatura.

En el fondo regional del Mediterráneo Occidental, el material particulado atmosférico fino ($PM_{2.5}$ y PM_1) está compuesto principalmente por (en orden de concentración) materia orgánica, sulfato, materia mineral, amonio, nitrato, aerosol marino, carbono elemental y elementos traza. La concentración media de $PM_{2.5}$ obtenida en la estación de muestreo (12.7 μg m^{-3}; 2002-2010) es más elevada que las registradas en otras estaciones de fondo regional de España, Escandinavia y Europa Occidental, y más baja que las concentraciones determinadas en zonas de Europa Central (el Norte de Italia, Austria y Suiza). Los niveles relativamente altos de $PM_{2.5}$ en la zona de estudio están parcialmente atribuidos a la influencia de las emisiones de origen antropogénico en la región. El predominio de la materia orgánica y del sulfato se refleja en una marcada estacionalidad de los niveles de PM, caracterizados por máximos de concentración en verano. Las concentraciones de PM son más bajas en invierno debido a la mayor precipitación y la mayor frecuencia de la advección Atlántica que favorecen la eliminación de los aerosoles. Por el contrario, las menores temperaturas invernales resultan en un incremento de las concentraciones de nitrato debido a la inestabilidad térmica de nitrato amónico.

El análisis de tendencias de series largas de $PM_{2.5}$ (2002-2010) obtenidas en varias estaciones de fondo regional en España y Europa evidencia una disminución estadísticamente significativa de las concentraciones de $PM_{2.5}$ en la última década. Se ha

estimado una reducción media de los niveles de $PM_{2.5}$ en Europa del 35%, que oscila entre el 7 y el 49%. Esta disminución generalizada se atribuye a la eficacia de las estrategias de reducción de la contaminación aplicadas por los países miembros de la UE, como las establecidas por las Directivas de la UE y las IPPC. Sobre esta tendencia decreciente se superponen otras oscilaciones de menor rango debidas al efecto de la meteorología a gran escala, que afecta a gran parte del continente aunque se evidencia una clara diferencia entre las condiciones meteorológicas entre el Norte y el Sur de Europa que afecta a las variaciones de los contaminantes. En invierno, la Oscilación del Atlántico Norte (NAO) controla las condiciones meteorológicas predominantes sobre el continente, y puede controlar la frecuencia de las intrusiones de polvo sahariano que afectan a la Península Ibérica. En determinados países se registró una bajada más pronunciada de los niveles de $PM_{2.5}$ en los últimos años, coincidiendo con la recesión económica, que puede estar relacionada con una reducción de las emisiones antropogénicas como consecuencia de la ralentización de la actividad económica

La disponibilidad de series largas de composición química de $PM_{2.5}$ permite identificar que la reducción de los niveles de $PM_{2.5}$ está relacionada con la disminución de las concentraciones de sulfato y carbono orgánico. Estos compuestos muestran una reducción estadísticamente significativa, gradual y uniforme desde 2002. La reducción en el sulfato es probablemente debida a la sustitución del fuel oil por gas natural como combustible en las centrales térmicas la última década. Sin embargo, las concentraciones de nitrato permanecen relativamente constantes hasta la crisis económica y los niveles de $PM_{2.5}$ caen bastante a partir de 2008, probablemente como consecuencia de la reducción del tráfico vehicular y por la meteorología inusual de los últimos dos inviernos del periodo de estudio. Se observa también una reducción marcada de las concentraciones de muchos elementos traza de origen antropogénico, específicamente aquellos controlados por las Directivas (Pb, As, Cd y Ni).

El estudio de contribución de fuentes identifica seis fuentes que afectan a PM_1, incluyendo sulfato secundario, aerosol orgánico secundario, combustión de fuel oil, tráfico rodado y quema de biomasa, industria y nitrato secundario. El sulfato secundario y el aerosol orgánico secundario son más altos en verano como consecuencia de la elevada fotoquímica, y en el caso del material orgánico por las mayores emisiones biogénicas y episodios de quema de biomasa (incendios forestales). El aerosol orgánico secundario es también elevado en invierno como consecuencia del impacto de las emisiones de compuestos orgánicos antropogénicos que se acumulan dentro la capa de

mezcla durante episodios de contaminación intensa. La fuente combustión de fuel oil se identifica por la presencia de trazadores típicas como V, Ni y Sn. La influencia de las emisiones de barcos en la fuente fuel oil se relaciona con la presencia de trazadores de aerosoles marinos como Mg y Na, y es más importante en verano por la mayor intensidad de las brisas marinas. La fuente mixta de tráfico rodado y quema de biomasa, identificada por la presencia de carbono elemental y orgánico y de trazadores típicos de tráfico, como Sb y Sn, contribuye a la mayoría del carbono elemental en el emplazamiento de estudio (78%). La fuente industrial está caracterizada exclusivamente por la presencia de elementos traza (Pb, As, Cd, Sn, Cu, Zn, Cr, Fe y Mn) y por esta razón contribuye poco a la masa total de PM. Ambas, la fuente industrial y la de tráfico rodado y quema de biomasa, tienen contribuciones mínimas durante el periodo de vacaciones en verano. El nitrato secundario es más abundante en invierno. La influencia de las actividades antropogénicas se caracteriza por la reducción de las concentraciones durante los fines de semana de las fuentes típicamente antrópicas como el nitrato, la industria, el tráfico rodado y la quema de biomasa y la combustión de fuel oil.

Se han identificado cinco fuentes con impacto en el número de partículas sub-micrónicas: industria + tráfico rodado + quema de biomasa, formación de partículas nuevas y crecimiento, sulfato secundario y combustión de fuel oil, materia mineral y nitrato. La fuente llamada "formación de partículas nuevas y crecimiento" se caracteriza por altas concentraciones de partículas en la moda ultrafina (partículas menores de 100 nm de diámetro), contribuyendo a la mayoría de partículas en esta moda, y por la alta radiación solar debido a la importancia de la nucleación fotoquímica. Las otras fuentes contribuyen típicamente a la moda de acumulación, aunque la fuente industria + trafico rodado + quema de biomasa puede contribuir también a la moda de ultrafino. Las partículas de nitrato son más abundantes en invierno, especialmente durante episodios duraderos de contaminación, y en estas condiciones las partículas de la moda de nucleación son muy bajas. De manera similar, los episodios de contaminación caracterizados por partículas de sulfato que tienen lugar durante los periodos cálidos también tienen bajos los niveles de partículas en la moda de nucleación.

Las concentraciones de número de partículas tienen una estacionalidad similar a las de PM, con concentraciones más elevadas en los meses más cálidos respecto al invierno. La variabilidad diaria de las partículas está controlada por la meteorología local, donde las brisas de montaña, activadas por la insolación, transportan masas de aire

contaminadas acumuladas en la capa de mezcla hacia la estación de MSY, incrementando significativamente los niveles de contaminantes y partículas, especialmente en invierno. Sin embargo, en ausencia de esta brisa con una elevada carga de partículas pre-existente, las concentraciones de partículas de las modas de nucleación y Aitken inferior incrementan como consecuencia de los procesos de formación y crecimiento de partículas. Esto es probablemente debido al incremento de la fotoquímica y a los elevados niveles de vapores orgánicos condensables producidos a partir de la oxidación fotoquímica de precursores gaseosos de aerosoles orgánicos secundarios y de emisiones biogénicas en los meses cálidos.

Se han identificado las condiciones ideales para la formación de nuevas partículas que incluyen la existencia de una fuente de ácido sulfúrico, que permita formar clusters de nucleación, y elevada radiación solar para activar reacciones fotoquímicas. En los meses más fríos, la nucleación ocurre típicamente bajo condiciones de masas de aire limpias, aunque también puede ocurrir en condiciones contaminadas en función de la disponibilidad de aerosoles orgánicos condensables que contribuyen al crecimiento de partículas después de la nucleación. Se han identificado también reducciones en los diámetros de las modas, indicando disminución del diámetro de las partículas, que se atribuyen a la evaporación de especies semi-volátiles desde la fase particulada a la fase gas. Los procesos de evaporación están favorecidos en situaciones de altas temperaturas, radiación solar intensa, humedad relativa baja y dilución atmosférica.

Resum

La contaminació de l'aire és una àrea d'estudi de gran interès a l'actualitat degut a les implicacions per la salut de la exposició als contaminants aeris i als efectes dels aerosols atmosfèrics en el clima. L'exposició humana a la contaminació atmosfèrica causa, només en la Unió Europea, 380,000 morts prematures. Des de la Revolució Industrial, al segle XVIII, s'ha estimat un augment de la temperatura mitjana del món de 0.8ºC com a conseqüència de l'increment de les emissions antropogèniques. Per aquestes raons s'han implantat lleis i directives a escala nacional i europea per combatre els efectes negatius associats a la contaminació atmosfèrica.

Per poder identificar les tendències dels aerosols i investigar la influència de la meteorologia a escala sinòptica és necessari utilitzar estacions de fons regional que siguin representatives d'una àrea més extensa i que permetin discriminar processos de transport de contaminants a llarga distància. La conca del Mediterrani Occidental es caracteritza per una dinàmica atmosfèrica i uns processos meteorològics complexes que controlen el comportament dels aerosols atmosfèrics després de la seva emissió. La topografia abrupta de la regió, la recirculació de les masses d'aire, el baix volum de precipitació, la intensa radiació solar que afavoreix les reaccions fotoquímiques i les condicions convectives que incrementen la resuspensió local del sòl, confereixen a aquesta regió unes qualitats pròpies que la diferencien d'altres zones d'Europa. Aquestes característiques, combinades amb altres factors com les elevades emissions atmosfèriques antropogèniques al llarg de la costa Mediterrània (emissions urbanes, polígons industrials, vaixells, agricultura, construcció, crema de biomassa, entre d'altres), les elevades concentracions d'aerosols primaris d'origen natural, la importància dels processos de formació i transformació de partícules secundàries i la interacció entre partícules i contaminants gasosos, resulten en una complexa fenomenologia dels aerosols atmosfèrics en la regió.

En aquest treball es presenta un estudi detallat dels processos físics i químics i de les fonts que afecten als aerosols atmosfèrics en un emplaçament de fons regional situat al Montseny (MSY) en el Mediterrani Occidental. L'objectiu d'aquesta tesi és identificar i caracteritzar els processos físico-químics dels aerosols atmosfèrics que tenen lloc al fons regional del Mediterrani Occidental. S'ha analitzat una llarga sèrie de dades de nivells i composició de $PM_{2.5}$ (partícules de diàmetre aerodinàmic inferior a 2.5 μm)

amb la finalitat d'identificar les tendències i fluctuacions en les concentracions i descriure les possibles causes d'aquestes fluctuacions. D'altra banda, s'han identificat les fonts d'emissió amb impacte sobre els nivells de concentració en massa de partícules de diàmetre aerodinàmic inferior a 1 μm (PM1) i en el nombre de partícules submicròniques, amb l'objectiu de determinar si les fonts que afecten a aquests dos paràmetres són similars o es troben relacionades, així com determinar variacions diàries i estacionals en aquestes fonts d'emissió.

L'objectiu final es realitzar, per primera vegada en el fons regional del Mediterrani Occidental, un estudi en detall de la concentració i distribució segons la mida del nombre de partícules ultrafines, que ha permès identificar l'estacionalitat i la moda de la distribució granulomètrica de les partícules, els processos de formació de noves partícules i, possiblement, els processos d'evaporació, aquests últims poc freqüents en la literatura.

En el fons regional del Mediterrani Occidental, el material particulat atmosfèric fi ($PM_{2.5}$ i PM_1) està compost principalment per (en ordre de concentració) matèria orgànica, sulfat, matèria mineral, amoni, nitrat, aerosol marí, carboni elemental i elements traça. La concentració mitjana de $PM_{2.5}$ obtinguda en l'estació de mostreig (12.7 μg m^{-3}; 2002-2010) és més elevada que les registrades en altres estacions de fons regional d'Espanya, Escandinàvia i Europa Occidental, i més baixa que les concentracions determinades en zones de l'Europa Central (al Nord d'Itàlia, Àustria i Suïssa). Els nivells relativament alts de PM2.5 de la zona d'estudi s'atribueixen parcialment a la influència de les emissions d'origen antropogènic de la regió. El predomini de la matèria orgànica i del sulfat es reflexa en una marcada estacionalitat dels nivells de PM, caracteritzats per màxims de concentració a l'estiu. Les concentracions de PM són més baixes a l'estiu degut a la major precipitació i la major freqüència de l'advecció Atlàntica que afavoreixen l'eliminació dels aerosols. Contràriament, les menors temperatures de l'hivern resulten en un increment de les concentracions de nitrat degut a la inestabilitat tèrmica del nitrat amònic.

L'anàlisi de tendències de sèries llargues de $PM_{2.5}$ (2002-2010) obtingudes en varies estacions de fons regional a Espanya i Europa evidencia una disminució estadísticament significativa de les concentracions de $PM_{2.5}$ en l'última dècada. S'ha estimat una reducció mitjana dels nivells de $PM_{2.5}$ a Europa del 35%, que oscil·la entre el 7 i el 49%. Aquesta disminució generalitzada s'atribueix a la eficàcia de les estratègies de reducció de la contaminació aplicades per els països membres de la UE, com les establertes per

les Directives de la UE i de l'IPCC. Sobre aquesta tendència decreixent se superposen altres oscil·lacions de menor rang degudes a l'efecte de la meteorologia a gran escala, que afecta a gran part del continent, encara que s'evidencia una clara diferència entre les condicions meteorològiques entre el Nord i el Sud d'Europa que afecta a les variacions dels contaminants. A l'hivern, la Oscil·lació de l'Atlàntic Nord (NAO) controla les condicions meteorològiques predominants sobre el continent i pot controlar la freqüència de les intrusions de pols del Sàhara que afecten a la península Ibèrica. En determinats països es va registrar una baixada més pronunciada dels nivells de $PM_{2.5}$ en els últims anys, coincidint amb la recessió econòmica, que pot estar relacionada amb una reducció de les emissions antropogèniques com a conseqüència de l'alentiment de l'activitat econòmica.

La disponibilitat de sèries llargues de composició química de $PM_{2.5}$ permet identificar que la reducció dels nivells de $PM_{2.5}$ està relacionada amb la disminució de les concentracions de sulfat i carboni orgànic. Aquests compostos mostren una reducció estadísticament significativa, gradual i uniforme des del 2002. La reducció del sulfat és deu probablement a la substitució del fuel oil per gas natural com a combustible en les centrals tèrmiques durant la última dècada. No obstant, les concentracions de nitrat romanen relativament constants fins la crisi econòmica i els nivells de $PM_{2.5}$ cauen bastant a partir del 2008, probablement com a conseqüència de la reducció del trànsit de vehicles i per la meteorologia inusual dels últims dos hiverns del període d'estudi. S'observa també una reducció marcada de les concentracions de molts elements traça d'origen antropogènic, específicament aquells controlats de les Directives (Pb, As, Cd i Ni).

L'estudi de contribució de fonts identifica sis fonts que afecten a PM_1, incloent-hi sulfat secundari, aerosol orgànic secundari, combustió de fuel oil, trànsit rodat i crema de biomassa, indústria i nitrat secundari. El sulfat secundari i l'aerosol orgànic secundari són més alts a l'estiu com a conseqüència de l'elevada fotoquímica i, en el cas del material orgànic, per les majors emissions biogèniques i episodis de crema de biomassa (incendis forestals). L'aerosol orgànic secundari és també elevat a l'hivern degut a l'impacte de les emissions de compostos orgànics antropogènics que s'acumulen dins la capa de barreja durant episodis de contaminació intensa. La font de combustió de fuel oil s'identifica per la presència de traçadors típics com el V, Ni i Sn. La influència de les emissions dels vaixells en la font de fuel oil es relaciona amb la presència de

traçadors d'aerosols marins com Mg i Na, i és més important a l'estiu per la major intensitat de les brises marines. La font mixta de trànsit rodat i crema de biomassa, identificada per la presència de carboni elemental i orgànic i de traçadors típics de trànsit, com Sb i Sn, contribueix a la majoria del carboni elemental a l'emplaçament d'estudi (78%). La font industrial es caracteritza exclusivament per la presència d'elements traça (Pb, As, Cd, Sn, Cu, Zn, Cr, Fe i Mn) i per aquesta raó contribueix poc a la massa total de PM. Ambdues fonts, la industrial i la de trànsit rodat i crema de biomassa, tenen contribucions mínimes durant el període de vacances a l'estiu. El nitrat secundari és més abundant a l'hivern. La influència de les activitat antropogèniques es caracteritza per la reducció de les concentracions durant els caps de setmana de les fonts típicament antròpiques com el nitrat, la indústria, el trànsit rodat i la crema de biomassa i la combustió de fuel oil.

S'han identificat cinc fonts amb impacte sobre el número de partícules submicròniques: indústria + trànsit rodat + crema de biomassa, formació de partícules noves i creixement, sulfat secundari i combustió de fuel oil, matèria mineral i nitrat. La font anomenada "formació de partícules noves i creixement" es caracteritza per altes concentracions de partícules en la fracció ultrafina (partícules de menys de 100 nm de diàmetre), contribuint a la majoria de partícules en aquesta moda, i per la importància de la nucleació fotoquímica deguda a l'alta radiació solar. Les altres fonts contribueixen típicament a la moda d'acumulació, tot i que la font indústria + trànsit rodat + crema de biomassa poden contribuir també a la moda ultrafina. Les partícules de nitrat són més abundants a l'hivern, especialment durant llargs episodis de contaminació, i en aquestes condicions les partícules de la moda de nucleació són molt baixes. De manera similar, els episodis de contaminació caracteritzats per partícules de sulfat, que tenen lloc durant els períodes càlids, també mantenen baixos els nivells de partícules de la moda de nucleació.

Les concentracions de número de partícules tenen una estacionalitat similar a las de PM, amb concentracions més elevades durant els mesos més càlids que a l'hivern. La variabilitat diària de les partícules està controlada per la meteorologia local, on les brises de muntanya, activades per la insolació, transporten masses d'aire contaminades acumulades a la capa de barreja cap a l'estació del MSY, incrementant significativament els nivells de contaminants i partícules, especialment a l'hivern. No obstant, en absència d'aquesta brisa (amb una elevada càrrega de partícules pre-existents), les concentracions de partícules de les modes de nucleació i Aitken inferior

incrementen com a conseqüència dels processos de formació i creixement de partícules. Això és degut, probablement, a l'increment de la fotoquímica i als elevats nivells de vapors orgànics condensables produïts a partir de l'oxidació fotoquímica de precursors gasosos d'aerosols orgànics secundaris i d'emissions biogèniques durant els mesos càlids.

S'han identificat les condicions ideals per a la formació de noves partícules que inclouen l'existència d'una font d'àcid sulfúric, que permet formar clústers de nucleació, i elevada radiació solar per activar reaccions fotoquímiques. Durant els mesos més freds, la nucleació té lloc típicament sota condicions de masses d'aire net, tot i que també pot ocórrer en condicions contaminades en funció de la disponibilitat d'aerosols orgànics condensables que contribueixen al creixement de partícules després de la nucleació. S'han identificat també reduccions en els diàmetres de les modes, indicant disminució del diàmetre de les partícules, que s'atribueixen a la evaporació de les espècies semi-volàtils des de la fase particulada a la fase gas. Els processos d'evaporació es veuen afavorits en situacions d'altes temperatures, radiació solar intensa, humitat relativa baixa i dilució atmosfèrica.

Chapter 1: Introduction

1. Introduction

1.1. Atmospheric Aerosols

Atmospheric aerosols are defined as solid and/or liquid particles that enter into the atmosphere in suspension (Mészáros, 1999). In atmospheric science, the term aerosol traditionally refers to suspended particles in air that contain a large proportion of condensed matter other than water, thus excluding clouds which are considered a separate phenomena (Pruppacher and Klett, 1997). Atmospheric aerosols range in size from a few nanometers to some tens of micrometers (μm). They can be emitted directly to the atmosphere as primary emissions, or can be formed through the physicochemical transformation of gaseous emissions (secondary emissions). Sources of atmospheric aerosols include both natural and anthropogenic emissions, and the type of source will largely govern both the physical properties of the aerosol (mass, size and density) and the chemical composition. The effects of aerosols on climate, human health and the atmosphere are among the most central topics in current environmental research.

1.1.1 Origin

On a global scale, natural primary emissions are the dominant source of atmospheric aerosols. Aerosols of natural origin include particles of windborne crustal material, sea spray, volcanic emissions (dust and sulphates from volcanic SO_2), naturally occurring biomass burning (such as wild forest fires), biogenic emissions (spores, pollens and sulphates from biogenic gases) and organic matter from biogenic sources (Seinfeld and Pandis, 1998). Calculation of global mass emissions of aerosols carries significant uncertainty, but it is certain that emissions on a global scale are predominantly natural (~12,100 Tg y^{-1}; 98 wt%), compared to anthropogenic emissions which are estimated to be around 300 Tg y^{-1} (Durant et al., 2010; Andraea and Rosenfeld, 2008). According to Andraea and Rosenfeld (2008), sea spray and mineral dust (mostly from deserts) contribute the largest amount to the global aerosol loading, accounting for 10,130 and 1,600 Tg y^{-1}, respectively (Figure 1.1). Marine aerosols, formed from wind and waves forcing air bubbles to burst on the sea surface, are believed to account for the largest mass emission flux of all aerosol types. On a regional scale, the contribution of marine

aerosol to the PM mass will depend on the geographical area, proximity to the coast and meteorology.

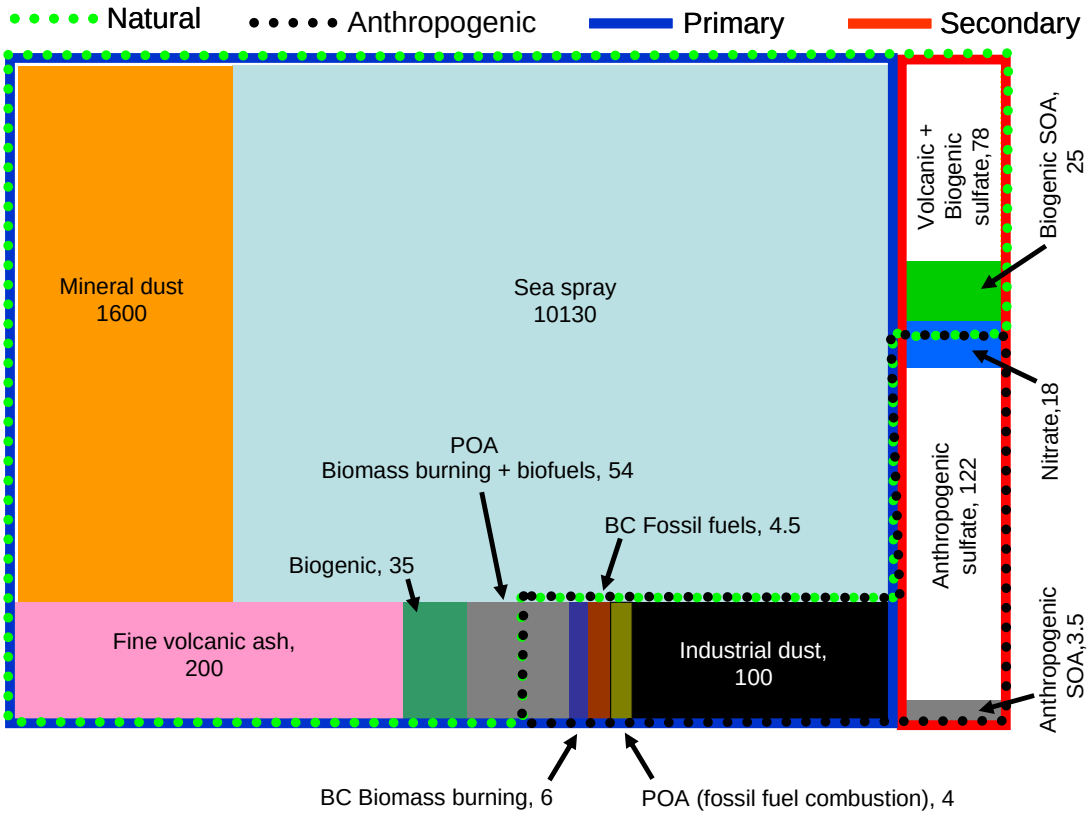

Figure 1.1. Global fluxes of primary and secondary atmospheric particulate matter (total of 12,400 Tg y^{-1}). The area of each square proportionally represents the contribution to the total loading. POA = primary organic aerosol; SOA = secondary organic aerosol; BC = black carbon. Taken from Gieré and Querol (2010).

Soil or mineral dust is the second most prominent aerosol type in the atmosphere according to Andraea and Rosenfeld (2008). Natural resuspension can be local, mostly from arid and semi-arid environments, or as a result of long-range transport from the major mid-latitude deserts (North Africa, Middle East and Central Asia) (Prospero et al., 2002). This long range transport can have serious implications for Europe considering the proximity of North Africa, and especially for the Iberian Peninsula (Escudero et al., 2007). Suspended crustal material can be transported from the Sahara to Southern Europe under suitable meteorological conditions and over long distances, increasing the particulate matter concentrations in the atmosphere. These African dust outbreaks across the Iberian Peninsula have been widely studied and documented (Querol et al., 1998a and b, 2002 and 2009; Rodríguez et al., 2001; Viana et al., 2002;

Escudero et al., 2005). Although the main global contribution of mineral PM to the atmosphere has a natural origin, in urban and industrial areas the mineral fraction is mainly from anthropogenic processes, such as industrial activities, construction/demolition, mining activities etc.

Anthropogenic sources of aerosols are mainly due to road traffic in urban areas (emission of precursor gases and ultrafine carbonaceous particles, brake and tyre wear and pavement erosion), fossil fuel combustion, energy plants, metallurgic industry and other industrial activities (mainly cement, ceramic and brick production), agricultural activities, waste treatment plants and fertiliser production plants (Gieré and Querol, 2010). Primary anthropogenic emissions, those emitted directly to the atmosphere from their source, account for 150 Tg y^{-1} (Andraea and Rosenfeld, 2008). In addition, an important proportion of anthropogenic aerosol is made up of secondary particles produced chemically from anthropogenic gaseous pollutants. Secondary anthropogenic are derived mostly from SO_2, NO_x and volatile organic compounds (VOCs) emitted from industrial and combustion processes, including road traffic emissions. In Mediterranean climates, photochemistry is a significant process in the formation of secondary particles i.e. aerosols released to the atmosphere can co-react under the presence of sunlight, producing secondary pollutants (Bougiatioti et al., 2013). Anthropogenic particles are usually unevenly distributed throughout the troposphere, with the highest concentrations typically found in urban areas, where there is a high volume of road traffic and industry (Putaud et al., 2004) and in specific hot spot regions such as China and India for example (Chan et al., 2008). However, long range transport of pollutants can occur and anthropogenic particles may reach remote locations (Wang, 2007; Fu et al., 2010).

1.1.2. Formation and transformation

Atmospheric aerosols can be further classified according to their formation processes. Primary emissions as particulate matter or gases are emitted directly to the atmosphere from their sources. Secondary emissions originate from the transformation of primary emissions through physical or chemical processes. They are formed from their precursor gases, such as SO_2, NO_x, NH_3 or VOCs. Gas-to-particle transformation is referred to as homogenous nucleation, whereby transformations resulting from the reaction between gases and pre-existing particles through coagulation and condensation

is referred to as heterogeneous nucleation (Warneck, 1988). Airborne particles undergo various physical and chemical interactions and transformations (atmospheric aging), changing in size, structure and composition. As particles grow in size through coagulation and condensation processes, they can be deposited to the Earth's surface by dry deposition or through wet deposition from precipitation or through their incorporation into cloud droplets (Pöschl, 2005). Removal processes are largely influenced by the size and chemical composition of the aerosol. Clouds are formed by the condensation of water vapour on pre-existing aerosol particles, thus removing particles from the atmosphere. If these clouds form precipitation, aerosols are further scavenged by water droplets and returned to the earth's surface. This process is referred to as wet deposition and is the main removal sink of aerosols from the atmosphere. Dry deposition involves removal of particulate aerosols by mechanical processes such as gravimetry, wind dispersion and diffusion as a function of size. Thus, the residence time of aerosols is heavily influenced by meteorological factors and the aerosol properties, and the lifetimes of aerosol particles can range from hours to weeks (Raes et al, 2010).

1.1.3. Composition

Owing to the broad range of aerosol sources and formation processes, the chemical composition of aerosols is often complex and varied. The relative abundance of various chemical components in atmospheric particles in any given region can depend on the prevalent emission source, meteorological conditions, the location and the size fraction, and vary spatially and temporally by an order of magnitude or more (Putaud et al., 2010). For example, the chemical composition of aerosols in an urban environment differs significantly from a remote site far from densely populated areas. For the purposes of this section, chemical composition will exclusively be discussed in the context of atmospheric particles, thus excluding gaseous pollutants. The major components of atmospheric particulate matter are crustal material, carbonaceous matter (elemental carbon and organic matter), marine aerosol, sulphate, nitrate, ammonium, trace elements and water. The predominance of any of these major components will depend heavily on the prevailing emission source and the formation mechanism of the particles.

Crustal material (or mineral matter) is the major component of the total PM mass present in the atmosphere. It is typically comprised of primary particles and its

composition varies depending on local geology, soils and anthropogenic activities. The most abundant element components are Al, Ca, Si, Fe, Ti, K and Mg, and the most abundant trace elements are Co, Rb, Ba, Sr, Li, Sc, Cs and Rare Earth Elements (Chester et al., 1996). The major mineral components of PM are calcite, quartz, dolomite, clay minerals and feldspars. Minor components include calcium sulphate and iron oxides but these may vary (Querol et al., 2002).

Marine aerosol is constituted mainly of NaCl, with minor contributions of other salts such as $MgCl_2$, $MgSO_4$, and Na_2SO_4 (Mészaros, 1999). Marine aerosol emissions are primary, generated by wind turbulence and waves in coastal areas and dispersion of sea foam and bubbles (Warneck, 1998). Dimethyl sulphide (DMS) is also an important marine aerosol, and is the most abundant biological sulphur compound emitted to the atmosphere, specifically by phytoplankton (Simpson et al., 1999). DMS is oxidised in the marine atmosphere atmosphere to various sulphur-containing compounds such as sulphur dioxide, dimethyl sulphoxide, dimethyl sulphone, methanesulphonic acid and sulphuric acid (Lucas et al., 2005).

Carbonaceous aerosols contribute around 133 Tg y^{-1} to the total global aerosol loading (Andraea and Rosenfeld, 2008). Carbonaceous aerosols are so called owing to the presence of carbon as the major component, although mineral carbon from carbonates is excluded as they are categorised as mineral matter. Thus, carbonaceous aerosols are divided into elemental carbon (EC) and organic carbon (OC). EC is graphitic carbon and is emitted directly at the source, i.e. it is a primary emission, and is produced from the incomplete combustion of fossil fuels and biomass (Goldberg, 1985). The main sources of EC in the atmosphere are from vehicle emissions (mainly diesel engines), power generation (especially coal-fuelled power plants), certain industrial processes, natural and anthropogenic biomass combustion and domestic emissions (Bond et al., 2013).

Anthropogenic sources of OC include fossil fuel combustion, biomass burning and agricultural emissions. Organic aerosols comprise a myriad of organic compounds of varied origin, such as polycyclic aromatic hydrocarbons (PAHs), alkanes, alkenes and organic acids, cellulose and humic acids among others (Seinfeld and Pandis, 1998). OC can be emitted directly either as primary organic aerosols (POA) or formed as secondary organic aerosols (SOA) through photochemical reactions and the condensation of VOCs (Jimenez et al., 2009). POAs include both anthropogenic organic aerosols and natural organic aerosols, such as bioaerosols, pollen and spores. Of the

natural sources of VOCs, vegetation is regarded as the greatest source on a global scale (Guenther et al., 2000). Oxidation of both natural and anthropogenic VOCs in the atmosphere produces less volatile compounds which can, in turn, undergo gas-to-particle transformation, forming SOA and contributing to the particle mass loading (Guenther et al., 2000). Formation and evolution of SOA is an area of study with a large degree of uncertainty (Volkamer et al., 2006). The formation of low-volatility compounds that make up SOA is governed by a complex series of reactions involving a large number of organic species, so the experimental characterisation and theoretical description of SOA formation presents a substantial challenge (Volkamer et al., 2006; Robinson et al., 2007; Jimenez et al., 2009). The most commonly studied mechanism of SOA formation is the oxidation of VOCs, but reactions of less volatile organics may also lead to the formation of particulate matter as well, so SOA may also be formed from chemical reactions or organic compounds emitted originally in the condensed phase (Robinson et al., 2007).

Secondary inorganic aerosols (SIA) are formed in the atmosphere from precursor gaseous species through gas-to-particle processes (Hidy, 1994). The major secondary inorganic compounds in the atmosphere are sulphate (SO_4^{2-}), nitrate (NO_3^-) and ammonium (NH_4^+), and they are formed from their precursor gaseous species (SO_2, NO_x and NH_3, respectively) through gas-to-particle transformation (Hidy, 1994). SIA contribute around 140 Tg y^{-1} of global planetary emissions (Andreae and Rosenfeld, 2008).

The oxidation of SO_2, emitted by coal and fuel oil combustion used for power generation and shipping, and natural sources such as volcanoes, in the atmosphere produces sulphuric acid aerosol. The sulphuric acid aerosol is readily neutralised in the atmosphere by NH_3 to form particulate $(NH_4)_2SO_4$, and to a lesser extent $CaSO_4$ or $NaSO_4$ after reaction with $CaCO_3$ or NaCl (Junge, 1963). $(NH_4)_2SO_4$ typically exists in the fine mode (<1 μm), whereas $CaSO_4$ or $NaSO_4$ is normally coarse (Mildford and Davidson, 1987).

NO_3^- is formed in the atmosphere from the gaseous precursors nitrogen oxides (NO_x), which are emitted into the atmosphere from natural sources (lightening, forest fires) and anthropogenic sources (high temperature fuel combustion). Nitric acid (HNO_3) is produced from the oxidation of NO_2, and the acid is subsequently neutralised by forming particulate NH_4NO_3, $NaNO_3$ or $CaNO_3$ (Meszarós, 1999). NH_3 is mostly emitted from agricultural emissions, but sources in urban areas include biological

sources such as sewage and waste (Reche et al., 2012; Pandolfi et al., 2012). NH_4NO_3 is thermally unstable at relatively high temperatures (>20-25ºC) and this governs the form particulate nitrate will take in the atmosphere (Seinfeld and Pandis, 1998). NH_4NO_3 species present a fine grain size (<1 μm), whereas $NaNO_3$ or $CaNO_3$ are mainly present in the coarse range (>1 μm) (Mildford and Davidson, 1987). Under warm and dry conditions, NH_4NO_3 is easily volatilised and gaseous HNO_3 may react with predominantly coarse components such as sea spray (NaCl) or mineral matter ($CaCO_3$), resulting in coarse particulate nitrate during the summer months (Harrison and Pio, 1983; Querol et al., 1998a). Under colder and more humid conditions, NH_4NO_3 is typically formed. Thus, in warmer regions nitrate undergoes a clear seasonal pattern with elevated concentrations in winter and a marked summer decrease as a consequence of the thermal instability of NH_4NO_3 (Querol et al., 2004a and b).

1.1.4. Size distribution

Atmospheric aerosols are typically categorised according to their size. Particle sizes can range from a few nanometres (nm) to tens of micrometres (μm), and a particle's size can often be loosely linked to its formation mechanism. The specific ranges of particle sizes are called modes, which include the nucleation mode (<20 nm), the Aitken mode (20-100 nm), the accumulation mode (100 nm – 1 μm) and the coarse mode (1-10 μm) (Seinfeld and Pandis, 1998). Particles can also be classified as nanoparticles, for particles with diameter <50 nm, ultrafine (<100 nm), fine (<1 μm) and coarse for particles of diameter 1-10 μm (Figure 1.2).

The nucleation mode incorporates all particles below 20 nm in diameter. Particles in this mode are associated with the formation of new particles through gas-to-particle transformations, and thus are considered secondary particles. However, nucleation mode particles can be emitted by traffic as primary particles. Nucleation mode particles are typically formed from gaseous precursors which nucleate spontaneously in the atmosphere. These gaseous precursors include H_2SO_4, NH_3 and VOCs (Kulmala et al., 2013). Several nucleation mechanisms have been proposed, including homogenous water-sulphuric acid nucleation, homogenous water-sulphuric acid-ammonia nucleation, ion-induced nucleation of organic or inorganic vapours, or kinetically controlled homogenous nucleation and the occurrence of nucleation depends on a number of variables (Kulmala and Kerminen, 2008, and references therein). Pre-existing particles

in the atmosphere can scavenge the gaseous precursors necessary for nucleation through condensation processes and thus clean air conditions are often more favourable for new particle formation processes (Rodríguez et al., 2005). Ambient air conditions, such as temperature, relative humidity and solar radiation are also believed to be influential factors on nucleation processes (Eastern and Peter, 1994). Photochemistry plays a pivotal role in new particle formation as it generates free radicals in the atmosphere that can react with gaseous precursors to produce the vapours necessary for nucleation (Pey, 2007). Following the formation of stabilised clusters through nucleation of the gaseous precursors mentioned (<1 nm), organic vapours are believed to activate these clusters causing the fresh particles to grow in size (Kulmala et al., 2013).

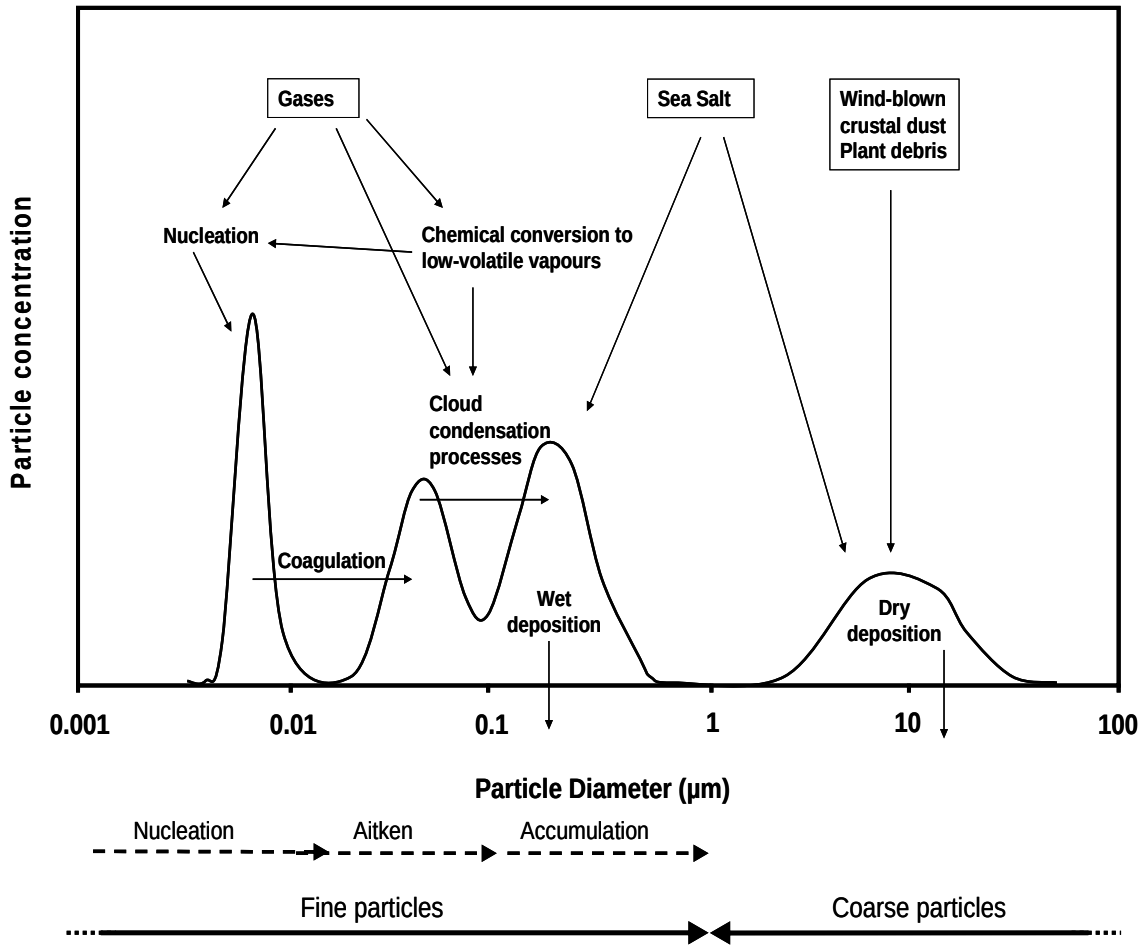

Figure 1.2. A simplified schematic illustration of atmospheric aerosols, including sources, transformations and sinks (adapted from Viana, 2003).

Nucleation has been observed to occur in almost all environments, including: the Polar Regions (Wiedensohler et al., 1996), high altitude sites (Venzac et al., 2009), continental boreal forests (Kulmala et al., 1998) and remote areas (Birmili et al., 2001), and urban environments (Pey et al., 2008; Dall'Osto et al., 2013), among many others. In urban environments, traffic emissions contribute significantly to nucleation processes through emissions of precursor gases necessary for nucleation, while also emitting primary particles with a typical size distribution in the nucleation mode (Casati et al., 2007; Harris and Maricq, 2001). The residence time of these particles is typically short as they grow rapidly through condensation and coagulation processes (Zhang and Wexler, 2004; Fine et al., 2002). In rural and remote regions, nucleation episodes are typically favoured under clean air conditions, as nucleation and the condensation of gaseous precursors on pre-existing particles are competing processes (Birmili et al, 2001; Rodriguez et al., 2005). However, nucleation can still occur under polluted atmospheric conditions provided the growth rate of the nucleating particles is sufficiently rapid to avoid being scavenged by pre-existing particles (Hamed et al., 2007).

Nucleation mode particles are typically removed from the atmosphere through condensation and coagulation processes, causing the particles to grow in size to Aitken and accumulation mode particles. Coagulation is produced by Brownian motion and diffusion, and is the most common removal process for nanoparticles (Mészáros, 1999). The rate of coagulation is proportional to the concentration of particles in the atmosphere, as collision between particles is more probable.

The Aitken mode refers to all particles of diameter between 20-100 nm. Particles in this mode result primarily from primary emissions and coagulation between pre-existing particles, usually from the nucleation mode (Lingard et al., 2006; Kerminen et al., 2007). In the urban environment this mode is especially prevalent owing to primary emissions from traffic such as black carbon, specifically from the incomplete combustion of fuels associated with diesel engines (Morawska et al., 1998 and 1999).

The accumulation mode includes all fine particles between 100 nm and 1 μm. This mode is associated with particles resulting from processes of coagulation between other particles, and/or the condensation of semi-volatile compounds on the surface of these particles (Seinfeld and Pandis, 2008). These particles may act as condensation nuclei

whereby low vapour gaseous species such as H_2SO_4, NH_3, HNO_3 and non-methane VOCs compounds can condense on the existing particle surface (Rose et al., 2006). The adsorption or condensation of gas phase components, and the coagulation of smaller particles to form accumulation mode particles, thus causes the particle number concentration to decrease, but the particle mass to increase. The accumulation mode is so named because particle removal mechanisms are least efficient in this regime and thus have a long residence time in the atmosphere compared to the inferior size modes (Seinfeld and Pandis, 2008). They can be transported over longer distances and this is especially relevant for transport from urban areas to rural areas.

Coarse particles are those of diameter greater than 1 μm. Air quality studies normally refer to mass concentrations of particulate matter with aerodynamic diameters less than 1 μm, 2.5 μm and 10 μm as PM_1, $PM_{2.5}$ and PM_{10} respectively. Coarse particles are mostly primary and are generated from mechanical processes such as resuspended mineral dust, marine aerosol, products from tyre and brake abrasion and biogenic emissions. However, coarse secondary particles can occur when gases chemically react with particles of marine or crustal origin (Querol et al., 1998a). Whereas coarse particles are typically primary and result from mechanical processes, the fine fraction (< 1μm) is dominated by secondary species (NO_3^-, SO_4^{2-} and NH_4^+ ions) and emissions from combustion processes (carbonaceous material) (Seinfeld and Pandis, 1998).

1.2. Effects of Aerosols

Atmospheric aerosols have played a pivotal role in the development of the Earth's atmosphere. Without atmospheric particles, rainfall would be non existent and the climate would be very different (Mészarós, 1999). However, anthropogenic emissions have changed the chemical composition of atmospheric aerosols significantly through emissions of particles and precursor gases from biomass burning and fossil fuel combustion, particularly since the industrial revolution (Pöschl, 2005). Numerous studies have demonstrated that atmospheric aerosols, both natural and anthropogenic, can impact health and climate, many of which will be referred to in the following sections.

1.2.1 Health effects

Epidemiological studies in humans and laboratory animals have consistently provided evidence that exposure to fine and ultrafine particulate air pollution is related to acute and chronic health effects such as respiratory and cardiovascular disease exacerbations (Brook et al., 2010; Rückerl et al., 2011; Anderson et al., 2012). Worldwide, it has been estimated that air pollution represents up to 8% of lung cancer deaths, 5% of cardiopulmonary deaths and 3% of respiratory infection deaths, according to the WHO global health risks (WHO, 2009). A recent review on evidence of health aspects of air pollution (REVIHAAP) by WHO (2013) suggested a possible link with neurodevelopment, cognitive function and diabetes, and strengthened the casual link between $PM_{2.5}$ and cardiovascular respiratory deaths. Recent estimates suggest that 3.5 million cardiopulmonary and 220,000 lung cancer annual deaths globally can be attributed to the anthropogenic component of $PM_{2.5}$ (Anenberg et al., 2010). Inhalation of airborne particles is the main mode of exposure and the effects are dependent on the concentration, size, shape and composition of the particles, and the extent of the exposure (Oberdörster, 2004). Short-term exposure to coarse particles is associated with adverse respiratory and cardiovascular health effects, even including premature mortality (Soukup and Becker, 2001). Furthermore, a relationship was observed for short-term exposure to PM during Saharan dust days with cardiovascular and respiratory mortality (Pérez et al., 2012).

Considering the adverse health effects of exposure to PM, the complex composition of particles makes it inherently difficult to identify with any great surety which components are culpable for the adverse health effects (Oberdörster et al., 2005). Some studies have focused on the direct health effects of specific components of aerosols, such as a report commissioned by WHO (2012) on the health implications of exposure to black carbon (BC). The report suggested that BC may not be a major directly toxic component of fine PM, but it may operate as a universal carrier of a wide variety of chemicals of varying toxicity to the lungs, the body's major defence cells and possibly the systematic blood circulation. The report states that, at present, it is not possible to say definitively whether health effects due to exposure to BC or PM mass are different qualitatively and/or quantitatively from each other. They attribute this partly to the fact that an insufficient number of controlled health studies have been implemented which

involve human subjects with simultaneous BC or EC measurements and other PM speciation.

Ultrafine particles are also attracting significant attention as they have been identified as a causal component of various negative health effects in humans (Knol et al., 2009; Hoek et al., 2010). Ultrafine particles contribute little to PM mass, but can contribute around 90% to the particle number concentration in areas influenced by vehicle emissions (Morawska et al., 2008). Ultrafine particles are believed to be particularly hazardous owing to their small size and large surface area, giving them the ability to penetrate deeper into the respiratory system, enter the circulatory system stream and deposit in the brain (Oberdörster et al., 2004; Samet et al., 2009). In urban environments, ultrafine particles are often associated with traffic emissions, containing components such as soot, certain organics and metals, and these components are believed to increase the risk of diseases (Ovrevik and Schwarze, 2006; Ostro et al., 2006).

1.2.2. Climate effects

Since the industrial revolution and the intensive use of fossil fuels for energy, the natural balance of aerosols in the atmosphere, and thus the radiative balance of the Earth, has changed dramatically. The IPCC (2007) has attributed a global increase of 0.8ºC in temperature compared to pre-industrial times. Anthropogenic or natural changes in atmospheric aerosol composition can disrupt the radiative balance by changing the amount of solar radiation reaching the earth's surface. Scattering and reflection of solar radiation by aerosols and clouds tend to cool the Earth's surface (negative radiative forcing), whereas the absorption of solar energy by aerosols, such as greenhouse gases, BC and clouds tend to have a warming affect (positive forcing; greenhouse effect; IPCC, 2007). Although the forcing by greenhouse gases such as CO_2 is known relatively accurately, the total forcing is more difficult to estimate due to the uncertain contribution of aerosols. This uncertainty arises from the great variety of aerosol types, their large number of sources, their distinct optical properties, their spatial distribution and atmospheric lifetimes.

Aerosol effects on climate are generally classified as direct or indirect with respect to radiative forcing of the earth's climate (Figure 1.3). Direct effects result from the scattering or absorbing of the incoming solar radiation and the outgoing terrestrial

radiation, whereas indirect effects result from aerosols acting as cloud condensation nuclei (CCN) or ice nuclei (IN), thus indirectly changing cloud formation and lifetimes. The residual forcing due to direct and indirect forcing by aerosols as well as semi-direct forcing from greenhouse gases and any unknown mechanism between 1970 and 2000 was estimated to be -1.1 ± 0.4 W m^{-2} (Murphy et al., 2009). The aerosol particle size, structure and chemical composition will largely decide the optical properties of the particle relevant to direct effects, such as the particle scattering, absorption and extinction coefficient, and ability to act as CCN and IN relevant to indirect effects.

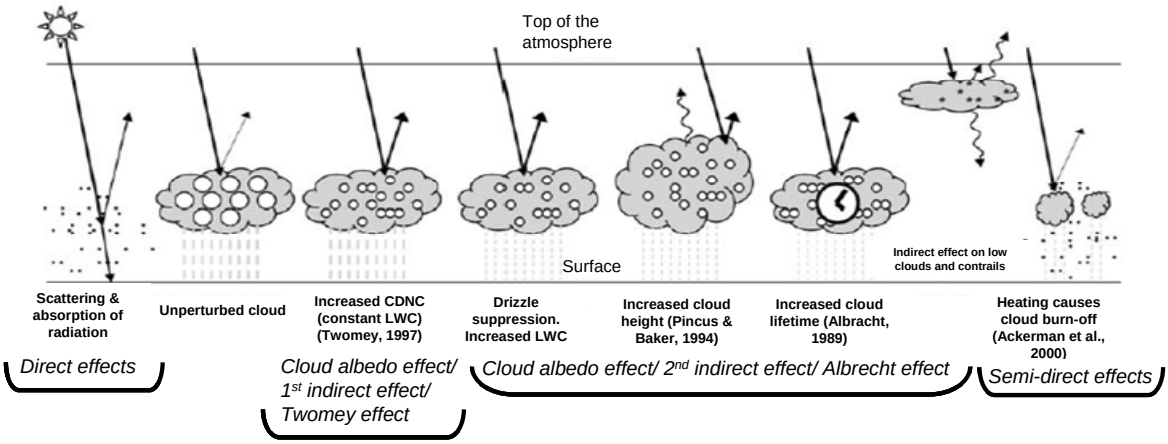

Figure 1.3. Direct, indirect and semi-direct climate forcing effects caused by aerosols (IPCC, 2007).

Thus, the radiative forcing properties of aerosols are strongly influenced by atmospheric processes such as chemical and physical transformations. This creates a large margin of uncertainty owing to the complex physical and chemical properties of aerosols. The mean total direct radiative forcing attributed to aersols is estimated to be around -0.4 W m^{-2} (IPCC, 2007). The global mean direct radiative forcing from the different components is estimated by IPCC and shown in Figure 1.4. Sulphate, for example, has a scattering effect of radiation, creating an overall cooling effect (-0.4 ± 0.2 W m^{-2}; IPCC, 2007). On the contrary, BC strongly absorbs radiation, trapping solar energy in the earth's atmosphere, causing a positive radiative forcing (estimated to be +1.1 W m^{-2}; Bond et al., 2013). The difficulty in estimation of the total radiative forcing of aerosols arises when the majority of the aerosols are emitted from the same sources. BC, for example, is usually emitted with other particles that cause cooling, therefore obscuring the observed net effects of real-world emissions (Shindell et al., 2012). That

same work suggested that control of BC emissions would produce a direct benefit through mitigation of climate change, and would also control emissions co-emitted with BC such as organic carbon compounds. However, this is disputed by some studies claiming that the forcing associated with BC may be overestimated (Cappa et al., 2012).

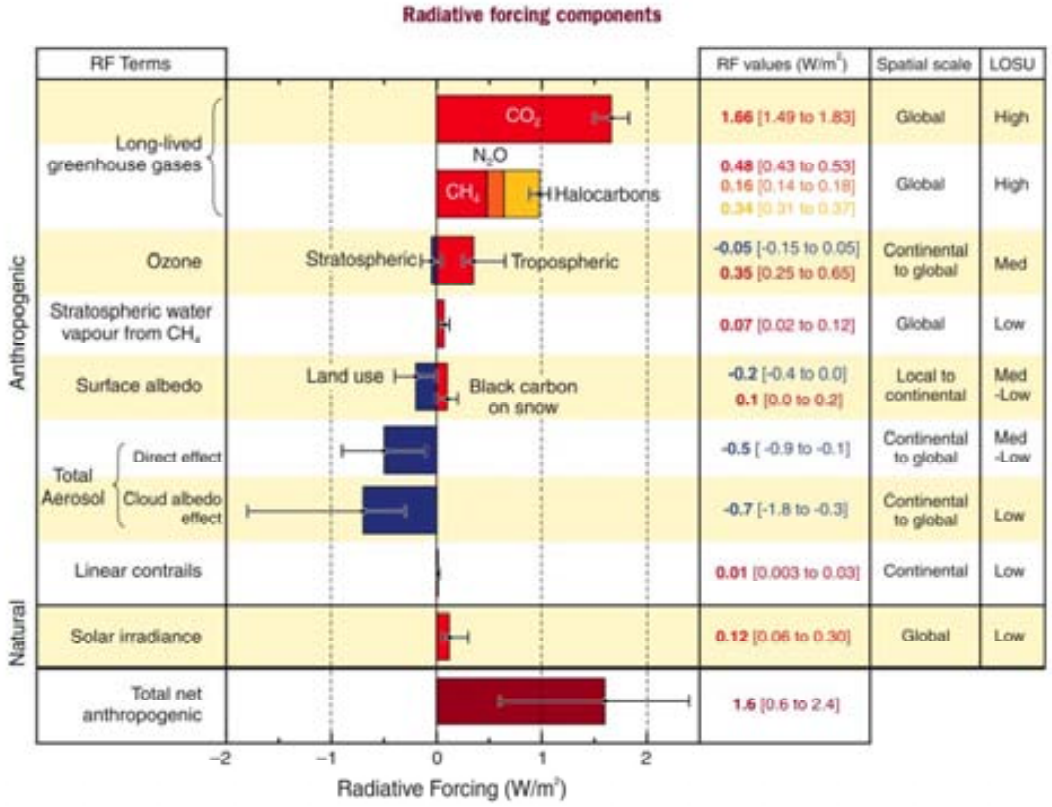

Figure 1.4. Average global radiative forcings and their 90% confidence intervals as of 2005 for greenhouse gases and atmospheric aerosols. Uncertainties are represented by error bars. (IPCC, 2007). LOSU: Level of Scientific Understanding.

An increase of atmospheric CCN and IN concentrations can have different effects on the formation and properties of clouds and, subsequently, precipitation. An increase in hygroscopic aerosol number concentrations tends to increase the CCN, which in turn can lead to increased cloud formation. Clouds scatter and absorb solar radiation and the cloud properties and size will determine their ability to disrupt the earth's radiative balance. The relationship between aerosols, clouds, precipitation and solar radiation influences the regional and global radiative energy balance and hydrological cycle, as well as the temperature, dynamics, and general circulation of the atmosphere and oceans (Andreae et al., 2005). The indirect effect of clouds is divided into the "cloud albedo

effect" and the "cloud lifetime effect" (IPCC, 2007), and the total aerosol indirect effect is estimated to be -0.7 W m^{-2}.

1.2.3. Regulation

Considering the detrimental health effects of atmospheric aerosols and their ability to disrupt the Earth's radiative budget, many countries aim to control and regulate ambient concentrations of atmospheric aerosols and specific emission sources. In order to reduce the negative effects of air pollution, the European Union (EU) has drawn up the European air quality directives 2008/50/EC and 2004/107/EC with the specific aim of regulating specific pollutant parameters in ambient concentrations. Member states are obliged to adhere to these regulations by implementing effective means to reduce air pollution at local, national and European levels. In the above air quality directives, criteria from previous directives were unified, while also taking into consideration the most recent scientific research and combined experience of member states. Thus, the parameters currently regulated at a European level include ambient concentrations of: PM_{10}, $PM_{2.5}$, Ozone, Benzene, Lead, As, Cd, Hg, Ni, PAHs, SO_2, NO_2, CO and NO_x. Furthermore, chemical composition monitoring of NO_3^-, SO_4^{2-}, Cl^-, NH_4^+, Na^+, K^+, Mg^{2+}, Ca^{2+}, OC and EC concentrations in $PM_{2.5}$ for rural areas has since become mandatory (Annex IV of the 2008/50/EC Directive).

Air quality standards for PM_{10} require that an annual mean limit value of 40 μg m^{-3} must not be exceeded, and a daily limit value of 50 μg m^{-3} must not be exceeded more than 35 times a year. An annual target value of 25 μg m^{-3} for $PM_{2.5}$ was enforced in 2010, and this will become an annual limit value by 2015. An annual limit value of 20 μg m^{-3} will be effective by 2020, pending revision by the European Commission in 2013 (the European Environment Agency's "Year of Air"), when the most recent information on PM health and environmental effects, technical viability and the experience obtained by the member states will be taken into consideration.

As well as controlling ambient concentrations of certain pollutants, certain EU air directives also aim to control emissions from specific sources, specifically exhaust emissions from vehicles and industrial emissions. Vehicular emissions are controlled under the EURO certification, whereby EURO 1 (1991/441/EC), 2 (1994/12/EC), 3 and 4 (1998/69/EC), 5 and 6 (2007/701/EC) controls light duty vehicles, and EURO I, II, etc. controls heavy duty vehicles. Emissions of NO_x, total hydrocarbon, non-methane

hydrocarbon, CO and PM are currently regulated for most vehicle types. Non compliant vehicles are not permitted to be sold in the EU. Industrial emissions are controlled by the Directive 2008/1/EC (the IPPC Directive, Integrated Pollution Prevention and Control), which replaces Directive 1996/61/EC. The Directive requires industrial and agricultural activities with a high pollution potential to have a specific permission, and this permit can only be issued if certain environmental conditions are met. The Directive establishes emissions ceilings for each specific type of industry, while taking into consideration BATNEEC (Best Available Techniques Not Exceeding Excessive Costs), which require industries to employ efficient pollution control that are economically viable.

Currently, there is much debate surrounding the inclusion of specific components of PM that should be controlled by environment agencies. As outlined previously, BC is a known contributor to climate forcing, and there are continuing studies in the adverse health effects of BC (WHO, 2012). Shindel et al. (2012) have shown how implementing specific practical emissions reductions chosen to maximise climate benefits would have important mutual benefits for near-term climate, human health and agriculture, among others. Bond et al. (2012) suggests that diesel engine and biomass burning sources of BC appear to offer the best mitigation potential to reduce near-term climate forcing. Furthermore, control of BC emissions would bring health benefits by additionally reducing PM exposure.

As discussed previously, ultrafine particles are believed to be the most harmful to human health, to the extent that the World Health Organisation has called for further research to establish the links between ultrafine particles, exposure and human health (WHO, 2013). The significance of fine and ultrafine aerosol concentrations in the context of impacts on human health has been well established in numerous studies which have outlined possible abatement measures (Kumar et al., 2010; Knibbs et al., 2011). However, there is no current legal threshold for controlling particle number concentrations (as opposed to particle mass concentrations which are controlled) even though there is evidence to suggest that ultrafine particles can be even more harmful to health (Knol et al., 2009).

1.3. Regional background environment

The Directive 2008/50/EC also requires the establishment of a monitoring network with an equilibrated number of hotspots, urban and rural monitoring sites, in order to appropriately monitor air quality. The Directive establishes criteria for the monitoring networks, such as location, type and number of sampling points, and provides measurement reference methods. The locations of the sites are chosen taking into consideration the major emission sources, and aim to categorise the exposure to populations. The directive also requires monitoring at rural/regional background sites located in areas far from direct anthropogenic pollution sources, thus providing information on background levels of pollutants on a regional scale.

Monitoring sites are classified according to the target environment under study in order to monitor air quality in different environments. These sites include traffic, industrial, urban, regional/rural or continental/remote monitoring stations, and are so chosen to provide information representative of that specific environment. Urban sites are located in urban areas separated from direct emissions from traffic or industry, with the aim of determining the average exposure of the general population to urban aerosols. According to the criteria outlined in directive 2008/50/EC, Van Dingenen et al. (2004) and Putaud et al. (2004), regional or rural background sites should be isolated from the direct influence of local anthropogenic emission sources, and should represent background pollutant levels from across the region in which they are located, with a distance of 10-50 km from significant pollution sources (Larssen et al., 1999). Ideally, regional background sites should be located in rural areas, distant from roads, populated areas and industries, but should be affected by regional sources of pollution, long-range transport and urban plumes of pollution. The relevance of these sites is most important for monitoring long-term trends of aerosols, the influence of synoptic meteorology and prevailing weather conditions on ambient air quality across the region, and the input of long-range transport of aerosols not emitted within the region. Furthermore, all the information compiled from these sites is essential for sufficient monitoring of a) air quality at a regional scale, b) climate change and the effect of aerosols in the region on the radiative balance, and c) the carrying potential of pollutants for eutrophication and acidification. Measurements from regional background sites also allow for more accurate quantification of urban emissions through comparison of urban levels and regional background levels of pollutants (Lenschow et al., 2001).

The importance of monitoring regional background aerosols is highlighted by the existence of international networks for pollutant monitoring. For example, the EMEP (European Monitoring and Evaluation Programme) network is a scientifically based and policy driven programme under the Convention of Long-Range Transboundary Air Pollution (CLRTAP) for international cooperation to solve transboundary air pollution problems (http://www.emep.int). The main objective of the EMEP programme is to regularly provide governments and subsidiary bodies under the LRTAP Convention with qualified scientific information on air pollutants throughout Europe. Pollutants currently monitored by EMEP include ground level ozone, persistent organic pollutants, heavy metals and particulate matter. The EMEP programme relies on three main elements: (1) collection of emission data, (2) measurements of air and precipitation quality, and (3) modelling of atmospheric transport and deposition of air pollutions. Through the combination of these three elements, EMEP fulfils its required assessment and regularly reports on emissions, concentrations and depositions of air pollutants, the quantity and significance of transboundary fluxes and related exceedances to critical loads and threshold levels.

The Aerosols, Clouds and Trace gases Research InfraStructure (ACTRIS) project, which identified the need for reliable information on the state of the atmosphere and its interactions through understanding the nature of atmospheric processes and components, aims to meet the challenges posed by global climate change, air quality and pollution (http://www.actris.net). ACTRIS is a research infrastructure launched in 2011 (formerly EUSAAR) and aims to integrate and homogenise the monitoring of the major atmospheric variables, with a strong focus on quality control of data collection. The parameters currently monitored under the ACTRIS network include remote sensing of the vertical aerosol distribution, in-situ chemical, physical and optical properties of aerosols (such as aerosol light absorption, size distribution, organic and elemental carbon), trace gases (NO_{xy}, VOCs) and cloud observations.

1.4. Specifics of the Western Mediterranean regional background

As described previously, atmospheric aerosols are complex in nature owing to the wide variety of natural and anthropogenic emission sources and atmospheric processes, both largely influencing the physical and chemical nature of the aerosols. The nature of atmospheric aerosols in any given region, in terms of both concentration and

composition, will also largely depend on other variables such as meteorology (temperature, humidity, solar radiation/photochemistry, precipitation, air mass movement) and geography (topography, proximity to the coast or to arid areas, soil cover, vegetative cover, land use). The characteristics and variability of the physical properties and chemical composition of atmospheric aerosols have been studied for many regional background sites across Europe, such as the variability of PM and chemical composition (Putaud et al., 2004 and 2010; Van Dingenen et al., 2004; Querol et al., 2009; Barmpadimos et al, 2012) and number size distributions and seasonality of sub-micron particles (Asmi et al., 2011; Birmili et al., 2001; Venzac et al., 2009). These studies have highlighted the wide variations in aerosols and their properties across the continent of Europe.

Northern Europe is very much under the influence of weather fronts from the Atlantic Ocean, bringing westerly winds and relatively high levels of precipitation associated with cold fronts and depressions. The Iberian Peninsula (IP), in contrast, is exposed to complex atmospheric dynamics and meteorology owing to its geographical position between two large bodies of water (the Atlantic Ocean and the Mediterranean), isolated from mainland Europe by the Pyrenees, and close proximity to the African continent. Meteorology and atmospheric dynamics in the western Mediterranean basin (WMB) have been previously described in detail (Millán et al., 1997 and 2000; Toll and Baldasano, 2000; Rodríguez et al., 2002 and 2003; Jorba et al., 2004; Pérez et al., 2004; Jiménez et al., 2006; Sicard et al., 2006). The WMB has peculiar atmospheric dynamics owing to a) the low atmospheric dispersive conditions b) the abrupt topography of the peninsula and c) to the influence of air masses originating in diverse regions such as desert areas or marine environments. Atmospheric circulation over the WMB is highly influenced by the Azores high pressure system and is balanced between two synoptic systems (Millan et al., 1997; Pérez et al., 2004; Sicard et al., 2006).

During the cold season, the displacement of the Azores high pressure system to the lower latitudes allows for the frequent movement of depression systems from the Atlantic across the IP (Lopez-Bustins et al., 2008). This scenario brings fresh, typically clean air masses to the WMB and consequently results in the renovation of air masses and removal of pollution. Displacement of the Azores high pressure system can also result in the movement of Central and Northern European air masses to the WMB, which are typically cold and polluted air masses, leading to an increment of pollutant levels on a regional level. However, in some instances, the Azores high can become

displaced over the IP, and this situation can continue for several days. Pey et al. (2010) describes this scenario as Winter Anticyclonic Episodes (WAE). WAE are associated with calm, sunny weather with little air mass renovation and thermal inversions, giving rise to stagnant conditions across the region. Due to the lack of advection, pollution emitted from urban and industrialised areas accumulates in the mixing layer, and a subsequent increase in pollutants is observed, lasting for several days until removed by advection of air masses from the Atlantic Ocean. Although the pollution typically remains close to the emission sources, local meteorology can transport some of this contaminated air mass to rural and remote areas. Owing to the mountainous topography of the Mediterranean coast and the meteorological conditions associated with WAE, mountain and sea breezes can be activated by insolation. These breezes can thus carry the accumulated pollution in the industrialised valleys and depressions to remote and rural areas, especially at higher altitudes, resulting in intense pollution episodes (Pérez et al., 2008; Pey et al., 2010).

During the warmer months, the Azores high is situated further to the north east, causing thermal lows to develop over the IP and the Sahara. This scenario favours a very weak pressure gradient over the WMB and consequently, local and regional circulations dominate the atmospheric dynamics (Pérez et al., 2004). Recirculation of air masses across the region are caused by the interaction of sea and mountain breezes, the topography of the region, the dominant north-western atmospheric air flows at high altitudes and the uplift of air masses in the central IP (Millán et al., 1997). This recirculation gives rise to aerosol aging and accumulation of pollutants across the region, and combined with low summer rainfall, intensified solar radiation inducing photochemical processes and increased soil resuspension, induce an aerosol seasonal pattern characterised by elevated levels of background aerosols during the summer in the WMB (Bergametti et al., 1989; Querol et al., 1998a; Rodríguez et al., 2002 and 2003; Viana et al., 2005). Furthermore, elevated levels of aerosols during the summer months are compounded by the frequent Saharan dust intrusions, owing to the IP's close proximity to the African continent, giving rise to sizeable increases in ambient aerosol concentrations often exceeding the EU Directive's daily limit value, especially in the coarse fraction (Querol et al., 1998a; Rodríguez et al., 2001; Viana et al., 2002; Escudero et al., 2005).

Elevated levels of mineral matter are also a result of local dust resuspension, owing to the low rainfall and dry and arid soils across the region (Querol et al., 2004a). The

presence of a high load of mineral matter in the atmosphere may favour the interaction with gaseous pollutants and give rise to a high proportion of secondary coarse particles (Harrison and Pio, 1983; Mamane and Mehler, 1987; Wall et al., 1988; Querol et al., 1998b). Warm conditions may favour the partitioning of atmospheric pollutants towards the gaseous phase, which in turn may interact with coarse components and increase the secondary coarse PM load (Harrison and Kito, 1990; Wakamatsu et al., 1996). These atmospheric recirculation episodes coupled with the sources of emissions typical of the Mediterranean coastline (densely populated and industrialised, shipping emissions, forest fires, biomass burning from agriculture, Saharan dust, soil resuspension) produces a complex aerosol phenomenology.

1.5. Previous knowledge and studies on regional background aerosols in the Western Mediterranean Basin

The variability of regional background aerosols across the entire Mediterranean region has been described in great detail by Querol et al. (2009). Important differences in PM were observed between the Western Mediterranean Basin (WMB) and Eastern Mediterranean Basin (EMB). PM in the EMB is characterised by higher levels of crustal material relative to the WMB owing to the higher frequency and intensity of African dust outbreaks. A clear seasonality in PM was observed for the WMB with higher levels in summer owing to lower precipitation, higher resuspension, photochemical transformations and more frequent African dust outbreaks. A broader pattern was observed for the EMB with maxima in spring due to higher frequency of dust episodes. Speciation data showed that PM in the EMB is characterised by higher levels of crustal material and SO_4^{2-} compared to the WMB, whereas OC + EC and NO_3^- were relatively constant across the Mediterranean. NO_3^- was seen to undergo a strong seasonal variability with maxima during colder months and reduced levels in the warmer months, related to the thermal instability of $NH_4NO_3^-$. SO_4^{2-} underwent a contrasting seasonal evolution with higher concentrations across the Mediterranean due to enhanced photochemistry, low air mass renovation at a regional scale, and the possible higher summer contribution of marine secondary sulphate from dimethyl sulphide (DMS) oxidation. OC levels were also higher in summer owing to enhanced formation of SOA from the oxidation of biogenic and anthropogenic VOCs, and forest fire emissions of VOCs. Compared to central European sites, PM across the Mediterranean was characterised by relatively high levels of SO_4^{2-} and crustal material, and with lower levels of OC + EC and nitrate. V and Ni across the Mediterranean were higher than in central Europe as a result of relatively high emissions of fuel-oil combustion in the region. Querol et al. (2009) clearly demonstrated why the Mediterranean is included among the most vulnerable regions globally in the context of climate destabilisation, as well as the significant and complicated role that aerosols play as a forcing driver.

Some other studies with specific focus on the WMB regional background have preceded this current work, specifically at the Montseny monitoring station in the northeast of the IP. The Montseny station is important for characterising regional background aerosols in the WMB, making it a unique station in a relatively

understudied region of Europe. For these reasons, the station has been incorporated into the EUSAAR project (currently ACTRIS) and participates in regular EMEP intensive measurement campaigns.

Numerous scientific articles and thesis have been published since the establishment of the Montensy site, such as "Interpretation of the variability of levels of regional background aerosols in the Western Mediterranean" (Pérez et al., 2008). In that work, levels and variability of atmospheric particulate matter in PM_{10}, $PM_{2.5}$ and PM_1 in function of different meteorological scenarios and seasons were evaluated, incorporating measurements since the installation of the station in 2002. Pérez et al. (2008) reported mean annual concentrations for PM_{10}, $PM_{2.5}$ and PM_1 at MSY to be 17, 13 and 11 μg m^{-3}, respectively. In winter, the periodical renovation of air masses and the increased precipitation resulted in relatively low concentrations of atmospheric particulate matter. However, the aforementioned WAE were also identified as key scenarios for causing large increments in pollution levels, as described in "Intense winter pollution episodes affecting the Western Mediterranean" (Pey et al., 2010). In summer, the combination of diverse factors gave rise to elevated levels of particulate matter, such as infrequent renovation of air masses on a regional scale and intensified photochemical activity resulting in an increment in levels of PM as a result higher SO_4^{2-} and organic matter concentrations. Episodes of advection from North Africa and enhanced soil resuspension owing to the low precipitation also caused increases in levels of mineral matter. Daily atmospheric dynamics were observed to be highly influenced by breeze circulations activated by insolation (mountain and sea breezes) transporting pollution from urbanised areas to rural areas. This mechanism was most pronounced during winter when the Montseny station resided above the mixing layer, resulting in very low concentrations at night increasing significantly during the day with the breeze (Pérez et al., 2008).

The chemical characterisation of regional background PM_{10} and $PM_{2.5}$ was studied and presented in "Geochemistry or regional background aerosols in the Western Mediterranean" (Pey et al., 2009a), where the effect of natural and anthropogenic emissions was investigated. For the coarse fraction, crustal material was observed to be the main contributor to the mass (24%), but contributed much less mass to $PM_{2.5}$ (9%; Pey et al., 2009a), with concentrations considerably higher in summer owing to elevated dust resuspension and to the higher frequency of African dust episodes (Pérez et al., 2008). Sporadic increases in mineral matter concentrations were recorded from

February to March, attributed mainly to intense African dust outbreaks. Organic matter was identified to be the most abundant component of $PM_{2.5}$ and the second most abundant in PM_{10}, with similar concentrations for both, suggesting organic matter exists mostly in the finer fraction (Pey et al., 2009a). SO_4^{2-} was found to be the next most abundant compound and was primarily in the finer size fraction, resulting from the prevalence of $NH_4SO_4^{2-}$. Secondary peak concentrations were also observed to occur during WAE (Pey et al., 2010). NO_3^- concentrations were mostly in the finer fraction due to the prevalence of fine NH_4NO_3, but coarser $NaNO_3$ and $CaNO_3$ particles caused NO_3^- concentrations to be slightly higher in the coarse fraction. Extremely intense NO_3^- episodes (up to 15 μg m^{-3} of daily mean nitrate levels) were recorded during the winter months, especially during WAE (Pey et al., 2009a). NH_4^+ concentrations were shown to vary only slightly throughout the year, with a strong partitioning in the finer fraction. During the colder months it typically exists in the atmosphere as NH_4NO_3, and in summer in the sulphate form. Elemental carbon also existed primarily in the finer fraction. Finally, sea spray was distributed evenly among both fractions and exhibited higher concentrations in summer due to increasing sea breeze circulation over the coast.

Following on from the chemical characterisation of PM_{10} and $PM_{2.5,}$ source apportionment studies were performed in order to identify the contribution of various sources to ambient particulate matter concentrations (Pey et al., 2009a). Four emission sources for both PM_{10} and $PM_{2.5}$ were identified. Sources in common to both fractions included mineral matter, identified by the high factor loadings for typical mineral matter tracers (Al_2O_3, Ti, Fe, La, Rb, Ca, La, Mg, K, Mn). A mixed anthropogenic industrial/road traffic source was identified in both fractions, with tracers for industrial emissions (total carbon, Zn, Cu, V, Ni, Pb; Querol et al., 2007), and road emissions (total carbon, Cu, Sn, Sb; Pacyna, 1986; Schauer et al., 2006) present. Secondary sulphate was identified in both fractions also, identified by the tracers SO_4^{2-} and NH_4^+, alongside V and Ni in $PM_{2.5}$. In the coarse fraction, SO_4^{2-} levels were correlated with Na, which was interpreted as the result of more intense sea breeze in summer transporting sea spray (Viana et al., 2005). A secondary nitrate source was also outlined, with main tracers of NO_3^- and NH_4^+. A marine source was identified by PCA that was not identified by PMF, with high factor loadings for typical marine aerosols.

The following is a timeline of previous projects (in chronological order) which led to a number of thesis and scientific publications focusing on the characterisation of

atmospheric particulate matter performed for the regional background of the north-eastern IP before the current work commenced:

- Project title: **Integrated study of atmospheric particulate matter and sulphur compounds originating from coal combustion in a large thermo-electrical plant (1995-1998).** This project was financed by the Comisión Interministerial de Investigación Científica y Técnica (AMB95-1102), which characterised levels and composition of PM_{10} around a coal-fired power station in Teruel, outlining the great seasonal variability of PM components (such as SO_4^{2-}, NO_3^-), and drew attention to the large influence of Saharan dust intrusions on ambient PM_{10} concentrations for the first time in Europe (Querol et al., 1998a and b).
- Project title: **Discrimination of external contributions on levels of emissions of atmospheric particulate matter in a regional air quality network (1998-2001).** This project was financed by the Comisión Interministerial de Investigación Científica y Técnica (AMB98-1044), and focused on the levels, composition and sources of particulate matter in urban environments (Querol et al., 2001).
- Project title: **Impact of the intrusion of African air masses on air quality of the Canary Islands and the Iberian Peninsula (2002-2005).** The project was financed by Plan Nacional (I+D+I, REN2001-0659-CO3-O3/) through collaboration with CREAF and the university of La Laguna. Through this project, a regional background monitoring station (Montseny, MSY) was established in the Montseny national park in 2002. PM_{10}, $PM_{2.5}$ and PM_1 levels were continuously measured in real-time, and total suspended particles (TSP) and $PM_{2.5}$ was monitored gravimetrically and chemically characterised (Castillo, 2006).
- Project title: **Influence of external contributions, regional and local, on levels and composition of atmospheric aerosols in background and urban stations in Spain (INTEREG: 2004-2007).** This project was financed by the Spanish Ministry of Education, Culture and Sport (CGL2004-05948-C07-02/CLI). In March 2003, TSP gravimetric measurements were replaced with PM_{10}. Thus, gravimetric and chemical speciation of PM_{10} and $PM_{2.5}$ were monitored continuously thereafter, as where measurements of real-time concentrations of PM_{10}, $PM_{2.5}$ and PM_1. Results were published in the thesis of Pey (2007).

- Project title: **European Super-sites for Atmospheric Aerosol Research, (EUSAAR: 2006 – 2010, ACTRIS: 2010 – present)**, under the action of scientific infrastructure with 21 European organisations I3, - **VI,** Marco Programme (RII3-CT-2006-026140).
- Project title: **Discrimination of the origin of atmospheric aerosols at a regional and urban scale (DOASUR: 2007-2010).** This project was also financed by the Spanish Ministry of Education, Culture and Sport (CGL2007-62505CLI). Publications resulting from this project (in conjunction with others) include: "Interpretation of the variability of levels of regional background aerosols in the Western Mediterranean" (Pérez et al., 2008) and "Geochemistry of regional background aerosols in the western Mediterranean" (Pey et al., 2009a), as well as the thesis of Pérez et al. (2010).
- Project title: **Climate Change and Impact Research: the Mediterranean Environment (CIRCE: 2007-2011).** This project was performed through collaboration with 65 European organisations. VI Marco Programme SUSTDEV-2005-3.I.3.1.
- Project title: **Determination of the sources of atmospheric Aerosols in Urban and Rural Environments in the western Mediterranean (DAURE: campaigns during winter 2009 and summer 2009).** Numerous publications were produced from the data obtained during the campaigns, including "Contrasting winter and summer VOC mixing ratios at a forest site in the Western Mediterranean Basin: the effect of local biogenic emissions" (Seco et al., 2011), "Fossil versus contemporary sources of fine elemental and organic carbonaceous particulate matter during the DAURE campaign in Northeast Spain" (Minguillon et al., 2011), and "Seasonal changes in the daily emission rates of terpenes by *Quercus ilex* and theatmospheric concentrations of terpenes in the natural park of Montseny, NE Spain**"** (Llusia et al., 2012), among others.
- Project title: **The combination of latest generation aerosol measurements at surface to interpret their time and spatial variability in the Western Mediterranean (VAMOS: 2011 - 2013)**. Funded by the Spanish Ministry of Science and Innovation CGL2010-19464 (sub-programme CLI).

1.6. Gaps in current knowledge

Investigation of atmospheric aerosols in the WMB regional background has thus far solely been concerned with PM, whereby the atmospheric dynamics such as mesoscale and synoptic meteorology, long range transport and air mass origins affecting PM has been thoroughly studied. Furthermore, the chemical characterisation of the PM_{10} and $PM_{2.5}$ and the processes affecting the chemical composition of PM has been similarly investigated in detail. In order to further understanding of the complexities of aerosols in the regional background of the WMB, it was necessary to develop upon these previous studies by:

- The continuation and subsequent compilation of all the years of PM data since the establishment of the MSY measurement station in order to study the temporal trends of PM levels and chemical speciation. An extensive set of data will allow better understanding of long-term trends of pollution levels, especially in terms of anthropogenic pollution. Furthermore, the influence of long-range transport can be better quantified and observed.
- Including chemical speciation of the fine fraction (PM_1). Until now, there have been no PM_1 speciation studies completed for the area and few exist within Europe. Anthropogenic aerosols are mainly found in the fine fraction and thus, it is an important parameter for monitoring anthropogenic emissions across the region. Furthermore, source apportionment studies on the fine fraction will help identify the specific sources affecting the fine fraction.
- Continuous measurements of aerosol optical properties, such as the mean aerosol absorption coefficient and aerosol scattering and backscattering coefficients, are important to observe the radiative forcing properties of aerosols in the region, and the trends of these types of aerosols. These parameters are important for determining the direct radiative forcing effect for climate studies.
- The particle number concentration and size distribution of sub-micron particles should be measured in order to observe the ultrafine aerosol processes occurring in the WMB regional background, such as nucleation and growth processes, and for investigation on the modality, the diurnal cycles, the seasonality and the sources of sub-micron particles at the site. Studies of this kind are currently scarce, or indeed non-existent, for this region of the IP.

- Coordinating a more in-depth characterisation of organic carbon aerosols in the area through employment of state-of-the-art techniques. Organic aerosols are still one of the most understudied components of atmospheric aerosols. Furthermore, organic aerosols in this region of the WMB are likely to be considerably different from other regions in Europe owing to the Mediterranean climate and increased solar radiation, the vegetation and biogenic emissions specific to the region and the influence of biomass burning on organic aerosol concentrations.

1.7. Objectives

Acknowledging the gaps in knowledge outlined in the previous section, this present study aims to fill a number of the above gaps through expansion of the existing measurement parameters and development of the monitoring station to incorporate measurements of other aerosol parameters. This allows for further in-depth analysis of the complex atmospheric aerosols occurring in the WMB regional background. Thus, the main objectives of this study are briefly described below:

1) Considering the extensive long-term measurements of $PM_{2.5}$ since 2002, the opportunity presents itself to study the time series of $PM_{2.5}$ concentrations and its chemical components for a relatively long period of time. To this end, specific chemical components of $PM_{2.5}$ can be analysed for statistically significant trends, and the temporal trends can be related to either anthropogenic emissions and/or fluxes in natural emissions, resulting from changes in meteorology for example. Long term chemical speciation studies are relatively few for regional background PM in southern Europe, and thus the objective here is to shed some light on the changes in PM and chemical composition over a long period of time (2002-2010).
2) The inclusion of measurements of PM_1 chemical composition at a regional background site will allow for better quantification of anthropogenic emissions in the fine fraction and source apportionment studies will help identify the main sources affecting PM_1 for the area.
3) Through the measurement of sub-micron particle number concentration and size distribution, the physical and chemical processes affecting sub-micron particles in the WMB regional background will be identified and explored. Processes such as new particle formation, growth and particle transformation will be identified. Furthermore, the interaction between sub-micron particles and a broad range of other pollutants (such as BC, pollutant gases and PM) and meteorological parameters measured simultaneously will be discussed in order to better understand the influencing factors on particle number concentration and size distribution. The modality, diurnal cycles and seasonal variation of particle number concentrations will be explored. Finally, the combination of particle number concentrations and size distribution with chemical speciation data of PM_1 will allow for the identification of specific emission sources of fine particles.

4) The final objective will be to investigate in detail specific episodes of interest concerning sub-micron particles, such as episodes of new particle formation and particle shrinkage. Through in-depth analysis of specific episodes of nucleation and shrinkage, the aim is to identify the ideal atmospheric properties and dynamics which may lead to such aerosol processes.

The following tasks were carried out in order to reach the objectives outlined above.

- The continuation of measurement and analysis of PM_{10} and $PM_{2.5}$ levels at the MSY site and the continuous chemical characterisation of both fractions through regular sampling and analysis for major and trace components. Including simultaneous measurements and chemical analysis of PM_1 for the first time.
- Introducing continuous measurements of particle number concentrations and size distribution for particles <1 μm, continuous on-line measurements of BC, pollutant gases and PM, and measurements of local meteorology on site not previously measured at the site.
- The identification and quantification of aerosol source contributions, both for mass and particle number concentrations, at the MSY site by source apportionment techniques, which have not been previously investigated.

1.8. Structure of the Thesis

Following this introduction, a methodology section will describe the monitoring station in detail, and outline the instrumentation and experimental techniques employed to reach the aforementioned objectives. The structure of this current work is that of a compilation of scientific articles published in peer-reviewed journals with a basis in atmospheric sciences. Taking this into consideration, the following methodology section will focus more on principles of operation for the instruments employed in order to avoid repetition, as the methodology is also described in each publication. Thus, the main body of results and discussion will comprise of four separate scientific articles. A summary discussion of the main findings in each article, and how the findings relate to each other, will be presented, followed by the main conclusions of this thesis. Finally, a brief section will discuss future research directions and implications of the work presented here.

The main chapters of this thesis are briefly described below:

- The investigation of a long-term time series (9 years) of $PM_{2.5}$ measurements and chemical speciation at a regional background site in the western Mediterranean basin. Trends in $PM_{2.5}$ and chemical components are analysed for statistical significance, and theories are suggested to explain the variance in PM and its chemical components. **Article 1: Cusack, M., Alastuey, A., Pérez, N., Pey, J., Querol, X.: Trends of particulate matter ($PM_{2.5}$) and chemical composition at a regional background site in the Western Mediterranean over the last nine years (2002-2010), Atmospheric Chemistry and Physics, 12, 8341-8357, 2012.**
- The chemical composition of PM_1 measured over a period of 2.5 years is presented in this publication. Source apportionment by PMF is applied to the entire dataset and the main emission sources affecting PM_1 are identified, and the weekly and seasonal trends of the sources are discussed. Subsequently, PCA is performed on the chemical speciation data and particle number concentrations in conjunction with other aerosol parameters such as black carbon, pollutant gases and meteorological variables, in order to identify the sources of particles at MSY. Finally, MLRA is applied to the same dataset in order to quantify the number of particles emitted by each source. **Article 2: Cusack, M., Pérez, N., Pey, J., Alastuey, A., Querol, X.:**

Source apportionment of fine PM and sub-micron particle number concentrations at a regional background site in the western Mediterranean: a 2.5 year study, Atmospheric Chemistry and Physics, in press.

- Article 3 focuses on the variability of sub-micrometer particle number size distributions and concentrations for an 8 month measurement period. Real-time measurements of PM, black carbon, pollutant gases and meteorological variables are included in this study. Particle concentrations and modality are discussed for different scenarios and seasons. **Article 3: Cusack, M., Pérez, N., Pey, J., Wiedensohler, A., Alastuey, A., Querol, X.: Variability of sub-micrometer particle number size distributions and concentrations in the Western Mediterranean regional background, Tellus B, 65, 19243, 2013.**
- Article 4 identifies specific episodes of interest concerning sub-micron particle number size distributions, such as new particle formation in clean and polluted atmospheres, the effect of air mass mixing, and possible particle shrinkage episodes. Thus, favourable atmospheric conditions leading to new particle formation are also identified. **Article 4: Cusack, M., Alastuey, A., Querol, X.: New particle formation and evaporation processes in the Western Mediterranean regional background, Atmospheric Environment, in review.**

Chapter 2: Methodology

2. Methodology

2.1. Monitoring site

In order to characterise atmospheric aerosols in the regional background of the WMB as outlined in the objectives, a monitoring site was established on one of the slopes of Montseny, in the first area of Spain declared as a biosphere reserve by the U.N. The **Montseny** (MSY) monitoring site is situated in the Catalan pre-coastal mountain range at an altitude of 720 m.a.s.l. (Figure 2.1). The mountain range has a Northeast-Southwest orientation running parallel to the Catalan pre-coastal ranges, and is generally sparsely populated and heavily forested. The station is located in *La Castanya* in the Montseny natural park (41º46'N, 2º21'E), approximately 40 km to the North-East of Barcelona city and 25 km from the Mediterranean coastline.

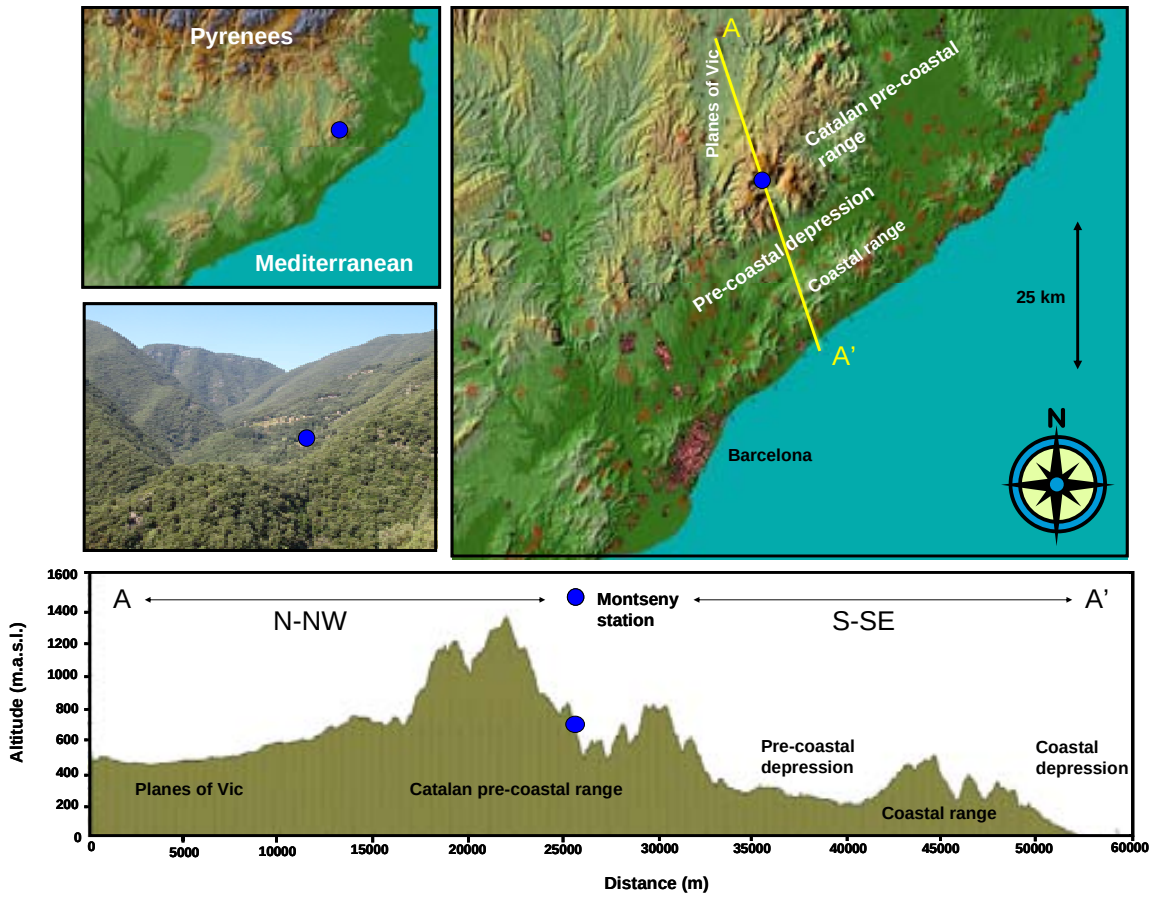

Figure 2.1. Location of the Montseny monitoring site and the topography of the surrounding area. The topography profile corresponds to the yellow line shown in the top-right figure.

The pre-coastal depression running alongside MSY is densely populated and industrialised, and the planes of Vic to the North and the valleys of the Catalan pre-coastal range are areas of intensive agriculture, especially pig farming in the case of the planes of Vic. Plumes of pollution can reach the site as a result of mountain and sea breezes, and mixing layer height development. The mountain and sea breezes are the most important processes affecting the daily variation of atmospheric pollutants for this site. The onshore breeze is activated by heating of the South-Eastern slopes of the mountain range in the morning (Millan et al, 1997; Jorba et al., 2004). Average annual temperatures are 11.4ºC, 75% relative humidity and 722 mm annual precipitation (based on 9 years of data since the establishment of the site). The site has been in operation since 2002, and has been a member of the ACTRIS network (formerly EUSAAR) since 2006. The site is also integrated in the Network of Control and Surveillance of Air Quality of the *Direcció General de Qualitat Ambiental* of *the Conselleria de Medi Ambient* of the *Generalitat de Catalunya*.

Figure 2.2. Climate controlled cabins at the MSY station containing aerosol monitoring equipment.

In spring 2008, the site was expanded extensively and two climate controlled cabins were installed at the site (Figure 2.2), coinciding with the beginning of this thesis. Within one cabin (Cabin 1 in Figure 2.2), continuous real-time measurements of PM_{10}, $PM_{2.5}$ and PM_1 are recorded by means of an optical particle counter (GRIMM 180) with an inlet supported around 0.5 m above the cabin roof. Within the same cabin on a separate sampling inlet continuous real-time measurements of pollutant gases O_3, NO_2, NO, CO, and SO_2 were collected, supplied by the Department of the Environment of the Autonomous Government of Catalonia.

Levels of gaseous pollutants in ambient air were determined by means of conventional principles such as ultraviolet fluorescence for SO_2 (Teledyne M100EU), chemi-luminescence for NO and NO_2 (Thermo 42iTL), ultraviolet photometry for O_3 (MCV 48 AUV) and non-dispersive IR for CO (Teledyne M300E). The second cabin (Cabin 2, behind Cabin 1 in Figure 2.2) contains two high volume samplers with sampling inlets for $PM_{2.5}$ and PM_1 placed above the cabin roof, an SMPS, a MAAP, a Nephelometer, an Aetholometer and a meteorological station. Figure 2.3 displays the inside of Cabin 2, with all the instruments listed above inserted within a supporting rack structure. The SMPS in Figure 2.3 is comprised of the DMA, CPC and voltage supply.

Figure 2.3. Measurement instruments inside Cabin 2.

2.2. Aerosol Monitoring: Instruments and methods

2.2.1. Instrumentation

Both off-line and on-line aerosol sampling techniques have been employed at the MSY site since its establishment in 2002, as shown in the time line of measurements and instrumentation in Figure 2.4.

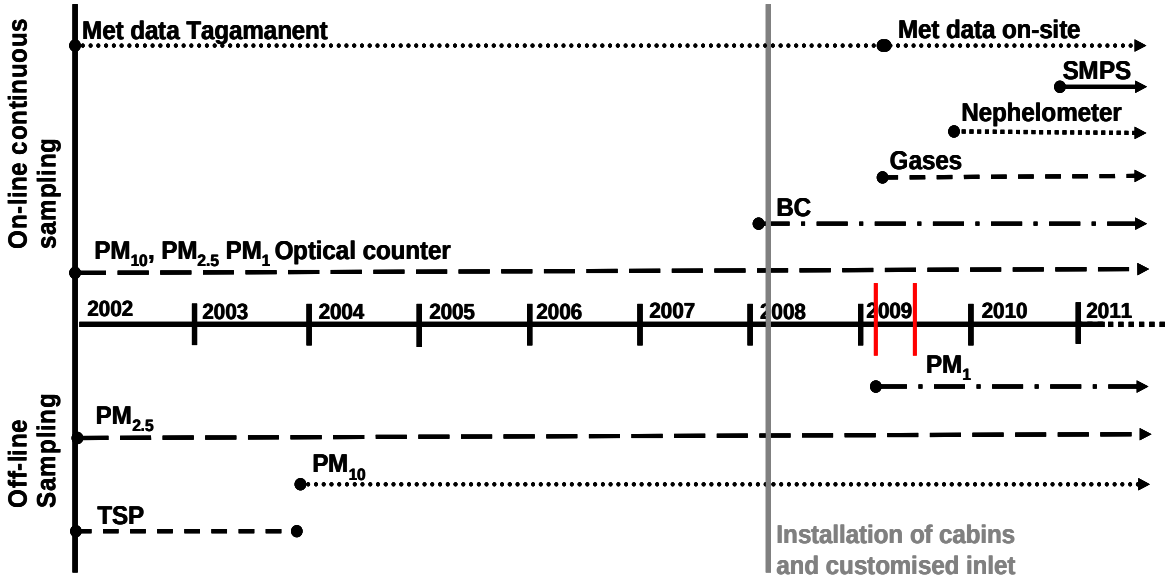

Figure 2.4 Time-line of the development of the MSY aerosol monitoring station since 2002. Red lines indicate when the DAURE winter and summer intensive measurement campaigns took place.

Off-line techniques

High volume sampling of PM

Regular sampling of PM_{10}, $PM_{2.5}$ and PM_1 was performed on site. Samples of TSP were taken until 2004, and eventually replaced by PM_{10} sampling. Thus, PM_{10} and $PM_{2.5}$ were collected for 24 hour periods roughly once a week until 2007, and consecutively every four days from 2008. Sampling of PM_1 commenced in September 2009, and all fractions were sampled simultaneously. Automatic sequential high-volume samplers were employed (DIGITEL-DH80 and MCV-CAV), and equipped with PM_{10}, $PM_{2.5}$ and PM_1 cut off inlets (DIGITEL DPM10/30/00, DIGITEL DPM2.5/30/00 and DPM01/30/00, respectively and PM1025-CAV for MCV instruments), working at 30

m^3 hr^{-1}. Air is sampled through the inlets (Figure 2.5) by means of an in-built pump, through the nozzles of the sampling head. The size of the nozzles will determine the cut-off diameter for the particle size fraction being sampled (PM_{10}, $PM_{2.5}$ and PM_1), whereby particles larger than those under study impact and adhere to a plate daubed with vaseline. The desired particles pass through and are collected on a filter, which is later weighed and analysed. The PM_1 inlet has a 2-stage impactor inlet whereby larger particles (>$PM_{2.5}$) are removed in the first impactor stage and subsequently particles $PM_{1\text{-}2.5}$ are removed in the second stage, hence the larger inlet head (the larger inlet labelled PM_1 as seen in Figure 2.5). In all cases, samples were collected on quartz fibre filters (15 cm diameter) which are previously conditioned in a procedure to be described anon.

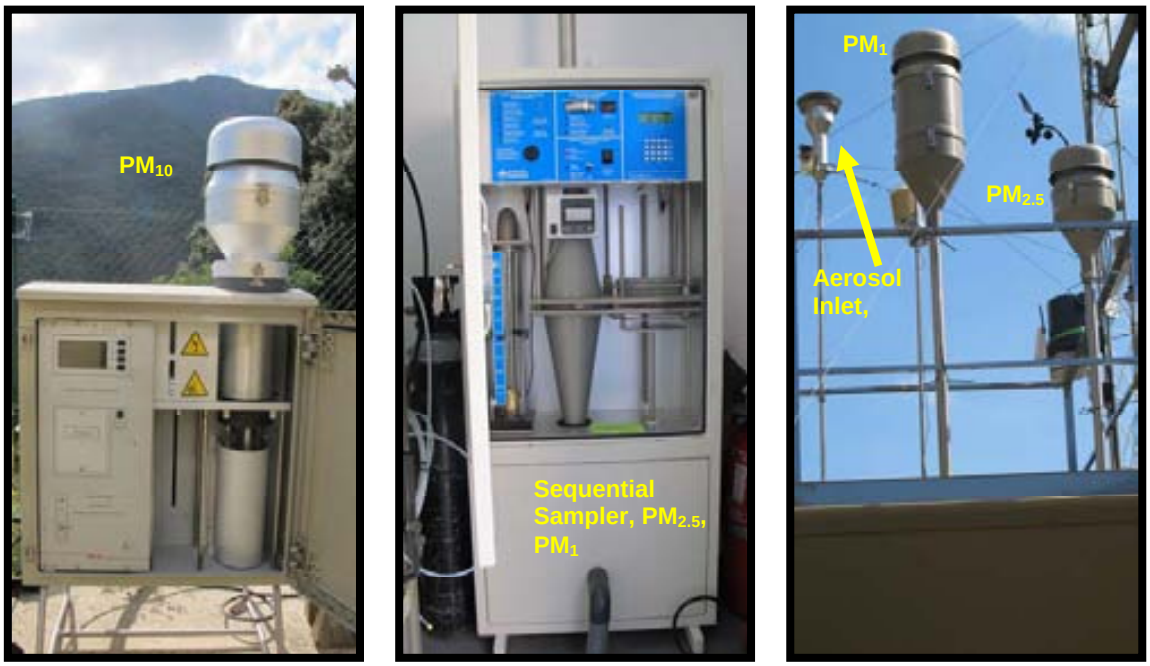

Figure 2.5. High-volume sampler MCV-CAV-A/M-S sequential high volume sampler (left) with an MCV inlet, DIGITEL DH-80 sequential high volume sampler inside the cabin (centre) and PM DIGITEL inlets for PM_1 and $PM_{2.5}$ protruding above the cabin roof (right). The custom designed aerosol inlet (Thermo, PM_{10}) is also shown (right).

On-line Sampling: Inlet design and drying system

Due to the hygroscopic growth of atmospheric aerosol particles at RH well below supersaturation, it is essential to control or limit RH when measuring aerosol optical properties (scattering, absorption) and particle number size distribution (Wiedensohler et al, 2012). In order to obtain comparable data sets for all member stations, as required

by EUSAAR/ACTRIS, the "dry" aerosol and particle number size distribution must be measured. Thus, in accordance with EUSAAR/ACTRIS requirements, the sampled aerosol must be maintained below a relative humidity of 40% at all times. In order to achieve this, a tailor-made inlet system with drying capabilities was designed by IfT and incorporated into the MSY station. The sampling in-let and head (Thermo, PM_{10}) above the cabin roof can be seen in Figure 2.5, and the set-up of the inlet is shown in Figure 2.6.

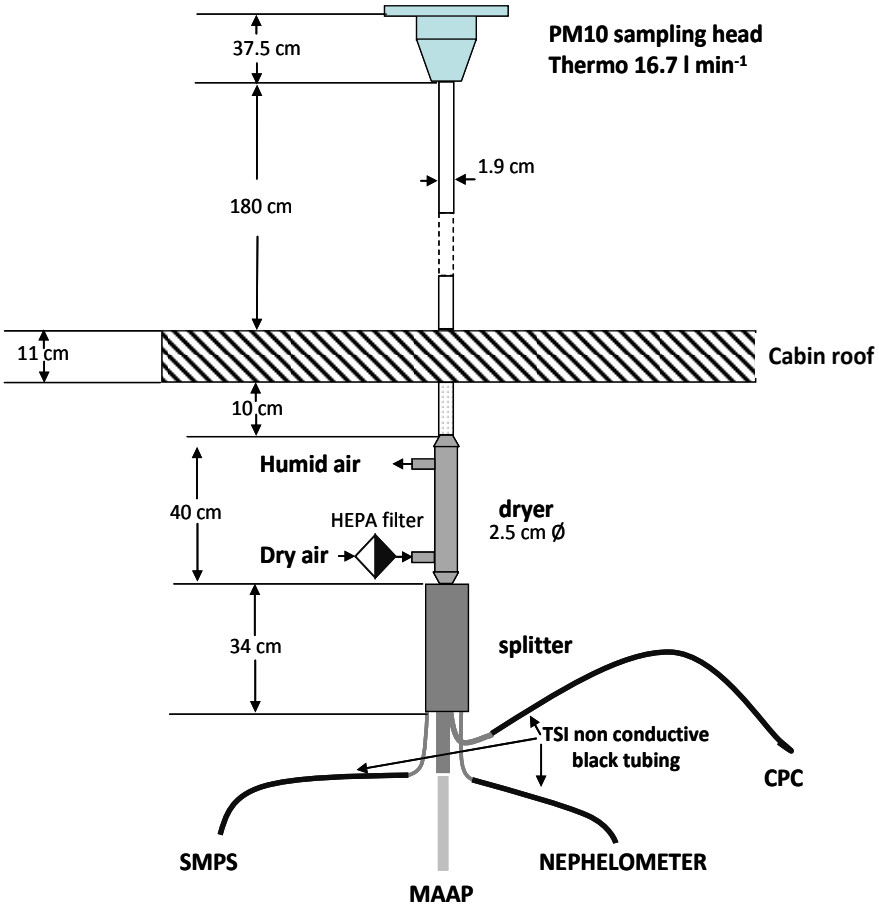

Figure 2.6. Sampling inlet for aerosols at the MSY site.

All components of the inlet are stainless steel except for the sampling inlets to each individual instrument after the splitter, where non-conductive black tubing (TSI) was used. Dry air was produced by passing ambient air through a silica based diffusion dryer and pumping this dried air to a nafion dryer placed in-line with the inlet above the splitter. Dry air enters at the bottom of the dryer and moisture from the sampled air is transferred to the dry air via the nafion dryer. The SMPS, MAAP and nephelometer are all connected to the same sampling line with this inlet, with a cut-off diameter of 10 µm,

placed at about 1.5 m above the roof of the cabin containing the instruments. The inlet flow was 1 m^3 h^{-1} (16.7 l min^{-1}). The Reynolds number for the described inlet was around 1300 (Pandolfi et al., 2012).

Particle number concentration and size distribution

Sub-micrometer particle number size distribution was measured using a mobility particle size spectrometer operated in the scanning mode, referred to as a Scanning Mobility Particle Sizer (SMPS). The SMPS system comprises a Differential Mobility Analyzer (DMA) connected to a Condensation Particle Counter (CPC, Model TSI 3772).

A schematic drawing of the SMPS set up is shown in Figure 2.7. Thus, the principle of operation of the DMA is as such:

1) The movement of electrically charged particles through an electric field will depend on the particle's electrical mobility
2) The electrical mobility of a particle depends on the size of the particle and its electrical charge
3) The smallest particles will have the largest electrical mobility
4) Particles with a large electrical charge will have a large electrical mobility.

Thus, the sampled aerosol enters the system through the sampling inlet, is dried, and is passed to a bipolar charger (neutralizer) which neutralizes the particles. The particles then enter the DMA where the particles are classified according to their electrical mobility, with only particles of a certain mobility (related to their size) exiting the DMA and passing through to the CPC which determines the particle concentration for that size range.

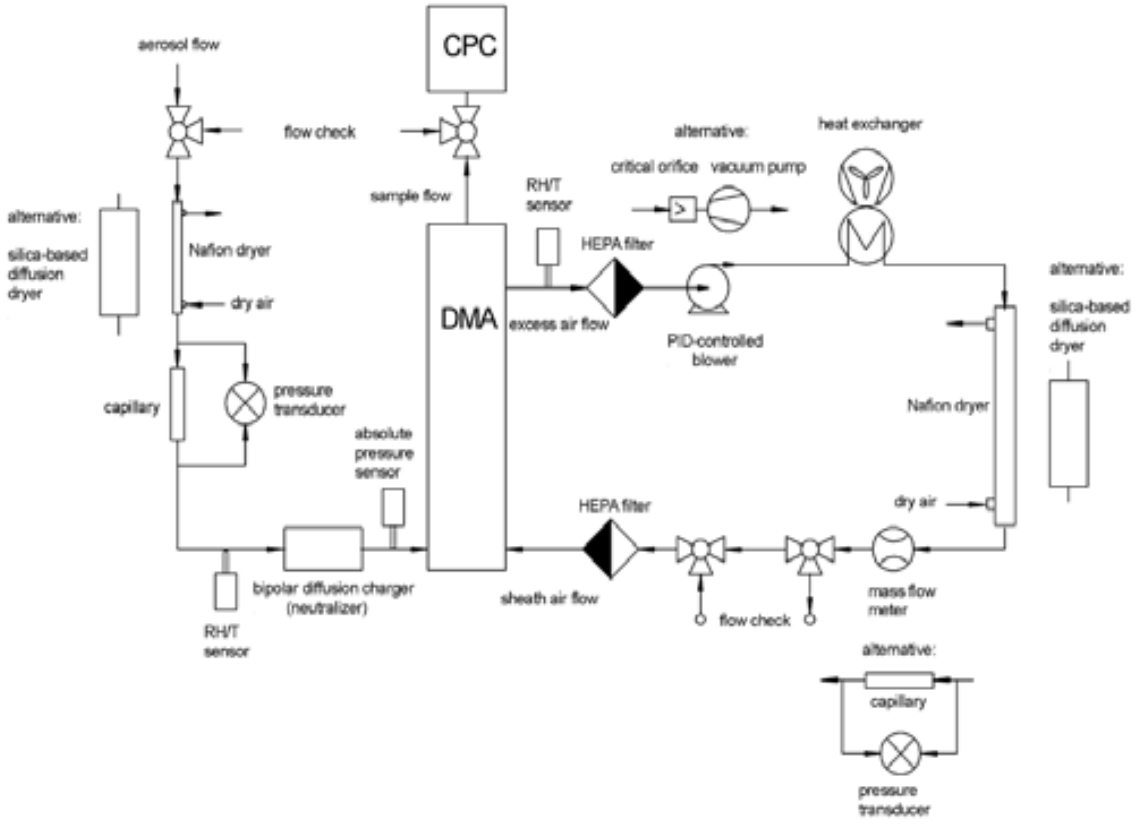

Figure 2.7. Schematic sketch of the SMPS set-up. The set-up includes dryers for aerosol flow and sheath air, heat exchanger, particle filters, as well as sensors for aerosol and sheath air flow rate, relative humidity and temperature of aerosol flow and sheath air, and absolute pressure (Wiedensohler et al. 2012).

The DMA consists of a cylinder with a negatively charged rod in the centre, and the main flow of air through the DMA is particle free sheath air with laminar flow. The sampled air with particles enters the DMA and particles with a positive charge move across the sheath flow towards the negatively charged central rod, at a rate determined by the particle's electrical mobility. Thus, particles of a certain mobility pass through the exit slit, while all other particles are carried away by the sheath flow. The size of particles exiting through the slit to the CPC is determined by the particle size and charge, the central rod voltage and flow within the DMA. By scanning the voltage across the central rod in the DMA, a full particle size distribution is accumulated.

The CPC specifically measures the particle number concentration by optical methods. The principle of operation is the enlargement of small particles (nm in diameter) using a condensation technique to a size that is large enough to be detected optically. This occurs by passing the sampled air with particles through a gaseous medium at 35ºC supersaturated with butanol. The supersaturated sampled air passes to a

condenser which is maintained at 10ºC, causing the condensation of butanol on the particles and in consequence the size of the particles increases. In this way, particles which were initially too small to be measured by optical means can reach diameters of some μm, which are detected by an optical detector. Each particle droplet produces a light pulse and these pulses are counted. Thus, particle number concentrations are expressed as the number of particles per cm^{-3} of air.

The entire SMPS system was designed and manufactured in the framework of the EUSAAR project at the Leibniz Institute for Tropospheric Research (IfT) in Leipzig, Germany. The full specifications for the *IFT-SMPS* are shown in Table 2.1 (Wiedensohler et al., 2012).

Table 2.1. Description of the SMPS system and hardware specifications

IFT-SMPS	Description
Range:	9-825 nm
DMA:	Hauke-type (custom-made); inner diameter 50 mm, outer diameter 67 mm, length 280 mm
Bipolar diffusion charger:	^{85}Kr
CPC:	TSI model 3772
Software:	IFT scanning programme
Sheath air flow:	Closed loop system with blower, heat exchanger, mass flow meter, Nafion dryer, maintained at 5 l min^{-1}
Aerosol flow:	Δp capillary for volumetric flow and Nafion dryer
Sensors:	T, RH in aerosol and sheath air flows, p in aerosol
HV power supply:	Positive

An intercomparison was carried out on the SMPS system in 2010 at the World Calibration Centre for Physical Aerosol Research (WCCAP) at IfT. IfT has designed a calibration programme for aerosol instrument maintenance and comparison and the institute is endorsed by the WMO. The intercomparison found the SMPS at MSY to measure within 10% of the reference mobility size spectrometer for particles 20-200 nm (Wiedensohler et al., 2012). In that same article, it was observed that measurement accuracy for particles <20 nm and >300 nm was less reliable than for particles 20-200 nm, and thus concentrations reported in this work for these size ranges could be more

qualitative in nature rather than quantitative. Furthermore, it is important to note that diffusion loses were not calculated in this work which can affect accurate measurement of ultrafine particles. The SPMS system provided a complete particle number size distribution of the number of particles between 9 and 825nm ($N_{9\text{-}825}$), and completed one scan every five minutes. The aerosol is dried prior to sampling to maintain a relative humidity below 40 % using a nafion dryer, in line with EUSAAR/ACTRIS requirements. Aerosol inlet flow was maintained at 1 l/min and sheath air flow at 5 l/min (which was also dried in a system using a nafion dryer in a closed loop). The dry air is the same dry air used for the drying system described for the sampling inlet.

Continuous SMPS measurements were obtained from October 2010 to June 2011 and again from October 2011 to December 2011. The period with unavailable data resulted from instrument break-down and reparation. Thus, data coverage for the period when the SMPS was operating correctly is 85%.

BC measurements

Real-time monitoring of BC concentrations was continuously obtained every minute from April 2008 until the present by means of a Multi-Angle Absorption Photometer (MAAP). The BC MAAP monitor used (CARUSSO, Thermo ESM Anderson Instrument) monitors the absorption coefficient expressed as the mass concentration of elemental carbon (EC, ng m^{-3}) in ambient air. In the MAAP instrument the optical absorption coefficient of aerosol collected on a filter is determined by radiative transfer considerations which include multiple scattering effects and absorption enhancement due to reflections from the filter. The MAAP uses a complex inversion algorithm that is based on a radiation transport analysis of the aerosol layer and filter matrix system and thus incorporates the scattering effect of the aerosol into the analysis. Thus, the MAAP measures the aerosol absorption coefficients directly and provides the cross-section absorption coefficient at 637 nm. However, it should be noted that even though the manufacturer specifies that the wavelength of the MAAP is 670 nm, the actual wavelength is 637 nm, as described by Müller et al. (2011).

$$BC = \frac{abs.coefficient}{MAC} \quad (1)$$

As shown in equation 1, equivalent BC measurements provided by MAAP are calculated by the instrument software by dividing the measured absorption coefficient σ_{ap} (λ) by 6.6 m^2 g^{-1} which is the mass absorption cross section (MAC) at 637 nm (Müller et al., 2011).

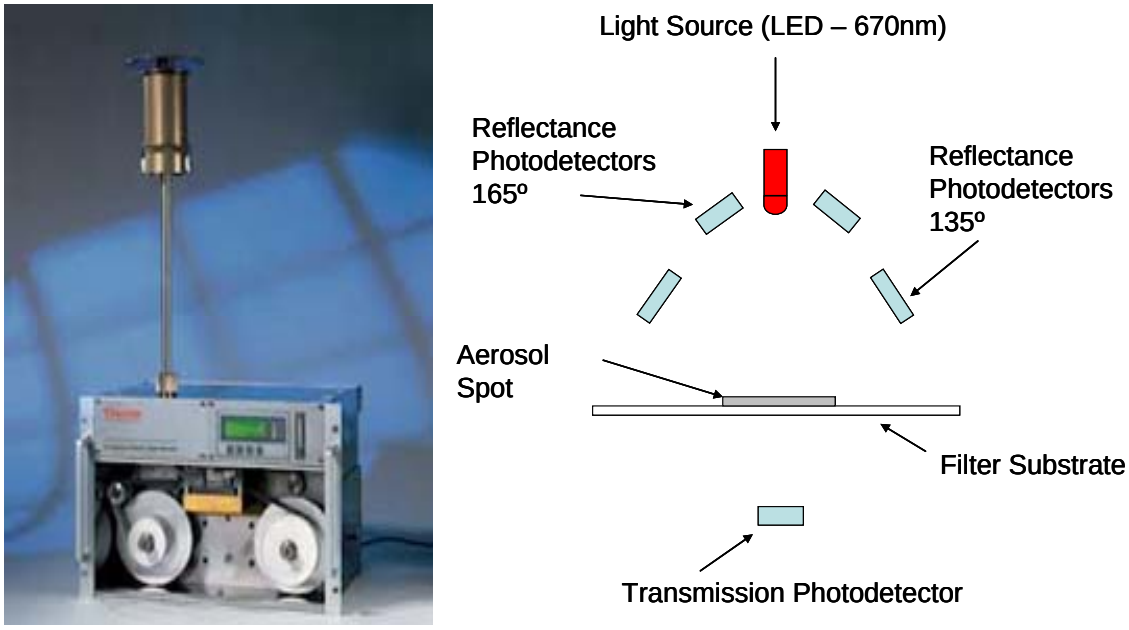

Figure 2.8. MAAP BC monitor (left) and schematic diagram of the MAAP detector block showing the arrangement of the detectors used relative to the sample collected on the filter (Thermo ESM Anderson Instruments).

During the development of this thesis, it was found that MAC may vary depending on the aerosol composition and age, and may differ depending on the area under study. For example, polluted air masses related with both winter and summer regional conditions of stagnation and accumulation over the MSY area were linked with an increase in MAC. Conversely, during clean air episodes such as Atlantic Advection, the MAC was observed to be significantly lower. In accordance with these findings (Pandolfi et al., 2011), the absorption coefficient values measured at MSY provided by the MAAP were converted into BC mass/volume units by dividing by a factor of 10.4 m^2 g^{-1}, which was calculated as the mean MAC for the study area. The detection limit of the MAAP is 100 ng m^{-3} over 2 minute integration. The aerosol flow through the inlet was maintained at 16.7 l min^{-1} and is dried by the drying system described previously.

Real-time measurements of PM concentration levels

Levels of PM_{10}, $PM_{2.5}$ and PM_1 were measured continuously on an hourly basis by means of an optical particle counter (GRIMM Technologies, Inc. model 108). GRIMM dust monitors measure concentration levels of particles of diameter between 0.3 and 15 μm. The operation principle is based on the measurement of particle number. The sampled air flow passes through a laser beam and the light scattered by the particles is detected at a 90º angle by a mirror and transferred to a recipient diode. Then a 15 channel pulse height analyser for size classification detects the scattered signals, and the number of single particle counts registered in each channel is converted to mass in this study using the gravimetric PM_{10}, $PM_{2.5}$ or PM_1 data obtained simultaneously with high volume samplers.

2.2.2. Chemical analysis and speciation

Filter pre-treatment and preparation for chemical analysis

As mentioned previously, gravimetric analysis of PM was performed using high volume samplers equipped with filters upon which PM is collected. Quartz fibre filters manufactured by Schleicher and Schuell, QF20 were used until 2009, after which time filters manufactured by Munktell were employed. The filters were baked in an oven at 200ºC for at least four hours to eliminate volatile impurities. The filters were then conditioned in a climate controlled chamber with temperature of 20º and relative humidity of 25% for 24 hours. The blank filters were then weighed three times on three consecutive days, and subsequently preserved individually in aluminium foil until they were used for sampling. For every set of 9 filters, 3 were retained for blank analysis in the subsequent chemical analysis.

After sampling in the high-volume samplers, the filters were conditioned once again in the same climate controlled chamber at the same conditions mentioned above for 24 hours. The filters were then weighed twice on two consecutive days in order to obtain a definitive weight. The difference in weight between the blank and sampled filter corresponds to the total mass of PM, and the ambient concentration is calculated from the volume of air sampled.

Following weighing of the filters, they were then processed for chemical analysis according to the procedure outlined by Querol et al. (2001). One half of each filter was acid digested (2.5 ml HNO_3 and 5 ml HF) into a closed PFA vesicle at 90ºC for at least 8 hours. After cooling, the PFA vessels were opened and 2.5 ml $HClO_4$ was added. The acids were then completely evaporated by placing the PFA vessels on a heating plate at 230ºC. The remaining dry residue was dissolved with 2.5 ml HNO_3, diluted with distilled water (MilliQ) to 50 ml, obtaining a solution of 5% HNO_3. This solution was then analysed for major elements (Al, Fe, K, Ca, Na, Mg, S, P, Ba, Cr, Cu, Mn, Ni, Sr, Pb, Ti, V, Zn) by ICP-AES (IRIS Advantage TJA Solutions THERMO). Minor elements (Li, Be, Sc, Ti, V, Cr, Mn, Co, Ni, Cu, Zn, Ga, Ge, As, Se, Rb, Sr, Y, Zr, Nb, Mo, Cd, Sn, Sb, Cs, Ba, La, Ce, Pr, Nd, Sm, Eu, Gd, Tb, Dy, Ho, Er, Tm, Yb, Lu, Hf, Ta, W, Tl, Pb, Bi, Th, U) were analysed by ICP-MS (X Series II THERMO).

For every batch of samples acid digested, corresponding blank filters were digested using the exact same procedure. Blank filter analysis is necessary in order to quantify the elements present in the blank filters and subtract those concentrations present from those attributed to the PM chemical components on the sampled filters. In addition, detection limits of the analysis techniques are calculated from the standard deviations from the blank filter analyses alongside the analytical uncertainties. A control was also used to help identify possible analytical or calibration errors. 10 mg of a reference material (NBS1663b, fly ash) was also digested alongside each set with half a blank filter.

Another quarter of each filter was leached in water to dissolve water soluble ions, and this leachate was then analysed by ion chromatography (nitrate, sulphate and chloride) and ammonium was analysed by ion specific electrode (Electrode MODEL 710 A+, THERMO Orion). The filter segment was put in a PVC vessel with 30 ml of distilled water, placed in an ultrasound bath for ten minutes and then heated at 60ºC for 6 hours. The resulting solution is then filtered and analysed by ion chromatography (High Performance Liquid Chromatography; WATERS IC-pakTM anion column and WATERS 432 conductivity detector).

The remaining quarter of each filter is then analysed for elemental and organic carbon by a thermal-optical technique (Birch and Cary, 1996) using a Sunset Laboratory OCEC Analyser with the EUSAAR2 temperature programme.

Some indirect determinations of components were also applied using empirically obtained factors (Dulac et al., 1992; Molinaroni et al., 1993; Querol et al., 2001) such as

SiO_2 = Al_2O_3 * 3 and CO_3^{2-} = Ca * 1.5. To calculate the organic matter (OM) component, OC is multiplied by a factor. According to Turpin and Lim (2001), a conversion factor of 1.6±0.2 is suitable for urban areas, whereas 1.9-2.3 was more suitable for aged aerosols and 2.2-2.6 for aerosols originating from biomass burning. Based on these results and considering the regional background status of MSY i.e. relatively ages aerosols with some influence of biomass burning emissions, a multiplier of 2.1 was applied.

All the procedures outlined, from sampling (uncertainty in the volume of air sampled) to digestion, analysis and blank filter subtraction, among others, involve some amount of uncertainty. Therefore, Amato (2010) developed an equation for calculating uncertainty, determined experimentally using a similar methodology to that described by Thompson & Howarth (1976). In order to include all sources of uncertainty, the overall uncertainty is represented by the following formula:

$$\sigma_{ij}^2 = \sqrt{\frac{\sigma_A^2}{V_i^2} + \left(\beta . x_{ij}\right)^2} \tag{2}$$

where σ_A is the analytical determination uncertainty, V_i is the air volume sampled, β is a coefficient estimated to be 0.15 which might account for the error in the flow rate and other additional sources of uncertainty, and x_{ij} is the concentration value of a species or compound for each sample.

The detection limit (DL) is widely accepted as a measure of the inherent detection capability of an instrument to measure the minimum analyte signal, amount or concentration. DL, along with uncertainty calculations, is required for source apportionment studies (specifically Positive Matrix Factorisation). The following formula, devised by Amato (2010), consists of propagating the estimates of the two uncertainties associated with the instruments employed for analysis (ICP-MS, ICP-AES, HPLC, Sunset, ion specific electrode) and the blank subtraction (IUPAC, 1995).

$$DL_j = \frac{\sqrt{\sigma_{0\,j}^2 + \sigma_{BLK\,j}^2}}{V} \tag{3}$$

where $\sigma^2_{o\,j}$ is the analytical error and $\sigma^2_{BLK\,j}$ is the standard deviation of the blank filters that were analysed with the samples. DL and σ^2_{ij} are for the j^{th} analyte are shown in Table 2.2.

Table 2.2. Estimate of Detection Limit and uncertainty for PM components.

	DL (µg m^{-3})	σ_{BLKj} (µg/filter)		DL (µg m^{-3})	σ_{BLKj} (µg/filter)
OC	0.17154	123.10	**Rb**	0.00002	0.0145
EC	0.02092	15.402	**Sr**	0.00037	0.2651
Al	0.09780	70.119	**Cd**	0.00002	0.0168
Ca	0.03458	24.791	**Sn**	0.00009	0.0619
K	0.04834	34.660	**Sb**	0.00011	0.0765
Na	0.01786	12.731	**Pb**	0.00012	0.0885
Mg	0.01487	10.662	**Li**	0.00002	0.0129
Fe	0.01297	9.302	**Se**	0.00003	0.0239
Mn	0.00079	0.5557	**La**	0.00008	0.0547
Ti	0.00113	0.8052	**Ba**	0.00282	2.0250
P	0.01386	9.9363	**Zr**	0.00333	2.3879
V	0.00005	0.0376	**Hf**	0.00017	0.1151
Cr	0.00074	0.5278	**SO_4^{2-}**	0.14808	-
Ni	0.00151	1.0859	**NO_3^-**	0.02483	-
Cu	0.00032	0.2261	**Cl**	0.44648	371.60
Zn	0.00298	2.1370	**NH_4^+**	0.03801	27.639
As	0.00004	0.0285			

2.3. Source apportionment techniques

Following complete chemical characterisation of PM and the compilation of a range of other aerosol parameters in the study area, receptor modelling can be applied to a dataset in order to determine and quantify the sources of aerosols.

Principal Component Analysis and Multi-Linear Regression Analysis (PCA-MLRA)

Principal component analysis (PCA) identifies possible correlation between a number of different variables, in this case PM chemical components, particle number concentration in different size ranges, pollutant gases or meteorological variables, and the principal components that explain the variance in the data are interpreted as possible sources. Through the combination of the data, a number of principal factors may be obtained, and these factors are the result of linear combinations of all the parameters considered (Thurston & Spengler, 2005).

A matrix is compiled containing all the different variables to be included in the analysis for each day of PM sampling (thus, other parameters will be averaged over 24

hours), and a number of factors are obtained. These factors are the result of the lineal combinations of all the parameters considered. In order to maximise the distance between factors, an orthogonal transformation is applied (Varimax normalised), forming the component matrix. In principal, each of the factors corresponds to a source of aerosols, presenting the components that characterise a source with highest coefficients, or factor loadings, to a maximum of 1. The maximum number of factors will not be greater than the total number of components or variables, but not all the factors given will have a physical meaning (Pey et al., 2009b).

The number of factors is determined by the variance of the original components, which will all have a variance of 1 after they have been normalised. The first step for determining the suitable number of factors is by the factor's variance (eigenvalue) which must be higher than 1 (Andrade et al., 1994). Once this criterion has been met, the physical significance of each factor must be determined from their chemical profile. Thus, knowledge of the possible emission sources is necessary in order to identify the likelihood of a source. The accumulated variance of all the factors must also be higher than 75% before the analysis can be considered really representative. Following these steps, the factors should be identified, as well as the components that characterise them, the variance value and the mean concentration that explains each factor.

After extracting the factors described above, it is possible to quantitatively estimate the daily contribution of each factor to the number of particles by applying a Multi-Linear Regression Analysis (MLRA), as described previously by Thurston & Spengler (2005). This method uses the scores obtained from the daily number concentrations, and these factors will be proportional to the daily number concentration of each source. The concentration values are then normalised, therefore normalising the scores, and they now equate to average concentration values. This requires that the score for a zero concentration must be calculated and this score must be subtracted from the daily scores, giving the absolute scores. Using these absolute scores for each daily sample and the particle number concentration in specific size ranges corresponding to each sample, multilinear regression is applied to the matrix, giving the coefficients for transforming the absolute daily scores to the contribution of each source to the particle number concentration. In the same way that the daily contribution of each source to the total particle number concentration was estimated, it is possible, also by multilinear regression, to determine the contribution of each source to the individual particle number size ranges ($N_{9\text{-}20,}$ $N_{20\text{-}50}$, $N_{50\text{-}100}$ etc.) taking the daily concentration in each size

range as the dependent variable and the daily contribution of each source to the particle number concentration as the independent variable. This procedure has been performed by Pey et al. (2009b).

Positive Matrix Factorisation (PMF)

Positive matrix factorisation (PMF) is a widely applied receptor model based on a weighted least squares fit (Paatero, 1997; Paatero and Tapper, 1994). PMF is used for the identification and quantification of sources of atmospheric particulate matter. PMF provides estimates of the chemical composition of PM associated with different sources and the mass contribution of PM attributed to each source. In this study, EPA PMF v3.0 (Norris et al., 2008) was employed.

PMF is a multivariate factor analysis tool that decomposes a matrix of speciated sample data into two matrices – factor contributions and factor profiles – which then need to be interpreted by an analyst as to what types of source types are represented using measured source profile information, wind direction analysis and emission inventories (Norris et al., 2008). A speciated data set can be viewed as a data matrix X of *i* by *j* dimensions, in which *i* number of samples and *j* chemical species were measured. The goal of multivariate receptor modelling, for example with PMF, is to identify a number of factors *p*, the specific profile *f* of each source, and the amount of mass *g* contributed by each factor to each individual sample (Equation 3):

$$x_{ij} = \sum_{k=1}^{p} g_{ik} f_{kj} + e_{ij} \quad (4)$$

where e_{ij} is the residual for each sample/species.

Results are constrained so that no sample can have a negative source contribution. PMF allows each data point to be individually weighed. This feature allows the analyst to adjust the influence of each data point, depending on the confidence in the measurement. For example, data below detection can be retained for use in this model, with the associated uncertainty adjusted so these data points have less influence on the solution than measurements above the detection limit (Norris et al., 2008). The PMF solution minimises the object function *Q* (Equation 4), based upon these uncertainties (*u*):

$$Q = \sum_{i=1}^{n} \sum_{j=1}^{m} \left[\frac{x_{ij} - \sum_{k=1}^{p} g_{ik} f_{kj}}{u_{ij}} \right]^2 \quad (5)$$

Variability in the PMF solution can be estimated using a bootstrapping technique, which is a re-sampling method in which "new" data sets are generated that are consistent with the original data. Each data set is decomposed into profile and contribution matrices, and the resulting profile and contribution matrices are compared with the base run. Instead of inspecting point estimates, this method allows the analyst to review the distribution for each species to evaluate the stability of the solution.

The uncertainties were calculated as outlined previously (Amato, 2010).

2.4. Additional analyses

Trend analysis: Mann-Kendall test

The Mann-Kendall test can be applied to analyse temporal trends of PM and chemical composition. The MAKESENS template application (Mann-Kendall test for trend and Sen's slope estimates, Salmi et al., 2002) consists of the nonparametric Mann-Kendall test for the calculation of the trend and the nonparametric Sen's method for determining the magnitude of the trend. The method was originally developed for the detection and estimation of trends in the time series of annual values of parameters such as atmospheric concentrations and precipitation.

MAKESENS performs two types of statistical analysis. The presence of a monotonic increasing or decreasing trend is tested with the nonparametric Mann-Kendall test and the slope of the linear trend is estimated with the nonparametric Sen's method (Gilbert, 1987). The Mann-Kendall test is only applicable to the detection of a monotonic trend of a time series with no seasonal or other cycle, and therefore the method is usually applied to mean annual concentrations. However, it can be applied to data with a marked seasonal cycles by comparing the same month or season throughout the different years of analysis. In the Sen's method, it is assumed that the trend is linear and the residuals are from the same distribution with zero mean. The time series should

fulfil these presumptions in order to produce correct statistical results with MAKESENS.

Calculation of the Condensation Sink (CS)

The aerosol condensation sink determines how rapidly molecules will condense onto pre-existing aerosols and depends strongly on the shape of the size distribution (Pirjola et al., 1999). CS in this study has been calculated according to the method described by Kulmala et al. (2001). The condensation sink is obtained by integrating over the aerosol size distribution:

$$CS = 2\pi D\int_0^\infty dp\beta_M(d_p)n(d_p)dd_p = 2\pi D\sum_i \beta_M d_{p,i}N_i \qquad (6)$$

Here D is the diffusion coefficient, d_p is particule radius, β_M is the transitional correction factor for the mass flux, $n(d_p)$is the particle size distribution function and N_i is the concentration or particles in the size section i. CS is reported as s^{-1}.

Chapter 3: Results

Article 1

Cusack, M., Alastuey, A., Pérez, N., Pey, J., Querol, X.

Trends of particulate matter ($PM_{2.5}$) and chemical composition at a regional background site in the Western Mediterranean over the last nine years (2002-2010).

Atmospheric Chemistry and Physics, 12, 8341-8357, 2012

Pages: 83-99
Published in: September 2012
Impact factor of Journal: 5.52

Atmos. Chem. Phys., 12, 8341–8357, 2012
www.atmos-chem-phys.net/12/8341/2012/
doi:10.5194/acp-12-8341-2012

Atmospheric Chemistry and Physics

Trends of particulate matter ($PM_{2.5}$) and chemical composition at a regional background site in the Western Mediterranean over the last nine years (2002–2010)

M. Cusack[1,2], **A. Alastuey**[1], **N. Pérez**[1], **J. Pey**[1], **and X. Querol**[1]

[1]Institute of Environmental Assessment and Water Research, IDÆA, CSIC, C/Jordi Girona, 18–26, 08034, Barcelona, Spain
[2]Institute of Environmental Science and Technology (ICTA), Universitat Autónoma de Barcelona, 08193, Bellaterra, Barcelona, Spain

Correspondence to: M. Cusack (michael.cusack@idaea.csic.es)

Received: 13 March 2012 – Published in Atmos. Chem. Phys. Discuss.: 27 April 2012
Revised: 30 August 2012 – Accepted: 3 September 2012 – Published: 17 September 2012

Abstract. The time variability and long term trends of $PM_{2.5}$ (particulate matter of diameter $< 2.5\,\mu m$) at various regional background (RB) sites across Europe are studied and interpreted in this work. Data on mean annual levels of $PM_{2.5}$ measured at Montseny (MSY, North East Spain) and various RB sites in Spain and Europe are evaluated and compared, and subsequently analysed for statistically significant trends. The MSY site registered higher average $PM_{2.5}$ levels than those measured at a selection of other RB sites across Spain, Portugal, Germany and Scandinavia by percentage compared to the mean of all the stations in these countries, but lower than those measured in Switzerland, Italy and Austria.

Reductions in $PM_{2.5}$ were observed across all stations in Spain and Europe to varying degrees (7–49 %). MSY underwent a statistically significant reduction since measurements began, indicating a year-on-year gradual decrease ($-3.7\,\mu g\,m^{-3}$, calculated from the final year of data compared to the mean). Similar trends were observed in other RB sites across Spain ($-1.9\,\mu g\,m^{-3}$). Reductions recorded in $PM_{2.5}$ across Europe were varied, with many experiencing gradual, year-on-year decreases ($-1.8\,\mu g\,m^{-3}$). These reductions have been attributed to various causes: the introduction and implementation of pollution abatement strategies in EU member states, the effect of the current economic crisis on emissions of $PM_{2.5}$ and the influence of meteorology observed during the winters of 2009 and 2010. In addition, the North Atlantic Oscillation (NAO), a large scale meteorological phenomenon most prevalent during winter, was observed to influence the frequency of Saharan dust intrusions across the Iberian Peninsula.

Chemical composition of $PM_{2.5}$ at MSY is characterised by high levels of organic matter (OM) and sulphate, followed by crustal material, nitrate and ammonia. Sea Spray and elemental carbon (EC) comprised a minor part of the total $PM_{2.5}$ mass. Statistical trend analysis was performed on the various chemical components of $PM_{2.5}$ recorded at MSY to determine which components were accountable for the decrease in $PM_{2.5}$ concentration. It is shown that OM underwent the largest decrease over the time period with a statistically significant trend ($-1.3\,\mu g\,m^{-3}$ compared to the mean), followed by sulphate ($-0.8\,\mu g\,m^{-3}$), ammonium ($-0.5\,\mu g\,m^{-3}$) and nitrate ($-0.4\,\mu g\,m^{-3}$). Conversely, sea spray, EC and crustal material reductions were found to be negligible.

1 Introduction

One of the greatest challenges facing the global environment is the presence of tropospheric aerosols, both natural and anthropogenic, and their impact on health (Pope and Dockery, 2006), the Earth's climate (IPCC, 2007), visibility, ecosystems and building materials. For these reasons, emissions and ambient levels of atmospheric pollutants are currently regulated through various EC directives. The directive 2008/50/EC establishes limit and target values (annual average of $25\,\mu g\,m^{-3}$) for ambient air $PM_{2.5}$ in all member states of the European Union (EU). Although the target values for

$PM_{2.5}$ did not come into force until 2010 (with limit values being enforced in 2015), levels of $PM_{2.5}$ have been decreasing throughout Europe for a number of years, as outlined in this paper. Thus, it can be reasonably assumed that this Europe-wide reduction is a result of the implementation of emission abatement strategies enforced within the EU and the introduction of the Integrated Pollution Prevention and Control (IPPC) directive. The abatement strategies, until recently, have mostly focused on gaseous emissions and PM_{10}, but cleaner industrial practices and reduced traffic emissions would inevitably have a subsidiary reducing effect on other major pollutants, $PM_{2.5}$ included. Previous studies have observed a decreasing trend for $PM_{2.5}$ for many countries in Europe, as outlined in the EMEP report 4/2011 (Tsyro et al., 2011). In fact, the findings in the report show that almost all countries in Western Europe with long term $PM_{2.5}$ measurements have undergone varying degrees of reduction since 2000 (ranging from 7 to 49 %). Furthermore, a recent article has described PM variability in Europe, and highlighted how PM_{10} and $PM_{2.5}$ have decreased considerably over the past decade, and that the observed reduction was not solely due to meteorological factors (Barmpadimos et al., 2012).

Other factors appear to have had some influence on PM concentrations observed over the past decade. Since mid-2008, Europe and much of the developed world has been in the grips of a severe economic recession which, at the time of writing this article, appears to show no sign of abating. Indeed, this economic crisis has been most severely felt in the peripheral economic states of Europe such as Spain and Portugal, and Europe's fourth largest economy, Italy. A study performed by Arruti et al. (2011) has observed a direct link between levels of industrial trace elements and some economic indicators in northern Spain from 2008–2009. However, the study did not discover any direct relationship between the economic downturn and ambient PM levels. Anthropogenic activities have long been associated with air pollution, through fuel oil combustion, industrial activities, traffic emissions and construction, to name a few. The economic recession has severely impacted these activities, and the possible resulting effect is a net reduction in pollution.

Finally, unusual meteorology has possibly played a significant role in the changes in PM observed in the last two years. Millán et al. (1997), Soriano et al. (2001), Gangoiti et al. (2001), Rodríguez et al. (2002 and 2003), Jorba et al. (2004) and Pérez et al. (2004), among others, have all described the relationship between air quality in the Western Mediterranean Basin (WMB) and the effect of mesoscale and local meteorological processes. However, meteorology on a much larger scale also plays an important role on influencing annual PM levels. In the northern hemisphere, one of the most consistent and prominent large-scale patterns of atmospheric variability during the winter months is the North Atlantic Oscillation (NAO). Fluctuations between positive and negative phases of NAO (calculated from the pressure differences between the Icelandic low pressure and Azores high pressure systems) can produce large changes in wind speed, temperature and precipitation across Europe (Hurrell et al., 2003). The winters of 2009 and 2010 were characterised by intensely negative NAO index (NAOi) and extreme cold spells for much of Northern Europe. Vicente-Serrano et al. (2011) linked the intense negative phase of NAO to the extreme rainfall recorded in the Iberian Peninsula for the same period; higher precipitation would undoubtedly affect the levels of PM on a regional scale. Further studies have shown the effect of NAO on the transport of North African Dust (Moulin et al., 1997). The influence of North African dust outbreaks on PM in NE Spain is very significant (Querol et al., 1998a, b); the inhibition of Saharan dust reaching NE Spain would have an overall reducing effect on total PM levels.

The Montseny (MSY) monitoring station forms an important part of a Europe-wide measurement network EUSAAR (European Supersites for Atmospheric Aerosol Research), which aims to integrate and homogenise the monitoring of similar atmospheric aerosol properties performed by 21 stations across Europe. The MSY station provides important information on regional background (RB) aerosols in the Western Mediterranean Basin (WMB). The Spanish coastline, especially in the NE towards the border with France, is densely populated and highly industrialised. Measurements of aerosols performed at RB sites such as MSY, relatively distant from the influence of specific emissions sources, provide more accurate data on long-term trends of aerosols. A number of studies have outlined the variability of PM at MSY and the complex atmospheric dynamics that occur there (Querol et al., 2009; Pérez et al., 2008; Pey et al., 2010). The variability of levels of PM and chemical composition from 2002–2007 at MSY has also been well documented by Pey et al. (2009). This present work investigates the trends observed through the extension of the data time series (2002–2010), allowing for greater insight into the inter-annual PM trends occurring. The $PM_{2.5}$ trends for many stations across Europe, and to a greater extent Spain, are analysed and compared to those of MSY. These trends are analysed for statistical significance, in order to determine if the decreases observed are gradual and uniform. Special focus is then given to the in-depth investigation into the temporal trends observed, not only for $PM_{2.5}$, but also to the various chemical components of $PM_{2.5}$ at MSY.

2 Methodology

Table 1 lists the various stations (and corresponding countries) used in this study for comparison of $PM_{2.5}$ levels. The Montseny station (MSY) is located in the Montseny natural park 40 km to the NNE of the Barcelona urban area, and 25 km from the Mediterranean coast. The station is located on the upper walls of a valley extending perpendicularly from the Catalan Pre-Coastal ranges, in a densely forested area

Table 1. Location of the various monitoring sites, their respective altitude (meters above sea level), $PM_{2.5}$ concentration for corresponding first year and last year of measurements, average $PM_{2.5}$ ($\mu g\,m^{-3}$) and standard deviation (EMEP stations in bold).

Country	Site	Latitude	Longtitude	m a.s.l.	Period (years)	$PM_{2.5}$ (First Year)	$PM_{2.5}$ (Last Year)	$PM_{2.5}$ Mean ± Stan. Dev
Spain	**Montseny**[1]	41°46′ N	02°21′ E	720	2002–2010	14.0	8.9	12.6 ± 2.2
	Cabo de Creus[2]	42°19′ N	00°05′ E	23	2002–2010	12.9	7.9	10.8 ± 2.7
	Els Torms[2]	41°23′ N	00°43′ E	470	2002–2010	10.0	7.3	10.2 ± 2.1
	Zarra[2]	39°05′ N	01°06′ W	885	2002–2010	8.2	5.5	7.4 ± 1.2
	Viznar[2]	37°14′ N	03°28′ W	1265	2002–2010	10.3	9.2	10.1 ± 0.7
	Barcarrota[2]	38°28′ N	06°55′ W	393	2002–2010	12.5	7.6	8.8 ± 2.0
	O Saviñao[2]	42°28′ N	07°42′ W	506	2002–2010	9.4	6.2	8.1 ± 1.4
	Niembro[2]	43°26′ N	04°50′ W	134	2002–2010	10.1	9.2	9.8 ± 1.0
	Campisábalos[2]	41°16′ N	03°08′ W	1360	2002–2010	7.0	5.7	6.9 ± 0.9
	Peñausende[2]	41°17′ N	05°52′ W	985	2002–2010	8.0	4.9	6.9 ± 1.3
	Risco Llano[2]	39°31′ N	04°21′ W	1241	2002–2010	6.7	5.9	7.1 ± 1.0
Austria	**Illmitz**[2]	47°46′ N	16°45′ E	117	2002–2010	23.3	19.0	19.7 ± 3.2
Italy	**Ispra**[2]	45°48′ N	08°38′ E	209	2002–2009	29.4	19.2	26.2 ± 4.2
Switzerland	**Payerne**[2]	46°48′ N	06°56′ E	489	2002–2010	15.9	10.6	14.5 ± 3.0
Germany	Pfälzerwald-Hortenkopf[3]	49°16′ N	07°49′ E	606	2003–2009	12.6	9.0	9.7 ± 1.5
	Schwartenberg[3]	50°39′ N	13°27′ E	785	2002–2009	10.5	8.7	9.5 ± 2.0
	Schauinsland[2]	47°54′ N	07°54′ E	1205	2002–2009	10.2	6.9	7.2 ± 1.7
	Waldhof[2]	52°48′ N	10°45′ E	74	2003–2009	16.5	11.8	13.5 ± 2.3
Finland	Virolahti[3]	60°31′ N	27°40′ E	4	2004–2009	7.5	5.5	6.6 ± 1.1
	Utö[3]	59°46′ N	21°22′ E	7	2004–2009	6.7	5.3	5.9 ± 0.7
	Hyytiälä[1]	61°51′ N	24°17′ E	181	2002–2009	7.5	3.8	5.5 ± 1.3
Sweden	**Vavihill**[2]	56°01′ N	13°08′ E	163	2002–2010	10.5	7.2	9.9 ± 2.2
	Aspvreten[2]	58°48′ N	17°22′ E	25	2002–2010	8.9	5.7	7.5 ± 1.3
Norway	**Birkenes**[2]	58°23′ N	08°15′ E	190	2002–2010	6.0	3.4	4.3 ± 1.1
Portugal	Fundão[3]	40°08′ N	07°10′ W	473	2005–2010	9.9	6.9	8.3 ± 1.8
	Chamusca[3]	39°12′ N	08°16′ W	43	2003–2010	10.3	9.1	10.8 ± 2.1
	Lamas de Olo[3]	41°22′ N	07°47′ W	1086	2004–2010	11.0	3.6	9.0 ± 4.1
	Ervedeira[3]	40°35′ N	08°40′ W	32	2006–2010	13.9	11.9	10 ± 2.8

[1] This study; [2] EMEP; [3] Airbase, the European Air Quality Database (http://acm.eionet.europa.eu/databases/airbase/).

known as La Castanya. The station is situated relatively far from urban and industrial zones, but the region is generally densely populated and heavily industrialised, and local anthropogenic emissions can affect this site under specific meteorological conditions. Atmospheric dynamics and aerosol variability at MSY has been described in detail by Pérez at al. (2008).

Samples of $PM_{2.5}$ were collected on quartz fibre filters (Schleicher and Schuell, QF20 until 2009, Munktell thereafter) for 24 h periods roughly once a week until 2007, and consecutively every four days from 2008, with high volume samplers ($30\,m^3\,h^{-1}$) DIGITEL-DH80 and MCV-CAV, equipped with a $PM_{2.5}$ cut off inlet (manufactured by DIGITEL). Filters were treated prior to sampling by pre-heating at 200°C for 4 h, conditioned at 20–25 °C and 25–30 % relative humidity for at least 24 h, and weighed three times on three consecutive days. Sampling began in March 2002 and 403 samples of $PM_{2.5}$ were taken and chemically analysed from 22 March 2002 to 31 December 2010. PM mass concentrations were determined by standard gravimetric procedures (see Querol et al., 2001).

Filters were analysed using different instrumental techniques to determine concentrations of a range of elements and components, as described by Querol et al. (2008). After weighing, 1/2 of each filter was acid digested ($HF:HNO_3:HClO_4$) for the determination of major and trace elements. Major component (Al, Ca, Na, Mg, Fe, K) concentrations were determined by Inductively Coupled Plasma Atomic Emission Spectroscopy, ICP-AES (IRIS Advantage TJA solutions, THERMO). Trace element concentrations were determined by means of Inductively Coupled Plasma Mass Spectroscopy, ICP-MS (X Series II,

THERMO). Water soluble ions SO_4^{2-}, NO_3^-, NH_4^+ and Cl^- were determined from water leachates from 1/4 of the filter and analysed by Ion Chromatography HPLC (High Performance Liquid Chromatography) using a WATERS ICpakTM anion column and WATERS 432 conductivity detector. NH_4^+ was determined by an ion specific electrode. The remaining 1/4 of each filter was used for the elemental analysis of Organic and Elemental Carbon (OC and EC) by a thermal-optical transmission technique using a Sunset Laboratory OCEC Analyser. Organic Matter (OM) is calculated from OC by multiplying by a factor of 2.1 as suggested by Turpin et al. (2001) and Aiken et al. (2005). SiO_2 and CO_3^{2-} were indirectly determined from empirical formulas (Querol et al., 2001). These combined procedures allowed for the determination of concentrations of major components (OC, EC, SiO_2, CO_2^{3-}, Al, Ca, Na, Mg, Fe, K, NO_3^-, SO_4^{2-}, NH_4^+ and Cl^-) and trace elements (Li, P, Ti, V, Cr, Mn, Co, Ni, Cu, Zn, As, Se, Rb, Sr, Cd, Sn, Sb, Ba, La, Pb, among others). The combined sum of the aforementioned components accounted for 75–85 % of the total PM mass. All analyses and results were blank-filter corrected following the same methodology. For each set of ten filters, nine were sampled and one was reserved for blank analysis. The corresponding blank filter was analysed using the same procedures described for OC/EC, water soluble ions and for major/minor elements. Blank concentrations were subtracted from the total concentration measured for each sample, thus giving ambient concentrations.

Stations in Spain from which data was used in this study (Cabo de Creus, Els Torms, Zarra, Viznar, Barcarrota, O Saviñao, Niembro, Campisábalos, Peñausende and Risco Llano) are all members of EMEP (Co-operative Programme for Monitoring and Evaluation of the Long-Range Transmission of Air Pollutants in Europe). Measurements were performed gravimetrically on a daily basis using EN UNE 14907 high volume samplers (MCV PM1025) in accordance with standard procedures outlined by European Air Quality Directive 2008/50/CE and EN 14907:2005 standard. Of the remaining European sites, all measurements were determined gravimetrically on a daily basis except the following stations: Pfälzerwald-Hortenkopf, Virolahti, Utö, Fundão, Chamusca, Lamas de Olo and Ervedeira performed measurements by Beta Ray Attenuation providing hourly averages of $PM_{2.5}$. Measurements at Vavihill and Aspvreten were performed by TEOM with hourly resolution. Measurements at Hyytiälä were recorded on a daily basis using an impactor. Ispra employed a filter pack and measurements were performed on a daily basis. Finally, a Sierra Dichotomous Sampler was employed at Birkenes providing $PM_{2.5}$ measurements at a weekly resolution. All $PM_{2.5}$ data and details of the operational status and site characteristics of the stations can be found on the EMEP website (www.emep.int) and the AIRBASE website (http://acm.eionet.europa.eu/databases/airbase/).

Temporal trend analysis was performed for all the stations where sufficient data was available (see Table 2 for the list of stations) by means of the nonparametric Mann-Kendall test for the trend and the nonparametric Sen's method for the magnitude of the trend. The MAKESENS (**Ma**nn-**Ke**ndall test for trend and **Sen's** slope estimate) template application was employed to determine the statistical significance of the trend (Salmi et al., 2002). The Mann-Kendall test is applicable for the detection of a monotonic increasing or decreasing trend of a time series and the Sen's method estimates the slope of the linear trend (Gilbert, 1987). Thus, analysis was applied to the mean annual and monthly concentrations of $PM_{2.5}$ and its various chemical components. The significance of the trend is symbolised as (α) and the level of significance is weighted from most significant to the least significant as: ($\alpha = 0.001 > 0.01 > 0.05 > 0.1$).

Table 2. Percentage reduction of $PM_{2.5}$ and statistical significance of the decreasing trend (α) for various stations across Europe.

Site	First year	Last year	# data points	α	% reduction
Montseny	2002	2010	9	0.01	35
Cabo de Creus	2002	2010	9	0.001	49
Els Torms	2002	2010	9	0.05	40
Zarra	2002	2010	9	–	30
Viznar	2002	2010	9	–	14
Barcarrota	2002	2010	9	0.05	41
O Saviñao	2002	2010	9	0.01	36
Niembro	2002	2010	9	–	7
Campisábalos	2002	2010	9	0.05	34
Peñausende	2002	2010	9	0.001	42
Risco Llano	2002	2010	9	–	20
Illmitz	2002	2010	9	–	31
Payerne	2002	2010	9	0.05	36
Vavihill	2002	2010	9	0.05	35
Aspvreten	2002	2010	9	0.05	34
Birkenes	2002	2010	9	–	41

3 Results and discussion

3.1 Mean $PM_{2.5}$ levels

Mean $PM_{2.5}$ levels recorded at MSY (determined gravimetrically) from 2002 to 2010 were 12.6 µg m^{-3}. $PM_{2.5}$ levels were elevated when compared with Spanish EMEP stations (Table 1). The average $PM_{2.5}$ concentration for 10 EMEP RB sites across the Iberian Peninsula (IP) for the same time period was 8.6 µg m^{-3}, and the average value for two other RB stations in the NE IP (namely Els Torms and Cabo de Creus) was 10.5 µg m^{-3}. Thus, the MSY station registered higher levels of PM compared to average concentrations across Spain (+37 %) and those registered from stations in the NE of Spain (+18 %). This surplus may be attributed to anthropogenic influences. The greater area surrounding MSY, especially the valleys in the pre-coastal depression, is

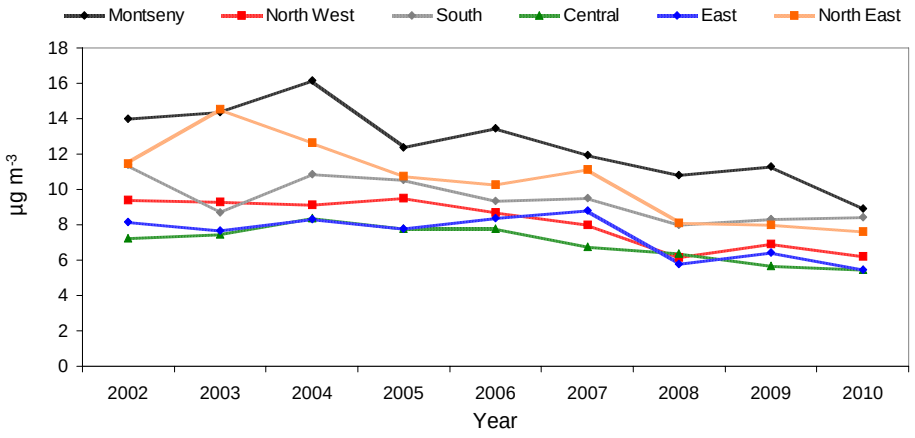

Fig. 1. $PM_{2.5}$ concentrations measured at RB sites across Spain from 2002–2010.

densely populated and highly industrialised, being a significant source of pollution reaching the MSY site.

Comparing these values with other RB sites across Europe (Table 1), concentrations measured at MSY were considerably higher (+34 %) than those in Portugal (9.4 µg m^{-3}), Germany (10 µg m^{-3}) and Scandinavia (6.6 µg m^{-3}). They were slightly lower than levels recorded in Switzerland (14.5 µg m^{-3}) and significantly lower than levels recorded in Austria (19.7 µg m^{-3}). Ispra recorded the highest levels of all the stations included in this work, with $PM_{2.5}$ of 26.2 µg m^{-3}. Climate conditions are likely to influence $PM_{2.5}$ levels at each of the RB stations mentioned, whereby differences in precipitation levels and prevailing wind systems could account for the differing concentrations observed, especially for Atlantic and Scandinavian countries. Anthropogenic influences are likely to be most prevalent in Ispra in Northern Italy, as it is subjected to intense episodes of pollution owing to thermal inversions in winter and emissions from nearby heavy industry in the Po valley (Van Dingenen et al., 2004). High pressure weather systems over Eastern Europe in winter can lead to stagnant conditions across Austria and Switzerland, causing the accumulation of pollutants (Barmpadimos et al., 2012). Furthermore, the regions can be affected by long range transport of pollution from central and Eastern Europe, and biomass burning emissions in winter.

3.2 Interannual trends across Spain and Europe

A decreasing trend for $PM_{2.5}$ has been observed in MSY since measurements began in 2002 (Fig. 1). Furthermore, this decreasing trend has been observed not only across Spain, but throughout Europe (Fig. 2). Of the stations listed in Table 1, statistical trend analysis using the Mann Kendall test was performed where 9 valid data points were available, with results shown in Table 2. Evidently, levels of $PM_{2.5}$ at all stations have decreased to some extent. However, not all have undergone a uniform reduction, with some having a statistically relevant trend (significance level $\alpha > 0.1$), where others have decreased in the absence of a statistically significant trend, in which case α is not shown. The three stations from the NE Iberian peninsula i.e. MSY, Els Torms and Cabo de Creus, have experienced reductions of 35 %, 40 % and 49 % with $\alpha = 0.01$, 0.05 and 0.001, respectively. Peñausende has also experienced a significant decrease ($\alpha = 0.001$) of 42 % since 2002.

On average, for the RB stations used in this study a reduction of 32 % has been observed in $PM_{2.5}$ levels since 2002 throughout Spain, 31 % at Illmitz, 36 % at Payerne, 34 % at Ispra, 35 % in Sweden, 32 % across Germany, 32 % in Finland, 41 % in Norway and 38 % in Portugal. There were only two stations, Niembro in the north and Viznar in southern Spain, which registered lower decreases of only 7 % and 14 %, respectively. The proximity of Viznar in southern Spain to the urbanised area of Granada (20 km) places it under greater influence of urban emissions, which may account for the comparatively smaller decrease of 14 % in $PM_{2.5}$. Furthermore, Viznar is located closer to North Africa and exposes the site to more frequent Saharan dust intrusions. However a 14 % reduction in $PM_{2.5}$, in the context of a RB site with some urban influence, is still quite significant. Niembro is a low altitude coastal site on the Atlantic coast. The station is located within close vicinity of a densely industrialised area which may be an important source of PM emitted locally, accounting for the lower reduction observed. Stations located in the central IP i.e. Risco Llano, Campisábalos and Peñausende all registered very low concentrations of $PM_{2.5}$ (Table 1). A statistically significant decreasing trend was not observed for Risco Llano, unlike that observed for Campisábalos and Peñausende, but $PM_{2.5}$ levels have decreased nonetheless.

Thus, excluding Viznar and Niembro, the percentage reduction observed across Spain and Europe ranges from a minimum of 20 % (Risco Llano) to a maximum of 49 % (Cabo de Creus). What is most striking is that these decreases are similar across Europe, the median percentage reduction being 35 %.

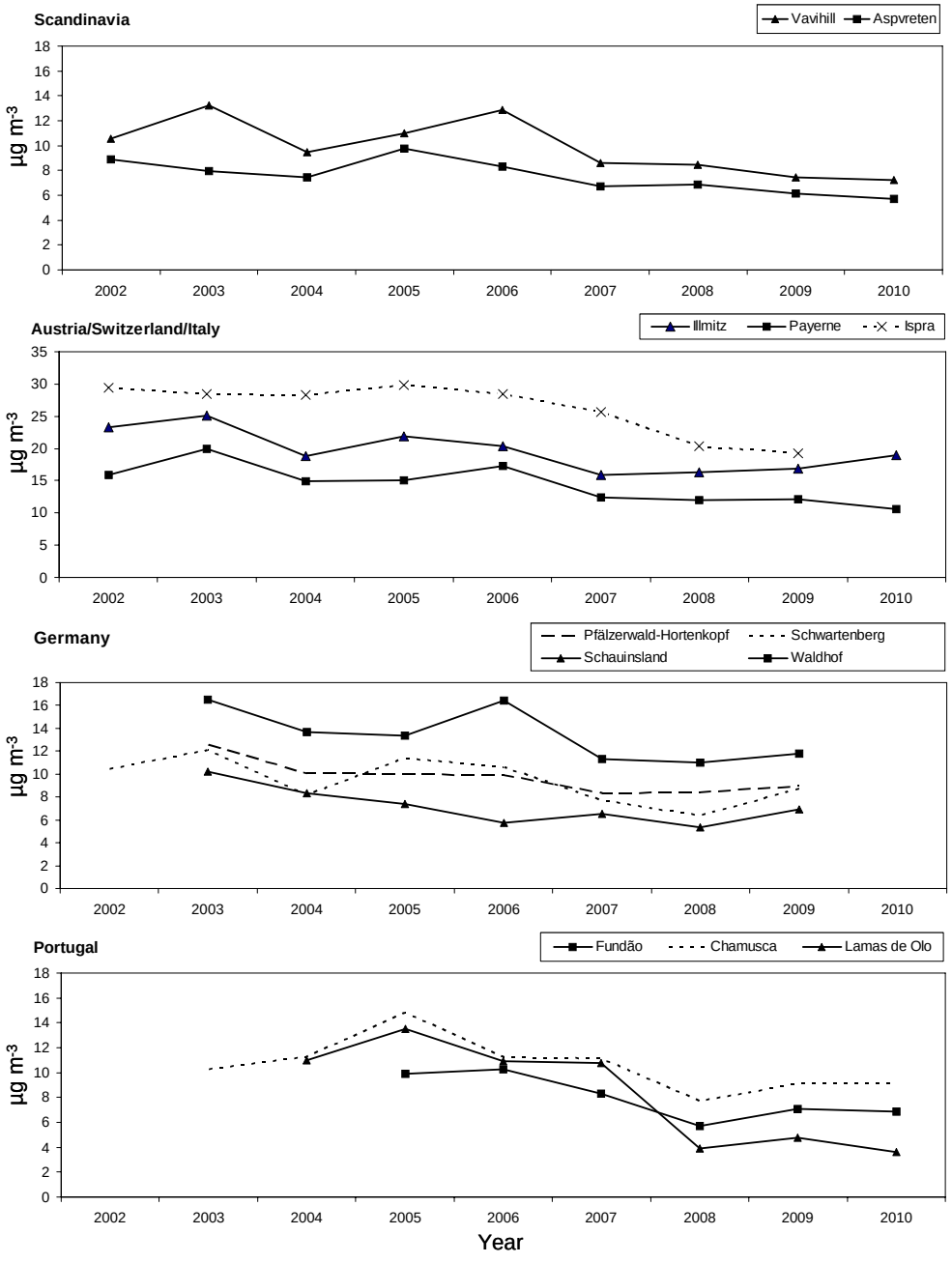

Fig. 2. $PM_{2.5}$ levels measured for various RB stations across Europe according to AIRBASE and EMEP data.

As illustrated in Fig. 1, a marked decrease was observed for each area of Spain through the decade, with minimum concentrations occurring from 2008 onwards. Stations are categorised according to their location in Spain and values are mean $PM_{2.5}$ concentrations of the stations for that location for each year: Niembro and O Saviñao are categorised as North; Viznar and Barcarrota are South; Peñausende, Campisábolos and Risco Llano are considered Central; Zarra is East; Cabo de Creus and Els Torms are North East. For many regions levels reached a minimum in 2008, followed by a slight increase in 2009 (for all except central Spain), and a reduction once again in 2010. MSY followed a similar trend to that observed for the other stations in the NE peninsula, albeit with slightly higher levels measured in comparison. The fact that the PM levels here follow a similar trend verifies that the trend is real and observed across the region. In fact, this decreasing trend is observed for many stations across Europe (Fig. 2).

For some stations in Germany, Austria, Switzerland, Finland and Sweden, levels of $PM_{2.5}$ experienced noticeable

decreases from 2007 onwards. For example, in Vavihill, Sweden and Waldhof in Germany, a sharp decrease was recorded of 4 µg m^{-3} and 5 µg m^{-3} between 2006 and 2007, respectively (Fig. 2). A similar reduction, although not quite as pronounced, was observed for stations Illmitz, Payerne, Utö, Aspverten, Virolahti, Schwartenberg and Schauinsland. This gradual reduction observed across Europe is possibly a direct result of the implementation of the aforementioned pollution abatement strategies. Indeed, the countries in which these stations are located have to a large extent avoided economic recession compared to the peripheral European states such as Spain, Portugal and Italy. Thus, reductions there have not been quite as pronounced as those recorded for the last two years in the IP and Ispra. However, it should be highlighted that PM levels in many of the stations, especially in Norway (mean $PM_{2.5}$ of 4.3 µg m^{-3}) and Finland (6.0 µg m^{-3}) for example, were comparatively low even at the beginning of the measurement period. Thus, even though a decreasing trend has been observed in these regions, it cannot be decisively ascertained that the economic recession and pollution abatement strategies have not impacted PM levels here, considering the low initial concentrations.

Stations in Portugal and Italy displayed similar reductions as those observed in Spain (Fig. 2). The sharpest reductions were observed between 2007 and 2008 (as compared to levels in most of the other European stations which dropped more gradually). Levels measured in Lamas de Olo fell 6.8 µg m^{-3} during 2007–2008 from 10.8 to 3.9 µg m^{-3} (Fig. 2). Decreases in Fundão and Chamusca were more gradual from 2007–2009, decreasing by 2.6 µg m^{-3} and 3.4 µg m^{-3}, respectively. This suggests that similar processes are influencing PM levels not only in Spain, but across the IP including Portugal. The reduction observed at Ispra in northern Italy was also most pronounced from 2008 onwards. Although levels do exhibit a decreasing trend across the time series, especially since 2005, a large drop in $PM_{2.5}$ was observed between 2007 (26 µg m^{-3}) and 2008 (20 µg m^{-3}). This observed decrease from 2008 onwards indicates that these stations in Spain, Portugal and Italy, although geographically distant, share some factor in common causing background levels of $PM_{2.5}$ to decrease all within the same time period. A reduction in emissions of pollutants as a result of the downturn in the economy may possibly be this factor. A recent study by Barmpadimos et al. (2012) also observed a decreasing trend in PM_{10} and $PM_{2.5}$ in various urban and rural background sites in Europe, some of which are also included in this study (namely, Illmitz, Waldhof, Payerne and Peñausende). The article concluded that PM_{10} and $PM_{2.5}$ have reduced considerably over the past ten years due to non-meteorological factors. Indeed, for the station at Peñausende, the authors concluded that a decrease in anthropogenic emissions was likely to be accountable for the reduction observed in $PM_{2.5}$ rather than meteorology.

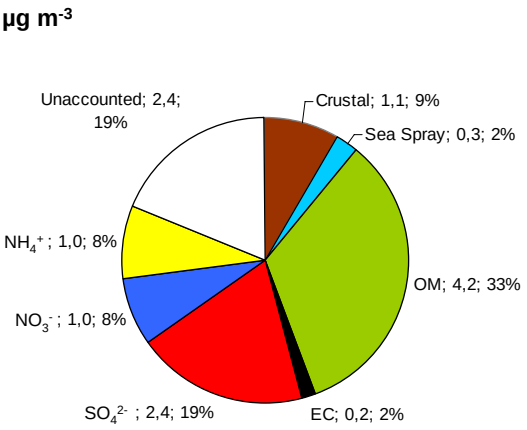

Fig. 3. Mean $PM_{2.5}$ composition (µg m^{-3}) at MSY for the study period (2002–2010).

3.3 PM speciation

As shown in Fig. 3 the main chemical components of $PM_{2.5}$ (12.6 µg m^{-3}) at MSY are: organic matter (OM; 4.2 µg m^{-3}; 33 %), SO_4^{2-} (2.4 µg m^{-3}; 19 %), crustal material (1.1 µg m^{-3}; 9 %), NO_3^- (1.0 µg m^{-3}; 8 %), NH_4^+ (1.0 µg m^{-3}; 8 %), sea spray (0.3 µg m^{-3}; 2 %) and finally elemental carbon (EC; 0.2 µg m^{-3}; 2 %). The unaccounted mass is 19 % of the total PM mass and is attributed to water retention on the filters. Usually, a simple mass closure approach yields a larger unidentified fraction compared to source receptor modelling such as PMF. This discrepancy has been attributed to its simplicity and inability to apportion the water mass to different source contributions.

In relative proportions, OM was by far the major component of $PM_{2.5}$ at MSY. Sources of OM at MSY are varied, and can be attributed to secondary organic aerosol (SOA) formed from the emissions of anthropogenic volatile organic compounds (VOCs) from industry, road traffic, biomass burning emissions and also biogenic VOCs (Peñuelas et al., 1999). Sulphate was the second most abundant compound measured at MSY and is associated with industrial, shipping and power generation emissions. Nitrate and ammonium levels recorded at MSY were similar, at 8 % for both compounds. Owing to the thermal instability of ammonium nitrate, the most common compound of nitrate at this site, the majority of nitrate was measured during the winter months. During summer months, when ammonium nitrate is volatilised, ammonium concentrations measured were typically in the sulphate form. Crustal material registered 9 % of the total mass in $PM_{2.5}$. The majority of crustal material at MSY is typically found in the coarse fraction ($PM_{2.5-10}$) and does not influence levels of $PM_{2.5}$ to a great extent, but Saharan dust intrusions can influence the crustal load measured in $PM_{2.5}$ (Pey et al., 2009). Levels of elemental carbon (EC) comprised only 2 % of the total mass. EC emissions

are associated with fuel-oil combustion and biomass burning emissions. Biomass burning, both anthropogenic and natural, could possibly be a significant source of EC at MSY, as it is a rural forested site with agricultural land nearby.

3.4 Inter-annual trends at MSY for $PM_{2.5}$ and chemical composition

The analysis of inter-annual trends of $PM_{2.5}$ levels measured at MSY, and the respective trend analysis of its chemical components, has revealed possible explanations for the reduction observed over the past 9 yr, and may possibly provide insight into the reduction observed across Europe. The seasonal trends are also supplied in the supplementary material.

3.4.1 $PM_{2.5}$ trends

Temporal trend analyses were applied to the annual and seasonal chemistry data sets from MSY from 2002 to 2010. The Mann-Kendall tests showed significant temporal trends for the total mass of $PM_{2.5}$ ($\alpha = 0.01$) with a 35 % decrease observed over the total measurement time period (Fig. 4), the equivalent of $6\,\mu g\,m^{-3}$ of $PM_{2.5}$. On a seasonal basis, winter was the only season that registered a statistically significant year-on-year decreasing trend ($\alpha = 0.05$), with a decrease of 35 %. MSY is regularly affected by intense anthropogenic pollution episodes that occur during the colder months i.e. from October to March. The occurrence of these polluted winter anticyclonic episodes (WAE), their intensity and their affect on pollution levels, has been outlined by Pey et al. (2010). The combination of various factors may account for this reduction that occurred only in the winter season; a reduction in anthropogenic emissions due to pollution abatement strategies, the economic recession and quite possibly the unusual meteorology that has occurred during winter for the last few years. The North Atlantic Oscillation (NAO) is a large-scale meridional oscillation in atmospheric mass, with centres of action near Iceland and over the subtropical Atlantic (Visbeck et al., 2001). It is one of the leading climate modes in the North Atlantic region (Hurrell et al., 2003), and influences climate variability, e.g. temperature, precipitation and wind, especially during the winter (Hurrell and Deser, 2009). When the pressure gradient between the Icelandic low and the subtropical high pressure centre during winter is more intense than normal (positive NAO), the westerly winds are stronger across northern Europe. This brings Atlantic air masses over the continent (associated with mild temperatures and higher precipitation) and dryer conditions across southern Europe. When this pressure gradient is low (negative NAO), cold and dry air masses often dominate over northern Europe, and the Atlantic weather systems and storm tracks tend toward a more southerly trajectory, bringing higher than normal precipitation levels across the Iberian peninsula (Vicente-Serrano et al., 2011), as occurred during winter 2009 and 2010. Indeed, winter 2010 was notable for two reasons; unusually high precipitation over the IP which coincided with one of the most negative NAOi since measurements began (reported in Vincente-Serrano et al. (2011) as the end of the 19th century or beginning of the 20th century), and one of the coldest winters in decades across northern Europe. Incidentally, winter 2010 also registered the lowest PM levels recorded at MSY since 2002. The cleaning effect of Atlantic Advection on MSY is significant and such episodes are associated with low PM events (Pérez et al., 2008). Thus, due to the intensified westerly Atlantic winds (as a result of the negative NAO), PM levels were observed to be considerably lower compared to other winters. As mentioned previously, the occurrence of Saharan dust intrusions over the IP can affect PM levels significantly. Figure 5 displays the linear relationship observed between the frequency of NAF episodes (in days) and the corresponding NAO index for the winter months December, January, February and March. It can be seen that for winters with positive (negative) NAO indices, NAF episodes were more (less) frequent. This suggests that when NAO is more intensely positive, the probability of air masses from North Africa reaching the IP is much higher. Conversely, when NAO is negative, intense Atlantic Advection directed over the IP can block North African air masses and prevent these air masses moving northward. This influence is most prominent in the north of the IP i.e. closer to the Atlantic Ocean, and the intensity weakens with greater distance from the Atlantic Ocean. However, for all parts of the peninsula, if the NAO index is sufficiently positive or negative, the effects are felt across the country. This theory agrees with that proposed by Moulin et al. (1997). Furthermore, a study by Ginoux et al. (2004) observed a high correlation between dust surface concentration and NAO over much of the North Atlantic and the western part of North Africa during winter.

3.4.2 Organic and elemental carbon

Figure 4 shows the temporal trends for OC and EC concentrations recorded from 2002 to 2010 by means of the Mann-Kendall test and Sen's method using MAKESENS. OC underwent a reduction of 48 % over the total measurement period, with very high statistical significance ($\alpha = 0.001$). This reduction is the equivalent of $1.6\,\mu g\,m^{-3}$ of OC from a maximum in 2004 of $2.9\,\mu g\,m^{-3}$ to a minimum of $1.3\,\mu g\,m^{-3}$ in 2010. This decreasing trend was observed across all seasons, with varying levels of significance (spring ($\alpha = 0.01$), summer ($\alpha = 0.01$), autumn ($\alpha = 0.05$), winter ($\alpha = 0.05$)), verifying that the reduction was observed across all seasons. Figure 6 shows the time evolution of a selection of components of $PM_{2.5}$, including OC. OC followed a clear seasonal trend, with maximum concentrations registered in summer coinciding with the lowest renewal of the atmosphere at a regional scale (Rodríguez et al., 2002; Pérez et al., 2008) and higher biogenic emissions of VOCs (Seco et al., 2011). Secondary

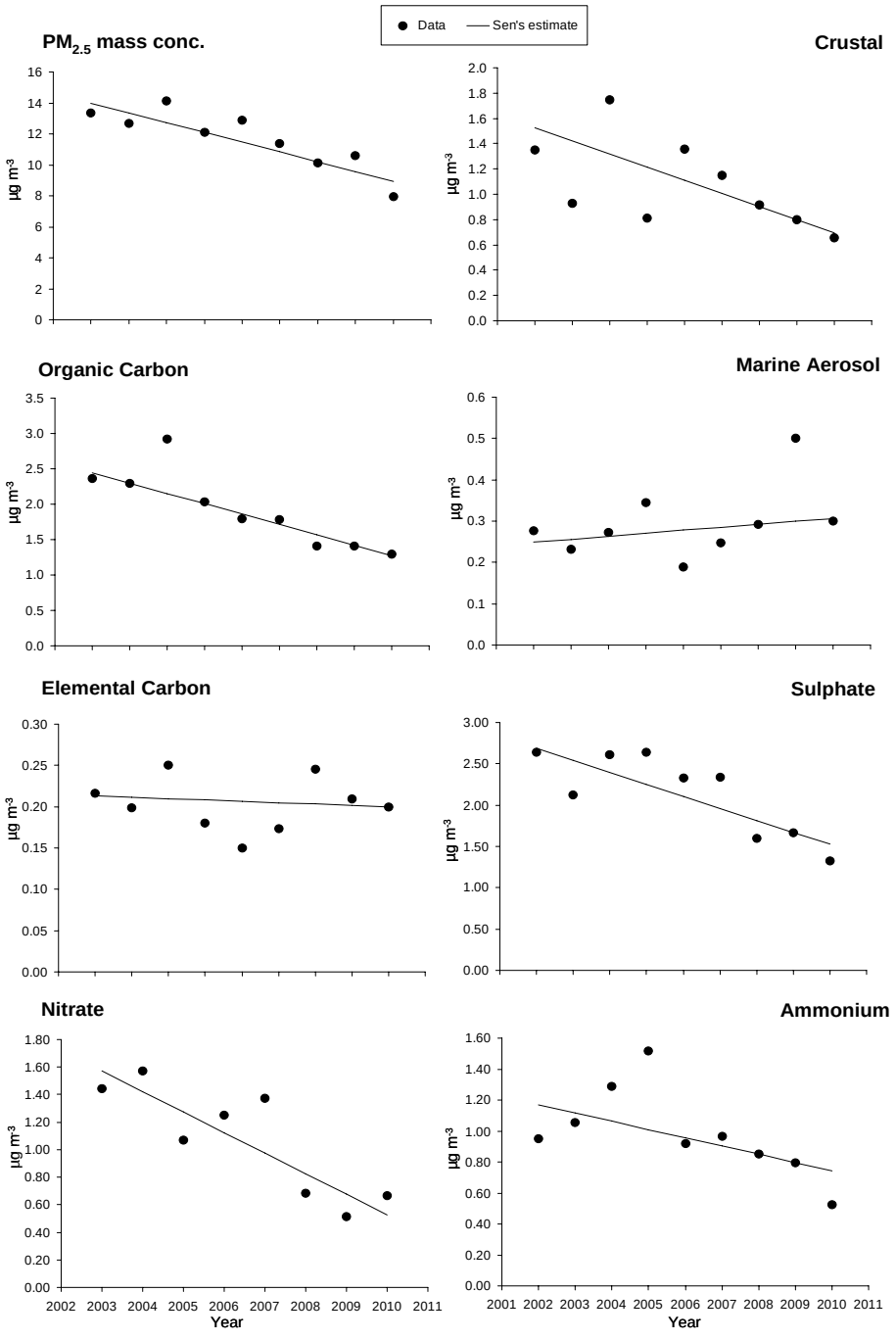

Fig. 4. Temporal trends for $PM_{2.5}$ and its various major chemical components by means of the Mann-Kendall test and Sen's method using MAKESENS (Salmi et al., 2002).

peaks in concentration also occurred during WAE, followed by sharp reductions in spring due to higher precipitation and Atlantic Advection episodes. The intensity of the seasonal cycles clearly began to diminish from 2007 onwards. The reduction observed in OC is most probably a result of a reduction of OC emissions or precursors from anthropogenic sources, as natural emissions of OC would not be expected to decrease. Previous studies at MSY have shown that the fraction of OC in PM_1 that is mainly attributed to road traffic, accounts for 31 % of total OC in winter and 25 % in summer (Minguillón et al., 2011). Measurements of known tracers for biomass burning emissions, such as K^+ (which was not analysed), would be useful to help determine the contribution of biomass burning to levels of OC at MSY. As stated

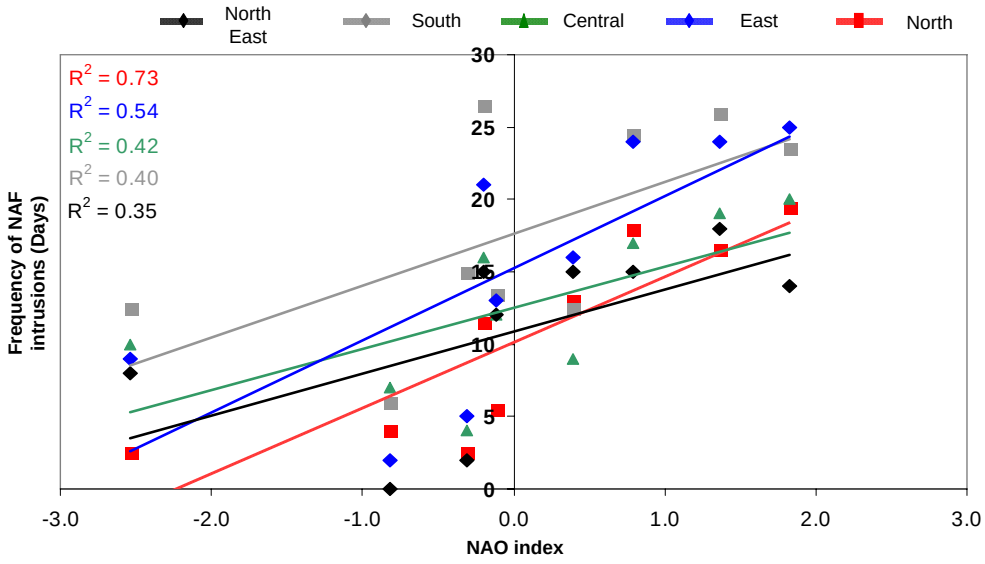

Fig. 5. Correlation plot of NAO index and the frequency of Saharan dust intrusions (NAF) in days during winter for 2002–2010 for different regions of Spain.

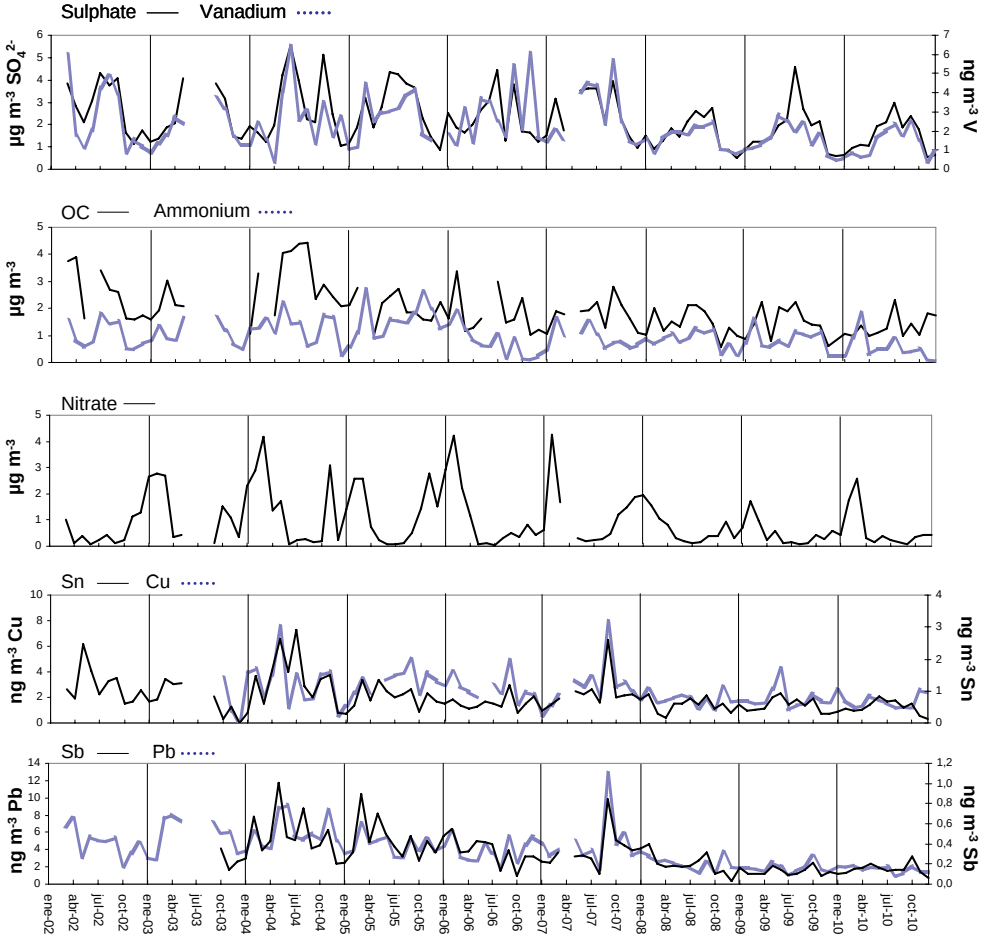

Fig. 6. Time evolution of concentration levels of SO_4^{2-}, V, OC, NH_4^+, NO_3^-, Cu, Sn, Pb and Sb at MSY.

previously, OM (calculated from measured OC) accounted for 44 % of total $PM_{2.5}$. Thus, much of the reduction observed for $PM_{2.5}$ can partly be attributed to the reduction in OC.

EC levels have not shown any statistically significant trend since measurements began, and levels did not vary very much on a yearly basis (0.15–0.25 $\mu g\,m^{-3}$). A minimum value was recorded in 2006 (0.15 $\mu g\,m^{-3}$) and maximum values were recorded in 2004 and 2008 (0.25 $\mu g\,m^{-3}$). Maximum and minimum concentrations did not differ significantly. On a seasonal basis, there is an indication that EC levels have actually shown an increasing trend since 2008, especially in winter and autumn. This is contrary to what has been observed for many other anthropogenic pollutants at MSY, but EC may be closely related to local domestic and agricultural biomass burning emissions.

3.4.3 Secondary inorganic aerosols

A significant reduction has also been observed for the Secondary Inorganic Aerosols (SIAs) at MSY, including sulphate, nitrate, and ammonium. As stated previously, SIAs comprised 44 % of the total sum of the chemical components of $PM_{2.5}$. Thus, a reduction in SIA would have an overall reducing effect on the total $PM_{2.5}$ mass. Figure 4 shows the temporal trends observed for sulphate, nitrate and ammonium and Fig. 6 shows the time series for the concentrations of these three components over the measurement period. Anthropogenic sulphate concentrations (where the fraction of marine sulphate has been removed) at MSY decreased by 43 % from 2002 to 2010 ($\alpha = 0.05$). The EMEP Report 4/2011 reported a reduction in sulphur oxides (SO_x) emissions of 23 % in Spain from 2008–2009 alone, which would contribute to the reduction observed in secondary sulphate. Sulphate and V showed similar trends on a yearly basis (Fig. 6), with many intense peaks for both components coinciding. It is clearly visible that sulphate and V have decreased from 2008 onwards. Sulphate emissions are associated with fuel oil combustion for power generation and industry, as well as shipping. Vanadium and Nickel are also associated with these types of emissions and often correlate closely with sulphate measured at MSY. For the total measurement period, SO_4^{2-} correlates very well with V ($R^2 = 0.74$) and Ni ($R^2 = 0.71$). Thus, the decrease could be a result of reduced combustion emissions and the implementation of emission abatement strategies, such as the IPPC directive (Directive 2008/1/EC), employed by industry and power plants. Power plants in Barcelona and the surrounding area began to phase out the use of fuel oil in exchange for natural gas, and by 2007 all power plants were using natural gas (Bruno et al., 2007). This has undoubtedly impacted levels of SO_4^{2-}, V and Ni and likely accounts for the reduction observed since 2007.

Sulphate levels were highest during the summer; possibly as a result of enhanced photochemistry associated with more intense solar radiation, lower air mass renovation at a regional level, the increase in height of the summer mixing layer depth and higher regional transport, favouring the regional mixing of polluted air masses. Sulphate levels, along with many other components, undergo intense concentration increases under WAE (as described by Pey et al., 2010), These scenarios are associated with unseasonably warm and calm weather, with little advection, causing the local air mass to stagnate and pollution levels to increase over a period of days and weeks. Trend analysis on a seasonal basis did not show any significant trend, but the reductions observed from 2008 onwards are still pronounced.

Nitrate levels exhibited strong seasonal variability, giving highest concentrations during the colder winter months (especially during WAE), with minimum concentrations in summer. This trend is associated with the thermal instability of ammonium nitrate (Harrison and Pio, 1983; Querol et al., 2004), the most frequent form of nitrate at this site. These intense peaks of nitrate have been observed since measurements began, occurring from January to March, with secondary peaks often recorded in November. They are typically followed by marked decreases in April, when WAE are less frequent and wetter weather is more prevalent. Since 2008, these winter nitrate episodes have diminished considerably. From 2002 to 2007, nitrate levels remained relatively consistent, but dropped sharply from 2008 onwards, as shown in Fig. 6. Trend analysis of annual nitrate levels have shown that the reduction has not followed a pattern as linear as that of OC or sulphate, but the reduction was still significant ($\alpha = 0.05$), having reduced by 61 %. On a seasonal basis, statistically significant reductions of nitrate only occurred in winter ($\alpha = 0.05$), very similar to the annual trend. As the majority of nitrate measured at MSY occurred in winter, this similarity is to be expected. The seasonal evolution of nitrate for the remaining seasons did not display any significant trends. As the presence of ammonium nitrate varies with temperature (due to its thermal instability), the trends were not as pronounced during warmer seasons.

Yearly ammonium concentrations followed a relatively unusual trend as compared to nitrate and sulphate, with concentrations increasing year-on-year to 2005, followed by a sharp drop in 2006, maintaining a decreasing trend thereafter until 2010. The reduction was statistically significant ($\alpha = 0.05$), giving a percentage decrease of 37 %. Ammonium underwent a bimodal seasonal variation, with intense winter peak concentrations during WAE, followed by generally elevated levels over the entire summer period. Ammonium measured on site was typically in the form of ammonium nitrate in the winter months and as ammonium sulphate during the warmer summer months, as will be discussed anon. Ammonium did not show significant trends on a seasonal basis except in winter ($\alpha = 0.05$), but a marked decrease since 2008 was observed.

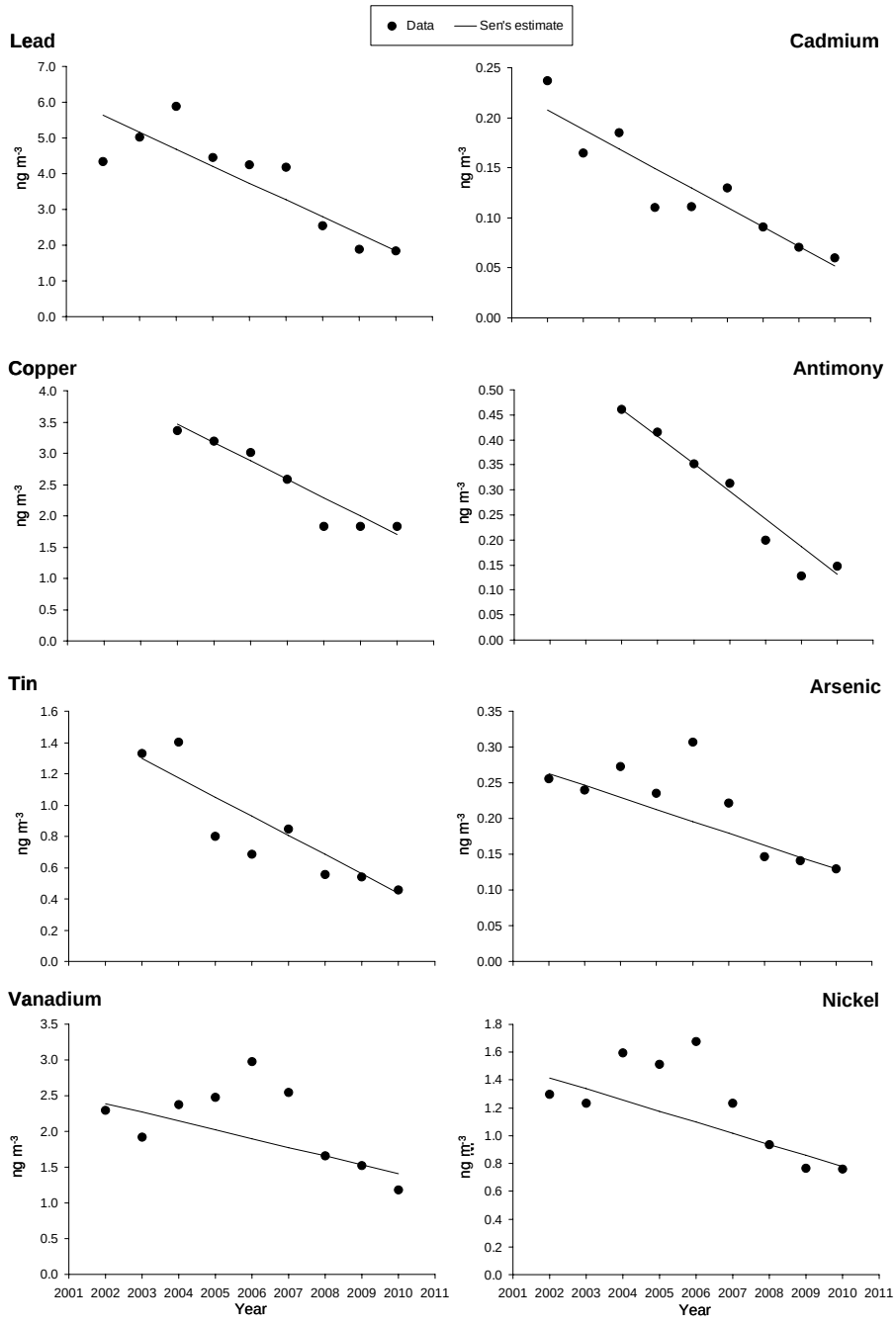

Fig. 7. Temporal trends for a selection of trace anthropogenic chemical components by means of the Mann-Kendall test and Sen's method using MAKESENS (Salmi et al., 2002).

3.4.4 Crustal and marine aerosols

As stated previously, crustal material and marine aerosol comprised 9 % and 2 % respectively of the total sum of the chemical components registered at MSY. Thus, marine aerosols did not influence the total $PM_{2.5}$ mass significantly. Elevated levels of crustal material are associated with high soil resuspension and episodes of Saharan dust intrusions (Pérez et al., 2008) i.e. they are mostly natural, and the crustal load of $PM_{2.5}$ increases significantly under NAF episodes. A minor decreasing trend has been observed for the crustal material measured at MSY ($\alpha = 0.05$), beginning in 2006 (Fig. 4). The unusual weather conditions experienced for the last two winters in the IP, as a result of the unusually negative NAO index, could be the cause for this slight reduction observed in crustal material. As stated previously, NAO

Table 3. Percentage reduction of various trace elements, mean concentration ($ng\,m^{-3}$) and statistical significance of the decreasing trend (α) recorded at MSY (elements with statistically significant reductions in bold).

Element	Measurement Period	Mean Conc. ($ng\,m^{-3}$)	α	% reduction
Pb	2002–2010	3.82 ± 1.41	0.01	67
Cd	2002–2010	0.13 ± 0.06	0.01	75
Cu	2004–2010	2.52 ± 0.69	0.05	44
Sb	2004–2010	0.29 ± 0.13	0.01	58
Sn	2004–2010	0.76 ± 0.32	0.01	58
As	2002–2010	0.22 ± 0.06	0.05	51
V	2002–2010	2.11 ± 0.57	–	41
Cr	2002–2010	0.82 ± 0.20	–	34
Ni	2002–2010	1.22 ± 0.34	0.1	45
Co	2002–2010	0.06 ± 0.02	0.05	53
Li	2002–2010	0.06 ± 0.02	–	43
Ti	2002–2010	3.51 ± 1.19	–	34
Mn	2002–2010	1.94 ± 0.49	0.1	37
Ga	2002–2010	0.04 ± 0.02	0.1	53
Rb	2002–2010	0.14 ± 0.03	–	43
Sr	2002–2010	0.47 ± 0.26	–	49
La	2002–2010	0.07 ± 0.01	–	34
Ce	2002–2010	0.13 ± 0.02	–	17
Pr	2002–2010	0.02 ± 0.01	0.05	46
Nd	2002–2010	0.06 ± 0.02	0.1	49

can potentially control the frequency of Saharan dust intrusions reaching the IP, which would affect the mean crustal load concentrations. In addition, increased Atlantic Advection (associated with negative phases of the NAO) would have a cleaning effect on the atmosphere. Indeed, marine aerosol registered a spike in annual concentrations in 2009 ($0.5\,\mu g\,m^{-3}$). It could also be hypothesised that some part of the crustal material measured at MSY is a product of the construction industry. The construction industry in Spain has been especially affected by the current economic recession, and crustal material produced by this industry may have contributed to the crustal load in $PM_{2.5}$. Analysis of seasonal trends of crustal material did not show any specific statistical trend. Marine aerosol is also of natural origin and, as expected, has not undergone any clear declining trend.

3.4.5 Trace elements

Various anthropogenic pollution tracers associated with industrial and traffic emissions (Pb, Cd, Cu, Sb, Sn, As, V, Cr, Ni, Co) and elements of natural origin (Li, Ti, Mn, Ga, Rb, Sr, La, Ce, Pr, Nd) were analysed for statistically significant trends and are listed in Table 3. Those experiencing the greatest percentage reductions since measurements began are Cd, Sb, Sn and Pb ($\alpha = 0.01$). Cu and As have recorded a reduction in the range of 44–51 % ($\alpha = 0.05$), followed by Ni ($\alpha = 0.1$) at 45 % and V at 41 %. Finally, Co underwent a reduction of 53 % ($\alpha = 0.05$). Limit values are set by the European Union for Pb, (2008/50/CE) and target values are set for Cd, As, and Ni (2004/107/CE) and the reduction observed may be a direct result of the enforcement of this legislation. V, Ni and As all displayed peak concentrations in 2006 of $3\,ng\,m^{-3}$, $1.7\,ng\,m^{-3}$ and $0.3\,ng\,m^{-3}$ respectively, but from 2007 began to decrease in a similar fashion, as shown in Fig. 7. V and Ni are both associated with fuel oil combustion and correlate very well ($R^2 = 0.64$). Of the remaining trace elements, all have followed similar decreasing patterns over the measurement time period. Figure 6 shows typical anthropogenic pollution tracers Sn, Cu, Sb and Pb, all of which follow similar patterns over time, with many coinciding peaks in concentration (as occurs in September 2007, for example). In general they do not follow a clear seasonal trend. The variation of trace element concentrations at MSY during an intensive measurement campaign was described by Moreno et al. (2011), and outlined the inherent difficulty in distinguishing exact sources of trace elements at MSY due to PM mixing and dilution during transport to MSY. The reductions and correlations between Pb and As ($R^2 = 0.64$) and Pb and Cd ($R^2 = 0.62$), all of which are regulated by legislation, suggest the efficacy of the abatement strategies and also that they may be of the same source, most likely industrial.

All the elements shown in Fig. 7 show a marked decrease in concentrations from 2008 onwards, quite possibly for the same reasons as those mentioned previously for the major PM components. V and Ni are tracers for the combustion of fuel oil and the reduction observed coincides with both the replacement of fuel oil in power generation with natural gas and also with the beginning of the economic recession. A similar study performed in Cantabria, in the north of Spain, has observed a comparable effect, linking the effects of the economic recession to some industrial trace metal emissions (Arruti et al., 2011).

Some trace elements associated with crustal material (Li, Ti, Mn, Ga, Rb, Sr, La, Ce, Pr, and Nd) are also listed in Table 3. Some of these elements (Mn, Ga, Pr and Nd) have undergone statistically significant reductions similar to those observed for the total crustal material measured in $PM_{2.5}$. The percentage reductions observed for all the crustal elements are a result of the reduction observed in 2009 and 2010, as was the case for the crustal material, and the causes for this reduction are most likely the same.

On a seasonal basis, Pb exhibits a similar statistical trend for each season to that of its annual trend, with each season having $\alpha = 0.05$ and a drop in ambient concentrations of Pb were recorded for each season from 2008 onwards. Cd also maintains the decreasing trend for each season with similar statistical significance ($\alpha = 0.01$). Even though mean annual values of Cu and Sn show a reduction on a yearly basis, they do not undergo any apparent seasonal trend. Sb and As trend analysis shows a significant decreasing trend for spring and summer ($\alpha = 0.01$) but in autumn and winter there is no perceptible trend.

Table 4. Regression analysis of SO_4^{2-} vs. various major and minor components of $PM_{2.5}$ for the different seasons.

Winter		Spring	
Component	R^2	Component	R^2
SO_4^{2-}-V	0.70	SO_4^{2-}-V	0.76
SO_4^{2-}-Ni	0.65	SO_4^{2-}-Ni	0.82
SO_4^{2-}-NH_4^+	0.60	SO_4^{2-}-NH_4^+	0.62
SO_4^{2-}-NO_3^-	0.74		
NO_3^--NH_4^+	0.83	NO_3^--NH_4^+	0.43
NO_3^--As	0.79		
NO_3^--Cl^-	0.90		
OC-Pb	0.53	OC-Pb	0.70
OC-Cl^-	0.89	OC-NH_4^+	0.76
OC-Na	0.66		
Summer		**Autumn**	
Component	R^2	Component	R^2
SO_4^{2-}-V	0.60	SO_4^{2-}-V	0.74
SO_4^{2-}-Ni	0.79	SO_4^{2-}-Ni	0.70
SO_4^{2-}-NH_4^+	0.76	SO_4^{2-}-NH_4^+	0.80
OC-Pb	0.71	OC-Pb	0.63
OC-Fe	0.70		

3.5 Seasonal trends

It is difficult at MSY to ascertain the exact sources of pollutants measured at the site due to the mixed state of the aerosol during transport to the site, as stated previously. By analysing the seasonal variations in the chemical components it may be easier to identify the sources of pollutants. $PM_{2.5}$ and its chemical components are influenced by clear seasonal patterns and variations. To aid in the identification of the sources of the various chemical components, linear regression analysis was used comparing known tracers for both anthropogenic and natural components on a seasonal basis. Table 4 shows the correlation coefficients for the annual concentrations of various major components of $PM_{2.5}$ and various minor trace elements. The seasons for this study are defined as: winter (December, January, February and March), spring (April, May), summer (June, July, August) and autumn (September, October, November).

Sulphate exhibited year round correlation with the main tracers for fuel oil combustion such as V and Ni, as shown in Table 4, suggesting that these three components are from the same source and undergo linear changes in concentrations. The correlation between sulphate and NH_4^+ improves in the summer as ammonium at this time of year is most likely in the form of ammonium sulphate. The influence of intense winter pollution episodes and the mixed state of the aerosols arriving to MSY is highlighted by the correlation observed between sulphate and nitrate ($R^2 = 0.74$) in winter.

Nitrate, as explained earlier, displays a strong seasonal variability with elevated concentrations during the colder months due to the thermal instability of ammonium nitrate. Querol et al. (2009) reported that the ratio of $PM_{2.5}/PM_{10}$ nitrate in the colder months is almost 90 % at MSY, indicating only 10 % exists as coarse nitrate species (Ca and Na nitrate compounds). Thus, linear regression analyses could only be performed for winter, as levels are low in spring and autumn, and negligible in summer. However some relationship was observed between nitrate and ammonium in spring. Table 4 lists the correlation coefficients of nitrate with various components. In contrast to summer, ammonium was better correlated with nitrate in winter ($R^2 = 0.83$). During spring and autumn, it can be reasonably assumed that ammonium exists as a mixture of both the nitrate and sulphate form (and possibly as organic ammonium, see below), depending on the meteorological conditions. Correlation was also observed with As ($R^2 = 0.79$), which is typically an anthropogenic element emitted by industrial practices, which may also be a source of nitrate at MSY. Finally, excellent anti-correlation was observed for nitrate and chlorine ($R^2 = 0.90$) indicating that Atlantic Advection episodes and marine breezes (containing high chlorine concentrations) have a cleaning effect at MSY, removing nitrate from the atmosphere.

Organic Carbon shows correlation with Pb for each season, improving in spring and summer, as shown in Table 4. In fact it is the only trace element that displayed consistent correlation with OC throughout the year. Why Pb (a specifically anthropogenic pollutant), as compared to the other tracers, correlated so well with OC is not clearly understood. Interestingly, OC had very good anti-correlation with marine aerosol components Na and Cl in winter ($R^2 = 0.66$ and 0.89, respectively), as observed previously with nitrate. Again, this was possibly due to the cleaning effect of Atlantic Advection and the influence of cleaner sea breezes from the nearby Mediterranean. The relationship between ammonium and OC was only evident in spring (April and May). It is possible that they were emitted independently in the same region, and arrived at MSY simultaneously. However it could also suggest that there is a significant source of organic ammonium (amines) that is specific to that time of year only. Few studies appear to exist on the importance of atmospheric amines and their sources. A review on atmospheric sources of amines by Ge et al. (2011) lists many possible sources, including agriculture (livestock), industry, traffic, human waste, biomass burning and vegetation. Considering that the relationship between OC and NH_4^+ solely existed in spring indicates that the source was seasonally dependent. The presence of biomass burning in the surrounding area of MSY could well be the driving force behind this relationship. The burning of vegetation is strictly controlled in the area (to minimise risk of forest fires) and has a date limit after which it is prohibited, typically in late spring. Also, vegetative emissions of amines

could also be important as MSY is densely forested, and the seasonal activity of the surrounding trees and plant life may result in the release of amines to the atmosphere. Indeed, this is a new and unexpected discovery, and is worthy of further investigation.

4 Conclusions

The findings in this article provide good evidence that the implementation of pollution abatement strategies in Europe is having a direct effect on the levels of $PM_{2.5}$ and its various components. It is also hypothesised that the current economic climate, in recession since mid 2008 in Spain and many countries in Europe, is also affecting atmospheric pollutants through a reduction in activities associated with a healthy economy (increased road traffic, industrial processes, construction etc.). A reduction in $PM_{2.5}$ concentrations has been observed in Spain and across Europe, and, in most cases, this reduction has been gradual and consistent over time, implying the success of cleaner anthropogenic activities. Additional to this progressive trend, in some cases and especially for RB stations in the IP and Ispra in northern Italy, a marked decrease has been recorded since 2008, coinciding with the beginning of the economic crisis. The effect of the economic crisis on ambient trace element concentrations in northern Spain has also been observed (Arruti et al., 2011) and a reduction in black carbon owing to the economic crisis has been described in an urban area of south-east Spain (Lyamani et al., 2011). Indeed, Spain and Portugal, and to a lesser extent Italy, have all been especially affected by the current crisis, with specific industries, such as the construction industry, and employment suffering to a large extent.

Considering MSY as a representative site for the study of RB aerosols in the WMB, the temporal trends of the major and minor chemical components of $PM_{2.5}$ for a significant time-series of data were investigated. Temporal trends have shown that PM levels at MSY have been steadily decreasing over almost a decade, with statistical significance. The majority of this reduction in mass has been attributed to organic matter and secondary inorganic aerosol, the presence of which in the atmosphere is associated with anthropogenic emissions. Meanwhile, concentrations of marine aerosol have remained unchanged and crustal material has reduced only slightly. This is possibly a result of a decrease in anthropogenic mineral dust but also as a result of unusual meteorology recorded over the last few winter seasons. Intense periods of Atlantic Advection episodes as a result of unusually negative NAO may have had a cleaning effect on aerosols at MSY. Furthermore, the frequency of NAF episodes during winter appears to be influenced by the NAO, whereby positive (negative) episodes of NAO allow for more (less) frequent Saharan dust intrusions.

A similar reduction has been observed for many anthropogenic trace elements verifying this decreasing trend, and point to an ever improving situation regarding air quality. Many of these reductions, through statistical analysis using the Mann-Kendall test and Sen's estimate, have proven statistically significant over the past decade, meaning the reduction has been gradual and uniform.

In order to better understand the sources of the major and minor components that comprise $PM_{2.5}$, linear regression analyses were used to help define the possible sources of aerosols at MSY. The analysis was performed on a seasonal basis to investigate the changing source profiles and the effect of meteorology on aerosols onsite. Sulphate emissions were determined to be closely related with fuel oil combustion tracers V and Ni. Some of the reduction in ambient levels of sulphate, V and Ni may be related to the conversion of power plants employing fuel oil to natural gas, the last power plant having converted in 2008. Nitrate correlated closely with ammonium during the colder months, suggesting ammonium nitrate is the dominant compound of nitrate in winter. Finally, organic carbon correlated well with ammonium exclusively in spring, suggesting that amines may be an important source of organic carbon at MSY at certain times of year.

Supplementary material related to this article is available online at: http://www.atmos-chem-phys.net/12/8341/2012/acp-12-8341-2012-supplement.pdf.

Acknowledgements. This study was supported by the Ministry of Economy and Competitivity of Spain and FEDER funds under the project CARIATI (CGL2008-06294/CLI) and by the project VAMOS (CGL2010-19464/CLI). The Montseny site forms part of the ACTRIS network (European Union Seventh Framework Programme (FP7/2007–2013) project No. 262254), formerly EUSAAR (EUSAAR R113-CT-2006-026140). The authors would like to extend their gratitude to Jesús Parga and Jordi Gil for their technical support, to AEMET and also to the various stations that provided information and data from Spain under the EMEP network. Finally, we would like to express our gratitude to Airbase-EEA and EMEP for allowing free access to ambient PM levels recorded at a large number of sites in Europe, much of the data having been presented in this study.

Edited by: E. Gerasopoulos

References

Aiken, A. C., DeCarlo, P. F., Kroll, J. H., Worsnop, D. R., Huffman, J. A., Doherty, K., Ulbrich, I. M., Mohr, C., Kimmel, J.r., Sueper, D., Zhang, Q., Sun, Y., Trimborn, A., Northway, M., Ziemann, P. J., Canagaratna, M. R., Onasch, T. B., Alfarra, R., Prévôt, A. S. H., Dommen, J., Duplissy, J., Metzger, A., Baltensperger, U., and Jimenez, J. L.: O/C and OM/OC Ratios of Primary, Secondary, and Ambient Organic Aerosols with High Resolution Time-of-Flight Aerosol Mass Spectrometry, Environ. Sci. Technol., 42, 4478–4485, 2005.

Arruti, A., Fernández-Olmo, I., and Irabien, A.: Impact of the global economic crisis on metal levels in particulate matter (PM) at an urban area in the Cantabria Region (Northern Spain), Environ. Pollut., 159, 1129–1135, 2011.

Barmpadimos, I., Keller, J., Oderbolz, D., Hueglin, C., and Prévôt, A. S. H.: One decade of parallel fine ($PM_{2.5}$) and coarse (PM_{10}–$PM_{2.5}$) particulate matter measurements in Europe: trends and variability, Atmos. Chem. Phys., 12, 3189–3203, doi:10.5194/acp-12-3189-2012, 2012.

Bruno, J., Pon, J., and Russi, D.: Report on Air Quality and Health: the cost of improvement of air quality (in Catalan), Generalitat de Catalunya, Departament de Medi Ambient i Habitatge, December, 2007.

Gangoiti, G., Millán, M. M., Salvador, R., and Mantilla, E.: Long range transport and re-circulation of pollutants in the Western Mediterranean during the RECAPMA-Project, Atmos. Environ., 35, 6267–6276, 2001.

Ge, X., Wexler, A. S., and Clegg, S. L.: Atmospheric amines-Part 1. A review, Atmos. Environ., 45, 524–546, 2011.

Gilbert, R. O.: Statistical methods for environmental pollution monitoring, Van Nostrand Reinhold, New York, 1987.

Ginoux, P., Prospero, J. M., Torres, O., and Chin, M.: Long-term simulation of global dust distribution with the GOCART model: correlation with North Atlantic Oscillation, Environ. Modell. Softw., 19, 113–128, 2004.

Harrison, R. M. and Pio, C.: Size differentiated composition of inorganic aerosol of both marine and continental polluted origin, Atmos. Environ., 17, 1733–1738, 1983.

Hurrell, J. and Deser, C.: North Atlantic climate variability: the role of the North Atlantic oscillation, J. Marine Syst., 78, 28–41, 2009.

Hurrell, J., Kushnir, Y., Otterson, G., and Visbeck, M.: An overview of the north Atlantic oscillation. The North Atlantic Oscillation: climate significance and environmental impact, Geophys. Monogr., 134, 1–35, 2003.

IPCC: Climate Change 2007: The Physical Science Basis, Contribution of Working Group I to the Fourth Assessment Report of the IPCC, ISBN 978 0521 88009-1 Hardback; 978 0521 70596-7 Paperback, 2007.

Jorba, O., Pérez, C., Rocadenbosch, F., and Baldasano, J. K.: Cluster Analysis of 4-Day Back Trajectories Arriving in the Barcelona Area (Spain) from 1997 to 2002, J. Appl. Meteorol, 43, 887–901, 2004.

Lyamani, H., Olmo, F.J., Foyo, I., and Alados-Arboledas, L.: Black carbon aerosols over an urban area in south-eastern Spain: Changes detected after the 2008 economic crisis. Atmos. Environ. 45, 6423–6432, 2011.

Millán, M., Salvador, R., Mantilla, E., and Kallos, G.: Photooxidant dynamics in the Mediterranean basin in summer: results from European research projects, J. Geophys. Res., 102, 8811–8823, 1997.

Minguillón, M. C., Perron, N., Querol, X., Szidat, S., Fahrni, S. M., Alastuey, A., Jimenez, J. L., Mohr, C., Ortega, A. M., Day, D. A., Lanz, V. A., Wacker, L., Reche, C., Cusack, M., Amato, F., Kiss, G., Hoffer, A., Decesari, S., Moretti, F., Hillamo, R., Teinilä, K., Seco, R., Peñuelas, J., Metzger, A., Schallhart, S., Müller, M., Hansel, A., Burkhart, J. F., Baltensperger, U., and Prévôt, A. S. H.: Fossil versus contemporary sources of fine elemental and organic carbonaceous particulate matter during the DAURE campaign in Northeast Spain, Atmos. Chem. Phys., 11, 12067–12084, doi:10.5194/acp-11-12067-2011, 2011.

Moreno, T., Querol, X., Alastuey, A., Reche, C., Cusack, M., Amato, F., Pandolfi, M., Pey, J., Richard, A., Prévôt, A. S. H., Furger, M., and Gibbons, W.: Variations in time and space of trace metal aerosol concentrations in urban areas and their surroundings, Atmos. Chem. Phys., 11, 9415–9430, doi:10.5194/acp-11-9415-2011, 2011.

Moulin, D., Lambert, C. E., Dulac, F., and Dayan, U.: Control of atmospheric export of dust from North Africa by the North Atlantic Oscillation, Nature, 387, 691–694, 1997.

Peñuelas, J., Llusia, J., and Gimeno, B. S.: Effects of ozone concentrations on biogenic volatile organic compounds emission in the Mediterranean region, Environ. Pollut., 105, 17–23, 1999.

Pérez, C., Sicard, M., Jorba, O., Comeron, A., and Baldasano, J. K.: Summertime re-circulations of air pollutants over the northeastern Iberian coast observed from systematic EARLINET lidar measurements in Barcelona, Atmos. Environ., 38, 3983–4000, 2004.

Pérez, N., Pey, J., Castillo, S., Viana, M., Alastuey, A., and Querol, X.: Interpretation of the variability of levels of regional background aerosols in the Western Mediterranean, Sci. Total Environ., 407, 524–540, 2008.

Pey, J., Pérez, N., Castillo, S., Viana, M., Moreno, T., Pandolfi, M., López-Sebastián, J. M., Alastuey, A., and Querol, X.: Geochemistry of regional background aerosols in the Western Mediterranean, Atmos. Res., 94, 422–435, 2009.

Pey, J., Pérez, N., Querol, X., Alastuey, A., Cusack, M., and Reche, C.: Intense winter pollution episodes affecting the Western Mediterranean, Sci. Total Environ., 408, 1951–1959, 2010.

Pope, C. A. and Dockery, D. W.: Health effects of fine particulate air pollution: lines that connect, J. Air. Waste Manage., 56, 709–42, 2006.

Querol, X., Alastuey A., Puicercus, J. A., Mantilla, E., Ruiz, C. R., Lopez-Soler, A., Plana, F., and Artíñano, B.: Seasonal evolution of suspended particles around a coal-fired power station: particulate levels and sources. Atmos. Environ., 32, 719–731, 1998a.

Querol, X., Alastuey A., Puicercus, J. A., Mantilla, E., Ruiz, C. R., Lopez-Soler, A., Plana, F., and Artíñano, B.: Seasonal evolution of suspended particles around a coal-fired power station: particulate levels and sources, Atmos. Environ., 32, 1963–1978, 1998b.

Querol, X., Alastuey, A., Rodríguez, S., Plana, F., Mantilla, E., and Ruiz, C. R.: Monitoring of PM_{10} and $PM_{2.5}$ around primary particulate anthropogenic emission sources, Atmos. Environ., 35, 845–858, 2001.

Querol, X., Alastuey, A., Viana, M. M., Rodríguez, S., Artíñano, B., Salvador, P., Santos, S. G. D., Patier, R. F., Ruiz, C. R., Rosa, J. D. L., Campa, A. S. D. L., Menedez, M., and Gil, J. I.: Speciation and origin of PM_{10} and $PM_{2.5}$ in Spain, J. Aerosol Sci., 35, 1151–1172, 2004.

Querol, X., Pey, J., Minguillón, M. C., Pérez, N., Alastuey, A., Viana, M., Moreno, T., Bernabé, R. M., Blanco, S., Cárdenas, B., Vega, E., Sosa, G., Escalona, S., Ruiz, H., and Artíñano, B.: PM speciation and sources in Mexico during the MILAGRO-2006 Campaign, Atmos. Chem. Phys., 8, 111–128, doi:10.5194/acp-8-111-2008, 2008.

Querol, X., Alastuey, A., Pey, J., Cusack, M., Pérez, N., Mihalopoulos, N., Theodosi, C., Gerasopoulos, E., Kubilay, N., and Koçak, M.: Variability in regional background aerosols

within the Mediterranean, Atmos. Chem. Phys., 9, 4575–4591, doi:10.5194/acp-9-4575-2009, 2009.

Rodríguez, S., Querol, X., Alastuey, A., and Mantilla, E.: Origin of high PM_{10} and TSP concentrations in summer in Eastern Spain, Atmos. Environ., 36, 3101-3112, 2002.

Rodríguez, S., Querol, X., Alastuey, A., Viana, M., and Mantilla, E.: Events affecting levels and seasonal evolution of airborne particulate matter concentrations in the Western Mediterranean, Environ. Sci. Technol., 37, 216–222, 2003.

Salmi, T., Määttä, A., Anttila, P., Ruoho-Airola, T., and Amnell, T.: Detecting trends of annual values of atmospheric pollutants by the Mann-Kendall test and Sen's slope estimates-the Excel template application MAKESENS, in: Publications on Air Quality No. 31, Finnish Meteorological Institute, 35 pp., 2002.

Seco, R., Peñuelas, J., Filella, I., Llusià, J., Molowny-Horas, R., Schallhart, S., Metzger, A., Müller, M., and Hansel, A.: Contrasting winter and summer VOC mixing ratios at a forest site in the Western Mediterranean Basin: the effect of local biogenic emissions, Atmos. Chem. Phys., 11, 13161–13179, doi:10.5194/acp-11-13161-2011, 2011.

Soriano, C., Baldasano, J. M, Buttler, W. T., and Moore, K.: Circulatory Patterns of Air Pollutants within the Barcelona Air Basin in a summertime situation: Lidar and Numerical Approaches, Bound.-Lay. Meteorol., 98, 33–55, 2001.

Tsyro, S., Yttri, K. E., and Aas, W.: Measurement and model assessment of particulate matter in Europe, 2009. EMEP Transboundary particulate matter in Europe Status Report, 4/2011, 23–52, 2011.

Turpin, B. J. and Lim, H. J.: Species contributions to $PM_{2.5}$ mass concentrations: Revisiting common assumptions for estimating organic mass, Aerosol Sci. Technol., 35, 602–610, 2001.

Van Dingenen, R., Raes, R., Putaud, J. P., Baltensperger, U., Charron, A., Facchini, M. C., Decesari, S., Fuzzi, S., Gehrig, R., Hansson, H. C., Harrison, R. M., Hüglin, C., Jones, A. M., Laj, P., Lorbeer, G., Maenhaut, W., Palmgren, F., Querol, X., Rodriguez, S., Schneider, J., ten Brink, H., Tunved, P., Tørsed, K., Wehner, B., Weingartner, E., Wiedensohler, A., and Wåhlin, P.: A European aerosol phenomenology-1: physical characteristics of particulate matter at kerbside, urban, rural and background sites in Europe, Atmos. Environ., 38, 2561–2577, 2004.

Vicente-Serrano, M. S., Trigo, M. R., López-Moreno, J. I., Liberato, M. L. R., Lorenzo-Lacruz, J., Beguería, S., Morán-Tejeda, E., and El Kenawy, A.: Extreme winter precipitation in the Iberian Peninsula 2010: anomalies, driving mechanisms and future projections, Clim. Res., 46, 51–65, 2011.

Visbeck, M. H., Hurrell, J. W., Polvani, L., and Cullen, H. M.: The North Atlantic Oscillation: past, present and future, P. Natl. Acad. Sci. USA, 98, 12876–12877, 2001.

Article 2

Cusack, M., Pérez, N., Pey, J., Alastuey, A., Querol, X.

Source apportionment of fine PM and sub-micron particle number concentrations at a regional background site in the western Mediterranean: a 2.5 year study.

Atmospheric Chemistry and Physics, 13, 5173-5187, 2013

Pages: 103-117

Published in: May 2013

Impact factor of Journal: 5.52

Atmos. Chem. Phys., 13, 5173–5187, 2013
www.atmos-chem-phys.net/13/5173/2013/
doi:10.5194/acp-13-5173-2013

Atmospheric Chemistry and Physics Open Access

Source apportionment of fine PM and sub-micron particle number concentrations at a regional background site in the western Mediterranean: a 2.5 year study

M. Cusack[1,2], N. Pérez[1], J. Pey[1], A. Alastuey[1], and X. Querol[1]

[1]Institute of Environmental Assessment and Water Research, IDÆA, CSIC, C/ Jordi Girona, 18–26, 08034, Barcelona, Spain
[2]Institute of Environmental Science and Technology (ICTA), Universitat Autónoma de Barcelona, 08193, Bellaterra, Barcelona, Spain

Correspondence to: M. Cusack (michael.cusack@idaea.csic.es)

Received: 4 December 2012 – Published in Atmos. Chem. Phys. Discuss.: 13 February 2013
Revised: 11 April 2013 – Accepted: 25 April 2013 – Published: 22 May 2013

Abstract. The chemical composition and sources of ambient fine particulate matter (PM_1) over a period of 2.5 years for a regional background site in the western Mediterranean are presented in this work. Furthermore, sub-micron particle number concentrations and the sources of these particles are also presented. The mean PM_1 concentration for the measurement period was 8.9 µg m^{-3}, with organic matter (OM) and sulphate comprising most of the mass (3.2 and 1.5 µg m^{-3} respectively). Six sources were identified in PM_1 by Positive Matrix Factorisation (PMF): secondary organic aerosol, secondary nitrate, industrial, traffic + biomass burning, fuel oil combustion and secondary sulphate. Typically anthropogenic sources displayed elevated concentrations during the week with reductions at weekends. Nitrate levels were elevated in winter and negligible in summer, whereas secondary sulphate levels underwent a contrasting seasonal evolution with highest concentrations in summer, similar to the fuel oil combustion source. The SOA source was influenced by episodes of sustained pollution as a result of anticyclonic conditions occurring during winter, giving rise to thermal inversions and the accumulation of pollutants in the mixing layer. Increased levels in summer were owing to higher biogenic emissions and regional recirculation of air masses. The industrial source decreased in August due to decreased emissions during the vacation period. Increases in the traffic + biomass burning source were recorded in January, April and October, which were attributed to the occurrence of the aforementioned pollution episodes and local biomass burning emission sources, which include agriculture and domestic heating systems. Average particle number concentrations (N_{9-825} nm) from 5/11/2010 to 01/06/2011 and from 15/10/2011 to 18/12/2011 reached 3097 cm^{-3}. Five emission sources of particle of sub-micron particles were determined by Principal Component Analysis (PCA); industrial + traffic + biomass burning, new particle formation + growth, secondary sulphate + fuel oil combustion, crustal material and secondary nitrate. The new particle formation + growth source dominated the particle number concentration (56 % of total particle number concentration), especially for particles < 100 nm, followed by industrial + traffic + biomass burning (13 %). Secondary sulphate + fuel oil combustion (8 %), nitrate (9 %) and crustal material (2 %) were dominant for particles of larger diameter (> 100 nm) and thus did not influence the particle number concentration significantly.

1 Introduction

The negative impacts of particulate matter (PM) on human health have been well established in literature (Pope and Dockery, 2006). Furthermore, the ability of ambient PM to impact the Earth's climate (IPCC, 2007), visibility and natural ecosystems has made it the focus of intensive study for many decades now. Current legislation in Europe enforces controls on emissions and ambient levels of PM_{10} (particles of diameter < 10 µm) and $PM_{2.5}$ (< 2.5 µm), such as the European Directive 2008/50/EC. Particle size is an important factor when considering the ability of particles to penetrate

into the human respiratory system (Lighty et al, 2000) and the fine fraction (PM_1) and sub-micron particle number concentration may be more detrimental to human health owing to their capacity to penetrate deeper into the lungs. Despite this fact, the fine PM fraction and its chemical composition remain relatively understudied, especially outside urban areas. In recent years much attention has been focused on the aerosol sub-micron particle number concentration, which has been shown to have an inverse relationship with mass (Rodríguez et al., 2007; Pey et al., 2008). This implies that a reduction of ambient PM concentrations, as encouraged by pollution abatement strategies, might actually increase sub-micrometer particle number concentrations. Thus, understanding the chemical composition and sources of fine PM and sub-micron particles is vital. Of the few studies performed on PM_1, most are concerned with the urban environment, and were characterised during short measurement campaigns (Vecchi et al., 2008; Richard et al., 2011). Cozic et al. (2008) published results on organic and inorganic compounds in PM_1 for 7 years at a high alpine site in Switzerland (Jungfraujoch). Bourcier et al. (2012) studied PM_1 concentrations and seasonal variability over one year at the high altitude site of puy de Dôme in France. However, of the studies mentioned, source apportionment was only performed for PM_1 at urban sites by Vecchi et al. (2008) and Richard et al. (2011). Minguillón et al. (2012) performed source apportionment of PM_1 at a rural site in Switzerland but only for short measurement campaigns during summer and winter. Source apportionment studies are important to help identify the major pollution sources affecting ambient PM and particle number concentrations. The characterisation of the sources of sub-micron particles has been performed in urban environments using Principal Component Analysis (Pey et al., 2009b) and Positive Matrix Factorisation (Harrison et al., 2011).

The accumulation of a relatively long series of PM_1 levels and chemical composition data in this study (September 2009 to January 2012) has allowed for the investigation of the daily and seasonal variation in PM_1 and the identification of a number of sources affecting PM_1 at a regional background site in the western Mediterranean. Furthermore, in the present study a large number of parameters, including PM_1 chemical components, gaseous pollutants and meteorological variables have been combined with particle number size distribution in order to identify and quantify the contribution of various sources to atmospheric sub-micron particle concentrations. To the author's knowledge, no similar study exists in the literature for regional background sites.

2 Methodology

2.1 Sampling site

Regular sampling of PM_1 for gravimetric analysis was performed at a regional background (RB) site in the North East of the Iberian Peninsula. The site Montseny (MSY; 41°46′ N, 02°21′ E, 720 m.a.s.l.) is located in the Montseny natural park, 40 km from the greater urbanised area of Barcelona and 25 km from the Mediterranean coast. The mountainous region in which the site is located is sparsely populated and densely forested, but pollution from the region affects the area regularly, which is especially influenced by mesoscale and synoptic meteorology. The cyclical nature of prevailing mountain and sea breezes can transport urban and industrial emissions from the densely populated valleys and depressions below MSY to the site. Furthermore, MSY can be subjected to sustained episodes of pollution during winter (winter anticyclonic episodes; WAE), whereby calm weather creates a stagnant air mass and the accumulation of aerosols, increasing pollutant levels substantially. These pollution episodes (associated with anticyclonic pressure systems) tend to persist until removed by less calm weather such as strong winds which disperse the air mass. In summer, high pressure systems and insolation create regional recirculation of air masses, causing the aging and recirculation of air masses containing aerosols, particularly ammonium sulphate, over a larger area. Furthermore, episodes of Saharan dust intrusions are more frequent in summer, although they can occur year-round. Lower rainfall in summer also promotes the resuspension of soils and intensified solar radiation increases biogenic emissions and photochemical reactions of aerosols (Seco et al., 2011). These factors combined result in generally higher aerosol levels across the region for the summer months. Winter time levels are comparatively lower owing to higher precipitation and Atlantic advection, except when anticyclonic conditions prevail. For further information and details on atmospheric dynamics and PM trends at MSY see Pérez et al. (2008), Pey et al. (2010) and Cusack et al. (2012).

2.2 Measurements

Samples of PM_1 were collected on quartz fibre filters (Pallflex) consecutively every four days from September 2009 to January 2012 with high volume samplers ($30\,m^3\,h^{-1}$) DIGITEL-DH80, equipped with a PM_1 cut-off inlet (also DIGITEL). 182 samples were collected in total. Filter pre-treatment consisted of oven-baking the filters at 200 °C for 4 h to remove impurities, followed by conditioning for 24 h at 20–25 °C and 25–30 % relative humidity. Following sampling, the filters were weighed three times on three consecutive days. PM mass concentrations were determined by standard gravimetric procedures, and complete

chemical analysis for all filters was performed following the procedures described by Querol et al. (2001).

Chemical analysis was performed by a range of instrumental techniques to determine concentrations of various elements and components. Acid digestion ($HF:HNO_3:HClO_4$) of ½of each filter was carried out and subsequently analysed by Inductively Coupled Plasma Atomic Emission Spectroscopy, ICP-AES (IRIS Advantage TJA solutions, THERMO) to determine concentrations of major components (Al, Ca, Na, Mg, Fe, K). Trace element concentrations were determined by means of Inductively Coupled Plasma Mass Spectroscopy, ICP-MS (X Series II, THERMO). ¼ of the filter was analysed for water soluble ions SO_4^{2-}, NO_3^-, NH_4^+ and Cl^- and analysed by Ion Chromatography HPLC (High Performance Liquid Chromatography) using a WATERS IC-pakTM anion column and WATERS 432 conductivity detector. NH_4^+ was determined by an ion specific electrode. Organic and Elemental Carbon (OC and EC) were measured using the remaining ¼ of each filter by a thermal-optical transmission technique using a Sunset Laboratory OCEC Analyser. The EUSAAR2 protocol was employed (as outlined by Cavalli et al., 2010). Organic Matter (OM) is calculated from OC by multiplying by a factor of 2.1 as suggested by Turpin et al. (2001) and Aiken et al., (2005). SiO_2 and CO_3^{2-} were indirectly determined from empirical formulas (Querol et al., 2001). A complete dataset of major components (OC, EC, NO_3^-, SO_4^{2-}, NH_4^+, Cl^- Al, Ca, Na, Mg, Fe and K) and trace elements (Ti, V, Cr, Mn, Ni, Cu, Zn, As, Rb, Sr, Cd, Sn, Sb, La, Pb, among others) was thus compiled. Crustal material was determined from the sum of concentrations of Al_2CO_3, SiO_2, CO_3^{2-}, Ca, K, Mg and Fe. Sea spray was determined from the sum of Na^+ and Cl^-. The combined sum of the determined chemical components accounted for almost 70 % of the total PM mass. For each set of ten filters, nine were sampled and one was reserved for blank analysis. The corresponding blank filter was analysed using the same procedures described for OC/EC, water soluble ions and for major/minor elements. Blank concentrations were subtracted from the total concentration measured for each sample, thus giving ambient concentrations.

Sub-micron particle number size distribution was measured using a mobility particle size spectrometer operated in the scanning mode. In the following article, we call the system a Scanning Mobility Particle Sizer (SMPS). The SMPS system comprises a Differential Mobility Analyzer (DMA) connected to a Condensation Particle Counter (CPC, Model TSI 3772). The DMA system was designed and manufactured in the framework of EUSAAR project at the Leibniz Institute for Tropospheric Research (IfT) in Leipzig, Germany. The SMPS system provided a complete particle number size distribution of the number of particles between 9 and 825nm (N_{9-825}), and completed one scan every five minutes. Prior to sampling, the aerosol is dried using a nafion dryer in order to maintain a relative humidity below 40 %. The sampled aerosol flow was maintained at $1\,l\,min^{-1}$ at the inlet and the dried sheath air flow was maintained at $5\,l\,min^{-1}$.

Black Carbon (BC) concentrations were measured continuously using a Multi Angle Absorption Photometer (MAAP, model 5012, Thermo). Real time measurements of O_3, NO, NO_2, CO and SO_2 were obtained on-site, supplied by the Department of the Environment of the Autonomous Government of Catalonia. Hourly levels of wind direction, wind speed, solar radiation, temperature, relative humidity and precipitation were recorded in real-time on site. See Pérez et al. (2008) for further details. Solar radiation is presented in this work as the sum of hourly averages of solar radiation.

2.3 Source apportionment

2.3.1 Positive Matrix Factorisation

Source apportionment analysis was performed on the data set of PM_1 using Positive Matrix Factorisation (PMF) by means of EPA PMF v3.0 software. PMF is a multivariate tool used to determine source profiles by decomposing a matrix of data composed of chemical species into two matrices – factor contributions and factor profiles. The method employed in this work is based on that described by Paatero and Taper (1994). Individual estimates of the uncertainty associated with each data value are required as PMF is a weighted least-squares method. The individual estimates of uncertainty in the data set were determined following the methodology described by Amato et al. (2009). This methodology is similar to that described by Thompson and Howarth (1976), but also considers the uncertainty associated with blank filter subtraction from each sample. Elements used in this study (OC, SO_4^{2-}, NO_3^-, NH_4^+, EC, Al, Ca, K, Na, Mg, Fe, Mn, Ti, V, Cr, Ni, Cu, Zn, As, Rb, Sr, Cd, Sn, Sb, Pb and La) were selected according to their signal to noise ratio (S/N), whereby species with $S/N < 2$ were defined as weak, and species with $S/N > 2$ defined as strong. These criteria resulted in 12 strong species and 15 weak species. The total PM_1 concentration was set as the "total variable" and thus automatically categorised as "weak", increasing the uncertainty of this variable by a factor of three so as not to affect the PMF solution. In total, the matrix included 182 cases. After a variety of factor numbers were tested, it was observed that a 6 factor solution provided the most meaningful results, with a correlation coefficient (R^2) of 0.71 between the modelled and experimental PM_1 concentrations, with Q values of 2816 (Robust) and 2833 (True). Correlation coefficients (R^2) between modelled and measured concentrations for OC, sulphate and nitrate were 0.97, 0.95 and 0.99 respectively. These Q values were investigated for different FPEAK values, with FPEAK = 0 found to be the most reasonable. 100 bootstrap runs with a minimum R^2 of 0.6 were also performed to test the uncertainty of the resolved profiles, with all 6 factors being mapped, verifying the stability of the results.

2.3.2 Principal component analysis

Principal component analysis (PCA) was performed using the software STATISTICA v4.2. The orthogonal transformation method with Varimax rotation was employed, retaining principal components with eigenvalues greater than one. The dataset used for PCA was comprised of the PM_1 total mass and its constituents OC, EC, Al_2O_3, Ca, Fe, K, Mg, Na, SO_4^{2-}, NO_3^-, NH_4^+, Ti, V, Mn, Ni, Cu, Zn, As, Cd, Sn, Sb, La, Ce and Pb. The following variables were also included: NO_2, SO_2, BC, temperature, solar radiation and wind speed. Particle number concentrations were calculated for different size bins; N_{9-30}, N_{30-50}, N_{50-100}, $N_{100-300}$, $N_{300-500}$, $N_{500-825}$. Days whereby simultaneous measurements of particle number size distribution and chemical analysis were performed were included for PCA analysis, which totalled 61 cases, from 05/11/2010 to 01/06/2011 and from 15/10/2011 to 18/12/2011 (the instrument was under repair from June to October 2011). A typical robust PCA analysis requires a large dataset (> 100 cases), which is significantly more than presented in this work, and therefore the reduced dataset may propose a limitation in the data analysis presented. This technique allows for the identification of potential sources (principal components) with respect to the particle number concentration in different size ranges. Furthermore, a multilinear regression analysis (MLRA) allows for the calculation of the daily contribution of each source to the particle number concentration following the methodology proposed by Thurston and Spengler (1985) and Pey at al. (2009b). MLRA was applied to the data set using the particle number concentrations in each of the aforementioned size bins as the dependent variables and the principal component factor scores as the independent variables. The comparison between the experimental number concentration and the modelled concentration provided good correlation ($R^2 = 0.86$).

3 Results and Discussion

3.1 PM concentrations and composition

The average PM_1 concentrations (arithmetic mean) for the entire measurement period (24/09/2009 to11/01/2012) were $8.9 \pm 4\,\mu g\,m^{-3}$. PM_1 concentrations at MSY undergo a clear seasonality with minimum concentrations in winter ($6.6\,\mu g\,m^{-3}$), followed by autumn ($7.6\,\mu g\,m^{-3}$), spring ($9.4\,\mu g\,m^{-3}$) and summer ($11.2\,\mu g\,m^{-3}$). OM is the largest component of PM_1 ($3.2\,\mu g\,m^{-3}$; 37 %), as shown in Fig. 1. OM sources at MSY are varied, but are mostly attributed to secondary organic aerosol (SOA) produced from anthropogenic volatile organic compounds (VOCs) emitted from industry and road traffic, mixed anthropogenic/natural sources such as biomass burning, and natural sources such as biogenic emissions (Seco et al., 2011). Sulphate is the second most abundant compound in PM_1 ($1.5\,\mu g\,m^{-3}$; 16 %)

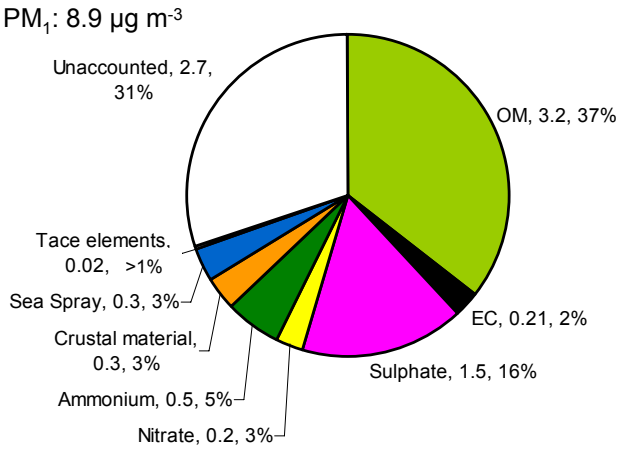

Fig. 1. Chemical composition of PM_1 at MSY from 24/09/2009 to 11/01/2012.

and is associated with power generation, industrial and shipping emissions, followed by ammonium ($0.5\,\mu g\,m^{-3}$; 5 %) and nitrate ($0.2\,\mu g\,m^{-3}$; 3%). Nitrate concentrations are significantly elevated in winter and much lower in summer owing to its thermal instability (Harrison and Pio, 1983, Querol et al, 2001). Ammonium nitrate can be volatilised in the atmosphere in warmer conditions associated with the Mediterranean climate, especially in summer. However, a negative artefact may also account for the reduced concentrations measured in summer, due to the volatilisation of ammonium nitrate from the filter during and after sampling. Crustal material, sea spray and EC (from traffic and biomass burning emissions) make up the remainder of the major components of PM_1, with concentrations of 0.3, 0.3 and $0.21\,\mu g\,m^{-3}$ respectively. The sum of trace element concentrations is $0.02\,\mu g\,m^{-3}$.

Long term PM_1 measurements at RB sites are relatively scarce in literature. Long term measurements of PM_1 were performed at a high altitude site (Jungfraujoch, 3580 m.a.s.l.) in Switzerland (Cozic et al., 2008). A clear seasonality for chemical components was observed at the site with low concentrations during winter owing to the residence of the site in the free troposphere, and higher concentrations in summer owing to enhanced vertical transport of boundary layer pollutants. A similar seasonality was observed for PM_1 at puy de Dôme (1465 m.a.s.l.) with higher summer concentrations and a winter minimum (Bourcier et al., 2012). Both these sites are high altitude sites, at higher altitudes than MSY (720 m.a.s.l.), and are considerably more influenced by free tropospheric air, although MSY exhibits a similar seasonal trend. Spindler et al. (2010) reported average concentrations of 12–13 $\mu g\,m^{-3}$ of PM_1 for a RB site in Germany (Melpitz). A study by Minguillón et al. (2012) compared PM_1 concentrations at a RB site in Switzerland (Payerne) for one month in winter and in summer. The concentrations of PM_1 at this site were $12\,\mu g\,m^{-3}$ and $6\,\mu g\,m^{-3}$ in winter and

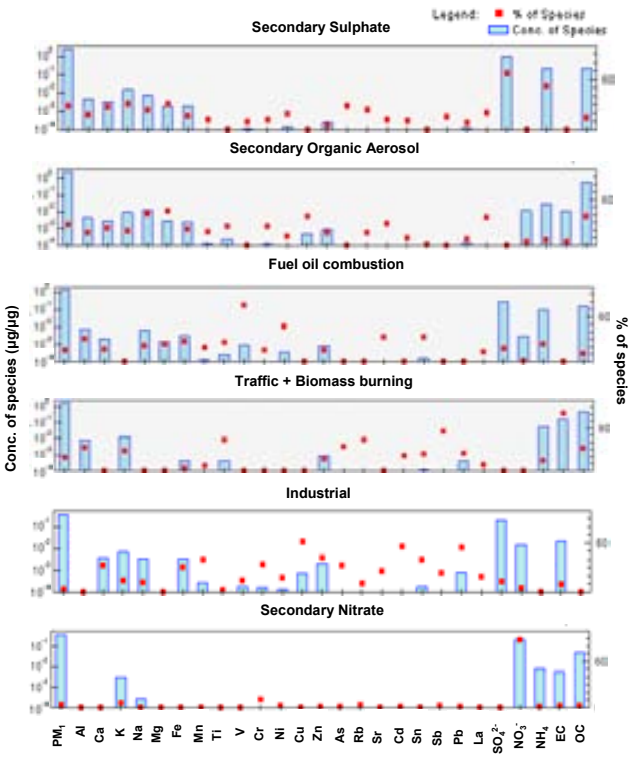

Fig. 2. Source profiles (µg/µg) identified for PM_1 measured at MSY. All available PM_1 samples (182) were used. The mass of each species apportioned to the factor (blue bar, left axis) and the percent of each species apportioned to each factor (red square, right axis) is shown.

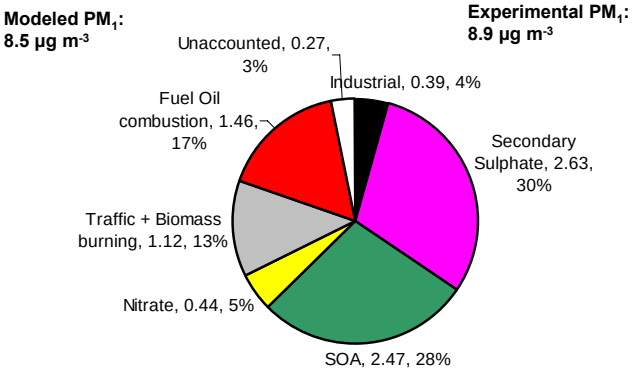

Fig. 3. Average contribution of each source ($\mu g\,m^{-3}$) to PM_1 obtained by PMF.

summer respectively (overall mean of $9\,\mu g\,m^{-3}$). The winter maximum at Payerne is a result of increased biomass burning emissions and intense thermal inversions, causing the accumulation of pollutants in populated valleys. These seasonal concentrations are in contrast to MSY, whereby winter concentrations are lower ($6.6\,\mu g\,m^{-3}$) than in summer ($11.2\,\mu g\,m^{-3}$). At MSY, all components give the lowest concentrations in winter and highest in summer, except for nitrate and sea spray (Table 1). EC concentrations were also lowest in summer but highest in the autumn.

This winter to summer increase in PM_1 can be attributed to the year-round dominance of SO_4^{2-} and OM concentrations on the overall mass. Sulphate and OM levels are higher during summer owing to; enhanced photochemistry associated with more intense solar radiation, lower air mass renovation on a regional scale (Rodríguez et al., 2003), and the increase of the mixing layer height giving higher regional transport that favours the regional mixing of polluted air masses (Pey et al., 2009a). Furthermore, biogenic emissions from surrounding vegetation at MSY in summer are considerably increased, affecting OM concentrations (Seco et al., 2011).

Increased levels of sulphate, ammonium, OM, EC and nitrate can also occur under specific atmospheric conditions such as WAE, whereby calm, cold, sunny weather favours the stagnation of air masses and accumulation of pollutants over several days (Pey et al., 2010). During these episodes, pollution that has accumulated around the industrialised and urbanised valleys below MSY is carried to the site by mountain breezes during the day, with cleaner tropospheric air present at night when the breeze retreats.

3.2 Source contribution to ambient PM levels

3.2.1 Identification of emission sources by PMF

Twenty six PM_1 chemical species with a signal to noise ration (S/N) greater than 0.2 were used in order to identify various sources. Six PM_1 sources were identified by PMF analysis. Figure 2 shows the source profiles and the percentages of ambient species concentration apportioned by each source.

The six PM_1 sources, in order of contribution to the PM_1 mass (Fig. 3) were: secondary sulphate ($2.63 \pm 2.85\,\mu g\,m^{-3}$), secondary organic aerosol (SOA; $2.47 \pm 1.84\,\mu g\,m^{-3}$), fuel oil combustion ($1.46 \pm 1.41\,\mu g\,m^{-3}$), traffic + biomass burning ($1.12 \pm 0.83\,\mu g\,m^{-3}$), industrial ($0.39 \pm 0.33\,\mu g\,m^{-3}$) and secondary nitrate ($0.44 \pm 1.13\,\mu g\,m^{-3}$). Although OM was identified as the major component of PM_1, SOA was not found to explain the largest variance in PM_1, probably because OC levels were consistently high (and less variable) compared to other components, thus reducing the explained variance of PM_1 by the SOA source. Thus, the secondary sulphate source accounted for the largest variance in PM_1 (28 %). Secondary sulphate is characterised mostly by ammonium sulphate, and accounts for 55 % of the variance of ammonium. Ammonium sulphate is associated with pollution across the region, when atmospheric recirculation causes the accumulation and aging of pollutants, especially in summer (Fig. 4). It is also characterised by many other components associated with both crustal elements (Al, Ca, La, Mg, Fe) and anthropogenic emissions (EC, As, Sb), highlighting the regional nature of this factor. A crustal source was not specifically identified by PMF analysis, but the presence of

Table 1. Mean annual and seasonal concentrations for major components of PM_1 at MSY, and sum of concentrations of trace elements (TE), in $\mu g\,m^{-3}$.

	PM_1	Crustal	Sea Spray	SO_4^{2-}	NO_3^-	NH_4^+	EC	OM	$\sum$ TE
Annual	8.9	0.3	0.3	1.5	0.2	0.5	0.21	3.2	0.021
Spring	9.4	0.3	0.2	1.3	0.2	0.4	0.22	2.9	0.018
Summer	11.2	0.4	0.4	2.4	0.1	0.7	0.16	3.8	0.028
Autumn	7.6	0.3	0.2	1.4	0.1	0.5	0.24	3.2	0.020
Winter	6.6	0.2	0.5	0.6	0.6	0.4	0.22	2.8	0.016

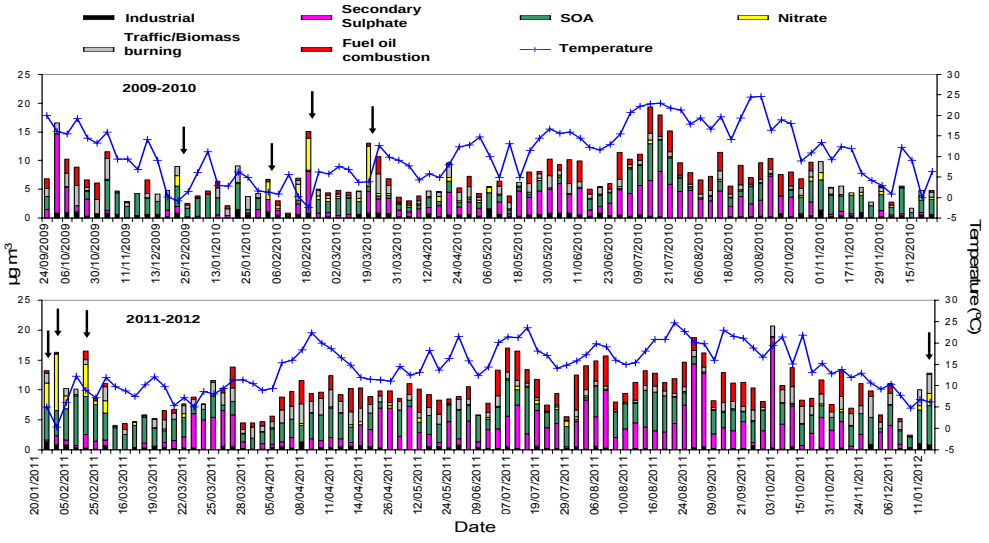

Fig. 4. Daily contribution of each source to total PM_1 mass concentration ($\mu g\,m^{-3}$) and temperature (°C) for 24/09/2009 to 19/12/2010 (above) and 20/01/2011 to 11/01/2012 (below). Intense winter pollution episodes are marked by black arrows.

crustal material was observed in both the secondary sulphate source and the SOA source. This is likely due to seasonal and meteorological influences, as soil resuspension and Saharan dust intrusions are most common in summer (Pérez et al., 2008), also when secondary sulphate and SOA are more abundant. In verification of this theory, the secondary sulphate source also explains 19 % of the variance in OC. This is probably due to the influence of summer recirculation episodes and more intense solar radiation, as emissions of OC and sulphate are likely to be independent of each other. Elevated levels of the secondary sulphate source also occur during episodes of pollution in winter such as WAE, as indicated by the arrows in Fig. 4.

The source titled SOA is the second most important source concerning PM_1 mass concentrations, comprising 28 % of the total mass. It is mostly characterised by OC (explaining 43 % of the total variance in OC). The annual variation of this source is mostly driven by two processes; (1) as is evident in Fig. 4, this source undergoes increased levels during prolonged episodes of winter pollution, mainly as a result of SOA produced from anthropogenic VOC and possibly biomass burning emissions. For example, elevated concentrations of SOA and nitrate were recorded at the beginning of 2011. (2) The observed increasing summer trend can be attributed to increased biogenic emissions from local vegetation, and enhanced photochemical reactions (Seco et al., 2012). A study performed by Minguillón et al. (2011) reported that the fraction of OC attributed to biomass burning at MSY in winter was 17–21 % and only 12 % in summer. In the same study, it was found that the fraction of OC attributed to fossil fuel consumption (mainly traffic emissions) was 34 ± 4 % and 31 ± 4 % for winter and summer respectively. Considering the clear seasonality of this source with elevated concentrations in summer, the low contribution of biomass burning to OC concentrations reported by Minguillón et al. (2011), the absence of EC in this source and the prohibition of open burning of agricultural biomass during summer (Spanish Decreto 64/1995), it can be reasonably assumed that this source is SOA with negligible input from biomass burning. As observed for the secondary sulphate source, some typical crustal elements such as La, Rb, Ti, Ca, Al, Mg, Fe and Sr are present, for the same reasons already described.

The third most important source in terms of contribution to the PM_1 mass is fuel oil combustion (17 %). This source is characterised by typical tracers V, Ni, and Sn (Pandolfi et al., 2011), and accounts for 19 % of the variance in sulphate and 24 % of ammonium, indicating that there is some overlap between the secondary sulphate source, specifically ammonium sulphate, and the fuel oil combustion source. Querol et al. (2009) reported that concentrations of V are elevated in the Mediterranean region owing to increased consumption of fuel oil for power generation, shipping and industrial emissions. The separation of this factor from that of secondary sulphate may give an indication of the age of the aerosol. SO_2 emissions from fuel oil combustion, emitted alongside V and Ni, may not be oxidised to SO_4^{2-} before reaching MSY, whereas the secondary sulphate source is older and representative of emissions across the region. This behaviour has also been observed in the Eastern Mediterranean (Öztürk et al., 2012). The presence of Na and Mg, typical marine aerosols, in the fuel oil combustion source may indicate the influence of shipping emissions. A source apportionment study of PM_{10} and $PM_{2.5}$ for the MSY site was performed by Pey et al. (2009a). In that study, the secondary sulphate and fuel oil combustion sources were not separated, but correlation was observed for secondary sulphate and sea spray emissions, indicating some influence of shipping emissions. Furthermore, it was shown that sea spray concentrations were considerably higher in summer at MSY owing to the increased sea breeze circulation over the coastal area (25 km from MSY).

The source of traffic + biomass burning (13 % of variance in PM_1) is identified from the presence of typical traffic tracers EC, OC, Sb and Sn (Amato et al., 2009; Minguillón et al., 2012). This source explains 78 % of the variance in EC. Minguillón et al. (2011) reported that 66–79 % of EC measured at MSY had a fossil origin, with the remainder attributed to biomass burning. The influence of biomass burning is highlighted by the presence of K, a known biomass burning tracer (Pio et al., 2008). An industrial source was identified, characterised by typical industrial tracers such as Pb, As, Cd, Sn, Cu, Zn, Cr, Fe and Mn (Viana et al., 2006; Belis et al., 2013). This source does not contribute substantially to the total PM mass (4 %) as it is mostly comprised of trace elements.

Finally, a secondary nitrate source was identified and was characterised to a very small extent by EC (3% of the total variance of EC) and K (7 %), probably as a result of mixing with aged traffic and biomass burning emissions. Some fraction of nitrate in PM_1 at MSY can exist as potassium nitrate, especially during WAE. Nitrate is most abundant in winter when temperatures are lower, and negligible in summer, as shown in Fig. 4. Thus, nitrate comprises little of the total PM_1 mass on a yearly basis (5 %), but its contribution to the mass increases to 19 % in winter.

To the author's knowledge, there are few existing source apportionment studies on fine PM, especially at RB sites. Most existing studies were performed at urban sites, such as that of Vecchi et al. (2008) and Richard et al. (2011). In the study by Vecchi et al. (2008), PMF was performed on PM_1 samples from three different urban areas across Italy, but major chemical components such as OC, EC, NH_4^+ and NO_3^- were not included. Minguillón et al. (2012) identified five sources during two month-long (summer and winter) measurement campaigns at a rural site in Switzerland, which were ammonium nitrate, ammonium sulphate + K + road traffic, industrial, road traffic and background V, Ni and Fe. This current study is the first of its kind to perform source apportionment studies on PM_1 and particle number concentrations at a RB site that comprises a large database of chemical species with long term measurements.

3.2.2 Daily and monthly variation

Figure 5 shows the daily variation of each source. The secondary sulphate source is generally elevated during the week with a decreasing trend at weekends. It undergoes an unusual weekly cycle in that concentrations decrease on Tuesday and Wednesday, which may be a result of some seasonal fluctuations rather than reflecting the true nature of the weekly trend. Episodes of regional pollution which most influence sulphate concentrations, especially in summer, induce the accumulation of pollutants from across the region over time, independent of the time of emission, which would affect the weekly cycle. However, a weekend decrease is observed, probably owing to lower SO_2 emissions on weekends. SOA does not undergo any discernible weekly pattern, as a large proportion of this source is natural, especially in summer. As stated previously, this source can be associated with anthropogenic activities in winter, but such seasonality is obviously not reflected in the weekly trend.

Conversely, sources identified as traffic + biomass burning, fuel oil combustion and industrial all undergo a marked weekly evolution with increasing concentrations throughout the week followed by a considerable reduction at weekends, when traffic flow and industrial activity would be diminished. Finally, the nitrate source undergoes a similar variation to that of traffic + biomass burning and the industrial source, with increasing concentrations during the week followed by minimum values at weekends.

The monthly variation of each source highlights the influence of meteorology and anthropogenic activities on each source (Fig. 6). The secondary sulphate source undergoes a clear monthly variation with highest concentrations recorded in summer, owing to the aforementioned regional pollution episodes and more intense insolation. Secondary sulphate concentrations in winter are reduced, when nitrate concentrations are at their highest, highlighting the thermal instability of particulate nitrate. Traffic + biomass burning is highest in January, April and October. Traffic emissions throughout the year should remain relatively constant, thus the observed variation must be due to other variable factors such as the aforementioned WAE and the influence of local meteorology (mountain breezes, thermal inversions), and also to

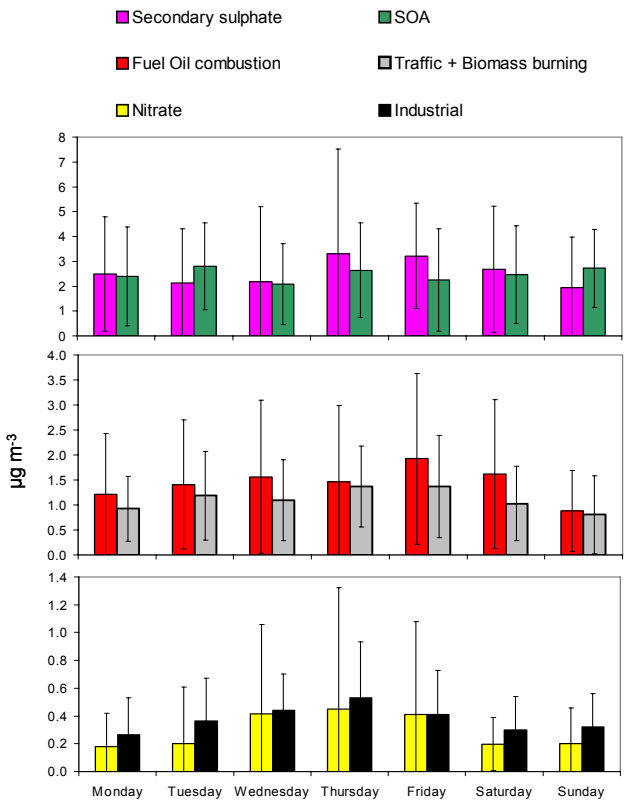

Fig. 5. Average daily concentrations ($\mu g\,m^{-3}$) of each source.

some extent emissions from biomass burning. The peak observed in January may be directly related to local emissions from domestic heating systems. The peaks observed in April and October may be explained by controlled biomass burning from local agriculture, which is common during these months. The impact of this factor is reduced at the height of summer (July and August), when biomass burning is prohibited to minimise risk of uncontrolled forest fires, and a reduction in traffic emissions occurs due to the vacation period in July/August. This also impacts the industrial source which is lowest in August. Finally, the fuel oil combustion source undergoes a similar variation to that of secondary sulphate, as this source would be influenced by the same factors. Furthermore, as noted previously, sea breeze circulation is substantially more influential during the summer months (Pey et al., 2009a). Therefore, shipping emissions are likely to be more influential owing to the enhanced sea breezes and may provide some explanation of the seasonality observed for the fuel oil combustion source. Furthermore, the presence of sulphate (19 % of the variance) and ammonium (24 %) in this source likely accounts for some of the seasonal variation observed in the fuel oil combustion source.

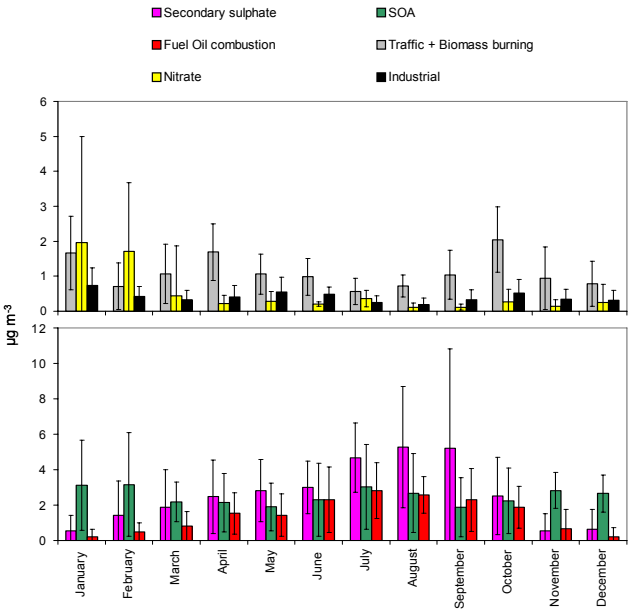

Fig. 6. Average monthly concentrations ($\mu g\,m^{-3}$) of each source.

3.3 Particle number concentrations

Average particle number concentrations (N_{9-825} nm) for the entire measurement period (5/11/2010 to 01/06/2011 and from 15/10/2011 to 18/12/2011) were 3097 cm^{-3}. While median values or geometric means are normally considered better suited for analysis of particle number size distributions to avoid giving too much weight to outlier values, arithmetic means are used here because PM_1 and its chemical components are daily averages, and outlier values occurring during 24 hr sampling can affect these concentrations similarly. For this reason, arithmetic mean particle number concentrations are reported in order to include, for example, short-lived or sudden changes in concentrations that would similarly affect PM_1 concentrations, BC, gaseous pollutants etc.

The Aitken mode (N_{30-100}) is the dominant particle mode with average concentrations of 1601 cm^{-3}, followed by the accumulation mode ($N_{100-825}$) at 881 cm^{-3}. The nucleation mode (N_{9-30}) registered the lowest concentrations of 616 cm^{-3}. A comparison of particle number concentrations measured at various sites across Europe found mean levels to range from 2000–10 000 cm^{-3} for continental boundary layer sites (Spracklen et al., 2010). Comparisons with particle number concentrations reported in that study suggest that levels at MSY most closely reflect those measured in Schauinsland, Germany (2772 cm^{-3}), which is a mid-level mountain station affected by regional pollution under certain conditions, similarly to MSY. Data was not available to include in this study from June to October, but there is evidence to suggest that summer concentrations of particles are substantially higher in summer at MSY. Thus, the mean annual particle number concentration given in this study is

likely to be underestimated due to the omission of summer measurements. This should be taken into consideration when comparing particle number concentrations with other sites.

3.4 Source contribution to ambient sub-micron number concentration

3.4.1 Identification of emission sources by PCA

The measurement of particle number concentrations and their size distribution (9–825 nm) in tandem with detailed chemical composition of PM_1 have also allowed for the identification of various sources affecting particle number concentrations. Similar studies have been performed with $PM_{2.5}$ chemical constituents in an urban environment (Pey et al., 2009), but few, if any, have been performed using PM_1 for a RB site. The application of PCA to the database explained 71 % of the variance of the data and allowed for the identification of five principal components, as shown in Table 2, which are: industrial + traffic + biomass burning, new particle formation + growth (NPF + G), secondary sulphate + fuel oil combustion, crustal material and secondary nitrate. These sources reflect the sources described previously for PMF, but the significantly reduced dataset used in the PCA analysis (61 daily samples) compared to PMF analysis (182 daily samples) resulted in the merging of some of the emission factors described in PMF, such as occurs for industrial + traffic + biomass burning, and secondary sulphate + fuel oil combustion. Unfortunately SOA was not identified by PCA, probably also as a result of the reduced dataset and incomplete summer measurements. A larger dataset with more cases (typically more than 100 cases for a robust analysis) may allow for the separation of these sources, or indeed the identification of new sources.

The principal component of industrial + traffic + biomass burning (34 % of the total variance) exhibits high factor loadings for variables typically associated with traffic emissions (EC, BC, OC, NO_2, Sn, Sb), industrial emissions (Pb, Zn, Cd, Mn, Cu) and biomass burning (OC, EC, BC, K). This component is closely associated with particles of 100–300 nm and 500–825 nm in diameter, suggesting this source mostly influences aerosol number concentrations in these two diameter ranges. Fresh emissions that are transported to MSY relatively quickly after emission would be expected to be smaller ($N_{100-300}$). Enduring regional pollution episodes, such as those that occur in winter, would promote the condensation of smaller particles onto the surface of larger particles within the aged air mass, and give rise to higher concentrations of larger particles ($N_{500-825}$).

The second component (12 % of the total variance) exists almost exclusively in the ultrafine mode (< 100 nm) in terms of concentration, and is not associated with any component of PM_1 or gaseous pollutant. However some relationship exists with temperature and solar radiation, suggesting this source is a result of photochemical nucleation and subsequent growth into particles of larger diameter. A negative factor loading is also observed for relative humidity (RH; –0.18), as RH is believed to have an inverse relationship with NPF (Hamed et al., 2011). The negative association with nitrate could indicate two alternative processes; (1) nitrate is most abundant when temperatures are lower, while on the other hand the component NPF + G bears some positive relationship with temperature, as evidenced in Table 2. Therefore, opposite meteorological conditions favour either the nitrate source or the NPF + G source. (2) In addition, the presence of coarse nitrate particles would act as a condensation sink and scavenge the gaseous precursors necessary for NPF. Fig. 7 highlights the opposing variation of nitrate concentrations and particle number concentrations in the nucleation mode.

Secondary sulphate + fuel oil combustion is marked by high factor loadings of ammonium sulphate and V and explains 10 % of the variance in particle number concentration. As previously observed with PMF analysis, this factor also strongly influences PM_1 concentrations, and exists across all size ranges (100–825 nm). The association with temperature/solar radiation is further indicative of this factor being most abundant under regional pollution episodes most typical in warmer seasons.

The component titled crustal material (10 % of the total variance) exhibits high factor loadings of Ce, La, Fe, Ni and Al_2O_3. This source contributes very little to the particle number concentration, as it most likely contributes to particles between 825 nm and 1 µm and coarse PM (not included in this study). Finally, nitrate is, similarly to that observed for PMF, characterised by NO_3^-, K and to a lesser extent NH_4^+ in the range of 300–825 nm. The presence of K may suggest some influence of biomass burning in this factor. Temperature is negatively correlated with this source as expected. This component explains the least amount of variance of all the sources (5 %). Attention must be drawn to the presence of N_{9-30} in this component (factor loading of 0.18), as this is in stark contrast to the theory that the presence of nitrate adversely affects NPF. As highlighted in Fig. 7, nitrate and N_{9-30} are, for the most part, anti-correlated. However, situations arise (indicated by the blue arrow) whereby their variation in the time series are similar, especially when nitrate concentrations are very low, and thus, PCA has identified these two variables as bearing some relationship. Rather than the nitrate source actually contributing to the nucleation mode (as suggested in Fig. 9; top graph), this is simply a limitation of PCA, whereby two variables that undergo similar variations coincidentally are considered to be related. It may also be hypothesised that NPF is occurring before the arrival of the polluted breeze (containing nitrate), however this seems unlikely as, if this were the case, the other sources such as industrial + traffic + biomass burning or secondary sulphate would also be present. This highlights the disadvantage of using 24 h PM_1 chemical component concentrations rather than, ideally, hourly concentrations.

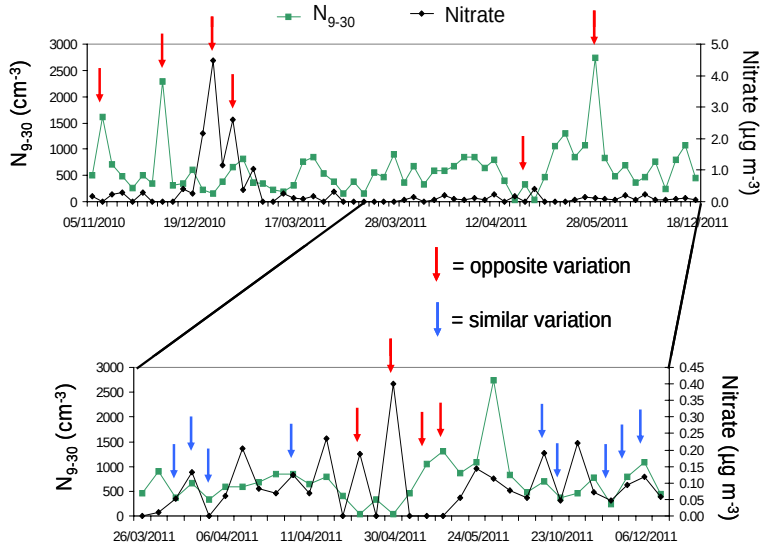

Fig. 7. Time variation of nitrate concentration ($\mu g\,m^{-3}$) and particle number concentration (cm^{-3}) of the nucleation mode (N_{9-30}) for the entire measurement period (above graph) and for a section of the data (below). Red arrows highlight opposing variations in concentrations and blue arrows indicate similar variations in concentrations.

Table 2. Factors/sources and factor loadings (< 1) identified by applying Principal Component Analysis on a dataset composed of PM_1 chemical components, particle number concentration for different size ranges, gaseous pollutant concentrations and some meteorological variables.

Industrial + Traffic + Biomass burning		New particle formation + growth (NPF + G)		Secondary Sulphate + Fuel oil combustion		Crustal material		Secondary Nitrate	
BC	0.90	N_{9-825}	0.88	SO_4^{2-}	0.85	Ce	0.91	K	0.56
Pb	0.89	N_{30-50}	0.92	NH_4^+	0.84	La	0.85	NO_3^-	0.51
EC	0.86	N_{9-30}	0.75	$N_{300-500}$	0.64	Ni	0.72	SR	–0.41
Zn	0.84	N_{50-100}	0.74	PM_1	0.74	Al_2O_3	0.63	T	–0.40
NO_2	0.81	T	0.61	V	0.59	Fe	0.46	$N_{300-500}$	0.39
Cd	0.80	SR	0.42	$N_{100-300}$	0.40	$N_{500-825}$	0.18	$N_{500-825}$	0.33
OC	0.76	$N_{100-300}$	0.39	$N_{500-825}$	0.36			NH_4^+	0.33
$N_{100-300}$	0.74	NO_3^-	–0.34	T	0.39			N_{9-30}	0.18
$N_{500-825}$	0.72	RH	–0.18	SR	0.34				
Sn	0.72								
Mn	0.65								
K	0.64								
Cu	0.55								
Sb	0.53								
NO_3^-	0.51								
Eigenvalues	11.9		4.3		3.8		3.4		2.1
% total var. exp.	34		12		10		10		5

3.4.2 Contribution of each source to particle number concentration

The application of MLRA allowed for the determination of the contribution of each factor to the total particle number concentration. As shown in Fig. 8, the component titled NPF + G comprises the largest part of the total particle number concentration with $1715 \pm 1724\,cm^{-3}$ (56 %). As stated previously, this factor is not related to any known emission source. It is probable that the source of these particles is from new particle formation and growth, either occurring in situ or being transported to the site. The component industrial + traffic + biomass burning is the second most influential factor in terms of particle number

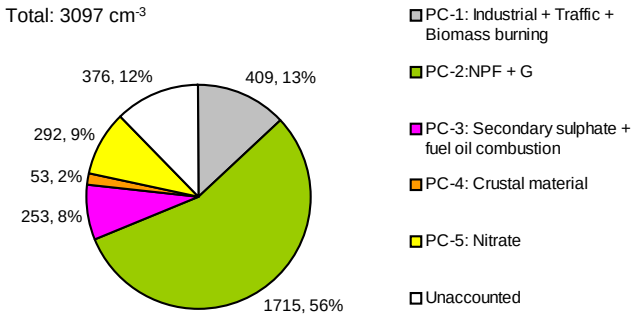

Fig. 8. Mean daily contribution to N_{9-800} (cm^{-3} and %) for the different factors identified by PCA analysis.

concentration ($409 \pm 654\,cm^{-3}$; 13 %), followed by the nitrate source ($292 \pm 344\,cm^{-3}$; 9 %). As outlined previously, the contribution of nitrate to the particle number concentration may be overestimated. Finally, the source secondary sulphate + fuel oil combustion contributes 8 % to the total particle number concentration ($253 \pm 378\,cm^{-3}$), followed by crustal material ($53 \pm 91\,cm^{-3}$; 2 %).

Figure 9 displays the mean daily contribution of each factor to the particle number concentration for different size ranges. Furthermore, specific episodes of interest are highlighted. Episodes of pollution (WAE) are highlighted in blue, occurring from 20/01/2011 to 13/02/2011 (A), and from 22/03/2011 to 26/03/2011 (B). These episodes are characterised by increased solar radiation with cool temperatures (mean of 5.1 °C and 9.4 °C for A and B, respectively), and high concentrations of NO_2 and PM_1. During episode A, particles of diameter > 50nm dominate, with the industrial + traffic + biomass burning and nitrate sources being most significant. Interestingly, the traffic + biomass burning source identified by PMF (Fig. 9; bottom graph) does not influence the PM_1 mass to the same extent as particle number concentrations. The nitrate source does influence both the mass and particle number concentration during this episode, and SOA is also substantial in the PM_1 mass. The second episode (B) differs from A in that it is dominated by the secondary sulphate source for both particle number concentrations of diameter > 100 nm and also the PM_1 mass. The warmer temperatures result in increased sulphate and reduced nitrate concentrations.

As is evidenced by Fig. 9, the component titled NPF + G undergoes a clear seasonality with levels increasing as solar radiation intensity and temperatures increase, such as occurs in April (C; highlighted in green) suggesting the sources of these particles have some relationship with photochemical reactions. Sulphate and nitrate related particles are not significant, as they would scavenge the gaseous precursors necessary for new particle formation through condensation and coagulation processes. The source of industrial + traffic + biomass burning is present in the accumulation mode however, along with elevated NO_2 concentrations, suggesting that transport of ultrafine particles, possibly emitted by traffic and biomass burning, may also be of influence here. SOA is also abundant in the mass concentration, indicating that SOA may be influential in NPF + G. Two episodes of nucleation are highlighted by the red arrows in Fig. 9. The first, occurring on 7/12/2010, coincides with elevated concentrations of SOA and relatively little contribution from the other sources. The second, on the 28/05/2011, coincides with elevated concentrations of SOA, secondary sulphate and PM_1, indicating that nucleation can occur at this site even in the presence of high concentrations of background coarse particles.

An episode of regional pollution during the warmer period is highlighted in red (D; mean temperature of 13 °C) in Fig. 9, when sulphate particles are at their highest concentrations. Particle number concentrations are generally very low, and particles of diameter > 300 mm dominate as a result of particle interaction through coagulation and condensation within the air mass. PM_1 concentrations are high and PM_1 is also comprised significantly of the secondary sulphate source. Once again, NPF + G is negligible owing to the high background concentrations of larger sulphate particles.

Figure 10 displays the mean particle number size distribution recorded over the measurement period, with the majority of particles existing in the Aitken mode (N_{30-100}). Furthermore, the mean contribution of each component to the particle number concentration for various size bins is also shown. Beginning with the smallest particles (N_{9-30}), the NPF + G source contributes the majority of particles in this range. The nitrate source, as observed in Fig. 8, contributes a significant number of particles to this mode, owing to an artefact caused by the limitation of the current analysis, as described previously. In a similar way, the component called crustal material was also found to artificially contribute particles to this mode. One would expect crustal material to contribute little to particle number concentration as it mostly found in the coarse mode and only contributes 3 % to PM_1 mass. As observed during PMF analysis, a significant proportion of crustal material was identified in the source SOA, owing to meteorological conditions which favour increased concentrations of both SOA and crustal material. Although SOA was not identified by PCA to contribute to particle number concentration, the presence of crustal material in the nucleation mode may be related to the fact that SOA and crustal material are controlled by similar conditions, and SOA could contribute to the growth of nucleating particles (O'Dowd et al., 2002b). NPF + G dominates particle number concentrations below 100 nm and, to a lesser extent proportionally, to particles between 100–300 nm, as continued growth into particles of this size is less likely. The influence of transport of nanoparticles may be influential; especially considering that the highest particle number concentrations for NPF + G were recorded for N_{30-100}, indicating that this source is not just from local NPF, but also from transport of newly formed

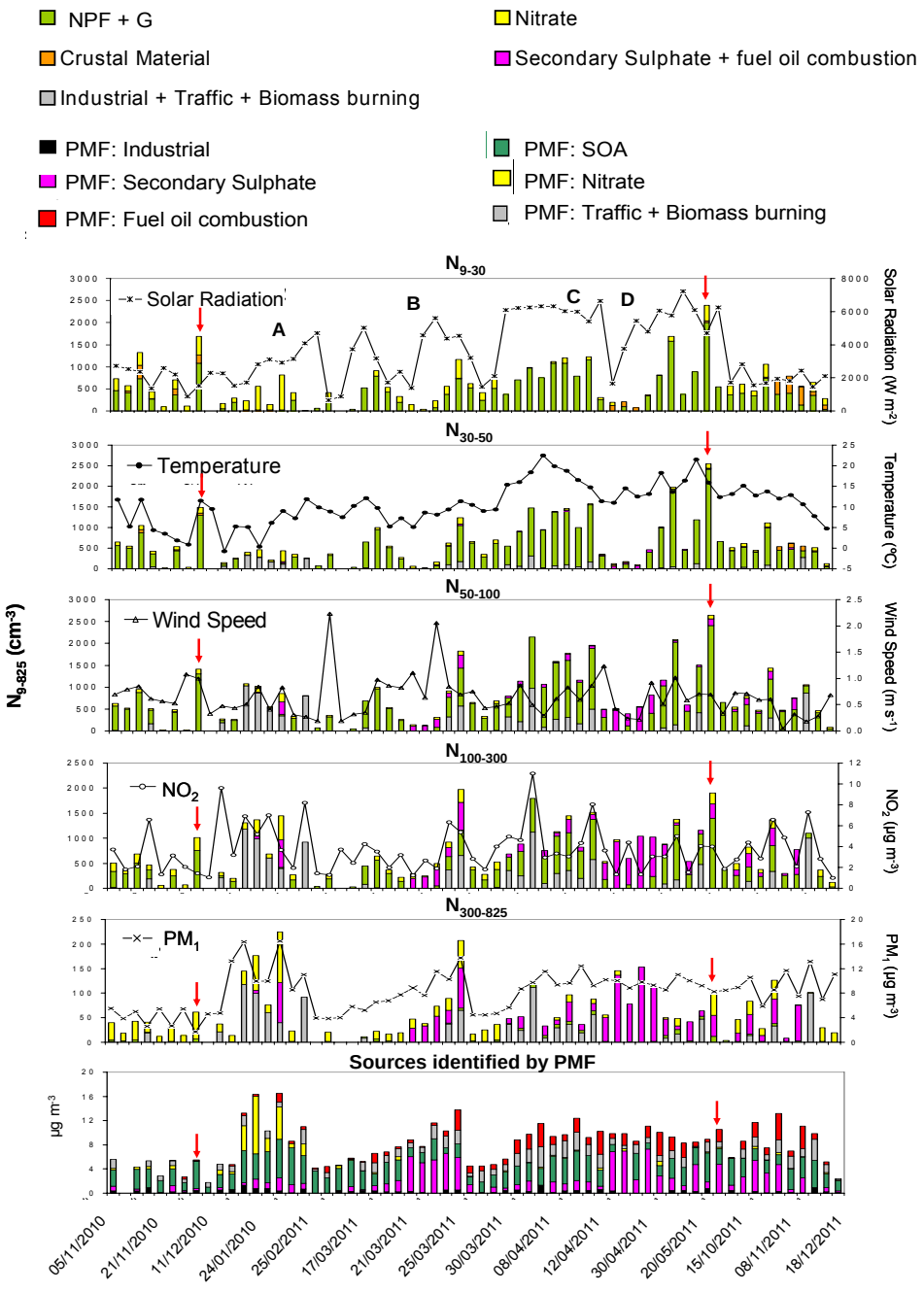

Fig. 9. Mean daily contribution of each source to the particle number concentration in various size ranges (N_{9-825} (cm^{-3})) identified by PCA analysis. Specific aerosol episodes are highlighted: blue (A, B; WAE), green (C; NPF), red (D; summer regional recirculation). The bottom graph shows the source contribution of factors identified by PMF for the same days. Occurrence of intense NPF are highlighted by the red arrow.

particles to the site. Industrial + traffic + biomass burning begins to emerge in the size ranges N_{30-50} and its influence increases with increasing diameter. As expected, secondary sulphate and nitrate particles are present in the larger ranges, contributing much less to the overall particle number, but significantly to the mass.

4 Conclusions

The levels and chemical composition of PM_1 recorded at the RB site of MSY over a period of almost 2.5 years are presented in this work. PM_1 mass at MSY is dominated by OM and secondary sulphate. Concentrations of chemical components were found to undergo a clear seasonality

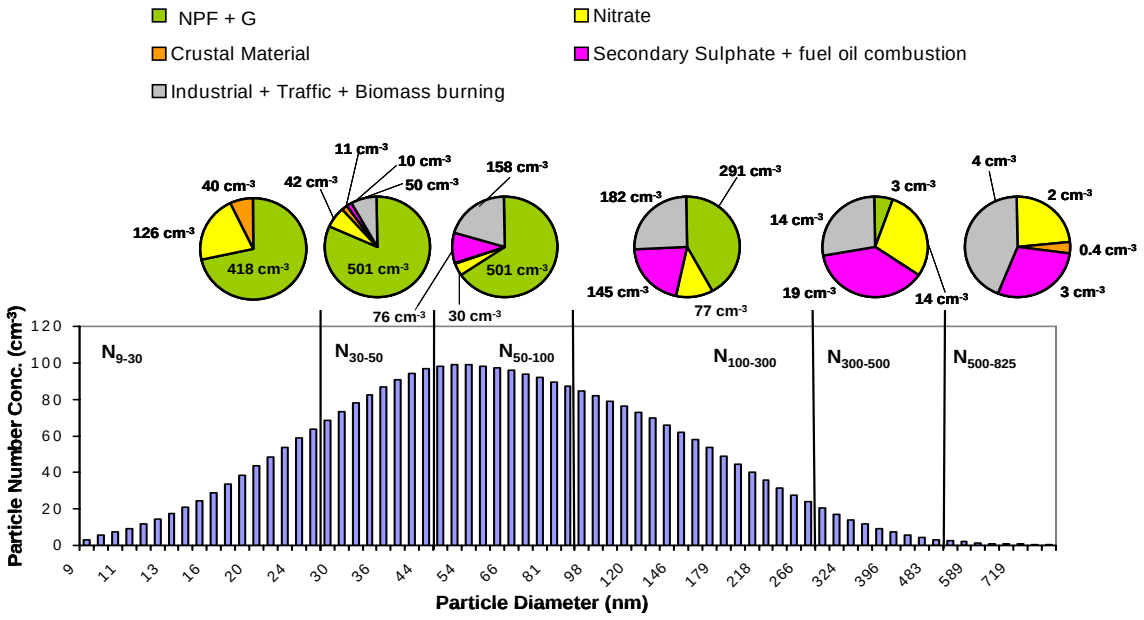

Fig. 10. Mean size distribution for particle concentrations (cm^{-3}) recorded at MSY and the corresponding contribution of each PC to the particle number concentration for various size groups (N_{9-30}, N_{30-50}, N_{50-100}, $N_{100-300}$, $N_{300-500}$, $N_{500-825}$).

with highest concentrations recorded in summer for OM, sulphate, ammonium and crustal material owing to the regional recirculation of air masses and, in the case of OM, from higher biogenic emissions. Nitrate concentrations were at their highest in winter, as was the marine aerosol. The identification of emission sources that contribute to PM_1 were identified using PMF. Six sources were identified, namely; secondary sulphate, traffic + biomass burning, industrial, SOA, secondary nitrate and fuel oil combustion. The secondary sulphate source accounted for the largest variance in PM_1 (32%), and was characterised by sulphate and ammonium. This source was most abundant in summer owing to higher insolation and air mass recirculation across the region, favouring the accumulation of pollutants emitted over a larger area. The SOA source was the second most important source in terms of mass, accounting for 28 % of the total variance, and was identified by the presence of OC (explaining 43 % of the variance in OC). SOA can be from both a natural source, such as biogenic emissions, or from anthropogenic emissions which are most influential during winter anticyclonic pollution episodes. Species associated with crustal material were found in both the secondary sulphate and SOA sources, as the meteorological conditions that favour these sources would also favour elevated levels of crustal material. Secondary nitrate was identified as a source with most influence on PM during winter, with highest concentrations in January and February. The traffic + biomass burning source was identified by the presence of typical traffic tracers (EC, OC, Sb and Sn) and biomass burning tracer K. This factor accounted for 78 % of the total variance of EC and 26 % of K. Concentrations were observed to be highest in January, April and October, as a result of local biomass burning emissions and winter pollution episodes. An industrial source was identified by the presence of typical tracers associated with industrial emissions such as Pb, As, Cd, Sn, Cu, Zn, Cr, Fe and Mn. This factor contributed little mass to PM_1, accounting for only 4 % of the total variance. A decrease in industrial emissions was observed in August owing to reduced industrial activity during the vacation period. Finally, a fuel oil combustion source was easily identifiable by the presence of V and Ni which are known emissions specific to fuel oil combustion.

Average particle number concentrations at MSY for the period 05/11/2010 to 01/06/2011 and from 15/10/2011 to 18/12/2011 were 3097 cm^{-3}, with the Aitken mode (N_{30-100}) being the dominant mode (52 % of the total particle number concentration). Principle Component Analysis of the particle number concentration for various size bins, coupled with chemical speciation data, gaseous pollutant concentrations and a range of meteorological data allowed for the identification of 5 factors affecting ambient particle number concentrations. These five factors reflected those identified by PMF, but some of the sources merged owing to the reduced data set. The five principal components identified were; industrial + traffic + biomass burning, NPF + G, secondary sulphate + fuel oil combustion, crustal material and nitrate. The source of industrial + traffic + biomass burning explained 34 % of the variance and was characterised by tracers associated with traffic emissions (EC, BC, OC, NO_2, Sn, Sb), industrial emissions (Pb, Zn, Cd, Mn, Cu) and biomass burning (OC, EC, BC, K). The second most important component (12 % of the total variance) was NPF +

G. This component was not observed to be associated with any other parameter except for temperature and solar radiation, suggesting that this source may be influenced by new particle formation due to the high loading of particle concentrations in the nucleation mode. The use of multilinear regression analysis allowed for the calculation of the contribution of each source to the daily particle number concentration. The NPF + G source was the largest contributor to the total particle number concentration, explaining 56 % of the total concentration. Furthermore, NPF + G dominated particle concentrations below 100 nm, but its influence diminished for particles > 100 nm. Episodes of elevated influence of NPF + G were identified during periods of more intense solar radiation and decreased levels of the nitrate and sulphate sources. Three episodes of prolonged pollution were identified, two in winter and the other in late spring. The winter pollution episodes were characterised by the industrial + traffic + biomass burning source and the nitrate source. Conversely, the spring regional pollution episode was mostly influenced by secondary sulphate particles. An artefact highlighting the limitation of MLRA for particle number concentrations was identified by the presence of the nitrate source in the nucleation mode, which was a result of coincidental parallel variations in 24 h nitrate concentrations and nucleation mode particle concentrations.

The utilisation of two source apportionment techniques for fine PM and chemical components, namely PMF and PCA, in conjunction with sub-micrometer particle number concentrations has allowed for the identification of the various sources affecting aerosols at MSY. Such a novel approach has highlighted the broad range of processes and sources that can influence aerosols at the site.

Acknowledgements. This study was supported by the Ministry of Economy and Competitiveness and FEDER funds under the projects CARIATI (CGL2008-06294/CLI), VAMOS (CGL2010 19464/CLI) and GRACCIE (CSD 2007-00067). The research leading to these results has received funding from the European Union Seventh Framework Programme (FP7/2007-2013) ACTRIS under grant agreement no. 262254 and the Generalitat de Catalunya (AGRUAR-2009SGR8). The authors would like to extend their gratitude to Jesús Parga and Jordi Gil for their technical support.

Edited by: E. Gerasopoulos

References

Amato, F., Pandolfi, M., Viana, M., Querol, X., Alastuey, A., Moreno, T.: Spatial and chemical patterns of PM10 in road dust deposited in urban environment, Atmos. Environ., 43, 1650–1659, 2009.

Belis, C. A., Karagulian, F., Larsen, B. R., and Hopke, P. K.: Critical review and meta-analysis of ambient particulate matter source apportionment using receptor models in Europe, Atmos. Environ., 69, 94–108, 2013.

Bourcier, L., Sellegri, K., Chausse, P., and Pichon, J. M.: Seasonal variation of water-soluble inorganic components in aerosol size-segregated at the puy de Dôme station (1465 m.a.s.l.), France, J. Atmos. Chem., 69, 47–66, 2012.

Cavalli, F., Viana, M., Yttri, K. E., Genberg, J., and Putaud, J. P.: Toward a standardised thermal-optical protocol for measuring atmospheric organic and elemental carbon: the EUSAAR protocol, Atmos. Meas. Tech., 3, 79–79, 2010, http://www.atmos-meas-tech.net/3/79/2010/.

Cozic, J., Verheggen, B., Weingartner, E., Crosier, J., Bower, K. N., Flynn, M., Coe, H., Henning, S., Steinbacher, M., Henne, S., Collaud Coen, M., Petzold, A., and Baltensperger, U.: Chemical composition of free tropospheric aerosol for PM1 and coarse mode at the high alpine site Jungfraujoch, Atmos. Chem. Phys., 8, 407–423, doi:10.5194/acp-8-407-2008, 2008.

Cusack, M., Alastuey, A., Pérez, N., Pey, J., and Querol, X.: Trends of particulate matter ($PM_{2.5}$) and chemical composition at a regional background site in the Western Mediterranean over the last nine years (2002–2010), Atmos. Chem. Phys., 12, 8341–8357, doi:10.5194/acp-12-8341-2012, 2012.

Hamed, A., Korhonen, H., Sihto, S.-L., Joutsensaari, J., Järvinen, H., Petäjä, T., Arnold, F., Nieminen, T., Kulmala, M., Smith, J. N., Lehtinen, K. E. J., and Laaksonen, A.: The role of relative humidity in continental new particle formation, J. Geophys. Res., 116, D03202, doi:10.1029/2010JD014186, 2011.

Harrison, R. M. and Pio, C.: Size differentiated composition of inorganic aerosol of both marine and continental polluted origin, Atmos. Environ., 17, 1733–1738, 1983.

Harrison, R. M., Beddows, D. C. S., and Dall'Osto, M.: PMF analysis of Wide-Range Particle Size Spectra Collected on a Major Highway, Environ. Sci. Tech., 45, 5522–5528, 2011.

IPCC: Climate Change 2007: The Physical Science Basis, Contribution of Working Group I to the Fourth Assessment Report of the IPCC, ISBN 978 0521 88009-1 Hardback; 978 0521 70596-7 Paperback, 2007.

Lighty, J. S., Veranth, J. M., and Sarofim, A. F.: Combustion aerosols: factors governing their size and composition and implications to you human health, J. Air Waste Manag., 50, 1565–1618, 2000.

Minguillón, M. C., Querol, X., Baltensperger, U., and Prévôt, A. S. H.: Fine and coarse PM composition and sources in rural and urban sites in Switzerland: Local or regional pollution? Sci. Total Environ., 427–428, 191–202, 2012.

Minguillón, M. C., Perron, N., Querol, X., Szidat, S., Fahrni, S. M., Alastuey, A., Jimenez, J. L., Mohr, C., Ortega, A. M., Day, D. A., Lanz, V. A., Wacker, L., Reche, C., Cusack, M., Amato, F., Kiss, G., Hoffer, A., Decesari, S., Moretti, F., Hillamo, R., Teinilä, K., Seco, R., Peñuelas, J., Metzger, A., Schallhart, S., Müller, M., Hansel, A., Burkhart, J. F., Baltensperger, U., and Prévôt, A. S. H.: Fossil versus contemporary sources of fine elemental and organic carbonaceous particulate matter during the DAURE campaign in Northeast Spain, Atmos. Chem. Phys., 11, 12067–12084, doi:10.5194/acp-11-12067-2011, 2011.

O'Dowd, C. D., Aalto, P., Hmeri, K., Kulmala, M., and Hoffman, T.: Aerosol formation: atmospheric particles from organic vapours, Nature, 416, 497–498, 2002b.

Öztürk, F., Zararsiz, A., Dutkiewicz, V. A., Husain, L., Hopke, P. K., Tuncel, G.: Temporal variations and sources of Eastern Mediterranean aerosols based on a 9-year observation, Atmos. Environ., 61, 463–475, 2012.

Paatero, P. and Tapper, U.: Positive matrix factorisation: a non-negative factor model with optimal utilisation of error estimates of data values, Environmetrics, 5, 111-26, 1994.

Pandolfi, M., Gonzalez-Castanedo, Y., Alastuey, A., de la Rose, J. D, Mantilla, E., de la Campa, A. S., Querol, X., Pey, J., Amato, F., and Moreno, T.: Source apportionment of PM10 and PM2.5 at multiple sites in the strait of Gibraltar by PMF: Impact of shipping emissions, Environ. Sci. Poll. Res., 18, 260–269, 2011.

Pérez, N., Pey, J., Castillo, S., Viana, M., Alastuey, A., Querol, X.: Interpretation of the variability of levels of regional background aerosols in the Western Mediterranean, Sci. Total Environ., 407, 524–540, 2008.

Pey, J., Rodríguez, S., Alastuey, A., Moreno, T., Putaud, J. P., and Van Dingenen, R.: Variations of urban aerosols in the Western Mediterranean, Atmos. Environ., 42, 9052–9062, 2008.

Pey, J., Pérez, N., Castillo, S., Viana, M., Moreno, T., Pandolfi, M., López-Sebastián, J.M., Alastuey, A., Querol, X.: Geochemistry of regional background aerosols in the Western Mediterranean, Atmos. Res., 94, 422-435, 2009a.

Pey, J., Querol, X., Alastuey, A., Rodríguez, Putaud, J.P., Van Dingenen, R.: Source apportionment of urban fine and ultra-fine particle number concentration in a Western Mediterranean city, Atmos. Environ. 43, 4407-4415, 2009b.

Pey, J., Pérez, N., Querol, X., Alastuey, A., Cusack, M., Reche, C.: Intense winter pollution episodes affecting the Western Mediterranean, Sci. Total Environ., 408, 1951-1959, 2010.

Pope, C. A. and Dockery, D. W.: Health effects of fine particulate air pollution: lines that connect, J. Air. Waste Manage., 56(6), 709-42, 2006.

Querol, X., Alastuey, A., Rodríguez, S., Plana, F., Mantilla, E., Ruiz, C.R.: Monitoring of PM10 and PM2.5 around primary particulate anthropogenic emission sources, Atmos. Environ., 35, 845-858, 2001.

Querol, X., Alastuey, A., Pey, J., Cusack, M., Mihalopoulos, N., Theodosi, C., Gerasopoulos, E., Kubilay, N., Koçak, M.: Variability in regional background aerosols in the Mediterranean, Atmos. Chem. Phys., 9, 4575-4591, 2009, http://www.atmos-chem-phys.net/9/4575/2009/.

Richard, A., Gianini, M.F.D., Mohr, C., Furger, M., Bukowiecki, N., Minguillón, M.C., Lienemann, P., Flechsig, U., Appel, K., DeCarlo, P.F., Heringa, M.F., Chirico, R., Baltensperger, U., Prévôt, A.S.H.: Source apportionment of size and time resolved trace elements and organic aerosols from an urban courtyard site in Switzerland, Atmos. Chem. Phys., 11, 8945-8963, 2011, http://www.atmos-chem-phys.net/11/8945/2011/.

Rodríguez, S., Querol, X., Alastuey, A., Viana, M., and Mantilla E.: Events affecting levels and seasonal evolution of airborne particulate matter concentrations in the Western Mediterranean, Environ. Sci. Technol., 37, 216-222, 2003.

Rodríguez, S., Van Dingenen, R., Putaud, J.P., Dell'Acqua, A., Pey, J., Querol, X., Alastuey, A., Chenery, S., Ho, K.F., Harrison, R., Tardivo, R., Scarnato, B., Gemelli, V.: A study on the relationship between mass concentrations, chemistry and number size distribution of urban fine aerosols in Milan, Barcelona and London, Atmos. Chem. Phys., 7, 2217-2232, 2007, http://www.atmos-chem-phys.net/7/2217/2007/.

Seco, R., Peñuelas, J., Filella, I., Llusiá, J., Molowny-Horas, R., Schallhart, S., Metzger, A., Müller, M., Hansel, A.: Contrasting winter and summer VOC mixing ratios at a forest site in the Western Mediterranean Basin: The effect of local biogenic emissions, Atmos. Chem. Phys., 11, 20389-20431, 2011, http://www.atmos-chem-phys.net/11/20389/2011/.

Spindler, G., Brüggemann, E., Gnauk, T., Grüner, A., Müller, K., Herrmann, H.: A four-year size-segregated characterisation of particles PM_{10}, $PM_{2.5}$ and PM_1 depending on air mass origin at Melpitz, Atmos. Environ., 44, 164-173, 2010.

Spracklen, D. V., Carslaw, K. S., Merikanto, J., Mann, G. W., Reddington, C.L., Pickering, S., Ogren, J.A., Andrews, E., Baltensperger, U., Weingartner, E., Boy, M., Kulmala, M., Laakso, L., Lihavainen, H., Kivekäs, Komppula, M., Mihalopoulos, N., Kouvarakis, G., Jennings, S. G., O'Dowd, C., Birmili, W., Wiedensohler, A., Weller, R., Gras, J., Laj, P., Sellegri, K., Bonn, B., Krejci, R., Laaksonen, A., Hamed, A., Minikin, A., Harrison, R. M., Talbot, R., and Sun, J.: Explaining global surface aerosol number concentrations in terms of primary emissions and particle formation, Atmos. Chem. Phys., 10, 4775–4793, 2010, http://www.atmos-chem-phys.net/10/4775/2010/.

Thompson, M. and Howarth, R. J.: Duplicate analysis in geochemical practice. Part I. Theoretical approach and estimation of analytical reproducibility, Analyst, 101, 690–698, 1976.

Thurston, G. D. and Spengler, J. D.: A quantitative assessment of source contribution to inhalable particulate matter pollution in the Metropolitan Boston, Atmos. Environ., 19, 9–25, 1985.

Turpin, B. J. and Lim, H. J.: Species contributions to PM2.5 mass concentrations: Revisiting common assumptions for estimating organic mass, Aerosol Sci. Technol., 35, 602–610, 2001.

Vecchi, R., Chiari, M., D'Alessandro, A., Fermo, P., Lucarelli, F., Mazzei, F., Nava, S., Piazzalunga, A., Prati, P., Silvani, F., and Valli, G.: A mass closure and PMF source apportionment study on the sub-micron sized aerosol fraction at urban sites in Italy, Atmos. Environ., 42, 2240–2253, 2008.

Viana, M., Querol, X., Alastuey, A., Gil, J. I., and Menéndez, M.: Identifiaction of PM sources by principal component analysis (PCA) coupled with wind direction data, Chemosphere, 65, 2411–2418, 2006.

Article 3

Cusack, M., Pérez, N., Pey, J., Wiedensohler, A., Alastuey, A., Querol, X.

Variability of sub-micrometer particle number size distributions and concentrations in the Western Mediterranean regional background.

Tellus B: Chemical and Physical Meteorology, 65, 19243, 2013.

Pages: 121-139

Published in: January 2013

Impact factor of Journal: 4.382

Tellus SERIES B CHEMICAL AND PHYSICAL METEOROLOGY
PUBLISHED BY THE INTERNATIONAL METEOROLOGICAL INSTITUTE IN STOCKHOLM

Variability of sub-micrometer particle number size distributions and concentrations in the Western Mediterranean regional background

By MICHAEL CUSACK[1,2]*, NOEMÍ PÉREZ[1], JORGE PEY[1], ALFRED WIEDENSOHLER[3], ANDRÉS ALASTUEY[1] and XAVIER QUEROL[1], [1]*Institute of Environmental Assessment and Water Research, IDÆA, CSIC, Barcelona, Spain;* [2]*Institute of Environmental Science and Technology (ICTA), Universitat Autónoma de Barcelona, Barcelona, Spain;* [3]*Liebniz Institute for Tropospheric Research, Leipzig, Germany*

(Manuscript received 31 July 2012; in final form 22 January 2013)

ABSTRACT

This study focuses on the daily and seasonal variability of particle number size distributions and concentrations, performed at the Montseny (MSY) regional background station in the western Mediterranean from October 2010 to June 2011. Particle number concentrations at MSY were shown to be within range of various other sites across Europe reported in literature, but the seasonality of the particle number size distributions revealed significant differences. The Aitken mode is the dominant particle mode at MSY, with arithmetic mean concentrations of 1698 cm^3, followed by the accumulation mode (877 cm^{-3}) and the nucleation mode (246 cm^{-3}). Concentrations showed a strong seasonal variability with large increases in particle number concentrations observed from the colder to warmer months. The modality of median size distributions was typically bimodal, except under polluted conditions when the size distribution was unimodal. During the colder months, the daily variation of particle number size distributions are strongly influenced by a diurnal breeze system, whereby the Aitken and accumulation modes vary similarly to PM_1 and BC mass concentrations, with nocturnal minima and sharp day-time increases owing to the development of a diurnal mountain breeze. Under clean air conditions, high levels of nucleation and lower Aitken mode concentrations were measured, highlighting the importance of new particle formation as a source of particles in the absence of a significant condensation sink. During the warmer months, nucleation mode concentrations were observed to be relatively elevated both under polluted and clean conditions due to increased photochemical reactions, with enhanced subsequent growth owing to elevated concentrations of condensable organic vapours produced from biogenic volatile organic compounds, indicating that nucleation at MSY does not exclusively occur under clean air conditions. Finally, mixing of air masses between polluted and non-polluted boundary layer air, and brief changes in the air mass being sampled gave rise to unusual particle number size distributions, with specific cases of such behaviour discussed at length.

Keywords: Western Mediterranean, sub-micrometer particle size distribution, number concentration, nucleation, photochemistry

1. Introduction

The Western Mediterranean Basin (WMB) and Iberian Peninsula represent a very complex climate area owing to its geographical position. Its location between two large bodies of water, with Africa to the south and isolated from mainland Europe to the north, makes it considerably unique within Europe both climatologically and geographically. Atmospheric aerosols here are under the influence of both mesoscale and synoptic meteorology, being affected by marine aerosol, Saharan dust, regional pollution and long-range transport from mainland Europe. The variability of particle number size distributions in background sites throughout Europe has been well documented (Asmi et al., 2011), but the lack of similar studies at regional background (RB) sites in the WMB are noticeable by

*Corresponding author.
e-mail: michael.cusack@idaea.csic.es

Citation: Tellus B 2013, **65**, 19243, http://dx.doi.org/10.3402/tellusb.v65i0.19243

their absence. Previous studies performed in this area have described the variability of particulate matter (PM) (Pérez et al., 2008), the chemical speciation of PM (Cusack et al., 2012) and the aerosol optical properties of aerosols (Pandolfi et al., 2011). Sorribas et al. (2011) published results on sub-micron particle size distributions for a rural background site in southern Spain, which was observed to be heavily influenced by marine, Saharan and continental air masses and, in some circumstances, emissions from a nearby industrial estate. However, the study of particle number concentration and size distributions in the RB of north-east (NE) Spain, until now, has been largely underdeveloped.

The impact of sub-micron aerosols in the atmosphere is of great interest for various reasons: sub-micron particles can penetrate as far as the alveoli in the lungs (Wichmann et al., 2000), and they have the ability to absorb and scatter light and act as cloud condensation nuclei (Charlson et al., 1987), thus affecting the Earth's radiation balance. Sub-micron aerosols may be emitted directly to the atmosphere or may be formed from gaseous precursors. Usually, cleaner atmospheres are favourable for new-particle formation processes. These pristine environments include: the Polar Regions (Wiedensohler et al., 1996), high altitude sites (Venzac et al., 2009), continental boreal forests (Kulmala et al., 1998) and remote areas (Birmili et al., 2001), among others. In the WMB, photochemical nucleation episodes are thought to be very relevant since they are observed even in highly polluted environments (Pey et al., 2008; Reche et al., 2011).

New particle formation (NPF) and subsequent growth is a current topic of great interest. It is widely accepted that two phases are involved in NPF: (1) the nucleation of an initial cluster and (2) subsequent activation of these clusters resulting in particle growth to a detectable size (Kulmala et al., 2000). The formation of these initial clusters is part of the main focus of investigation, with numerous candidates thought to play a role in NPF, such as H_2O–H_2SO_4 (binary nucleation, Easter and Peters, 1994), H_2O–H_2SO_4–NH_3 nucleation (Eisele and McMurray, 1997), 'nucleation of low vapour pressure organic compounds' (O'Dowd et al., 2002), 'ion-induced nucleation' (Kim et al., 2002) and 'activation of existing neutral and/or ion clusters' (Kulmala et al., 2006). However, nucleation and subsequent growth are believed to be two separate processes, and species involved in initial nucleation may not be important for the growth of the nucleating clusters (Kulmala et al., 2004). There is increasing evidence to suggest that the condensation of organic vapours on the nucleating clusters play a pivotal role in particle growth. Such organic vapours include the oxidation products of biogenic emissions such as isoprene and terpenes (Allan et al., 2006; Laaksonen et al., 2008). Results shown in this work present unusual processes regarding ultrafine particles, especially nucleation mode particles that may be indicative of mixing of air masses whereby nucleation events with differing phases of particle formation and growth are sampled during the same day.

The objective of this article is to report the sub-micron particle number size distribution in the WMB RB at Montseny (MSY, NE Spain) with special focus on the aerosol formation and modification processes, and seasonal trends. Most studies on ultra-fine particle size distribution within Spain have focused on the urban environment (Rodriguez and Cuevas, 2007; Pey et al., 2008; Fernández-Camacho et al., 2010; Gómez-Moreno et al., 2011) and a rural background site in southern Spain frequently affected by local anthropogenic emissions (Sorribas et al., 2011), with relatively few focusing on the regional background environment. This article interprets the combination of a large range of aerosol parameters and properties and their influence on the particle size distribution. The objective is to determine the temporal variations of aerosols and aerosol size distribution occurring and the conditions and processes that govern these variations. Special attention is given to processes affecting the nucleation mode, where some peculiar processes have been observed to have taken place.

2. Methodology

2.1. Measurement site

From October 2010 to June 2011, simultaneous measurements of particle number and size distribution of sub-micron particles (85% data coverage based on hourly resolution), PM (92% data coverage) and Black Carbon (BC; 99% data coverage) mass concentrations, as well as gaseous pollutants ($\sim$98% data coverage) were carried out at a RB site at MSY (41°19′N, 02°21′E). The MSY station is located in the MSY natural park, 40 km to the N–NE of the Barcelona urban area, and 25 km from the Mediterranean coast. The station is located on the upper walls of a valley extending perpendicularly from the Catalan Pre-Coastal ranges, in a densely forested area known as La Castanya (720 m.a.s.l.). The station is situated relatively far from urban and industrial zones, but the region is generally densely populated and heavily industrialised, and local anthropogenic emissions can affect this site under specific meteorological conditions. Atmospheric dynamics and aerosol variability of aerosols at MSY has been described in detail by Pérez et al. (2008), Pey et al. (2008) and Seco et al. (2011). The MSY station, located in the WMB RB, is a member of the ACTRIS network. The ACTRIS (Aerosols, Clouds, and Trace gases Research InfraStructure Network; formerly EUSAAR) project aims to provide a reliable and quality-controlled network of aerosol measure-

ments across Europe and farther afield (Philippin et al., 2009). This project has harmonised and homogenised measurements of aerosol chemistry and physical and optical properties through the standardisation of protocols of instrument operation and maintenance, data submission and measurement procedures (Wiedensohler et al., 2012).

2.2. Measurements

Sub-micrometer particle number size distribution was measured using a mobility particle size spectrometer operated in the scanning mode. In the following article, we call the system a Scanning Mobility Particle Sizer (SMPS). The SMPS system comprises a differential mobility analyser (DMA) connected to a condensation particle counter (CPC, Model TSI 3772). The entire system was designed and manufactured in the framework of the EUSAAR project at the Leibniz Institute for Tropospheric Research (IfT) in Leipzig, Germany. The full specifications of the instrument, such as DMA dimensions, bipolar diffusion charger, and so on for the *IFT-SMPS* can be found in Wiedensohler et al. (2012). An intercomparison was carried out on the SMPS system in 2010 at the World Calibration Centre for Physical Aerosol Research (WCCAP) at IfT. IfT has designed a calibration programme for aerosol instrument maintenance and comparison and the institute is endorsed by the WMO. The intercomparison found the SMPS at MSY to measure within 10% of the reference mobility size spectrometer for particles 20–200 nm (see Wiedensohler et al., 2012 for further details). In that same article, it was observed that measurement accuracy for particles <20 nm and >300 nm was less reliable than for particles 20–200 nm, and thus concentrations reported in this work for these size ranges could be more qualitative in nature rather than quantitative. Furthermore, it is important to note that diffusion loses were not calculated in this work which can affect accurate measurement of ultrafine particles. The SPMS system provided a complete particle number size distribution of the number of particles between 9 and 825 nm (N_{9-825}), and completed one scan every 5 minutes. The aerosol is dried prior to sampling to maintain a relative humidity below 40% using a Nafion dryer, in line with EUSAAR/ACTRIS requirements. Aerosol inlet flow was maintained at 1 l/min and sheath airflow at 5 l/min (which was also dried in a system using a Nafion dryer in a closed loop).

Real-time measurements of PM_1 mass concentrations were continuously obtained using a GRIMM optical counter (model 180). Hourly PM_1 data provided by GRIMM were daily averaged and subsequently corrected by comparison with 24 hours gravimetric mass measurements of PM_1 collected by high volume samplers (sampled consecutively every 4 d). The cross-section absorption coefficient was measured continuously using a Multi Angle Absorption Photometer (MAAP, model 5012, Thermo). Equivalent BC measurements provided by MAAP are calculated by the instrument software by dividing the measured absorption coefficient $\sigma_{ap}(\lambda)$ by $6.6\,m^2\,g^{-1}$ which is the mass absorption cross section (MAC) at 637 nm (Müller et al., 2011). However, MAC may vary depending on the aerosol composition and age, and may differ depending on the area under study. In accordance with the findings of Pandolfi et al. (2011), the absorption coefficient values measured at MSY provided by the MAAP were converted into BC mass/volume units by multiplying by a factor of $10.4\,m^2\,g^{-1}$. Thus, BC results presented in this work are specifically Equivalent Black Carbon (EBC) as measurements are derived from optical methods.

The SMPS system and MAAP instruments were both connected to the same sampling line and inlet, with a cut-off diameter of 10 μm, placed at about 1.5 m above the roof of the cabin housing the instruments. The sampled aerosol for SMPS and MAAP was dried in the same sampling inlet before reaching the respective instruments. Humidity control of the sampled aerosol was performed by attaching a Nafion dryer to the sampling inlet. Real-time measurements of O_3, NO, NO_2, CO and SO_2 were obtained on-site on a separate sampling inlet, supplied by the Department of the Environment of the Autonomous Government of Catalonia. Hourly levels of wind direction, wind speed, solar radiation, temperature, relative humidity and precipitation were recorded in real time on site. See Pérez et al. (2008) for further details.

Measurements of sulphuric acid concentrations were not performed but a proxy, referred to as $[H_2SO_4]$, was calculated according to the proxy described by Mikkonen et al. (2011), whereby $[H_2SO_4]$ is the product of SO_2 concentrations and solar radiation, although the uncertainty associated with this simplified linear approach is somewhat higher than for non-linear proxies also described by Mikkonen et al. (2011). The dry aerosol condensation sink was calculated as described by Kulmala et al. (2001). Air mass back trajectory analysis was performed using HYSPLIT4 (Draxler and Rolph, 1998) for various altitudes, typically 750, 1500 and 2500 m.a.s.l., to determine air mass origins and to aid in establishing air mass mixing effects.

3. Results

3.1. Overview of aerosol concentrations

The measured particle number size distributions in this work are grouped in size bins, whereby the nucleation mode includes all particles of diameter between 9 and 20 nm, the Aitken mode includes particles of diameter 20–100 nm and finally the accumulation mode 100–825 nm.

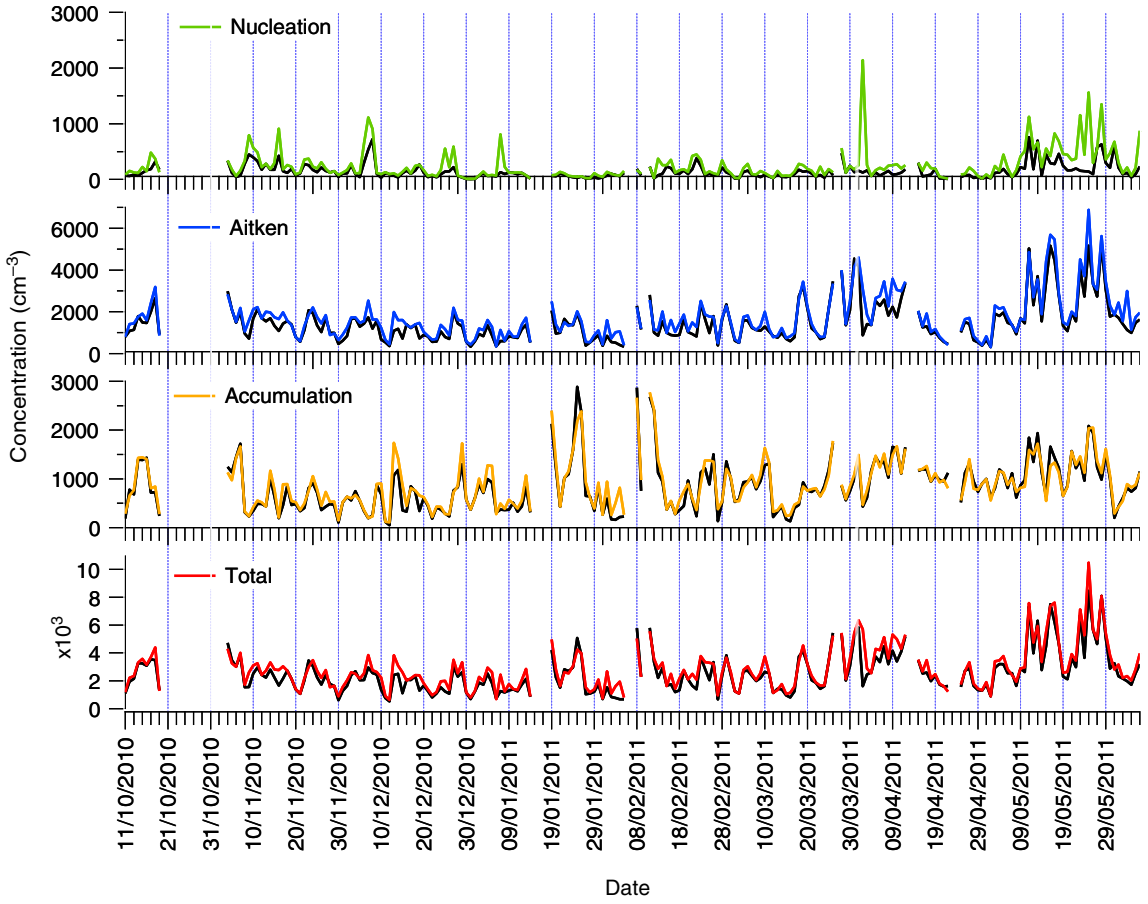

Fig. 1. Time series of daily mean total particle number concentration (coloured lines), median concentrations (black lines) and particle number concentration for the nucleation, Aitken and accumulation modes from 11 October 2010 to 6 June 2011. Warm period (October, April to June) is shaded in green and cold period (November to March) in blue.

Figure 1 shows the time variability from 11 October 2010 to 6 June 2011 of the total arithmetic mean (coloured line) and median (black line) daily particle number concentration ($N_{9–825}$) and the daily particle number concentration for the nucleation mode ($N_{9–20}$), Aitken mode ($N_{20–100}$) and accumulation mode ($N_{100–825}$). The daily arithmetic mean particle number concentration for the measurement period was 2856 cm^{-3} (median of 2292 cm^{-3}). The maximum daily value (9415 cm^{-3}) was recorded in May and was associated with an intense burst of NPF. The minimum total particle number concentration (537 cm^{-3}) occurred during a period of heavy rainfall.

Nucleation mode particles typically registered the lowest concentrations during the study period with a mean hourly concentration of 246 cm^{-3} (8.7% of the total particle number concentration) and a median concentration of 98.8 cm^{-3}. The large difference between the arithmetic mean and median concentrations can be attributed to nucleation events of short duration, whereby elevated concentrations of $N_{9–20}$ occurring for only a few hours influence the arithmetic mean concentrations while having a lesser impact on the median value. This is evident in Fig. 1 where the variation in the mean concentration of the nucleation mode in some instances differs significantly from that of median concentrations. Average concentrations of this mode increased significantly from April onwards, when the hourly mean concentration for April to early June increased to 352 cm^{-3} (Table 1). For the remaining time period (October to March inclusive), the time series for this mode is marked by relatively intense, short-lived peaks in concentrations, such as occurred on 7 January 2011 (daily mean concentration of 742 cm^{-3} and median of 128 cm^{-3}). Some of these intense peaks are related to NPF episodes, when low levels of upper Aitken and accumulation mode particles were recorded.

The Aitken mode is the dominant particle mode throughout the year, with a mean concentration of 1698 cm^{-3} (59% of the total) and a median concentration of 1227 cm^{-3}. Similar to that observed for nucleation mode particles, the mean concentration of Aitken mode particles increases

Table 1. Arithmetic mean (n) and median concentrations (ñ) of the Total, $N_{9–20}$, $N_{20–100}$ and $N_{100–825}$ mode particles recorded at Montseny (MSY) for the entire colder period (C) and warmer period (W), and under polluted and clean conditions for measurements from October 2010 to June 2011

	$N_{9–20}$ (cm^{-3})		$N_{20–100}$ (cm^{-3})		$N_{100–825}$ (cm^{-3})		Total (cm^{-3})	
	n	ñ	n	ñ	n	ñ	n	ñ
C: Total	191	95	1414	1070	778	598	2383	1879
W: Total	352	108	2274	1623	1071	1025	3697	2793
C: Polluted	164	92	1611	1287	987	822	2763	2339
C: Clean	366	173	1367	1002	440	376	2173	1680
W: Polluted	345	104	2628	1894	1274	1160	4247	3282
W: Clean	345	101	1958	1386	730	707	3033	2294

significantly in April and May (2274 cm^{-3}) compared to October to March (1414 cm^{-3}). Thus, the majority of sub-micron particles at MSY are of diameter 20–100 nm. The average accumulation mode concentrations registered 877 cm^{-3} (31% of the total) and median concentrations of 742 cm^{-3}. The accumulation mode bears some correlation with the upper Aitken mode ($R^2 = 0.57$ for the study period, hourly resolution, 4850 points), as the sources of accumulation mode particles may not always be the same as those of Aitken mode particles (such as during Saharan dust events or increased levels of secondary inorganic particles when larger particles are dominant). The autocorrelation coefficient (whereby the correlation between the accumulation mode and the upper Aitken is shifted for one or more hours for one of the variables), gives R^2 for x (t + 1) of 0.47 and x (t + 2) of 0.37. Hourly autocorrelations from here on will be referred to as R_0^2 for x (t), R_1^2 for x (t + 1) and R_2^2 for x (t + 2).

Comparisons of particle number concentrations with various other sites across Europe show that levels in MSY fall in line with other RB sites. A study performed by Spracklen et al. (2010) comparing particle number concentrations at various sites across Europe found mean levels at continental boundary layer sites to range from 2000 to 10 000 cm^3, and mid-latitude coastal stations to be between 1000 cm^{-3} and 2000 cm^{-3}, while Mace Head on the west coast of Ireland registered levels of 3000 cm^{-3}. Asmi et al. (2011) compiled particle number concentration data (for particles of diameter 30–500 nm) for various EUSAAR stations. Median concentrations in this range at MSY for the study period were 1764 cm^{-3}, which is lower than the mean of all the median concentrations of all the stations included in the study by Asmi et al. (2011; 2718 cm^{-3}). Comparing results with those observed for other Mediterranean sites included in the study, levels at MSY are significantly lower than those measured at Finokalia in the eastern Mediterranean which registered median concentrations of 2344 cm^{-3}, with most of this difference owing to elevated concentrations at Finokalia of $N_{50–100}$. Similar concentrations were also measured in Aspvreten (1786 cm^{-3}), which is a regional background station in Sweden surrounded by mixed coniferous and deciduous forest similarly to MSY, but is not typically influenced by anthropogenic activities, unlike MSY. The lack of complete summer measurements of particle number concentrations at MSY in this study, when photochemistry, soil resuspension and Saharan dust intrusions are most influential, means the annual particle number concentrations reported in this work are likely to be underestimated and thus, extended measurements including an entire year of data would make for better comparisons of the other EUSAAR/ACTRIS sites mentioned.

Concerning other stations in Spain, levels of particle number concentrations at a regional station on the southern Atlantic coast of Spain (Sorribas et al., 2011) recorded concentrations (for particles of diameter 14–673 nm) significantly higher than those at MSY (8660 cm^{-3}). This significant increase compared to MSY can be attributed to the influence of anthropogenic aerosols on particle number concentrations emitted from an industrial site close to the monitoring station. A study by Venzac et al. (2009) described in detail particle number concentrations and size distributions at the Puy de Dôme site. A strong diurnal and seasonal variability was observed at the site, attributed to the boundary layer height development during the day, reaching the height of the site during warmer months, which is a common occurrence at MSY.

The time series of various other aerosol parameters measured simultaneously are shown in Fig. 2. Average daily BC mass concentrations at MSY for the measurement period were 616 ng m^{-3}. BC was closely related to the accumulation mode ($R_0^2 = 0.84$, $R_1^2 = 0.72$, $R_2^2 = 0.54$; hourly resolution, 4850 points), but was not correlated with the Aitken mode ($R^2 = 0.21$), suggesting that BC at MSY exists mostly in the accumulation mode. BC and NO_2 exhibited high correlation ($R_0^2 = 0.69$, $R_1^2 = 0.64$, $R_2^2 = 0.41$), indicating they are of the same source, most likely from traffic and biomass burning emissions. No correlation was observed

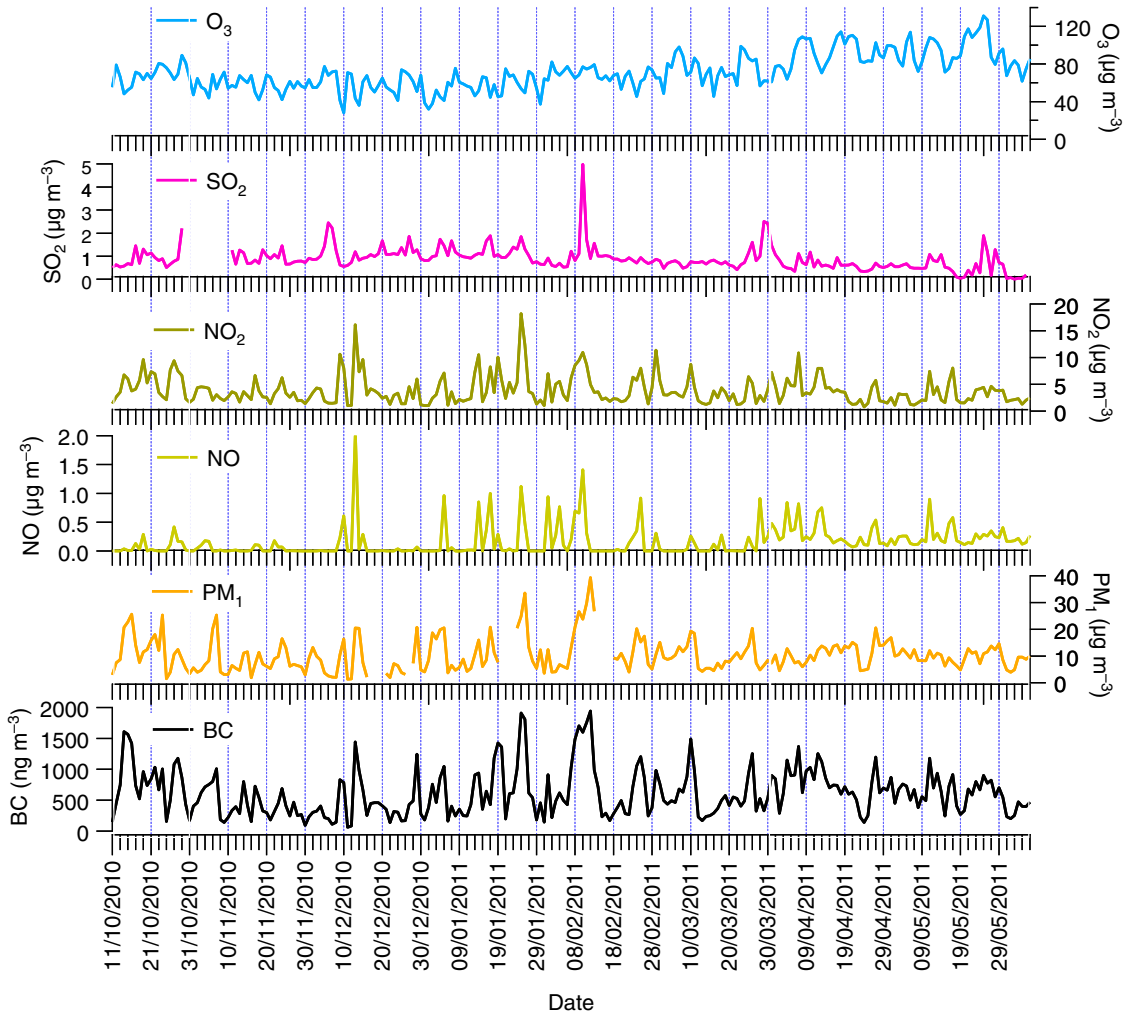

Fig. 2. Daily concentration levels for BC (ng m^{-3}), PM_1, SO_2 and NO_2, O_3 and NO (µg m^{-3}) from 11 October 2010 to 6 June 2011. Warm period (October, April to June) is shaded in green and cold period (November to March) in blue.

for SO_2 with other pollutants indicating sources of SO_2 at MSY are not related to sources of the other parameters measured.

3.2. *Particle number size distributions and seasonality at MSY*

During this study, two periods were identified according to temperature features in the colder and warmer seasons. The first period includes all data recorded from November 2010 to March 2011, when temperatures (average 7°C) were considerably lower than the second period (average 15°C; October 2010, April–June 2011), and thus the periods were accordingly entitled Cold (C) and Warm (W). Furthermore, periods were subdivided according to episodes of pollution and clean air episodes. Episodes of pollution were categorised according to concentrations of BC, and include all days whereby hourly averaged BC concentrations exceeded 700 ng m^{-3}. Clean episodes were classified similarly, and include all days whereby levels of BC hourly averages never exceeded 700 ng m^{-3}. Thus, the colder period was subdivided into C: Polluted (67 d) and Clean (31 d). The same criteria were applied for the warmer period, giving W: Polluted (32 d) and Clean (13 d). These periods will hitherto be referred to as C: Polluted and C: Clean for the colder periods, and W: Polluted and W: Clean for the warmer period. Tables 1 and 2 list the concentrations for various aerosol and meteorological parameters for each period. Analysis of 5-d back trajectories of air masses using HYSPLIT4 aided in verifying that air masses were likely to be clean or polluted. Of the 31 d classified as C: Clean, all were associated with Atlantic advection episodes or occurred after periods of heavy rainfall. The origins of air masses giving rise to episodes of elevated levels of

Table 2. Arithmetic mean and standard deviation for various aerosol parameters, pollutant gases and meteorological variables recorded at MSY for different periods throughout the measurement campaign

	PM_1 ($\mu g\ m^{-3}$)	BC ($ng\ m^{-3}$)	O_3 ($\mu g\ m^{-3}$)	NO ($\mu g\ m^{-3}$)	NO_2 ($\mu g\ m^{-3}$)	SO_2 ($\mu g\ m^{-3}$)	WS ($m\ s^{-1}$)	WD (°)	RH (%)	Temp (°C)	Days (#)
C: Total	10 ± 10	543 ± 692	62 ± 16	1.10 ± 1	3.9 ± 6	0.99 ± 1	1.66 ± 1.3	316	64	7	111
W: Total	11 ± 5	707 ± 452	88 ± 23	0.50 ± 0.5	3.8 ± 4	0.69 ± 6	1.13 ± 0.8	158	63	15	67
C: Polluted	13 ± 9	720 ± 674	60 ± 18	1.16 ± 1.1	5.2 ± 6.6	1.03 ± 0.8	0.90 ± 0.9	296	69	7	67
C: Clean	5 ± 4	230 ± 140	65 ± 10	1.00 ± 0.5	2.0 ± 1.1	0.93 ± 0.9	1.47 ± 1.2	318	65	7	31
W: Polluted	11 ± 4	786 ± 422	100 ± 21	0.28 ± 0.4	3.9 ± 4.2	0.69 ± 0.6	1.22 ± 1.5	163	61	16	32
W: Clean	8 ± 3.5	396 ± 203	88 ± 20	0.15 ± 0.1	1.7 ± 1.3	0.41 ± 0.5	1.20 ± 0.8	102	68	14	14

pollution were more varied than under clean conditions. As mentioned previously, local pollution is carried to the site by a mountain breeze with low nocturnal concentrations when MSY resides above the polluted mixing layer. The influence of long-range transport as opposed to local pollution is more difficult to ascertain but is usually evident when elevated nocturnal levels of pollutants occur. The most influential air masses bringing aerosols to MSY are from mainland Europe and North Africa. Saharan dust intrusions from North Africa occurred on 7 d and were associated with high concentrations of PM_{10} and BC, both during the day and at night. Long-range transport from Europe can occur when a high pressure system builds north of the peninsular as far as the British Isles, and air from mainland Europe travels south. This scenario occurred on 7 d during the colder period and was marked by low temperatures and very high levels of fine PM and BC both during the day and at night. Clean episodes during the warmer period resulted from either air masses from the Atlantic or from the nearby Mediterranean arriving at MSY. During the warmer period, phases of pollution are typically a result of air mass recirculation across the region, creating a continuous increment in pollution levels until it is replaced by a cleaner air mass or removed by precipitation. An intrusion of a polluted air mass from mainland Europe occurred during W lasting for a period of 5 d, resulting in continuously high levels of BC and fine PM.

Concerning particle number concentrations, levels in all modes were considerably higher during W than those recorded during C. The ratios of W to C mean concentrations for the nucleation ($N_{9–20}$), lower Aitken ($N_{20–50}$), upper Aitken ($N_{50–100}$) and accumulation ($N_{100–825}$) modes are 1.8, 1.7, 1.6 and 1.4, respectively. Higher levels of upper Aitken and accumulation mode particles in W compared to C can be attributed to the residence of MSY within the mixing layer for longer periods during the day in warmer months and lower precipitation (Pérez et al., 2008). Higher number concentrations of nucleation and lower Aitken mode particles are likely a result of increased NPF and growth, which will be discussed anon. Figure 3 shows histograms for concentrations of $N_{20–100}$ and $N_{100–825}$ for the measurement period. The accumulation mode presents the greatest differences between each period, with very low concentrations during C: Clean, and highest concentrations during W: Polluted. Elevated concentrations of Aitken mode particles under W: Polluted are more frequent as evidenced by the wider histogram shape. However, Aitken mode concentrations are similar in all periods, even though the sources are likely to be very different depending on the scenario.

The modality of median number size distributions under the different periods and scenarios was also investigated and are presented in Fig. 4. The fitted log-normal modes ($dN/d\log_{10}Dp$) are also shown underneath each graph (in red). The modal fittings in all cases are performed for day-time size distributions, i.e. 8–20 hours GMT [median night-time size distribution modality (20–8 hours) is represented in each figure by the solid black line]. All scenarios except C: Polluted exhibit a bimodal size distribution. During polluted conditions in C, the size distribution is unimodal with a median diameter (Dp_m) around 75 nm. Median size distributions for different seasons at a range of regional background sites across Europe were reported by Asmi et al. (2011). Using the results presented in that article, winter size distributions under polluted conditions at MSY most closely reflect those given for central European stations, indicating that size distributions and concentrations at MSY under these conditions are very similar to continental size distributions. Comparatively, the median size distribution under clean conditions during C is distinctly bimodal, with a Dp_m around 35 nm and a second mode with peak diameter around 150 nm, albeit with much lower concentrations. Interestingly, this modality is observed in winter at many of the high altitude sites reported by Asmi et al. (2011), such as at Jungfraujoch (3580 m.a.s.l.). Thus, under clean conditions during the colder period, it appears that MSY bears some similarities with high or mid altitude sites.

This bimodal behaviour is also evident during W, except the dominant modes in these cases are reversed when compared with C: Clean. The Aitken mode is dominant, with Dp_m between 80 and 90 nm under both W: Clean and

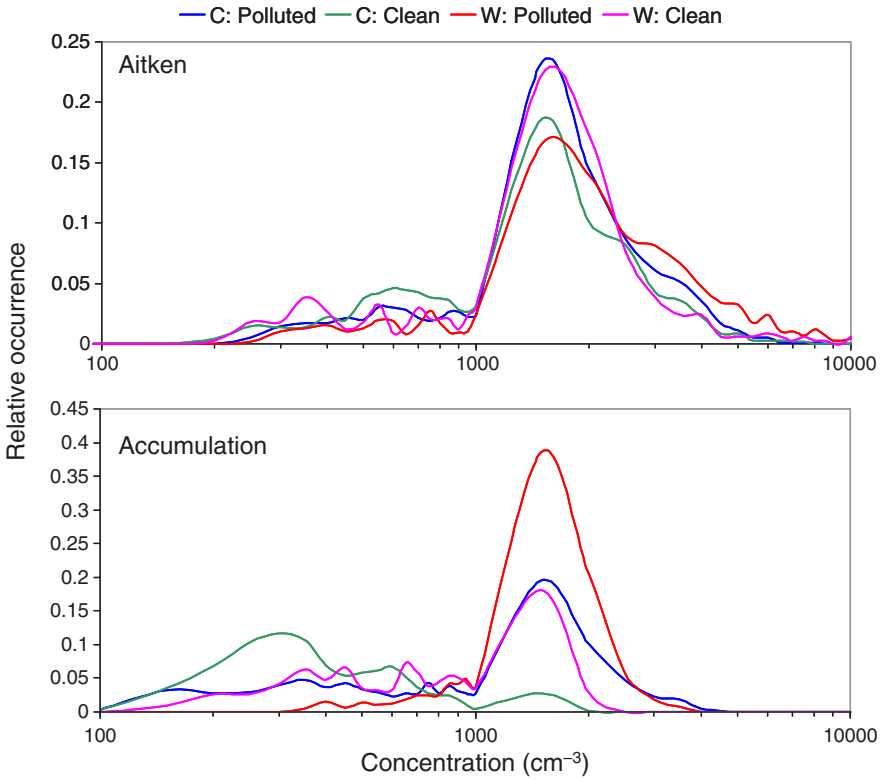

Fig. 3. Histogram of $N_{20–100}$ and $N_{100–825}$ hourly median concentrations at MSY for the different periods. The concentration bins are evenly distributed along the concentration axis (20 bins/decade) and the y-axis shows the occurrence of each bin relative to the total number of measurements.

W: Polluted, with a secondary mode between 20 and 30 nm. Although the modality for both clean and polluted conditions is very similar, concentrations are substantially lower under cleaner conditions. Referring once again to results published by Asmi et al. (2011), MSY displays similar spring time size distributions for the stations Bösel and Schauinsland in Germany. Bösel is a central European low altitude site situated among land mostly used for agriculture and some residential areas. Interestingly, springtime total particle number concentrations at MSY under clean conditions are similar to those reported for Schauinsland (Germany; 1210 m.a.s.l.), while under polluted conditions they are more similar to concentrations at Bösel.

3.2.1. Particle concentrations and variability during colder months. During the colder months, MSY undergoes sharp changes in pollutant concentrations, with daytime maxima and nocturnal minima for all pollutants, driven by the diurnal breeze system (Pérez et al., 2008; Pey et al., 2010) which advects pollutants from the semi-urban and urban areas at lower altitudes to the site during the day-time. Therefore, mixing effects between polluted and non-polluted boundary layer air masses can be very significant at this site. Aerosols accumulate in the valleys below MSY, and are transported towards elevated areas such as MSY during the day by the presence of mountain and sea breezes, activated by insolation (see wind speed and direction in Fig. 5). The nocturnal north-west (NW) winds and daytime southerly wind scenarios are related to the topography of the valley wherein the MSY site is located. The polluted southerly breeze proceeds up the valley during the day, followed by a nocturnal drainage flow from the north, removing pollutants from the site. Night-time levels of BC (minimum 374 ng m^{-3}) and PM_1 (7.6 µg m^{-3}) are relatively low, but undergo sharp increases during the day with maximum values being reached at 16:00 (1343 ng m^{-3} and 15.9 µg m^{-3}, respectively). The mixed state of the particle sizes is highlighted by the similar concentrations for the upper Aitken and accumulation mode. Nucleation mode particle concentrations are low (median concentration of 92 cm^{-3}) owing to the elevated condensation sink, which varies similarly to $N_{20–825}$, highlighting the aged state of the air mass having stagnated within the mixing layer before reaching MSY. As stated previously, the median size distribution of particles under these conditions is clearly unimodal with a Dp_m of 75 nm, both during the day and at night (Fig. 4).

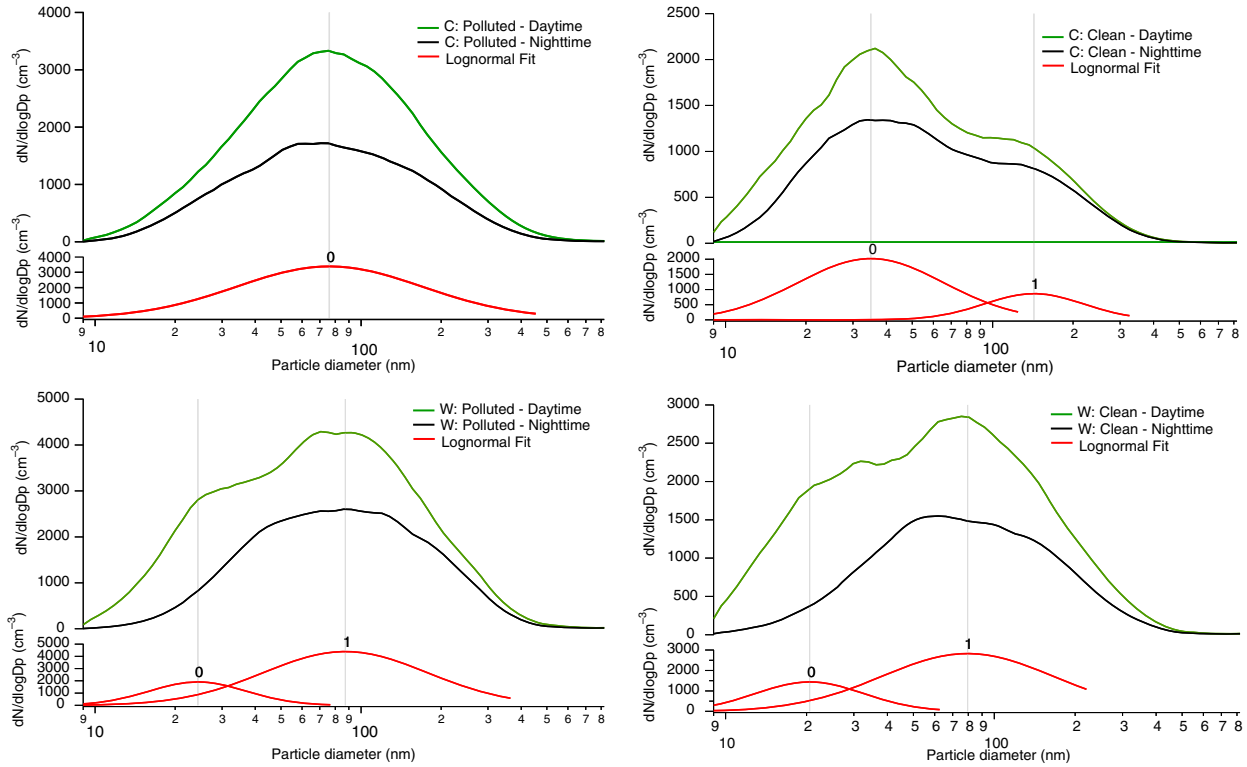

Fig. 4. Median distributions for daytime (green lines), night-time (black lines) and modal fittings of daytime distribution (red lines) for periods C and W under polluted and clean conditions.

Conversely, Fig. 6 shows the diurnal variations for almost the same parameters (temperature is replaced by solar radiation) under clean conditions during the colder months. The NW wind is maintained throughout the day with little change in wind direction and, thus, minimum influence of the polluted mountain breeze. Wind speeds are also slightly higher (1.47 ± 1.2 m s^{-1}) compared to polluted conditions (0.90 ± 0.9 m s^{-1}), especially during the day. The day and night variations are significantly reduced for many pollutants, with night-time minima of BC of 177 ng m^{-3} and day time maxima of 277 ng m^{-3}. The absence of abundant pre-existing particles allows for NPF to take place, giving rise to higher concentrations of nucleation mode particles. This is evident in the overall reduced condensation sink (daily mean of 2.6×10^{-3} s^{-1}) compared to polluted conditions (5.9×10^{-3} s^{-1}). Kulmala et al. (2005) reported condensation sink values for nucleation event days in Athens and Marseille to range between $5.9 \times 10^{-3} - 1.3 \times 10^{-2}$ s^{-1} and $3.2 \times 10^{-3} - 1.5 \times 10^{-2}$ s^{-1}, respectively, which are in line with values recorded at MSY in winter. Furthermore, the condensation sink reaches a minimum precisely when the nucleation mode begins to increase at 10:00 GMT. Concerning particle number size concentrations, less variation is observed for the accumulation and upper Aitken mode particle number concentrations between night and day, similarly to BC and PM_1. However, particle number concentrations of nucleation and lower Aitken mode particles are significantly increased and undergo a large diurnal variation unlike that of the other parameters measured. No correlation between either nucleation or lower Aitken and accumulation mode particle concentrations was observed ($R^2 = 0.006$ and 0.03, respectively), giving a strong indication that NPF is occurring in-situ and not by transport. Growth to the Aitken mode is possible considering the loose correlation observed for nucleation and the lower Aitken mode ($R_0^2 = 0.44$, hourly resolution, 671 data points), and this correlation actually improves slightly with R_1^2 (0.48). Further growth from the lower Aitken to the upper Aitken mode is not as efficient ($R_0^2 = 0.23$). As solar radiation approaches maximum values between 10 and 11:00 GMT, nucleation particle concentrations begin to increase continuously to a maximum median concentration of 480 cm^{-3} at 14:00 GMT, as shown in Fig. 6. The continuous increase in lower Aitken mode concentrations reaches a maximum of 1475 cm^{-3} at 18:00 GMT. The diurnal profile for ozone under polluted conditions (Fig. 5) is in stark contrast to that of ozone under clean conditions (Fig. 6). The absence of the polluted breeze loaded with NO_x allows ozone concentrations to increase throughout the day. Ozone may be a limiting factor in the growth of nucleating particles under

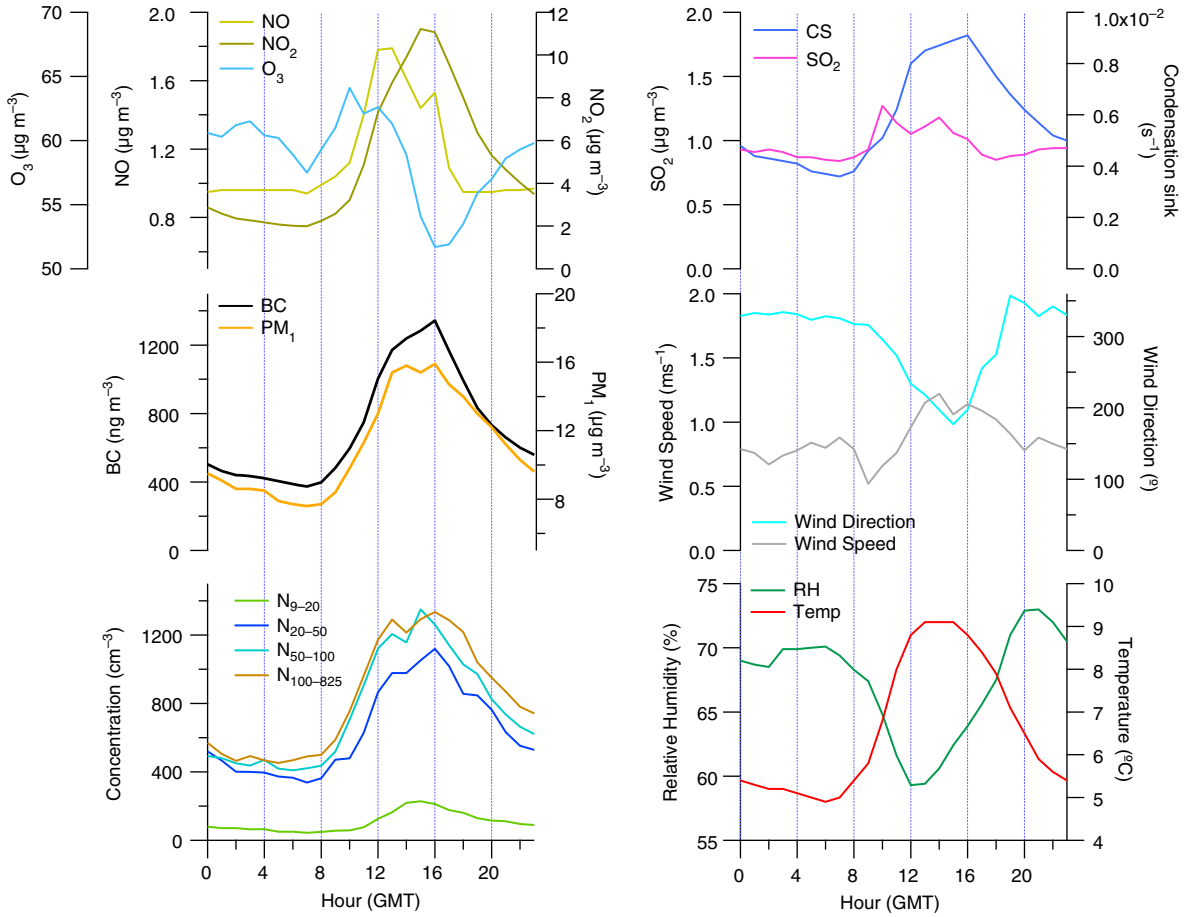

Fig. 5. Median diurnal variation of particle number concentrations of nucleation, lower Aitken, upper Aitken and accumulation mode particles (cm^{-3}); mean concentrations of BC ($ng\ m^{-3}$), PM_1, NO, NO_2, O_3, SO_2 ($\mu g\ m^{-3}$); temperature (°C), relative humidity (%), wind speed ($m\ s^{-1}$), wind direction (°) and condensation sink (s^{-1}) during C: Polluted.

these conditions, as it is responsible for the formation of condensable organic species through reactions with VOCs (Hallquist et al., 2009). These condensable organic species are not believed to be directly involved in NPF but are believed to promote more rapid growth of nucleating clusters.

Out of a total of 31 d of clean conditions, 14 episodes of elevated nucleation mode particle concentrations were observed, as shown in Fig. 7. However, episodes with elevated concentrations of nucleation mode particles were observed to occur at different times of day. As Fig. 7 outlines, for each date that elevated concentrations of nucleation mode particles occurred, the time (hour GMT) when maximum particle number concentrations of nucleation and lower Aitken mode was recorded for that respective day, and the particle number concentrations reached in those modes at that hour. This highlights how the occurrence of elevated nucleation particle number concentrations varies on different days. According to the classification of nucleation events outlined by Dal Maso et al. (2005), not all of the episodes when elevated $N_{9–20}$ were observed at MSY can be classified as nucleation events in the traditional sense. For example, elevated concentrations of nucleation mode particles recorded on 10 November 2010, 6 December 2010 and 8 January 2011 coincide with peak concentrations in the lower Aitken mode. In all three cases, a sharp increase was observed simultaneously for both nucleation and Aitken mode particle concentrations, suggesting that there is mixing of different air masses with differing aerosol processes occurring within the air mass. Similarly, days where nucleation mode concentrations are significantly lower than lower Aitken mode concentrations, and when peak concentrations occur quite late in the day such as on the 15 November 2010 and 26 November 2010, may be a result of transport of nucleating particles and accompanying growth particles, with some influence of mixing effects of air masses. Days of elevated nucleation mode particles when nucleation mode particle number concentrations are low are usually

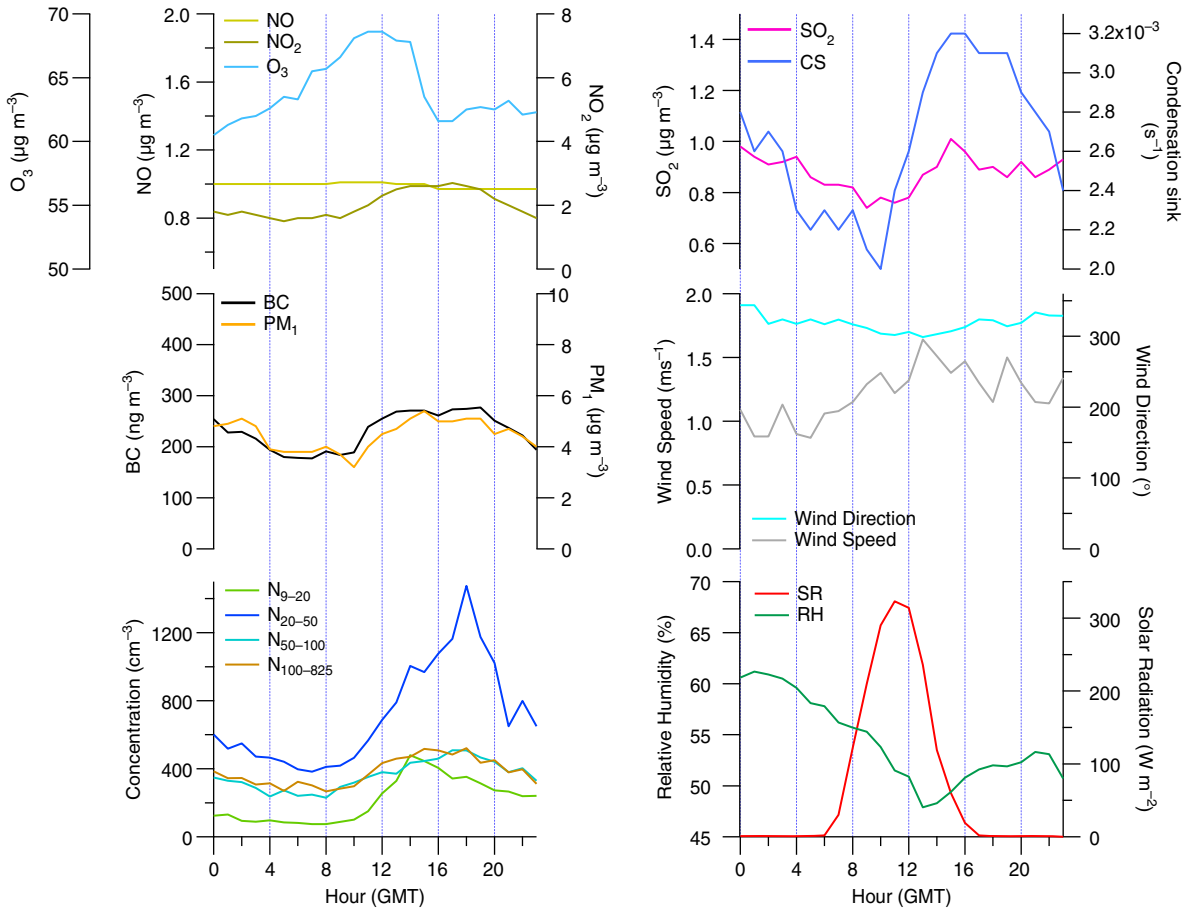

Fig. 6. Median diurnal variation of particle number concentrations of nucleation; lower Aitken, upper Aitken and accumulation mode particles (cm^{-3}); mean concentrations of BC ($ng\ m^{-3}$), PM_1, NO, NO_2, O_3, SO_2 ($\mu g\ m^{-3}$); solar radiation ($W\ m^{-2}$), relative humidity (%), wind speed ($m\ s^{-1}$), wind direction (°) and condensation sink (s^{-1}) during C: Clean.

accompanied by low lower Aitken mode particle number concentrations, and are not especially intense bursts of NPF. Nucleation events in the traditional sense, displaying the typical banana profile associated with NPF and growth, occurred on the 9 November 2010, 7 December 2010, 8 December 2010, 25 December 2010 and the 27 December 2010.

An example of a nucleation event that occurred on 25 December 2010 is shown in Fig. 8. NPF commences around 12:00 GMT, and nucleation mode particle number concentrations reach a maximum at 15:00 GMT. The lower Aitken mode continues to increase after the nucleation mode and reaches a maximum at 17:00 GMT, as the nucleation mode particles grow in diameter to Aitken mode particles. Upper Aitken and accumulation mode concentrations are comparatively much lower (note their concentrations are represented by the right axis), that is, the absence of larger particles allow NPF to take place. This is verified by the variation in the condensation sink, which varies similarly to the upper Aitken mode. SO_2 concentrations, and thus $[H_2SO_4]$, for this particular day were negligible and underwent little variation.

Continuous particle number size distribution measurements in Northern Italy (Ispra) were performed from June to December 1999 by Rodríguez et al. (2005). It was observed that nucleation events at the boundary layer site only occurred under clean air conditions. This also appears to be the case at MSY during the colder months, whereby nucleation tends to occur when clean-air conditions are prevalent.

3.2.2. Particle concentrations and variability during warmer months. The diurnal variations of pollutants measured during the warmer period (W) present significant differences to the variation observed during C. During the day, wind speeds are slightly higher and the daytime southerly breeze is much more stable and longer in duration, owing to the higher temperatures. The effect of the mountain breeze on the aerosol parameters is evident

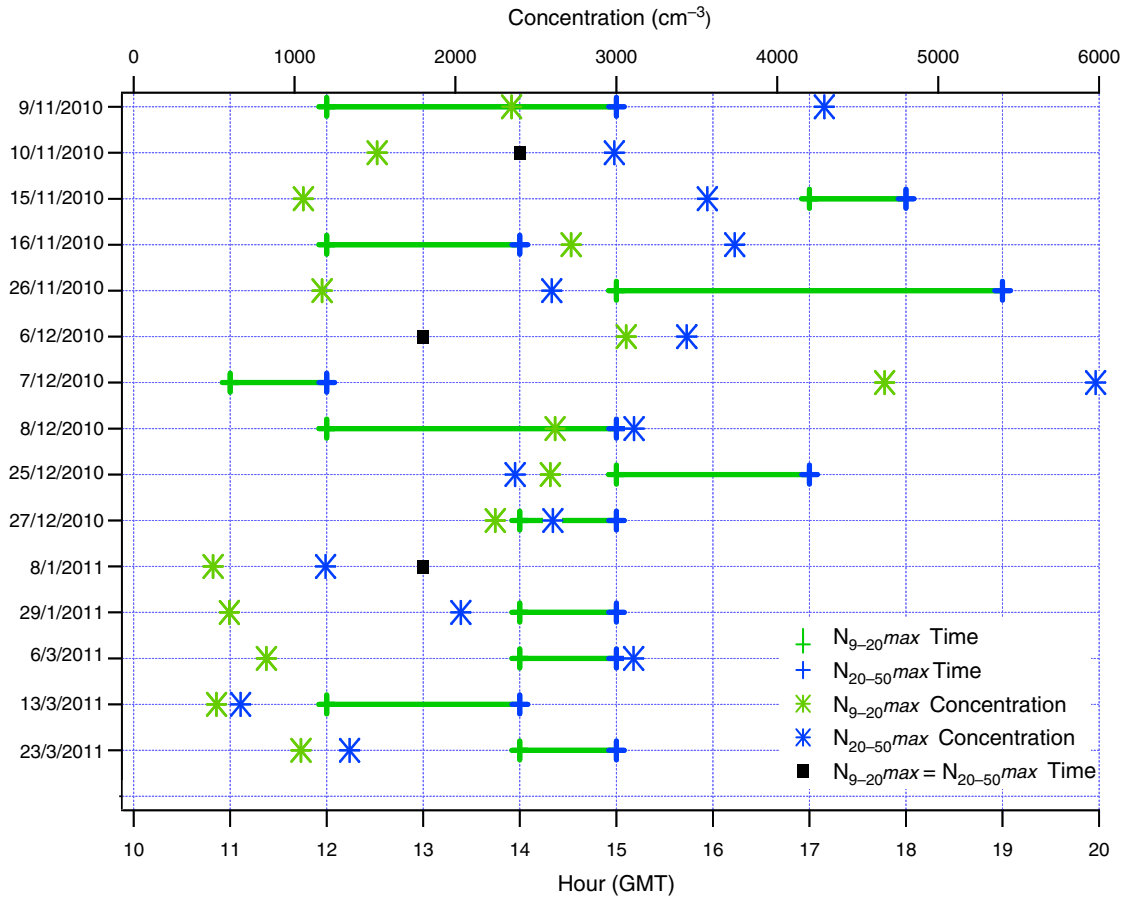

Fig. 7. Days when elevated levels of N_{9-20} occurred during C: Clean; the hour (GMT) when maximum particle number concentrations are reached for nucleation (green) and lower Aitken (blue) mode and the respective particle number concentrations. Black dots indicate when peak N_{9-20} and N_{20-50} particle number concentrations occur at the same time.

during this period also, but the duration of the peaks in pollutant concentrations are extended compared to C, owing to the higher temperatures, increase in mixing layer height and the increase in wind speed during the warmer months.

Figure 9 displays the diurnal trends for the same parameters presented in Fig. 5 for W under polluted conditions. BC and PM_1 concentrations are slightly elevated during the warmer months, with minimum night time concentrations for BC of 505 ng m^{-3} and PM_1 concentrations at 9.2 μg m^{-3}. Particle number concentrations are elevated for all modes compared to C. Upper Aitken and accumulation mode particles undergo similar diurnal variations as BC and PM_1 mass concentrations. Ozone concentrations are elevated owing to more intense solar radiation and increased photochemical reactions of VOCs, irrespective of the NO_x sink.

The diurnal variation of the nucleation and lower Aitken modes during the warmer period is unlike the variations observed for BC or PM_1. The nucleation mode peaks at 14:00 GMT coinciding with peak solar radiation, and also with maximum lower Aitken mode particle number concentrations. Thus, nucleation mode particle number concentrations increase even in the presence of the polluted breeze and elevated levels of upper Aitken and accumulation mode particles, indicating that NPF may be taking place even in the presence of pre-existing particles, as highlighted by the increased levels of the condensation sink. As observed for the size distribution modality under these conditions, a secondary mode is observed near the nucleation mode (25 nm; Fig. 4). Hamed et al. (2007) also observed higher nucleation events during the warmer months at the boundary layer site in the Po valley in Italy even under polluted conditions. High particle growth and formation rates of the nucleation particles were recorded, as freshly nucleated particles need to grow quickly before being scavenged by pre-existing particles.

Owing to the heavy particle loading of the polluted air mass arriving at MSY, and the short residence time of nucleation mode particles (reported as a few hours in a

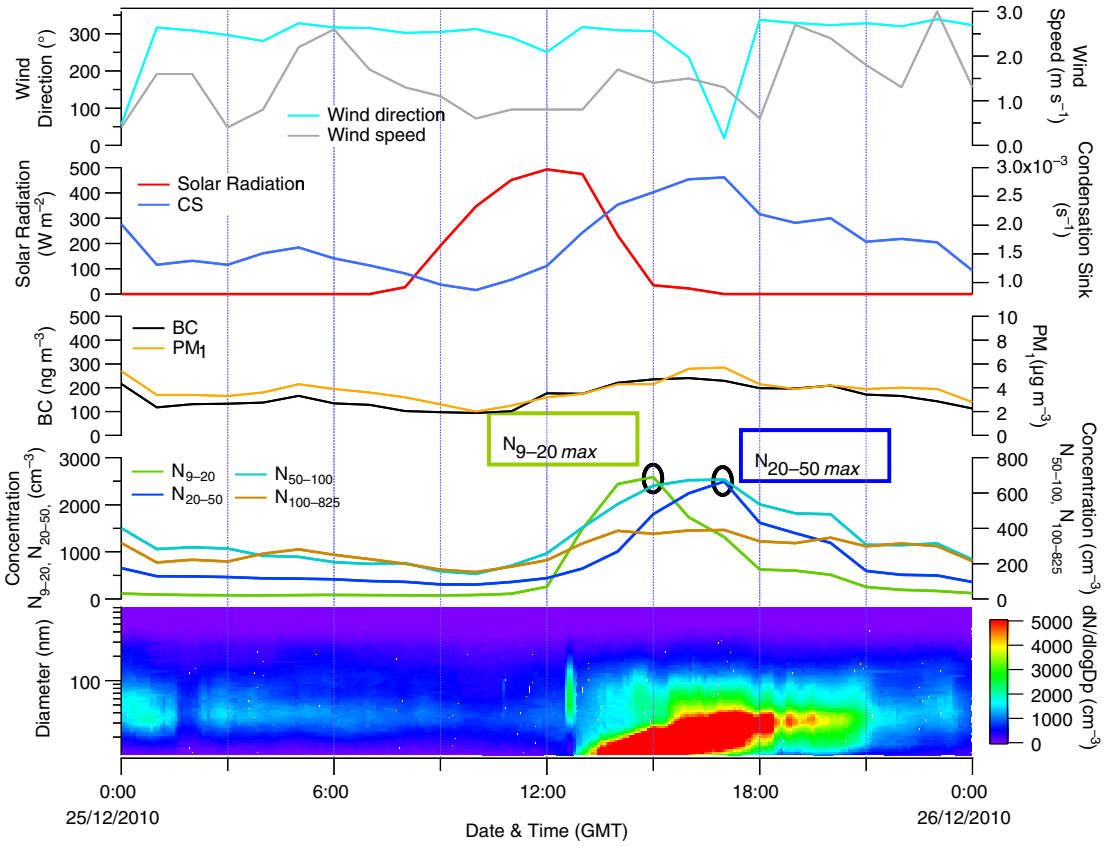

Fig. 8. Time series of a nucleation event recorded during C: Clean on 25 December 2010 showing the contour plot of the particle number size distribution, with median particle number concentration of nucleation and lower Aitken (left axis), and upper Aitken and accumulation mode (right axis) concentrations, PM_1, BC, condensation sink and solar radiation, wind speed and wind direction.

roadside environment by Charron and Harrison, 2003), the elevated particle number concentrations of nucleation mode particles at MSY are evidently forming and growing faster than they can be removed. Biogenic emissions from local vegetation may be a significant source of condensable organic vapours at MSY. Although organic vapours are not believed to play a role in the initial formation of new particles, subsequent growth of nucleated clusters is considered to be enhanced by oxidation products of biogenic organic vapours such as terpenes (O'Dowd et al., 2002). An abundance of such biogenic compounds in the atmosphere might indeed promote the growth of nucleating clusters to a detectable size before the gaseous precursors are lost through coagulation and condensation processes. Seco et al. (2011) reported VOC mixing ratios at the same site of MSY in summer and winter with the aim of determining the effect of biogenic emissions on VOC concentrations. It was reported that short-chain oxygenated VOCs and isoprenoids presented higher mixing ratios in summer, attributed to higher emissions by vegetation and increased photochemistry. This also resulted in higher ozone concentrations. The abundance of VOCs in the atmosphere during the warmer months most likely account for the increase in ultrafine particles observed. Furthermore, a study performed by Querol et al. (1999) in a rural area in NE Spain found midday oxidation rates of SO_2 to SO_4^{2-} (the intermediate compound H_2SO_4 is a known nucleating agent) were seasonally dependent, with oxidation ratios ranging seasonally from $<1\%\ h^{-1}$ (winter) to $6\%\ h^{-1}$ (summer). Thus, an abundance of H_2SO_4, VOCs and solar energy would likely enhance NPF and growth. Figure 10 displays an example of an episode with elevated levels of nucleation mode particles recorded on the 6 June 2011, a day with relatively elevated levels of pollutants.

As is evident in Fig. 10, an intense burst of NPF occurs at 9:00 GMT, where nucleation is evidently activated by the peak observed for $[H_2SO_4]$. NPF is relatively short lived as it is interrupted by the increasing condensation sink and BC concentrations. A drop in solar radiation is also observed which may be due to a passing cloud or cloud formation on site. As BC and PM_1 mass concentration levels begin to decrease as the morning progresses, the lower Aitken and nucleation mode begin to increase, peaking between 13:00 and 14:00 GMT. The lower Aitken mode decreases

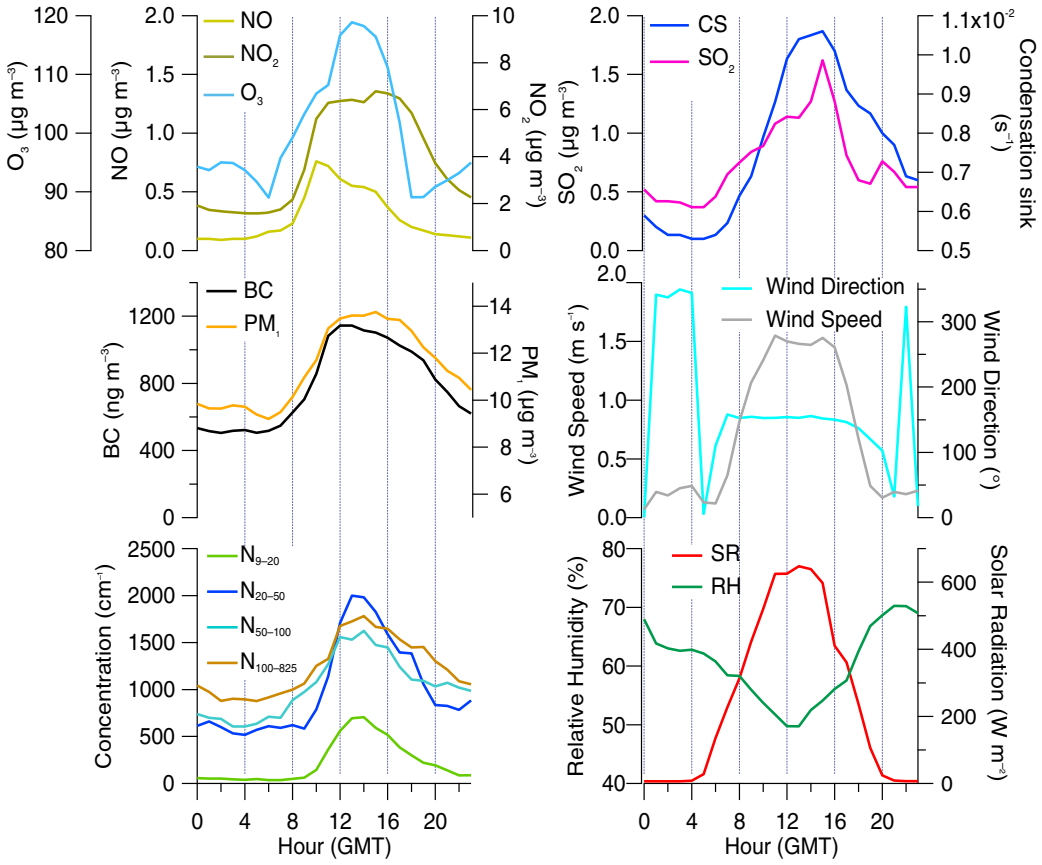

Fig. 9. Median diurnal variation of particle number concentrations of nucleation, lower Aitken, upper Aitken and accumulation mode particles (cm^{-3}); mean concentrations of BC (ng m^{-3}), PM_1, NO, NO_2, O_3, SO_2 (µg m^{-3}); solar radiation (W m^{-2}), relative humidity (%), wind speed (m s^{-1}), wind direction (°) and condensation sink (s^{-1}) during W: Polluted.

thereafter but unusually the nucleation mode concentrations are maintained for an hour after the lower Aitken mode decreases. There are various reasons that could explain this unusual behaviour. It is possible that a mixing event between different air masses occurred, whereby nucleation occurring in one of the air masses is replaced briefly by a more polluted air mass. Air mass back trajectory analysis showed a stable atmosphere for various altitudes throughout the day at MSY, but higher resolution analysis may prove that a mixing event is taking place. Thus, it could be suggested that (a) as background aerosol particle number and mass concentrations decrease, nucleation processes resume without further growth; (b) different parts of the air mass at different stages of a nucleation event are being sampled during the same day; (c) particles are actually evaporating from the lower Aitken mode to the nucleation mode. Particle evaporation, to the author's knowledge, has only been described in the urban environment of London (Dall'Osto et al., 2011) and Hong Kong (Yao et al., 2010). It was suggested that nanoparticle loss as a result of evaporation of the volatile/semi-volatile species caused this phenomenon. At MSY, episodes whereby a reversal of nucleated particle growth occurs in a 'reverse banana' profile occurred on 23 d during the entire measurement period. It is likely that these unusual processes are a result of mixing effects of air masses, but the possibility of particle evaporation cannot be ruled out. These findings are beyond the scope of this present work but will be further investigated in detail in future publications.

Figure 11 displays all the same variables for W under clean conditions. Mean particle number concentrations of nucleation mode particles are the same as under polluted conditions (345 cm^{-3}), whereas Aitken and accumulation mode particle number concentrations are significantly lower than under polluted conditions. Peak concentrations of nucleation mode particles are slightly higher (866 cm^{-3}) compared to polluted conditions (706 cm^{-3}). Maximum BC and PM_1 mass concentrations reach 532 ng m^{-3} and 9.5 µg m^{-3}, respectively. BC is closely related to accumulation mode particle number concentration ($R_0^2 = 0.67$, $R_1^2 = 0.54$, $R_2^2 = 0.40$; 336 data points) and undergo similar variations. The nucleation and lower Aitken modes undergo alternative

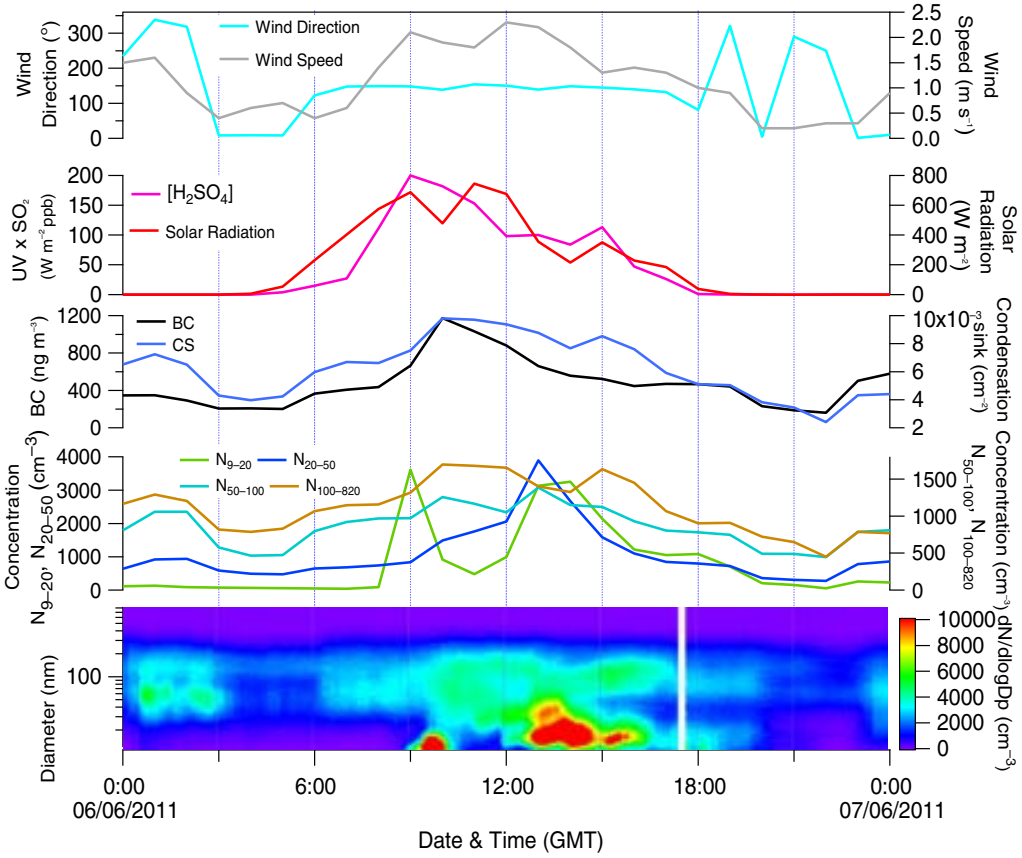

Fig. 10. Time series of a nucleation event recorded during W: polluted on 6 June 2010, with the contour plot of the size distribution and median particle number concentrations of nucleation, lower Aitken (left axis), upper Aitken and accumulation modes (right axis), BC mass concentration, condensation sink, solar radiation, a proxy for [H_2SO_4], wind speed and wind direction.

variations independent of the other parameters. Nucleation mode concentrations begin to increase in the early morning with increasing solar radiation, to a maximum of 866 cm^{-3} at 13:00 GMT, followed by a peak in lower Aitken mode concentrations (1718 cm^{-3} at 14:00 GMT). The condensation sink under clean conditions is significantly lower than under polluted conditions, but this does not seem to affect the nucleation mode concentrations. SO_2 concentrations also begin to increase around the same time as the nucleation mode. An input of sulphuric acid (produced from the oxidation of SO_2), a summer abundance of condensable organic vapours from vegetative and anthropogenic sources, elevated ozone concentrations and intense solar radiation, would provide perfect conditions for NPF and growth.

A measurement campaign performed at Monte Cimone from June to July was described by Van Dingenen et al. (2005). The diurnal trends during the study show remarkable similarities to those observed at MSY during the warmer months. Monte Cimone (2165 m.a.s.l.) is located at a much higher altitude than MSY (720 m.a.s.l.), but BC mass concentrations undergo similar diurnal trends to those observed at MSY. The diurnal trend at Monte Cimone for BC is attributed to the transport of pollution by upslope winds induced by heating of the mountain side, similar to MSY. Furthermore, the morning increase of submicron particle number concentrations is noticeably similar to that observed at MSY. The authors suggest that the mixing of polluted boundary layer air with the clean free troposphere air provided favourable conditions for photochemically induced homogenous nucleation to occur in-situ. The example of a nucleation event shown in Fig. 12 suggests that mixing of different air masses is similarly influential at MSY.

Figure 12 displays an example of NPF occurring at the beginning of April under clean conditions. Nucleation begins at 8:00 GMT and is followed by a rapid increase in concentrations relative to the lower Aitken mode. Peak concentrations of nucleation mode particles also coincide with peak [H_2SO_4] concentrations. Nucleation is interrupted as levels of BC and PM_1 increase suddenly at 12:00 GMT and the condensation sink increases, removing the nucleating particles through condensation and coagulation.

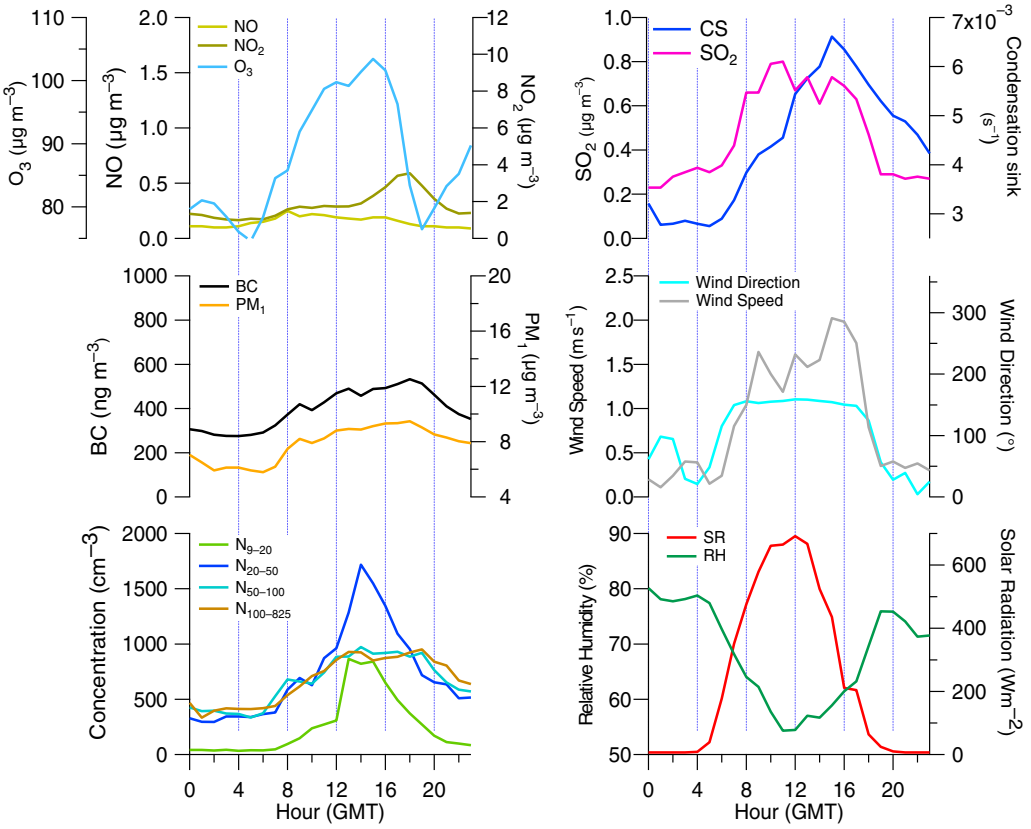

Fig. 11. Median diurnal variation of particle number concentrations of nucleation, lower Aitken, upper Aitken and accumulation mode particles (cm^{-3}); mean diurnal variation of BC ($ng\ m^{-3}$), PM_1, NO, NO_2, O_3, SO_2 ($\mu g\ m^{-3}$); solar radiation ($W\ m^{-2}$), relative humidity (%), wind speed ($m\ s^{-1}$), wind direction (°) and condensation sink (s^{-1}) during W: Clean.

The coinciding double peak observed in BC and the Lower Aitken mode suggests that the two parameters are closely related, and also that an abrupt change in the air mass is occurring. The change in wind direction and speed which occurs at the same time when lower Aitken mode concentrations begin to decrease and nucleation mode particles peak suggests that a mixing event is being observed, whereby different phases of a nucleation event within the air mass are sampled during the same day. Air mass back trajectory analysis (using HYSPLIT) at different altitudes did not show any evidence of mixing. However, taking into consideration the change in wind direction, it would seem likely that a nucleation event is being observed over a large area, and the nucleating particles at different stages of formation and growth are being sampled as the day progresses. The nucleation mode reaches a daytime minimum between the hours of 12:00 and 13:00 GMT, when BC and PM_1 are at their highest, that is, a polluted air mass has moved over MSY. The change in wind direction and coinciding drop in BC and particles > 20 nm, suggest that the polluted air mass is quickly replaced by a cleaner air mass, within which a nucleation episode is occurring.

4. Summary and conclusions

Eight months of sub-micrometer particle number size distributions at the RB site of MSY have been analysed and described to determine their variability in the western Mediterranean. The Aitken mode was observed to be the dominant size mode in terms of particle number concentration, followed by the accumulation and nucleation modes. Furthermore, particle number concentrations showed a clear seasonal variability, with concentrations significantly elevated during warmer months relative to colder months. Owing to this seasonality observed, the dataset was divided according to temperature; a cold period (C: November to March) and a warm period (W: October, April to June). Furthermore, these periods were categorised according to scenarios of clean and polluted episodes. Under polluted conditions during C, the observed daily variability of the various particle properties was related to a diurnal breeze system activated by insolation. This scenario was characterised by low nocturnal number and mass concentrations of aerosols when MSY resided above the polluted mixing layer, with elevated daytime concentrations due to transport

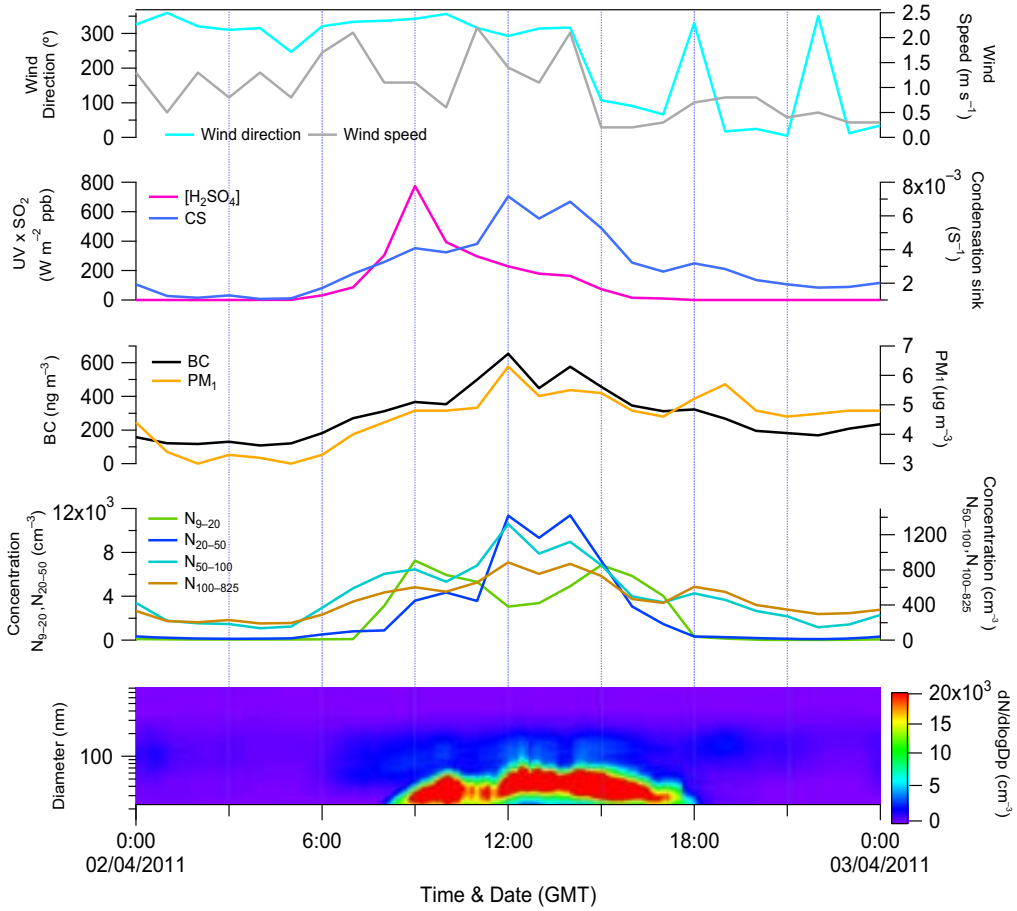

Fig. 12. Time series of a nucleation event recorded during W: Clean on 2 April 2011 with the contour plot of the size distribution and particle number concentration of nucleation, lower Aitken (left axis), upper Aitken and accumulation modes (right axis); PM_1 and BC mass concentrations; condensation sink; a proxy for $[H_2SO_4]$ concentrations, wind speed and wind direction.

of pollutants to MSY carried by upslope winds. Particle number size distributions during C: Polluted were clearly unimodal, both during the day and at night, with a modal diameter around 75 nm. Conversely, the diurnal profile under clean conditions during C presented little day-to-night variation for almost all the pollutant parameters except for the nucleation mode and lower Aitken mode. The absence of pre-existing particles in the form of coarser particles, as evidenced by lower values of the condensation sink, allowed for NPF to take place. The nucleation mode began to increase coinciding with minimum levels of the condensation sink and maximum intensity of solar radiation. The particle size distribution is bi-modal, with a dominant mode peaking at 35 nm and a secondary mode at 150 nm. Nucleation mode concentrations were observed to undergo significant increases at different times of day and to varying degrees of intensity, and this was related to NPF events in some cases. In others, mixing events between polluted and non-polluted boundary layer air gave rise to short intense bursts of nucleation mode particles.

Diurnal particle number concentrations for all modes during W were observed to be significantly different to the diurnal profiles observed during C. The nucleation and lower Aitken modes concentrations exhibited the largest difference between W and C, although particle number concentrations in all modes were elevated. Bimodal size distributions were recorded for both W: Polluted and W: Clean, with modal diameters around 80–90 nm and 20–30 nm, although particle concentrations are reduced under W: Clean. Nucleation mode particle number concentrations were elevated even under polluted conditions and the presence of an elevated condensation sink. NPF under polluted conditions was believed to be able to occur due to (a) increased solar radiation promoting photochemical reactions, and (b) elevated concentrations of condensable organic vapours produced from the photochemical oxidation of secondary aerosol precursor gases and biogenic emissions. An abundance of such condensable organic vapours in the atmosphere might promote the growth of nucleating clusters to a detectable size even in a

relatively polluted atmosphere. The diurnal profile for clean conditions during W differs significantly to that of C, specifically in that BC and PM_1 mass concentrations are higher and underwent a larger day-to-night variation. NPF clearly occurred even in the presence of pre-existing particles capable of scavenging potentially nucleating gaseous precursors. Finally, mixing effects between polluted and non-polluted boundary layer was observed to be an influential process at MSY, whereby it was observed that different phases of nucleation and growth processes within the same air mass was occurring and sampled at different times of day at the site, giving rise to unusual size distributions.

5. Acknowledgments

This study was supported by the Ministry of Economy and Competitiveness and FEDER funds under the projects CARIATI (CGL2008-06294/CLI), VAMOS (CGL2010 19464/CLI) and GRACCIE (CSD 2007-00067), and from the Generalitat de Catalunya 2009 SGR8. The research leading to these results has received funding from the European Union Seventh Framework Programme (FP7/2007-2013) ACTRIS under grant agreement no. 262254. The authors would like to extend their gratitude to Jesús Parga and Jordi Gil for their technical support. The authors also thank METEOCAT for the meteorological data and the NOAA Air Resources Laboratory (ARL) for the provision of the HYSPLIT transport and dispersion model and/or READY website (http://www.arl.noaa.gov/ready.html) used in this publication. Finally, the authors thank Dr. Zhibin Wang for his essential input.

References

Allan, J. D., Alfarra, M. R., Bower, K. N., Coe, H., Jayne, J. T. and co-authors. 2006. Size and composition measurements of background aerosol and new particle growth in a Finnish forest during QUEST 2 using an Aerodyne aerosol mass spectrometer. *Atmos. Chem. Phys.* **6**, 315–327.

Asmi, A., Wiedensohler, A., Laj, P., Fjaeraa, A.-M., Sellegri, K. and co-authors. 2011. Number size distributions and seasonality of submicron particles in Europe 2008–2009. *Atmos. Chem. Phys.* **11**, 5505–5538.

Birmili, W., Wiedensohler, A., Heintzenberg, J. and Lehmann, K. 2001. Atmospheric particle number size distribution in central Europe: statistical relations to air masses and meteorology. *J. Geophys. Res. D. Atmos.* **106**, 32005–32018.

Charlson, R. J., Lovelock, J. E., Andreae, M. O. and Warren, S. G. 1987. Oceanic phytoplankton, atmospheric sulphur, cloud albedo and climate. *Nature*. **326**, 655–661.

Charron, A. and Harrison, R. M. 2003. Primary particle formation from vehicle emissions during exhaust dilution in the roadside atmosphere. *Atmos. Environ.* **37**, 4109–4119.

Cusack, M., Alastuey, A., Pérez, N., Pey, J. and Querol, X. 2012. Trends of particulate matter (PM2.5) and chemical composition at a regional background site in the Western Mediterranean over the last nine years (2002–2010). *Atmos. Chem. Phys.* **12**, 8341–8357.

Dal Maso, M., Kulmala, M., Riipinen, I., Wagner, R., Hussein, T. and co-authors. 2005. Formation and growth of fresh atmospheric aerosols: eight years of aerosol size distribution data from SMEAR II, Hyytiälä, Finland. *Boreal. Environ. Res.* **10**, 323–336.

Dall'Osto, M., Thorpe, A., Beddows, D. C. S., Harrison, R. M., Barlow, J.F. and co-authors. 2011. Remarkable dynamics of nanoparticles in the urban atmosphere. *Atmos. Chem. Phys.* **11**, 6623–6637.

Draxler, R. R. and Hess, G. D. 1998. An overview of the HYSPLIT_4 modelling system for trajectories, dispersion and deposition. *Aust. Meteor. Mag.* **47**, 295–308.

Easter, R. C. and Peters, L. K. 1994. Binary homogenous nucleation: temperature and humidity fluctuations, nonlinearity and aspects of new particle production in the atmosphere. *J. Appl. Meteorol.* **33**, 775–784.

Eisele, F. L. and McMurray, P. H. 1997. Recent progress in understanding particle nucleation and growth. *Philos. Trans. R. Soc. Lond. B.* **352**(1350), 191–200.

Fernández-Camacho, R., Rodríguez, S., De La Rosa, J., Sánchez De La Campa, A. M., Viana, M. and co-authors. 2010. Ultrafine particle formation in the inland sea breeze airflow in Southwest Europe. *Atmos. Chem. Phys.* **19**, 9615–9630.

Gómez-Moreno, F. J., Pujadas, M., Plaza, J., Rodríguez-Maroto, J. J., Martínez-Lozano, P. and co-authors. 2011. Influence of seasonal factors on the atmospheric particle number concentration and size distribution in Madrid. *Atmos. Environ.* **18**, 3169–3180.

Hallquist, M., Wenger, J. C., Baltensperger, U., Rudich, Y., Simpson, D. and co-authors. 2009. The formation, properties and impact of secondary organic aerosol: current and emerging issues. *Atmos. Chem. Phys.* **9**, 5155–5236.

Hamed, A., Joutsensaari, J., Mikkonen, S., Sogacheva, L., Dal Maso, M. and co-authors. 2007. Nucleation and growth of new particles in Po valley, Italy. *Atmos. Chem. Phys.* **7**, 355–376.

Kim, C. S., Adachi, M., Okuyama, K. and Seinfeld, J. H. 2002. Effect of NO_2 on particle formation in SO_2/H_2O/air mixtures by Ion-induced and homogenous nucleation. *Aerosol. Sci. Tech.* **36**, 941–952.

Kulmala, M., Dal Maso, M., Mäkelä, J. M., Pirjola, L., Väkevä, M. and co-authors. 2001. On the formation, growth and composition of nucleation mode particles. *Tellus.* **53B**, 479–490.

Kulmala, M., Laakso, L., Lehtinen, K. E. J., Riipenen, I., Dal Maso, M. and co-authors. 2004. Initial steps of aerosol growth. *Atmos. Chem. Phys.* **4**, 2553–2560.

Kulmala, M., Lehtinen, K. E. J., Laakso, L., Mordas, G. and Hämeri, K. 2005. On the existence of neutral atmospheric clusters. *Boreal. Environ. Res.* **10**, 79–87.

Kulmala, M., Lehtinen, K. E. J. and Laaksoonen, A. 2006. Cluster activation theory as an explanation of the linear dependence

between formation rate of 3 nm particles and sulphuric acid concentration. *Atmos. Chem. Phys.* **6**, 787–793.

Kulmala, M., Pirjola, L. and Mäkelä, J. M. 2000. Stable sulphate clusters as a source of new atmospheric particles. *Nature*. **404**, 66–69.

Kulmala, M., Toivonen, A., Mäkelä, J. M. and Laaksonen, A. 1998. Analysis of the growth of nucleation mode particles observed in Boreal forest. *Tellus*. **50B**, 449–462.

Laaksonen, A., Kulmala, M., O'Dowd, C. D., Joutsensaari, J., Vaatovaara, P. and co-authors. 2008. The role of VOC oxidation products in continental new particle formation. *Atmos. Chem. Phys.* **8**, 2657–2665.

Mikkonen, S., Romakkaniemi, S., Smith, J. N., Korhonen, H., Petäjä, T. and co-authors. 2011. A statistical proxy for sulphuric acid concentration. *Atmos. Chem. Phys.* **11**, 11319–11334.

Müller, T., Henzing, J. S., de Leeuw, G., Wiedensohler, A., Alastuey, A. and co-authors. 2011. Characterization and intercomparison of aerosol absorption photometers: result of two intercomparison workshops. *Atmos. Meas. Tech.* **4**, 245–268.

O'Dowd, C. D., Aalto, P., Hämeri, K., Kulmala, M. and Hoffman, T. 2002. Aerosol formation: atmospheric particles from organic vapours. *Nature*. **416**, 497–498.

Pandolfi, M., Cusack, M., Alastuey, A. and Querol, X. 2011. Variability of aerosol optical properties in the Western Mediterranean Basin. *Atmos. Chem. Phys.* **11**, 8189–8203.

Pérez, N., Pey, J., Castillo, S., Viana, M., Alastuey, A. and co-authors. 2008. Interpretation of the variability of levels of regional background aerosols in the Western Mediterranean. *Sci. Total. Environ.* **407**, 527–540.

Pey, J., Pérez, N., Querol, X., Alastuey, A., Cusack, M. and co-authors. 2010. Intense winter pollution episodes affecting the Western Mediterranean. *Sci. Total. Environ.* **408**, 1951–1959.

Pey, J., Rodríguez, S., Querol, X., Alastuey, A., Moreno, T. and co-authors. 2008. Variability of urban aerosols in the Western Mediterranean. *Atmos. Environ.* **40**, 9052–9062.

Philippin, S., Laj, P., Putaud, J. P., Wiedensohler, A., de Leeuw, G. and co-authors. 2009. EUSAAR – an unprecedented network of aerosol observation in Europe. *J. Aerosol. Res.* **24**, 78–83.

Querol, X., Alastuey, A., Lopez-Soler, A., Plana, F., Puicercus, J. A. and co-authors. 1999. Daily evolution of sulphate aerosols in a rural area, northeastern Spain – elucidation of an atmospheric reservoir effect. *Environ. Pollut.* **105**, 397–407.

Reche, C., Viana, M., Moreno, T., Querol, X., Alastuey, A. and co-authors. 2011. Peculiarities in atmospheric particle number and size-resolved speciation in an urban area in the western Mediterranean: results from the DAURE campaign. *Atmos. Environ.* **45**, 5282–5293.

Rodriguez, S. and Cuevas, E. 2007. The contributions of "minimum primary emissions" and "new particle formation enhancements" to the particle number concentration in urban air. *J. Aerosol. Sci.* **12**, 1207–2119.

Rodríguez, S., Van Dingenen, R., Putaud, J. P., Martins-Dos Santos, S. and Roselli, D. 2005. Nucleation and growth of new particles in the rural atmosphere of Northern Italy – relationship to air quality monitoring. *Atmos. Environ.* **39**, 6734–6746.

Seco, R., Peñuelas, J., Filella, I., Llusià, J., Molowny-Horas, R. and co-authors. 2011. Contrasting winter and summer VOC mixing rations at a forest site in the Western Mediterranean Basin: the effect of local biogenic emissions. *Atmos. Chem. Phys.* **11**, 13161–13179.

Sorribas, M., de la Morena, B. A., Wehner, B., Lòpez, J. F., Prats, N. and co-authors. 2011. On the sub-micron aerosol size distribution in a coastal – rural site at El Arenosillo Station (SW–Spain). *Atmos. Chem. Phys.* **11**, 11185–11206.

Spracklen, D. V., Carslaw, K. S., Merikanto, J., Mann, G. W., Reddington, C. L. and co-authors. 2010. Explaining global surface aerosol number concentrations in terms of primary emissions and particle formation. *Atmos. Chem. Phys.* **10**, 4775–4793.

Van Dingenen, R., Putaud, J.-P., Martins-Dos Santos, S. and Raes, F. 2005. Physical aerosol properties and their relation to air mass origin at Monte Cimone (Italy) during the first MINATROC campaign. *Atmos. Chem. Phys.* **5**, 2203–2226.

Venzac, H., Sellegri, K., Villani, P., Picard, D. and Laj, P. 2009. Seasonal variation of aerosol size distributions in the free troposphere and residual layer at the puy de Dôme station, France. *Atmos. Chem. Phys.* **9**, 1465–1478.

Wichmann, H.-E. and Peters, A. 2000. Epidemiological evidence of the effects of ultrafine particle exposure. *Philos. Trans. R. Soc. A. Math. Phys. Eng. Sci.* **358**, 2751–2769.

Wiedensohler, A., Covert, D. S., Swietlicki, E., Aalto, P., Heintzenberg, J. and co-authors. 1996. Occurrence of an ultrafine particle mode less than 20 nm in diameter in the marine boundary layer during Arctic summer and autumn. *Tellus*. **48B**, 213–222.

Wiedensohler, A., Birmili, W., Nowak, A., Sonntag, A., Weinhold, K. and co-authors. 2012. Mobility particle size spectrometers: harmonization of technical standards and data structure to facilitate high quality long-term observations of atmospheric particle number size distributions. *Atmos. Meas. Tech.* **5**, 657–685.

Yao, X., Choi, M. Y., Lau, N. T., Lau A. P. S., Chan, C. K. and co-authors. 2010. Growth and shrinkage of new particles in the atmosphere in Hong Kong. *Aerosol. Sci. Tech.* **44**, 639–650.

Article 4

Cusack, M., Alastuey, A., Querol, X.

New particle formation and evaporation processes in the Western Mediterranean regional background.

Atmospheric Environment, in review

Pages: 142-165

Published in: submitted April 2013, in review

Impact factor of Journal: 3.465

New particle formation and evaporation processes in the Western Mediterranean regional background.

M. Cusack[a,b], A. Alastuey[a], X. Querol[a].

[a] {Institute of Environmental Assessment and Water Research, IDÆA, CSIC, C/ Jordi Girona, 18-26, 08034, Barcelona, Spain}

[b] {Institute of Environmental Science and Technology (ICTA), Universitat Autónoma de Barcelona, 08193, Bellaterra, Barcelona, Spain}

Correspondence to: Michael Cusack (michael.cusack@idaea.csic.es)

Tel: 0034 934006100 ext. 1543

Address: Institute of Environmental Assessment and Water Research, IDÆA, CSIC, C/ Jordi Girona, 18-26, 08034, Barcelona, Spain

Abstract

Case studies of new particle formation (NPF), subsequent growth and possible particle shrinkage occurring in the western Mediterranean regional background are presented in this work. Owing to the mid-altitude height of the station (720 m.a.s.l.), aerosol processes were highly influenced by mixing layer height and development, and mountain breezes. Nucleation processes were observed to occur both under cold and warm conditions, when solar radiation and sulphuric acid concentrations were sufficiently high. Intense bursts of NPF were recorded when the station resided above the polluted mixing layer with little influence of upslope transport of pollution. NPF and growth was also observed to occur within polluted air masses residing over the site, owing to the probable abundance of anthropogenic and natural volatile organic compounds (VOCs) promoting rapid particle growth after nucleation. Measurable growth rates for the NPF episodes ranged from 1.4 to 3.8 nm h^{-1}. Reductions in modal diameters, indicating particle shrinkage, were also frequently observed and were attributed to the evaporation of semi-volatile species from the particulate phase to the gas phase. Particle shrinkage was observed both for pre-existing particles and for freshly formed particles. In the latter case, an "arch" formation was observed in the size distribution contour plot, as the nucleating particles grew and subsequently evaporated until the mode disappeared completely. Furthermore, rapid particle shrinkage (32.8 nm h^{-1}) occurred after significantly rapid growth (21.6 nm h^{-1}) in the absence of an appreciable condensation sink. We suggest that such exaggerated growth rates for a relatively clean environment produced unstable particles from which semi-volatile species involved in the nucleation process evaporated readily. In agreement with the few articles on particle shrinkage published to date, evaporation appears to be favoured under warm temperatures, high solar radiation, low relative humidity and atmospheric dilution, causing particle-to-gas transformations.

Key words: ultrafine particles, nucleation processes, atmospheric aerosols, particle shrinkage

1. Introduction

Atmospheric NPF and growth has been the focus of intensive study for many decades. Understanding the processes behind the formation of new particles in the atmosphere, both by primary and secondary formation processes, is important both for climate and

epidemiology studies (Charlson et al., 1992; Donaldson et al., 1998). Atmospheric particles can affect climate directly by scattering and absorbing solar radiation (Ramanathan and Carmichael, 2008), or indirectly by forming cloud condensation nuclei (CCN, Clarke and Kapustin, 2010; Pöschl et al., 2010). Ultrafine particles (<100 nm) are believed to be especially toxic owing to their ability to penetrate deeper into the human respiratory system (Nel, 2006).

Secondary NPF involves gas to particle processes whereby homogenous or ion-induced nucleation of ion or neutral clusters occurs. H_2SO_4, formed from the oxidation of SO_2, is believed to be the most important nucleating agent in the atmosphere (Sipilä et al, 2010). However, it has been shown that sulphuric acid cannot account for the observed growth rates of nucleation clusters and other condensable vapour precursors are believed to play an important role in subsequent growth (Tunved et al., 2006; Jimenez et al., 2009). Thus, when sulphuric acid and other condensable vapours such as low-volatile organics, ammonia and water are in sufficiently high concentrations in the atmosphere, gas to particle processes can occur and grow rapidly before being scavenged by pre-existing particles (Kulmala et al., 2013).

Recent publications have suggested that new particle growth can be reversible under certain atmospheric conditions. Yao et al. (2010) observed particle shrinkage following NPF in an urban environment in Hong Kong, and suggested that the observed shrinkage was a result of evaporation of organic compounds and ammonium nitrate. Young et al. (2013) presented several examples of particle shrinkage in Taiwan which occurred following NPF and growth. The authors in this case similarly propose that semi-volatile NH_4^+, NO_3^- and organics in the particle phase are the likely evaporating species. Finally, Backman et al. (2012) observed particle shrinkage in São Paulo and suggested that changes in atmospheric conditions resulting in a decrease in precursor vapour concentrations might cause condensed semi-volatile species to evaporate, resulting in a shrinking of particle sizes.

This current work presents case studies of NPF at a regional background mid-altitude site in the western Mediterranean basin. Each case study presents considerably different scenarios when NPF occurs, and a broad range of variables are presented and discussed in order to determine the main influential factors on NPF, thus helping to identify the favourable conditions leading to nucleation events. The influence of air mass mixing between polluted and non-polluted boundary layer air, and NPF at different stages of

development within the same air mass, are presented. Finally, numerous occasions whereby apparent particle shrinkage occurs are also presented and discussed.

2. Methodology

2.1. Observation site

This current article is intended as a companion piece to a previous publication by Cusack et al. (2013), within which full details of the measurement site, the specifications of the instruments used, the methods used and general meteorological conditions can be found. The Montseny (MSY) station is located 40 km to the N-NE of the metropolitan area of Barcelona, and 25 km from the Mediterranean Sea. The area is mountainous (site elevation of 720 m.a.s.l.) and densely forested, located in the Montseny natural park. The site lies on the Eastern slopes of a valley stretching perpendicularly from the Catalan pre-coastal ranges. The greater region is generally densely populated and industrialised, and pollution from the region can affect the site regularly. Pey et al. (2010) and Pérez et al. (2008) have described the affect of meteorology and air mass origins on aerosols at the site. The MSY station is a member of the ACTRIS network (Aerosols, Clouds, and Trace gases Research InfraStructure Network; formerly EUSAAR), a Europe wide network of aerosol monitoring supersites.

2.2. Sampling and instrumentation

Particle number size distributions with mobility diameters between 9 and 825 nm were performed using a Scanning Mobility Particle Sizer (SMPS) operated in the scanning mode. The SMPS consists of a Differential Mobility Analyser (DMA) connected to a Condensation Particle Counter (CPC; TSI Model 3772). The system was designed by the Leibniz Institute for Tropospheric Research (IfT) in Leipzig, Germany in the framework of the ACTRIS project. Wiedensohler et al. (2012) has published the full specifications of the instrument, such as DMA dimensions, bipolar diffusion charger etc. The SMPS was set to provide size distribution data from an up and down scan every 5 minutes, with a sheath air flow of 5 lpm and an aerosol flow of 1 lpm. The sheath and sampled aerosol were both dried using a nafion dryer to maintain relative humidity below 40% in accordance with ACTRIS requirements. The case studies presented in this work were taken from a data set from October 2010 to June 2011. Surface plots of the time series of the number size distributions were made and, according to the procedure described by Kulmala et al. (2012), the dataset was visually analysed in order

to identify and classify NPF events. Furthermore, the growth rate was determined by using the log-normal distribution function method, as outlined by Kulmala et al. (2012). The shrinkage rate is calculated in the same way as the growth rate.

A Multi-Angle Absorption Photometer (MAAP, model 5012, Thermo) provided real time measurements of the cross section absorption coefficient, which was corrected according to Pandolfi et al. (2011) to provide equivalent Black Carbon (BC) concentrations. The sampling line and inlet for the SMPS and MAAP instruments reached 1.5 m above the roof of a climate controlled cabin, with a cut-off diameter of 10 µm. Pollutant gas concentrations (O_3, NO, NO_2, SO_2) were also measured on site and were provided by the Department of the Environment of the Autonomous Government of Catalonia. Meteorological data such as temperature, relative humidity, solar radiation, wind direction, wind speed and precipitation was recorded in real time on site. Absolute humidity (AH) was used as a tool to observe changes in the air mass over MSY.

The dry aerosol condensation sink (CS) was calculated according to Kulmala et al. (2001). A proxy for sulphuric acid, [H_2SO_4], was calculated from the measured SO_2 concentrations and CS measurements using the method described by Petäjä et al. (2009). For this approach, H_2SO_4 vapour is considered to be in a pseudo-steady state between condensational losses and gas-phase production:

$$[H_2SO_4] = \frac{k[SO_2]R}{CS} \quad (1)$$

Where k is an empirical constant (2.3×10^{-9} m^2 W^{-1} s^{-1}) and R is the measured solar radiation. CS is the condensation sink (s^{-1}) calculated from the SMPS measurements and [SO_2] is the measured SO_2 concentrations on site.

All times reported are in GMT.

3. Results and Discussion

Overview

The topography of the area in which MSY resides, the mid-altitude height (720 m.a.s.l.) and the station's orientation incurs unusual aerosol processes at the site. As occurs at most mountainous sites, MSY is regularly affected by a diurnal mountain breeze. Owing to the sites eastern orientation, mountain breezes are activated early in the day by insolation, which advects anthropogenic and natural emissions from the urbanised valleys below MSY to the site. In winter MSY typically remains above the mixing

layer, but injections of polluted mixing layer air can be brought to the site by the mountain breeze development. In contrast, during the warmer months the mountain breeze is still influential, but MSY also resides within the mixing layer for most of the day, regularly exposing the site to a broad range of both anthropogenic and natural emissions within the mixing layer, dilution processes and intense photochemical activity. Pey et al. (2010) describes in detail the synoptic and mesoscale meteorology that affects atmospheric aerosols at this site. Thus, the aerosol processes that occur at MSY are often complex, and the affect of air mass mixing between polluted and non-polluted boundary layer air gives rise to unusual particle number size distributions, as will be discussed anon. For in depth analysis on particle number size distributions, modality, seasonality and trends of particle number concentrations and various other parameters at the site, please see Cusack et al. (2013). In brief, it was concluded that during the colder months, NPF was usually observed to occur under clean air conditions, i.e. in the absence of the polluted mountain breeze and a significant CS. On the other hand, it was observed that during the warmer months increased concentrations of nucleation mode particles existed regardless of elevated pre-existing background particle concentrations, suggesting that with increased photochemistry and VOC concentrations, NPF can still occur. During the entire measurement period, 30 episodes of nucleation were recorded, and 10 episodes of particle shrinkage were observed. Of those 10 episodes of particle shrinkage, 5 occurred on the same day as nucleation was observed. It should be highlighted that complete summer measurements were not available, and there is evidence to suggest that nucleation processes are significantly enhanced during the summer months. In this current work, specific case studies of NPF are presented and discussed, as well as the effect of air mass mixing on particle number size distributions and the possibility of particle evaporation as a potential formation process of smaller particles in the ultrafine range at the site.

Case 1: New particle formation and growth under clean atmospheric conditions

Examples of new particle formation events which occurred on three consecutive days (6 to 8 December 2010) are presented in Fig. 1. The NPF episodes occurred during a period of relatively low pollution and particle loading (mean of 2.3 µg m^{-3} PM2.5 and 152 ng m^{-3} of BC for the three days). Average daily concentrations of $N_{9\text{-}20}$ for each of the days are 639 cm^{-3}, 1087 cm^{-3} and 920 cm^{-3} respectively, with maximum recorded

hourly concentrations for each day of 3128 cm^{-3}, 4644 cm^{-3}, and 2779 cm^{-3}. Nucleation on the first day occurs slightly later (13:00 h) than the following days (10:00 h). Considering the peak in BC and CS, and the slight dip in solar radiation, it is likely that NPF is delayed owing to the unavailability of condensable gaseous precursors necessary for NPF which are consumed by the pre-existing particles. This is reflected by the comparatively lower [H_2SO_4] on this day. Furthermore, solar radiation is significantly less intense on this day compared to the following days. There are two distinct modes; one appears to arrive with the peak in BC with a geometric mean diameter (GMD) in the lower Aitken mode around 30 nm. The second mode exists primarily in the nucleation mode, appearing at 12:30 h with a GMD of 14 nm, subsequently growing into the lower Aitken mode with a growth rate from 9 – 25 nm of 1.4 nm h^{-1}.

Of the three days, the most intense NPF event occurs on the second day in Fig. 1, as evidenced by the average and peak concentrations of $N_{9\text{-}20}$. NPF commences slightly earlier than the previous day at 10:30 h. The increased intensity of NPF on this day may be attributable to the reduced CS and BC concentrations at the same time that NPF commences. CS was 1.35 x 10^{-3} s^{-1} at the beginning of NPF on day 2, compared to 3.1 x 10^{-3} s^{-1} on day 1. Although SO_2 concentrations are significantly lower on day 2, [H_2SO_4] is higher and this, combined with the reduced CS and increased solar radiation, allows for NPF to occur with greater intensity. Furthermore, O_3 concentrations are significantly higher, which may be an important factor for the production of condensable organic vapours which would enhance particle growth after formation. The growth rate of the nucleating particles from 9-38 nm on day 2 was around 3.8 nm h^{-1}, more than double the growth rate recorded for the previous days.

Day 3 (8 Dec) undergoes a similar NPF event as that of the previous day, albeit with reduced concentrations. Considering NPF commences at more or less the same time as the previous day (10:00 h), with similar solar radiation intensity, CS and with slightly higher [H_2SO_4], one might expect NPF to produce similar or higher concentrations of $N_{9\text{-}20}$ on day 3. However, it appears that NPF and growth is briefly interrupted by a slight increase in CS and BC at 13:00 h, with these particles possibly consuming some of the gaseous precursors, preventing NPF and removing the newly formed particles through coagulation and condensation. However not all of the nucleated particles are removed, and when CS and BC concentrations reduce, growth of the fresh particles resumes. Although NPF is briefly interrupted, the GMD does maintain growth from 9 to 26 nm, with a growth rate of 1.7 nm h^{-1}.

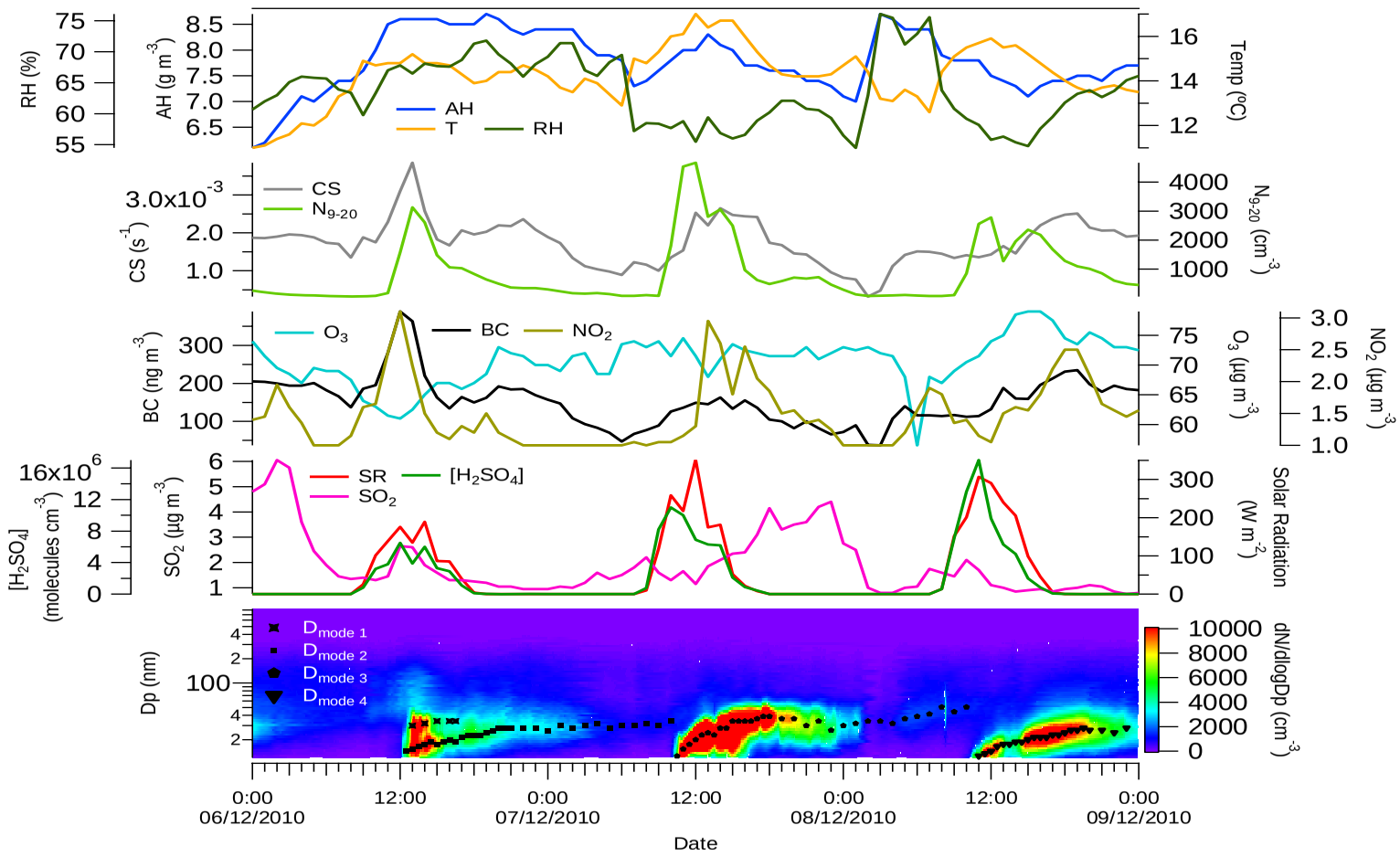

Fig. 1. Contour plot of the particle number size distributions, $N_{9\text{-}825}$, and particle mode diameter (D_{mode}) (bottom graph), $[H_2SO_4]$, SO_2, NO_2, O_3 and BC concentrations, solar radiation (SR), temperature (T), absolute humidity (AH) and relative humidity (RH), and condensation sink (CS) and nucleation mode concentrations ($N_{9\text{-}20}$).

A study of NPF at a remote rural site in the Sierra Nevada Mountains in Northern California was performed during winter 2009 (Creamean et al., 2011). Similarly to MSY, the site can be exposed to anthropogenic pollution brought to the site by up-slope winds, and NPF was observed to occur under clean atmospheric conditions and clear skies. Growth rates at that site of 4-7 nm h^{-1} were substantially higher than those recorded at MSY in this case study, but solar radiation was also significantly higher which would likely produce photochemical gaseous precursors in greater quantities.

Case 2: New particle formation and growth under polluted atmospheric conditions

Fig. 2 displays three consecutive days of new particle formation which occurred from the 25 to 27 December 2010. This case (case 2) differs significantly from the previous one (case 1) in many aspects: average temperatures over the three days reach 3.1ºC compared to 10.8ºC during Case 1. Solar radiation during Case 2 is also considerably more intense. Daily nucleation mode concentrations for day 1 to 3 (25 – 27 Dec) were 554 cm^{-3}, 212 cm^{-3} and 568 cm^{-3} respectively, with peak hourly concentrations of 2590 cm^{-3}, 735 cm^{-3} and 2178 cm^{-3}. The NPF event recorded on day 1 is similar to the NPF events recorded in Case 1, albeit with lower concentrations. Nucleation commences at 12 hr followed by continuous growth into the upper Aitken mode (50-100 nm) with a growth rate of 1.8 nm h^{-1}. The freshly nucleated particles grow to merge with the regional background mode (around 50 nm), which grows further into the accumulation mode over the three days. Furthermore, CS was at similar levels as those recorded during Case 1, with a daily mean of 1.71 x 10^{-3} s^{-1}. The low day-to-night variation recorded on day 1 for BC and NO_2 suggest little input of polluted mixing layer air throughout the day, allowing NPF to occur uninterrupted. On the contrary, NPF on the following day is much less intense, even though meteorological conditions and SO_2 concentrations are very similar. The lower intensity NPF can almost certainly be attributed to the peaks in BC and CS and brief drop in [H_2SO_4], occurring between 11:00 and 13:00 h, which is when NPF commenced the day before. NPF is evident however, and a new mode emerges in the nucleation mode at 14:30 h. The appearance and disappearance of this mode in tandem with varying levels of BC and NO_2 suggests that NPF is occurring within the relatively polluted air mass brought to the site by the diurnal breeze system. The previous day appears to occur in the cleaner atmosphere above the mixing layer.

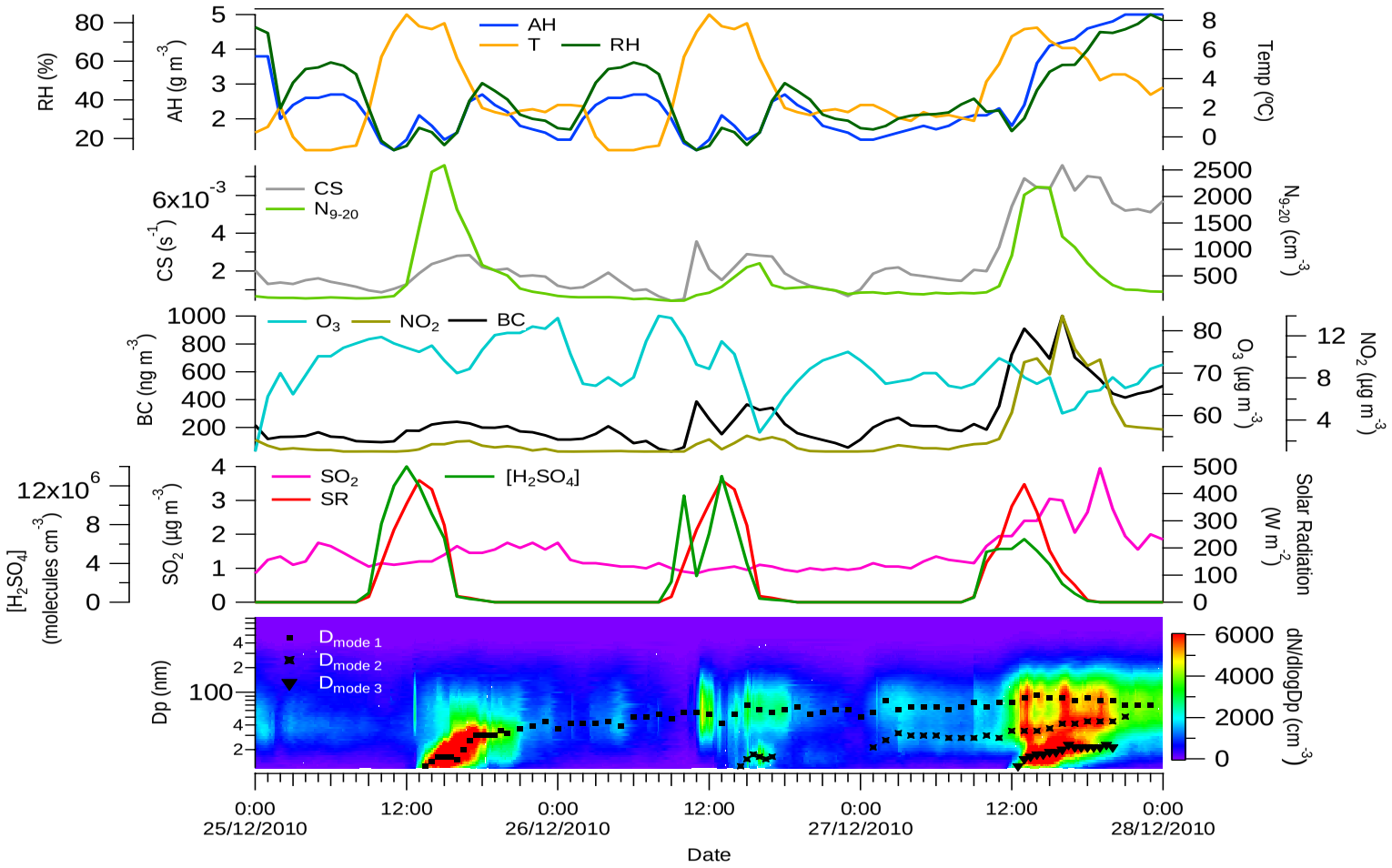

Fig. 2. Contour plot of the particle number size distributions, $N_{9\text{-}825}$, and particle mode diameter (D_{mode}) (bottom graph), $[H_2SO_4]$, SO_2, NO_2, O_3 and BC concentrations, solar radiation (SR), temperature (T), relative humidity (RH) and absolute humidity (AH), and condensation sink (CS) and nucleation mode concentrations ($N_{9\text{-}20}$).

The third day shows the effect of a change in the air mass residing over MSY, which is evidenced by the large increase observed in absolute humidity occurring around 10:00 h. The air mass is evidently polluted as a sizeable increase in BC (daily average of 434 ng m^{-3}), NO_2 and SO_2 is recorded, and CS daily average increases to 4 x 10^{-3} s^{-1}. There is a clear tri-modal size distribution occurring on this day, with GMDs around 80-90 nm, 40-50 nm and a well defined mode emerging in the nucleation mode around 12:30 h. Indeed, concentrations of the nucleation mode on this day are similar to those observed under clean air conditions on day 1. Solar radiation intensity is very similar to the previous days as are average temperatures. SO_2 concentrations are significantly higher on this day but [H_2SO_4] is lower owing to the higher CS. Considering that [H_2SO_4] is lower than on the previous days, but $N_{9\text{-}20}$ are still high, there must be a considerable amount of condensable organic vapours within the air mass that aids in particle growth before the fresh particles can be removed by coagulation. Seco et al. (2011) showed that VOC mixing ratios at MSY in winter were governed by the diurnal breeze system, with concentrations increasing significantly during the day with the approach of the mountain breeze. If sufficient concentrations of [H_2SO_4] to begin NPF and high VOC concentrations are present in the atmosphere, nucleation can occur even under relatively high background levels of pre-existing particles (Fiedler et al. 2005). This has been observed previously on day 1 of Case 1, whereby NPF occurred even in the presence of high CS owing to elevated concentrations of SO_2.

The growth rate of the nucleating particles (9-17 nm) is 3.7 nm h^{-1}, but further growth slows down significantly with a growth rate of 1.5 nm h^{-1} for particles 17-23 nm. Kulmala et al. (2005) showed that low growth rates are a feature of cleaner environments, whilst higher growth rates are required in more polluted environments before nucleating particles are scavenged by the pre-existing aerosol population.

Case 3: New particle formation and effect of air mass mixing

In this case, the effect of boundary layer air mixing between polluted air masses and cleaner air is highlighted. These processes are typical of medium to high altitude sites such as MSY, and can result in the sampling of different parts of air masses undergoing different aerosol processes, such as a nucleation event at different phases of development. As is evident in Figure 3, there is a dominant background mode with GMD around 80 nm ($D_{mode\ 1}$) that remains fairly constant over the three days. However, ultrafine particles vary considerably, and more than one NPF events are recorded even

during the same day. On 23 May a low intensity nucleation event begins at 10:00 h, coinciding with peak solar radiation and two hours before peak CS and BC. Growth of these particles is observed, as shown by the black stars ($D_{mode\ 2}$) tracing the GMD of the mode in Figure 3, but mixing of these growth particles is evident with the progressing breeze. As shown in Figure 3, a new mode ($D_{mode\ 3}$) emerges between 13:00 and 14:00 h on 23 May, marked by the continuous black line with GMD of 20 nm. The emergence of this mode coincides with peak [H_2SO_4], and also as CS and BC begin to decrease. This suggests that there is a nucleation episode occurring elsewhere which arrives at MSY after some growth has already occurred. Similar behaviour was observed during a summer measurement campaign on a mountain site in British Colombia, Canada (Pierce et al., 2012), whereby particles of ~20 nm were regularly recorded. The authors suggested this was due to the transport of nucleating and growing particles occurring in the valley floor to the site, or the entraining of nucleation particles from the free troposphere to the mixing layer during the day. The GMD of $D_{mode\ 3}$ actually begins to decrease at 15:00 h, from a maximum of 23 nm to 15 nm, which is maintained for an hour before the GMD begins to increase once again. Considering the effect of air mass mixing in this case and the inherent difficulty in distinguishing between modes under these conditions, it is difficult to ascertain what is causing the GMD of this mode to decrease. Numerous episodes of nucleation occurring within the same air mass at different phases of formation and growth is a possible explanation. The stability of absolute humidity suggests that there is no discernible change in the sampled air mass itself, but the abrupt changes observed for CS, BC and NO_2 suggest that aerosols are not evenly distributed within the air mass, or that dilution within the air mass is occurring. However, particle evaporation may be the cause of the shrinkage observed in the GMD which occurred on 23 May, which will be discussed in the next case study.

NPF is greatly reduced on 24 May, even though BC, CS and solar radiation are equivalent to the previous and next day. This is likely due to the lower concentrations recorded for [H_2SO_4] for the same day, once again highlighting the importance of sulphuric acid as a nucleating agent. Although no NPF is evident at the site, there is evidence that two growing nucleation modes are being sampled both at 12:00 h ($D_{mode\ 4}$) and another at 14:00 h ($D_{mode\ 5}$). This again indicates that freshly nucleated particles formed elsewhere are being carried to the site after the particles have grown to sizes greater than 20 nm.

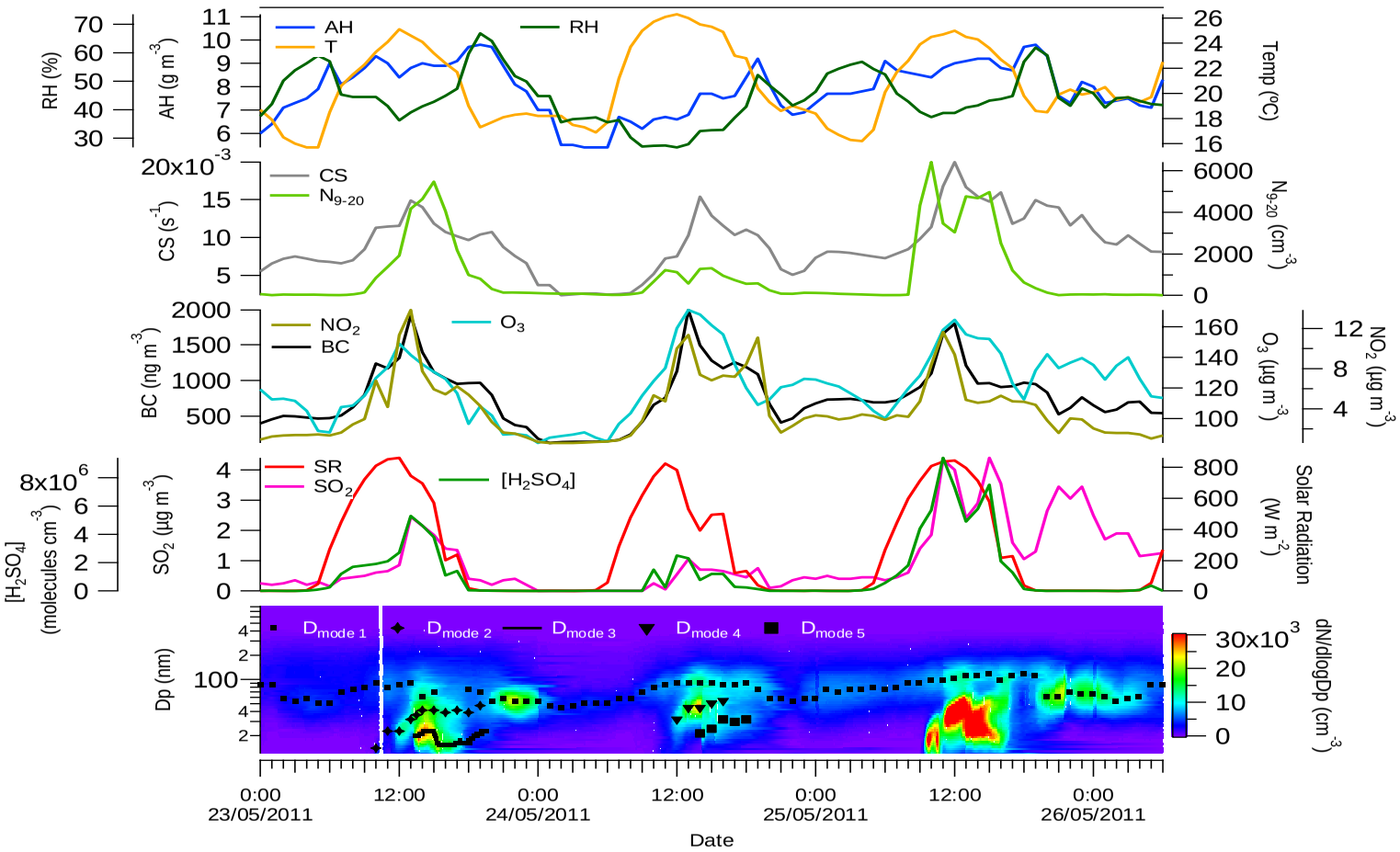

Fig. 3. Contour plot of the particle number size distributions, $N_{9\text{-}825}$, and particle mode diameter (D_{mode}) (bottom graph), $[H_2SO_4]$, SO_2, NO_2, O_3 and BC concentrations, solar radiation (SR), temperature (T), relative humidity (RH) and absolute humidity (AH), and condensation sink (CS) and nucleation mode concentrations ($N_{9\text{-}20}$).

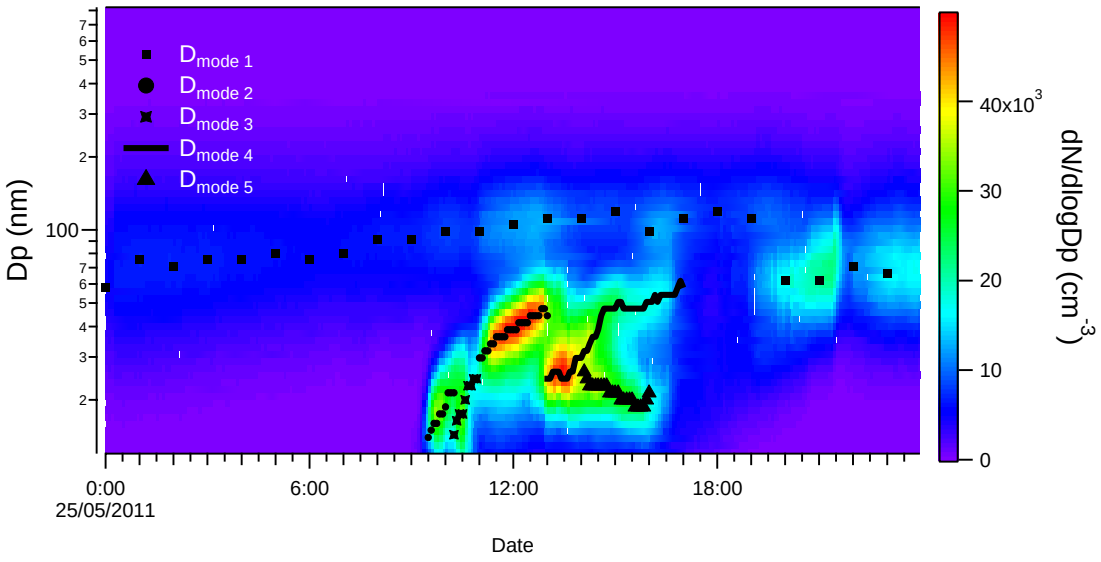

Fig. 4. Contour plot of particle number size distributions, $N_{9\text{-}825}$, and particle mode diameter (D_{modex}) for the 25/05/2011.

The complexity of air mass mixing is most evident on 25 May. NPF commences on this day around 10:00 h with much greater intensity than the previous days owing to the abundance of [H_2SO_4]. It is interrupted shortly thereafter as CS and BC increase to a maximum around midday. Nucleation mode concentrations begin to increase once again when BC and CS reduce but the source of these particles appear to not be from NPF. The number size distribution and particle mode diameters for this day are shown separately in Fig. 4. Closer inspection of the modality of the particle size distribution highlights the complex processes occurring on this day. Two episodes of brief NPF appear to occur within quick succession. The first begins (D_{mode} 1) at 9:30 h and grows rapidly until the mode disappears and a new nucleation mode (D_{mode} 2) emerges at 10:30 h. This mode grows similarly until it merges with the particles within the polluted breeze containing BC and NO_2 arriving at MSY. Following the apparent retreat of the breeze or dilution processes (marked by the decreasing BC and NO_2), two new modes emerge (D_{mode} 4 and 5; Fig. 4). D_{mode} 4 emerges at 13:00 h with a GMD of 24 nm and increases steadily to 62 nm until 17:00 h. D_{mode} 5 appears an hour later at 14:00 h with a similar GMD of 26 nm. However, this mode actually decreases over time, reducing to 18 nm around 16:00 h, and then returns to growth afterwards. Thus, an exceptionally complex size distribution is evident containing a tri-modal distribution: one relatively constant background mode (D_{mode} 1), a growing mode (D_{mode} 4) and a shrinking mode (D_{mode} 5).

Case 4: Particle shrinkage events

As indicated previously, there is evidence to suggest that particle shrinkage may also occur at MSY. Particle evaporation has been reported in São Paulo in Brazil (Backman et al., 2012), in subtropical central Taiwan (Young et al., 2013) and during the dry season in Hong Kong (Yao et al., 2010). Backman et al. (2012) observed particle evaporation from 36 nm to 16 nm and attributed this behaviour to 1) a decrease in the precursor vapour concentrations (possibly as a result of dilution with growth in PBL) causing the condensed semi-volatile species to evaporate and a resulting shrink in particle size or, 2) the evaporation of NH_4NO_3 when the equilibrium between $HNO_3/NH_3/NH_4NO_3$ favours the gas phase. Yao et al. (2010) attributed observed particle shrinkage in Hong Kong to the evaporation of organic components and ammonium nitrate. Furthermore, that same study in Hong Kong suggested that strong photochemical activity would likely produce increased ambient concentrations in secondary volatile and semi-volatile organic and inorganic species in the gas phase. Of the studies mentioned, all shrinkage events were observed in urban or urbanised areas, whereas MSY is a regional background site not directly influenced by local emission sources, although pollution plumes from the metropolitan area of Barcelona can affect the site.

An example of possible particle shrinkage on 1 May 2011 is shown in Fig. 5. A background accumulation mode with GMD around 160 nm is stable and continuous throughout the day. A secondary mode arrives around 9:00 h with the onset of the mountain breeze from a southerly direction, as highlighted by the increase in BC and CS. This mode, with GMD around 90nm, is stable until around 12:00 h, at which point it briefly disappears. When the mode reappears at 12:30 h the GMD is reduced (66 nm) and gradually begins to decrease from then on. Apart from the background accumulation mode, no other modes are observed i.e. the size distribution is bi-modal, indicating that air mass mixing is not occurring. If a mixing event was occurring, one might expect this mode to split at some point into different modes. Furthermore, the absolute humidity, wind direction and wind speed do not vary significantly suggesting the air mass is homogenous. Thus, the GMD of this mode at 13:00 h is 66 nm, and decreases thereafter to a minimum of 24 nm at 16:30 h, with a shrinking rate of 11 nm h^{-1}. This is similar to a particle shrinkage rate of 10.7 nm h^{-1} observed in Hong Kong (Yao et al., 2010), but higher than shrinkage rates observed in São Paulo (5.2 nm h^{-1}; Backman et al., 2012) and in Taiwan (5.1 – 7.6 nm h^{-1}; Young et al., 2013).

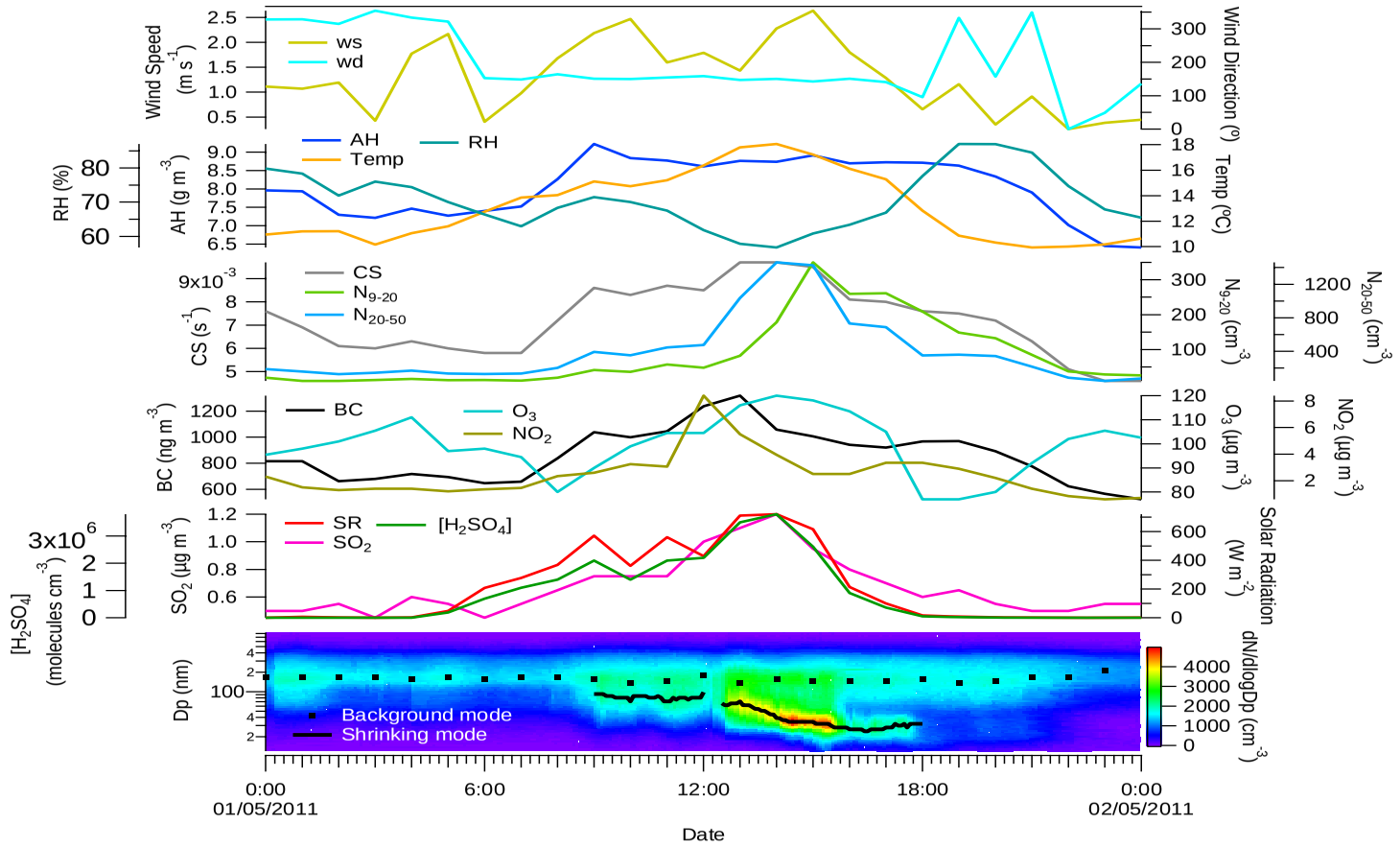

Fig. 5. Contour plot of the particle number size distributions, $N_{9\text{-}825}$, and particle mode diameters (bottom graph), $[H_2SO_4]$, SO_2, NO_2, O_3 and BC concentrations, solar radiation (SR), temperature (T), absolute humidity (AH) and relative humidity (RH), and condensation sink (CS), nucleation mode ($N_{9\text{-}20}$) and lower Aitken mode ($N_{20\text{-}50}$) concentrations on 01/05/2011.

However, as results on evaporation processes are so far not widely published, comparisons of shrinkage rates are vague. As indicated by the contour plot in Fig. 5, as the GMD of the shrinking mode decreases, the particle number concentration increases as larger particles are dissociating and producing greater concentrations of smaller particles. When evaporation eventually ceases at 16:30 hr, the GMD of this mode remains constant and no further growth/shrinkage occurs. Particle shrinkage appears to commence with maximum solar radiation intensity and ambient temperatures, which might favour the evaporation of volatile and semi-volatile particles from the surface of larger particles. Similarities exist between this example presented and that outlined by Backmann et al. (2012) in São Paulo. In both sites, the solar radiation suggests the early part of the day was partly cloudy, but around noon there was little or no cloud cover. Backmann et al. (2012) attributed this to either the breaking up of a stable nocturnal boundary layer, or an increasing of the boundary layer height. This might dilute particle concentrations and gas-to-particle processes are reversed. Yao et al. (2010) suggested that when a change in atmospheric conditions (such as meteorological parameters and pollution concentrations) occurs, a shift in gas/particle partitioning can take place, resulting in the evaporation of volatile and semi-volatile species. In the case presented in Fig. 5, a decrease in BC and CS and an increase in solar radiation and temperature occur precisely when particle shrinkage appears to commence.

An example of NPF directly followed by particle evaporation on the 2 April is shown in Fig. 6. Nucleation commences at 8:00 h with increasing [H_2SO_4] and as solar radiation intensifies. The direct relationship between [H_2SO_4] and NPF intensity is highlighted here as high concentrations in [H_2SO_4] also resulted in higher nucleation mode concentrations. The GMD of the nucleation mode increases from 10 nm to a maximum of 21 nm between 10:00 and 10:30 h, with a growth rate of 21.6 nm h^{-1}. Peak hourly N_{9-20} concentrations reach 7244 cm^{-3} coinciding with peak [H_2SO_4] of 2.1 x 10^7 molecules cm^{-3}. This mode then appears to shrink briefly to a GMD of 18 nm at 11:30 h. The wind direction is generally N-NW with light wind speeds (hourly maximum of 2.2 m s^{-1}).

An increase in BC, NO_2, O_3 and CS is also observed, with concentrations reaching maximum around midday, consuming the evaporating volatile and semi-volatile particles through condensation. The GMD of D_{mode} (around 30 nm) remains relatively constant when BC and CS are at their maximum between 12:00 and 14:00 h, but particle shrinkage recommences when BC and CS begin to decrease. As suggested by Backman et al. (2012), the reduction in BC and CS may indicate dilution, resulting in

evaporation of the condensed semi-volatile species. A secondary peak in $N_{9\text{-}20}$ concentrations was recorded at 15:00 h with concentrations of 6845 cm^{-3}. Thus, on this occasion, the rate of formation of nucleation mode particle concentrations through evaporation processes is almost equivalent to the production of new particles by NPF. From a maximum modal diameter of 30 nm at 14:00 hr, the GMD reduces to 11 nm at 18:00 hr before disappearing completely. The evaporation rate for the particle shrinkage observed in the afternoon was 33 nm h^{-1}. Evaporation does coincide with a change in wind direction but at that same point wind speeds are very low, suggesting that there is little movement within the air mass surrounding MSY.

This "arch-like" shape has been observed and studied in the subtropical environment of Taiwan (Young et al., 2013). Of the three publications mentioned previously where evaporation was observed to occur, namely Backman et al. (2012), Young et al., (2013) and Yao et al., 2010, the common feature between these sites and MSY must undoubtedly be similar meteorological conditions, specifically intensified solar radiation and higher temperatures, which would favour evaporation of volatile and semi-volatile species. Comparing the two examples of particle shrinkage shown (in Fig. 5 and 6), there are significant differences. In the first instance, particle evaporation is much slower (11 nm h^{-1}) than the second example (32.8 nm h^{-1}). Furthermore, the growth rate of nucleating particles on 2 April was also considerably higher (21.6 nm h^{-1}) than the previous case studies presented in this study (1.4-3.8 nm h^{-1}), which is in the upper range of average growth rates of 1-20 nm h^{-1} reported by Kulmala et al. (2004), but similar growth rates have been reported in São Paulo (9-25 nm h^{-1}; Backman et al., 2012). Considering particle shrinkage on 1 May does not occur after NPF, i.e. the particles arrive at MSY with GMD of 66 nm and decrease to 24 nm thereafter, this suggests that the evaporating species are volatilising from stable clusters that have been transported to the site. On the other hand, the evaporating particles on the 2 April appear to evaporate from freshly formed particles. This suggests that the evaporating species in the two examples may be different. As stated previously, high growth rates are typically associated with more polluted environments. However, on the 2 April the high growth rate in the absence of an appreciable CS may be creating unstable clusters from which the condensing species can easily evaporate. Thus, the authors suggest that the evaporating species on the 2 April are the same as the species involved in previous NPF. On the contrary, the evaporating species on the 1 May may be a result of the evaporation of volatile NH_4NO_3.

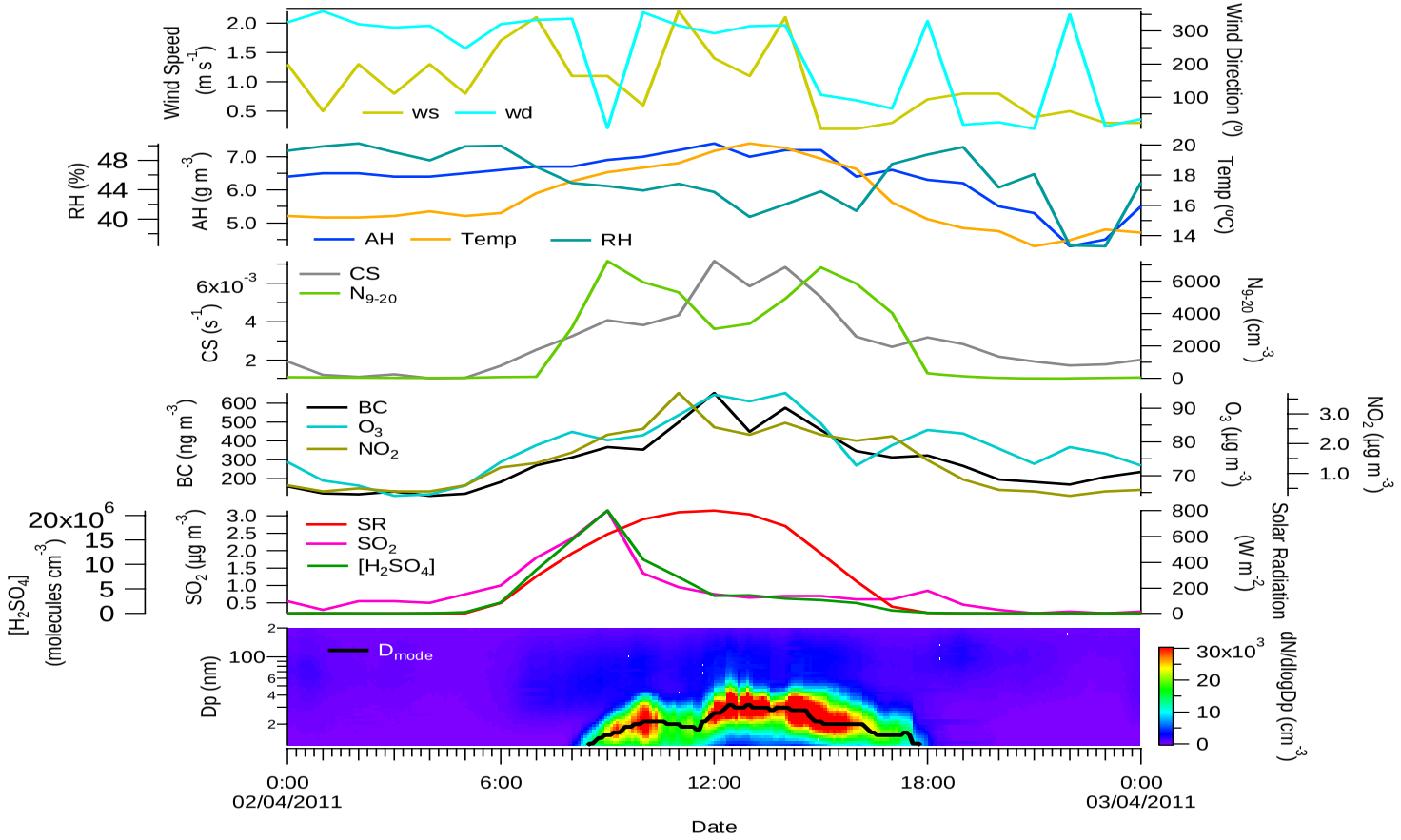

Fig. 6. Contour plot of the particle number size distributions, $N_{9\text{-}825}$, and particle mode diameter (D_{mode}) (bottom graph), $[H_2SO_4]$, SO_2, NO_2, O_3 and BC concentrations, solar radiation (SR), temperature (T), absolute humidity (AH) and relative humidity (RH), and condensation sink (CS) and nucleation mode concentrations ($N_{9\text{-}20}$) on 02/04/2011.

4. Conclusions

This study describes in detail specific episodes of NPF and particle shrinkage for a regional background site in the western Mediterranean Basin. Case studies are presented outlining aerosol dynamics and properties, meteorological conditions and air pollutant concentrations, with the aim of identifying favourable conditions for NPF. The site is classified as regional background but the variability of ultrafine particles is influenced by plumes of anthropogenic pollution from the populated and industrialised valleys below.

NPF was observed to occur under clean air conditions when MSY resided above the polluted mixing layer and there was minimal influence of a polluted mountain breeze, in which case NPF was observed to occur when solar radiation was at a maximum and [H_2SO_4] concentrations were sufficiently high. Continued growth after NPF was observed to be influenced by even slight increases in CS, which inhibited NPF or removed the growing particles through coagulation and condensation processes.

NPF was also observed to occur within polluted air masses when BC and CS were considerably higher. Even though [H_2 SO_4] concentrations were lower in this case, concentrations of nucleation mode particles were observed to be similar to concentrations recorded two days previously for an episode of NPF occurring under clean atmospheric conditions. This is likely due to elevated concentrations of anthropogenic and natural VOC concentrations which would promote fresh particle growth after nucleation, even in the presence of high CS. The effect of air mass mixing between polluted and non-polluted boundary layer typical of mid-altitude sites was also described.

Episodes of nucleation at different phases of formation and growth were recorded at the site at different times during the same day, indicating that there is a decoupling between NPF processes occurring within and above the mixing layer and that NPF may be quite localised in the region. Measurable growth rates for NPF episodes presented in this work ranged from 1.4-3.8 nm h^{-1}, except for one intense burst of NPF which had a growth rate of 21.6 nm h^{-1}.

Particle shrinkage was also observed to be an important formation process of ultrafine particles at the MSY site. In some cases, shrinkage was observed shortly after nucleation, and in others particles appeared to evaporate from the Aitken mode to particles of smaller diameter. In all cases, shrinkage appeared to occur after peak BC concentrations and CS, suggesting that dilution processes, which would reduce

precursor vapour concentrations, may allow condensed species to evaporate. Warm temperatures, high solar radiation and low relative humidity were also a common feature. The authors hypothesise that the evaporating species not preceded by NPF, i.e. evaporation from pre-existing particles, may be particle-to-gas transfer of particulate ammonium nitrate, producing NH_4^+ and NO_3^-, owing to the high volatility of particulate nitrate, and semi-volatile organics. The evaporating species involved in particle shrinkage occurring directly after NPF may be condensing species involved in the nucleation and growth process, with semi-volatile organics the most likely candidate. Finally, the authors suggest that rapid particle growth in the absence of a significant CS may produce unstable growing particles, which can readily lose condensed species through evaporation, under suitable ambient conditions.

Acknowledgements

This study was supported by the Ministry of Economy and Competitiveness and FEDER funds under the projects CARIATI (CGL2008-06294/CLI), VAMOS (CGL2010 19464/CLI) and GRACCIE (CSD 2007-00067). The research leading to these results has received funding from the European Union Seventh Framework Programme (FP7/2007-2013) ACTRIS under grant agreement n° 262254 and the Generalitat de Catalunya (AGAUR-2009SGR8).

References

Backman, J., Rizzo, L.V., Hakala, J., Nieminen, T., Manninen, H.E., Morais, F., Aalto, P.P., Siivola, E., Carbone, E., Hillamo, R., Artaxo, P., Virkulla, A., Petäjä, T., Kulmala, M., 2012. On the diurnal cycle of urban aerosols, black carbon and the occurrence of new particle formation events in springtime São Paulo, Brazil. Atmospheric Chemistry Physics 12, 11733-11751.

Charlson, R.J., Schwartz, S.E., Hales, J.M., Cess, R.D., Coakley Jr., J.A., Hansen, J.E., Hofmann, D.J., 1992. Climate forcing by anthropogenic aerosols, Science 255, 423-430.

Clarke, A. and Kapustin, V., 2010. Hemispheric aerosol vertical profiles: Anthropogenic impacts on optical depth and cloud nuclei. Science 329, 1488-1492.

Creamean, J.M., Ault, A.P., Ten Hoeve, J.E., Jacobson, M.Z., Roberts, G.C., Prather, K.A., 2011. Measurements of Aerosol Chemistry during New Particle Formation

Events at a Remote Rural Mountain Site. Environmental Science and Technology 45, 8208-8016.

Cusack, M., Pérez, N., Pey, J., Wiedensohler, A., Alastuey, A., Querol, X., 2013. Variability of sub-micrometer particle number size distributions and concentrations in the Western Mediterranean regional background. TellusB 65, 19243.

Donaldson, K., Li, X.Y., MacNee, W., 1998. Ultrafine (nanometre) particle mediated lung injury, Journal of Aerosol Science 29, 553-560.

Jimenez, J.L., Canagaratna, M. R., Donahue, N. M., Prevot, A. S. H., Zhang, Q., Kroll, J. H., DeCarlo, P. F., Allan, J. D., Coe, H., Ng, N. L., Aiken, A. C., Docherty, K. S., Ulbrich, I. M., Grieshop, A. P., Robinson, A. L., Duplissy, J., Smith, J. D., Wilson, K. R., Lanz, V. A., Hueglin, C., Sun, Y. L., Tian, J., Laaksonen, A., Raatikainen, T., Rautiainen, J., Vaattovaara, P., Ehn, M., Kulmala, M., Tomlinson, J. M., Collins, D. R., Cubison, M. J., Dunlea, E. J., Huffman, J. A., Onasch, T. B., Alfarra, M. R., Williams, P. I., Bower, K., Kondo, Y., Schneider, J., Drewnick, F., Borrmann, S., Weimer, S., Demerjian, K., Salcedo, D., Cottrell, L., Griffin, R., Takami, A., Miyoshi, T., Hatakeyama, S., Shimono, A., Sun, J. Y., Zhang, Y. M., Dzepina, K., Kimmel, J. R., Sueper, D., Jayne, J. T., Herndon, S. C., Trimborn, A. M., Williams, L. R., Wood, E. C., Middlebrook, A. M., Kolb, C. E., Baltensperger, U., and Worsnop, D. R., 2009. Evolution of organic aerosols in the atmosphere. Science 326, 1525-1529.

Kulmala, M., Dal Maso, M., Mäkelä, J.M., Pirjola, L., Väkevä, M., Aalto, P., Miikkulainen, P., Hámeri, K., O´Dowd, C.D. 2001. On the formation, growth and composition of nucleation mode particles. Tellus 53B, 479-490.

Kulmala, M., Vehkamäki, Petäjä, T., Dal Maso, M., Lauri, A., Kerminen, V.-M., Birmili, W., McMurry, P.H., 2004. Formation and growth rates of ultrafine atmospheric particles: a review of observations. Journal of Aerosol Science 35, 143-176.

Kulmala, M., Petäjä, T., Mönkkönen, P., Koponen, I.K., Dal Maso, M., Aalto, P.P., Lehtinen, K.E.J., Kerminen, V.-M., 2005. On the growth of nucleation mode particles: source rates of condensable vapour in polluted and clean environments. Atmospheric Chemistry and Physics 5, 409-416.

Kulmala, M., Petäjä, T., Mönkkönen, P., Koponen, I.K., Dal Maso, M., Aalto, P.P., Junninen, H., Paasonen, P., Riipinen, I., Lehtinen, K.E.J., Laaksonen, A., Kerminen,

V.M., 2012. Measurement of the nucleation of atmospheric aerosol particles, Nature Protocols 7, 1651-1667.

Kulmala, M., Kontkanen, J., Junninen, H., Lehtipalo, K., Manninen, H.E., Nieminen, T., Petäjä, T., Sipilä, M., Shobesberger, S., Rantala, P., Franchin, A., Jokinen, T., Järvinen, E., Äijälä, M., Kangasluoma, J., Hakala., J., Aalto, P.A., Paasonen, P, Mikkilä, J., Vanhanen, J., Aalto, J., Hakola, H., Makkonen, U., Ruuskanen, T., Mauldin III, R.L., Duplissy, J., Vehkamäki, Bäck, J., Kortelainen, A., Riipinen, I., Kurtén, T., Johnston, M.V., Smith, J.N., Ehn, M., Mentel, T.F., Lehtinen, K.E.J., Laaksonen, A., Kerminen, V.-M., Worsnop, D.R., 2013. Direct Observations of Atmospheric Aerosol Nucleation, Science 339, 943-946.

Nel, A., 2006. Toxic potential of materials at the nanolevel. Science 311, 622-627.

Ramanathan, V. and Carmichael, G., 2008. Global and regional climate changes due to black carbon, Nature Geoscience 1, 221-227.

Pandolfi, M., Cusack, M., Alastuey, A., Querol, X. 2011. Variability of aerosol optical properties in the Western Mediterranean Basin. Atmospheric Chemistry Physics 11, 8189-8203.

Pérez, N., Pey, J., Castillo, S., Viana, M., Alastuey, A., Querol, X., 2008. Interpretation of the variability of levels of regional background aerosols in the Western Mediterranean. Science of the Total Environment 407, 524-540.

Petäjä, T., Mauldin III, R. L., Kosciuch, E., McGrath, J., Nieminen, T., Paasonen, P., Boy, M., Adamov, A., Kotiaho, T., Kulmala, M., 2009. Sulfuric acid and OH concentrations in a boreal forest site. Atmospheric Chemistry Physics 9, 7435–7448.

Pey, J., Pérez, N., Querol, X., Alastuey, A., Cusack, M., Reche, C., 2010. Intense winter pollution episodes affecting the Western Mediterranean. Science of the Total Environment 408, 1951-1959.

Pierce, J.R., Leaitch, W.R., Liggio, J., Westervelt, D.M., Wainwright, C.D., Abbatt, J.P.D., Ahlm, L., Al-Basheer, W., Cziczo, D.J., Hayden, K.L., Lee, A.K.Y., Li, S.-M., Russell, L.M., Sjostedt, S.J., Strawbridge, K.B., Travis. M., Vlasenko, A., Wentzell, J.J.B., Wiebe, H.A., Wong, J.P.S., Macdonald, A.M., 2012. Nucleation and condensational growth to CCN sizes during a sustained pristine biogenic SOA event in a forested mountain valley. Atmospheric Chemistry Physics 12, 3147-3163.

Pöschl, U., Martin, S.T., Sinha, B., Chen, Q., Gunthe, S.S., Huffmann, J.A., Borrmann, S., Farmer, D.K., Garland, R.M., Helas, G., Jimenez, J.L., King, S.M., Manzi, A., Mikhailov, E., Pauliquevis, T., Petters, M.D., Prenni, A.J., Roldin, P., Rose, D.,

Schneider, J., Su, H., Zorn, S.R., Artaxo, P., Andreae, M.O., 2010. Rainforest Aerosols as Biogenic Nuclei of Clouds and Precipitation in the Amazon. Science 329, 1513-1516.

Seco, R., Peñuelas, J., Filella, I., Llusià, J., Molowny-Horas, R., Schallhart, S., Metzger, A., Müller, M.,Hansel, A., 2011. Contrasting winter and summer VOC mixing rations at a forest site in the Western Mediterranean Basin: the effect of local biogenic emissions. Atmospheric Chemistry Physics 11, 13161-13179.

Sipilä, M., Berndt, T., Petäjä, T., Brus, D., Vanhanen, J., Stratmann, F., Patokoski, J., Maudlin, R.L., Hyvärinen, A., Lihavainen, H., Kulmala, M., 2010. The Role of Sulfuric Acid in Atmospheric Nucleation. Science 327, 1243-1246.

Tunved, P., Hansson, H.-C., Kerminen, V.-M., Ström, J., Dal Maso, M., Lihavainen, H., Viisanen, Y., Aalto, P.P., Komppula, M., Kulmala, M., 2006. High natural aerosol loading over boreal forests. Science 312, 261-263.

Wiedensohler, A., Birmili, W., Nowak, A., Sonntag, A., Weinhold, K., Merkel, M., Wehner, B., Tuch, T., Pfeifer, S., Fiebig, M., Fjäraa, A.M., Asmi, E., Sellegri, K., Depuy, R., Venzac, H., Villani, P., Laj, P., Aalto, P., Ogren, J.A., Swietlicki, E., Williams, P., Roldin, P., Quincey, P., Hüglin, C., Fierz-Schmidhauser, R., Gysel, M., Weingartner, E., Riccobono, F., Santos, S., Grüning, C., Faloon, K., Beddows, D., Harrison, R., Monahan, C., Jennings, S.G., O`Dowd, C., Marinoni, A., Horn, H-G., Keck, L., Jiang, J., Scheckman, J., McMurray, P.H., Deng, Z., Zhao, C.S., Moerman, M., Henzing, B., De Leeuw, G., Löschau, G., Bastian, S., 2012. Mobility particle size spectrometers: Harmonization of technical standards and data structure to facilitate high quality long-term observations of atmospheric particle number size distributions. Atmospheric Measurement Techniques 5, 657-685.

Yao, X., Choi, M.Y., Lau, N.T., Lau, A.P.S., Chan, C.K., Fang, M., 2010. Growth and Shrinkage of New Particles in the Atmosphere in Hong Kong. Aerosol Science and Technology 44, 639-650.

Young, L.-H., Lee, S.-H., Kanawade, V.P., Hsiao, T.-C., Lee, Y.L., Hwang, B.F., Liou, Y.-J., Hsu, H.-T., Tsai, P.-J., 2013. New particle growth and shrinkage observed in subtropical environments. Atmospheric Chemistry and Physics 13, 547-564.

Chapter 4: Summarised Results and Discussion

Summarised Results and Discussion

The investigation of the physical and chemical processes affecting atmospheric aerosols in the Western Mediterranean Basin (WMB) during this thesis (2008-2011) has been possible by: a) maintaining continuous regular measurements of PM and its chemical characterisation since the establishment of the site (2002), b) observing the long-term trends of PM and chemical speciation and relating the trends to prevailing emission sources across the region and other outside factors, c) inclusion of measurements of fine PM and performing source apportionment studies on the fine PM fraction, d) expansion of the measurement site by introducing monitoring parameters previously not measured at the site such as BC, sub-micron particle number concentration and size distribution and pollutant gases and e) investigating the sources of sub-micron particles. The results obtained in this work for the specific regional background environment of the WMB provide a clearer picture of the aerosol phenomenology in the area, a region relatively understudied for many of the aerosol parameters included in this work. Building upon the previous knowledge obtained from theses and scientific publications preceding this work, a deeper understanding of atmospheric aerosols was developed.

4.1. Levels of $PM_{2.5}$, PM_1 and sub-micron particles

Continuous sampling of $PM_{2.5}$ since the establishment of the site in 2002 have allowed for the compilation of a relatively long-term time series of $PM_{2.5}$ concentrations (Article 1). PM_1 sampling was also introduced in 2009 (Article 2), and are especially relevant as the majority of anthropogenic emissions exist in the fine fraction, with less influence of primary natural emissions such as crustal material. Measurements of $PM_{2.5}$ are fairly common across Spain and Europe relative to PM_1, and comparisons of $PM_{2.5}$ concentrations with other sites in Spain showed that levels at MSY, as a representative site for the WMB, were higher (12.6 μg m^{-3}) than those recorded for most regional background stations in Spain (the mean $PM_{2.5}$ for all other regional background stations in Spain was 8.6 μg m^{-3}). The elevated levels in MSY were attributed to higher anthropogenic emissions across the region, which includes the metropolitan area of Barcelona and its industrialised and populated hinterland, especially in the pre-coastal depression. Comparisons of $PM_{2.5}$ concentrations with certain regional and rural sites of

Europe with similarly long time-series of data showed that levels were higher than Western Europe (Portugal and Germany) and Northern Europe (Scandinavia), but lower than those measured for Central Europe (Austria, Switzerland and Northern Italy). The surplus in $PM_{2.5}$ at those sites was attributed to heavy industrialisation in the case of Northern Italy (Van Dingenen et al, 2004), and intense pollution accumulation episodes as a result of thermal inversions arising from the mountainous topography of Austria and Switzerland (Barmpadimos et al., 2012). Furthermore, those sites can be more affected by long-range transport from Eastern Europe and substantial biomass burning emissions (Barmpadimos et al., 2012). As stated previously, long-term measurements of PM_1 concentrations in Spain and Europe are much less common. PM_1 concentrations at Melpitz in Germany (Spindler et al., 2010) were higher (12 µg m^{-3}) than those recorded at MSY, and levels at Payerne in Switzerland (Minguillón et al., 2012) were equivalent (9 µg m^{-3}), exhibiting a seasonality with higher concentrations in winter relative to summer. In MSY, the opposite was seen to be the case.

Article 1 and 2 showed a clear seasonality in PM for both fractions, which was related to prevailing meteorological conditions and emission sources across the region. In contrast to the seasonality reported for Payerne in Central Europe for example (Minguillón et al., 2012), PM concentrations at MSY were observed to be lowest in winter, maximum in summer and intermediate in spring and autumn. Weather conditions across the Mediterranean region, with hot, dry summers and relatively temperate winters induce atmospheric conditions largely different to Northern Europe. In summer, lower air mass renovation on a regional scale and the increase of the mixing layer height, which favours the regional mixing of polluted air masses, are important factors giving rise to elevated PM concentrations (Pérez et al., 2010). Furthermore, lower precipitation, higher soil resuspension, photochemical transformations and more frequent African dust outbreaks induce increments in PM levels (Querol et al., 2009). Low winter concentrations were a result of more effective dispersive conditions due to frequent Atlantic advection episodes, increased precipitation and the residence of MSY above the polluted mixing layer (Pérez et al., 2010).

Continuous measurements of particle number size distributions and concentrations commenced at the MSY site from October 2010, providing insight into sub-micron particle processes for the first time in the regional background of the WMB (Article 2 and 3). The Aitken mode was observed to be the dominant particle mode with average concentrations of 1698 cm^{-3}, followed by the accumulation mode (877 cm^{-3}) and the

nucleation mode (246 cm^{-3}). These concentrations were observed to fall in line with those reported in literature for other regional background sites across Europe, ranging from 281 to 10076 cm^{-3} (Asmi et al., 2011), however the lack of entire summer measurements included in this study make annual concentration comparisons not wholly reliable. Concentrations of sub-micron particles in the Eastern Mediterranean reported in that same work were substantially higher than those recorded for the WMB, and were dominated by a strong accumulation mode for most of the year, whereas the Aitken mode is dominant in MSY. In winter under polluted conditions, aerosol number size distributions at MSY bore many similarities with those reported by Asmi et al. (2011) for Central European sites, indicating that in winter particle size distributions can be similar across the continent with an overriding Aitken mode. In spring, a bi-modal distribution at MSY was similar to that reported for Schauinsland in Germany, which is at higher altitude (1210 m.a.s.l.), but is likely to be influenced by similar atmospheric processes as MSY, such as mixing layer development and mountain breezes. Similarly to the seasonality in PM, sub-micron particle number concentrations were also observed to increase considerably as the months became progressively warmer, especially for nucleation mode and Aitken mode particles which was also observed to occur in high-altitude sites in Europe as reported by Asmi et al. (2011).

4.2. Chemical composition of PM

Chemical analysis for the determination of the major and trace components comprising $PM_{2.5}$ and PM_1 was also performed and discussed in Article 1 ($PM_{2.5}$) and Article 2 (PM_1). Mean concentrations of $PM_{2.5}$ reported in Article 1 are for the period 2002-2010, whereas PM_1 means are calculated from autumn 2009 to early 2012. OM was found to be the major component in both fractions, existing mostly in PM_1 (3.2 µg m^{-3}) compared to $PM_{1-2.5}$ (1 µg m^{-3}). Sulphate was the second most abundant compound by a significant margin with concentrations in PM_1 and $PM_{1-2.5}$ of 1.5 and 0.9 µg m^{-3}, respectively. Ammonium was evenly distributed across both fractions (0.5 µg m^{-3} PM_1 and $PM_{1-2.5}$), whereas nitrate was mostly found in $PM_{1-2.5}$ (0.8 µg m^{-3} compared to 0.2 µg m^{-3} in PM_1). EC concentrations existed exclusively in PM_1, as did marine aerosol, although concentrations were low. Finally, crustal material was more abundant in $PM_{1-.25}$ (0.8 µg m^{-3}) relative to PM_1 (0.3 µg m^{-3}). However, it should be noted that there is only a 1.3 year overlap between $PM_{2.5}$ and PM_1 measurements as presented in this

work. As many components gave much higher concentrations (and subsequent gradual reductions) in $PM_{2.5}$ prior to commencement of PM_1 sampling, it should be taken into consideration when comparing the chemical composition of the two fractions.

Sulphate levels in $PM_{2.5}$ at MSY fall within the range for regional background sites in Central and Southern Europe and the UK (2-4 μg m^{-3}) but are higher than those measured at rural sites in Switzerland and Scandinavia (1-2 μg m^{-3}; Querol et al., 2009). Elevated concentrations across the Mediterranean are probably a consequence of high emissions from fuel-oil combustion from power generation, industrial and shipping emissions. Concentrations of OM for sites in Central Europe reported in literature (Putaud et al., 2004; Querol et al., 2009) are higher than those measured at MSY, probably as a result of increased biomass burning emissions, especially in winter. Mean nitrate levels in $PM_{2.5}$ at MSY (1.0 μg m^{-3}) are similar to concentrations measured at Ispra in Northern Italy and are substantially lower than those recorded for Central Europe and the UK (2-4 μg m^{-3}; Querol et al., 2009). The impact of nitrate on annual PM concentrations is closely related to its seasonality. In warmer climates such as that of MSY, ammonium nitrate concentrations are greatly reduced outside the winter months owing to its thermal instability (Querol et al., 2004).

Owing to the abundance of OM and sulphate, the aforementioned seasonality in PM concentrations was mostly attributed to the seasonal fluctuations of these compounds, as well as the atmospheric dynamics in the region described previously. Production of secondary aerosols as a result of intensified photochemistry in summer resulted in higher SOA formation, higher biogenic emissions, and elevated concentrations of sulphate. This seasonality will be further discussed in the following sections.

4.3. Trends of $PM_{2.5}$ and chemical components

Taking advantage of the availability of the extended time series of $PM_{2.5}$ and chemical component concentrations, the trends and variability over time were investigated for MSY and a selection of other regional background stations across Spain and Europe with similarly long term measurements (Article 1). Data from stations was collected from publicly accessible databases EMEP and AIRBASE (of the European Environment Agency). All the stations chosen for the trend analysis underwent decreases in ambient $PM_{2.5}$ concentrations to varying degrees. MSY recorded a drop of 35 % in ambient $PM_{2.5}$ concentrations over the measurement period of 2002-2010. This

trend was followed more or less all across Europe. On average, a reduction of 32% has been observed in $PM_{2.5}$ levels since 2002 throughout Spain, 31% at Illmitz, 36% at Payerne, 34% at Ispra, 35% in Sweden, 32% across Germany, 32% in Finland, 41% in Norway and 38% in Portugal. What was most striking of these statistics were the similarities in reductions shown across Europe, indicating that the forces responsible must be similar across the continent. It can be reasonably assumed that this continuous and, in most cases, gradual reduction is a reflection on the efficacy of pollution abatement strategies employed by member states of the E.U. The E.U. Directive 2008/50/EC specifically controls ambient concentrations of PM_{10} and $PM_{2.5}$ and targets industrial emissions (IPPC Directive, 2008/1/EC), and these measures clearly had a direct effect on pollutant levels in Europe. The introduction of cleaner industrial practices and more efficient combustion engines with lower emissions (as outlined in EURO certifications (1991/441/EC, 1994/12/EC, 1998/69/EC, 2007/701/EC) of vehicle emissions) showed that Europe is headed in the right direction with regards to atmospheric pollution abatement. This decreasing trend has also been described in a study by Barmpadimos et al. (2012). However, can all the reductions in $PM_{2.5}$ observed throughout Europe be attributed solely to the success of pollution abatement strategies, cleaner industrial practices and more efficient fossil fuel combustion?

As mentioned previously, all the stations included underwent a steady and gradual decrease for most of the duration of the study. However, yearly variations around the linear decrease must be related to outside factors which also vary and thus affect ambient $PM_{2.5}$ concentrations. For many of the stations of Europe (not including the Iberian Peninsula or Northern Italy), variations around the linear decrease are similar, with highest concentrations recorded in 2003 and 2006, and minimum concentrations in 2004 and 2007. This implies that the causes in fluctuations in PM are felt across the continent, and are most likely a result of large-scale meteorology. In the case of Central Europe, and possibly as far north as Scandinavia, high levels of PM are associated with high-pressure systems over Eastern Europe in winter that on the one hand lead to relatively stagnant weather conditions and on the other hand to transport of relatively polluted air masses from Eastern Europe to the west (Spangl and Nagl, 2010). Conversely, low-pressure weather systems in Western and North-Western Europe during winter facilitate the transport of relatively clean air masses from Western Europe and the Atlantic, and are associated with frequent weather fronts which remove PM effectively (Spangl and Nagl, 2010). In that same study, low concentrations of $PM_{2.5}$ in

2004, 2007, 2008 and 2009 and high concentrations in 2003 and 2006 were mostly attributed to meteorological conditions. Barmpadimos et al. (2012) showed the year-to-year variability of PM concentrations both in the raw data and adjusted data removing the influence of meteorology. They showed that once the effect of meteorology was removed, a linear decreasing trend was still observed. They attributed the peaks in PM measured in Central Europe in 2003 to meteorology favouring pollution episodes in winter and summer of that year. The summers of 2003 and 2006 were exceptionally warm summers in Europe, and the heatwave of 2006 was most pronounced in Northern Europe (Rebetez et al., 2009), which would have induced higher PM concentrations for the region through soil resuspension, elevated biogenic emissions, forest fires and air mass stagnation. Southern Europe remained relatively unaffected by these summer heatwaves (Rebetez et al., 2009) and may explain why the peak concentrations observed for Central and Northern Europe are not observed for the Mediterranean region.

The winter of 2006-2007 was the warmest across Europe since records began, and the anomalous warm and dry conditions were related to advection of warm air masses from the Eastern subtropical Atlantic as well as strong anticyclonic conditions over large parts of the continent (Luterbacher et al., 2007). Barmpadimos et al. (2012) noted an inverse relationship between temperature and $PM_{2.5}$ in winter and related that finding to the influence of space heating emissions in Central Europe. Space heating by wood burning has been shown to have a large influence on winter aerosol concentrations in Switzerland (Szidat et al., 2007; Sandradewi et al., 2008). Thus, it could be hypothesised that warmer temperatures during the winter of 2006-2007 required less use of domestic heating systems in Central Europe, which in turn reduced the impact of these emissions on overall PM levels. Furthermore, enhanced advection of anticyclonic conditions across Europe would also increase dispersion of PM, which under normal circumstances would accumulate as a result of thermal inversions and stagnation.

The decoupling of the climate of Northern and Central Europe to that of the Mediterranean most likely explains the differing maxima and minima in $PM_{2.5}$ recorded during the measurement period. In contrast to the reduction observed in 2007 in Central and Northern Europe, concentrations of $PM_{2.5}$ in Spain and Northern Italy increased slightly relative to the year previous. While the warm weather in Northern Europe resulted in lower $PM_{2.5}$ emissions, the same warm weather conditions may be related to elevated levels in the WMB, or rather, the air masses associated with such warm weather. Two of the main influential processes affecting atmospheric aerosols in the

WMB during the winter months are Saharan dust intrusions and intense episodes of pollution accumulation resulting from the stagnation of air masses under calm weather conditions. The effect of large-scale meteorological systems, with the ability to affect both Northern and Southern Europe, may go some way to explain such annual variations seen in $PM_{2.5}$.

The North Atlantic Oscillation (NAO) is a large scale oscillation in atmospheric mass, which is believed to be one of the most influential climate modes especially in winter in the North Atlantic region, influencing temperature, precipitation and wind speed across the European continent (Visbeck et al., 2001). The NAO index (NAOi) is a means of quantifying the fluctuations in the dominant pressure systems (the Azores high pressure system and the Icelandic low) over the Atlantic. When the NAO index is in a positive phase, strong winds, precipitation and mild temperatures from the Atlantic move across Northern Europe, and warm, dry weather is experienced in Southern Europe. However, when the NAO index is negative, the Atlantic weather fronts are directed toward a more southerly trajectory giving rise to wetter, windier weather across the Iberian Peninsula and colder weather across Northern Europe (Visbeck et al., 2001). During the warm winter of 2007, the NAOi was in a distinctly positive phase, whereas during winter 08/09 and winter 09/10, the NAOi was in a negative phase. These opposing phases of the NAO might have different implications for different areas of Europe. Whereas warmer conditions in winter for Northern Europe might equate to less domestic heating emissions, the same NAO conditions in Spain give rise to more frequent and more intense winter pollution episodes and stagnation of air masses. However, under negative phases of NAO the impact of these pollution episodes is diminished through dispersion and higher precipitation associated with Atlantic weather fronts. Indeed, winter 2010 was notable for two reasons; unusually high precipitation over the IP which coincided with one of the most negative NAOi since measurements began (Vincente-Serrano et al. (2011), and one of the coldest winters in decades across northern Europe. Incidentally, winter 2010 also registered the lowest PM levels recorded at MSY since 2002. Thus, the extreme negative phase of the NAO possibly had two important effects on ambient PM levels that winter at MSY: increased Atlantic advection and precipitation, and possibly less Saharan dust intrusions. As mentioned previously, the occurrence of Saharan dust intrusions over the IP can affect PM levels significantly. A linear relationship was observed between the frequency of NAF episodes (in days) and the corresponding NAO index for the winter months across the

Iberian Peninsula. This indicated that when NAO is more intensely positive, the probability of air masses from North Africa reaching the Iberian Peninsula is much higher. Conversely, when NAO is negative, intense Atlantic Advection directed over the Peninsula can block North African air masses and prevent these air masses moving northward.

Finally, one further influential factor may explain the decline in $PM_{2.5}$ concentrations observed. As outlined above, a declining trend was discernable throughout Europe, and variations around this trend are likely a result of meteorology. However, in some cases the annual variation in concentrations appeared to fluctuate less intensely relative to previous years. Furthermore, this appeared to be preceded by a drop in concentrations, specifically between 2007 and 2008. $PM_{2.5}$ levels thereafter fluctuate much less and in most cases do not exceed the linear decreasing trend. What the countries have in common where this occurred, such as in Spain, Portugal and Italy, is the on-going economic crisis. The countries which have been largely unaffected by the economic recession, such as Germany, Austria, Switzerland, Finland, Sweden and Norway, did not display any discernable larger decrease other than that which was observed for the previous years. For example, $PM_{2.5}$ concentrations at Ispra in the heavily industrialised Po valley in Northern Italy dropped 6 μg m^{-3} between 2007 and 2008, and this decrease was maintained for the year after, removing the likelihood that the decrease was anomalous. An even more dramatic decrease was observed across Portugal, especially for one station (Lamas de Olo) which underwent a 6.8 μg m^{-3} reduction between 2007 and 2008 alone. In Spain, this decrease was 1.7 μg m^{-3} (from an average of 9.8 μg m^{-3} before the crisis (2002-2007) to 7.4 μg m^{-3} since the crisis began (2008-2010)).

Considering MSY as a representative station for the WMB regional background, the analysis of the long-term time series of the chemical constituents of $PM_{2.5}$ allowed for the identification of the components causing the declining concentrations (Article 1). The largest decrease observed of all the components was for OC, with a total reduction of 48 % from 2002-2010. Considering the regional background status of MSY, it could be reasonably assumed that a large proportion of OC at the site is comprised of SOA produced from both anthropogenic and natural emissions. Natural emissions of organic aerosol would not be expected to fluctuate to any great extent, at least not linearly as was observed, and thus the reduction must be attributed to a reduction in anthropogenic emissions. EURO certifications control total hydrocarbon and non-methane

hydrocarbons for vehicular emissions and the implications of this may be a net reduction in ambient OC concentrations. SIA also decreased significantly: sulphate concentrations underwent a declining trend and this was attributed to the phasing out of the combustion of fuel oil for power generation around Barcelona (Bruno et al., 2007), as V and Ni concentrations dropped similarly over the same period. Sulphate and OC concentrations decreased gradually (and with statistical significance) and this is likely a direct result of pollution abatement strategies. However nitrate concentrations remained relatively constant from 2002-2007, but from 2008 onwards registered comparatively lower concentrations. This indicates that, unlike sulphate and OC, the decline in nitrate concentrations may be more related to a decrease in economic activity, especially road traffic, rather than the efficacy of air quality control measures alone. Intense peaks in nitrate concentrations are common during the winter months owing to pollution episodes, but the impact of these pollution episodes on annual nitrate levels was diminished considerably in the last few years, which may also be a result of the aforementioned negative phase of NAO.

Trace elements varied considerably throughout the measurement period, many of which experienced declining concentrations with statistical significance. Those which experienced the greatest percentage reductions since measurements began were typical anthropogenic emission tracers Cd, Sb, Sn and Pb, followed by Cu, As, Ni and V. Some of these tracers (Pb, Cd, As, Ni) are specifically targeted by pollution abatement programmes (2008/50/CE, 2004/107/CE) and the observed decline for these trace elements can be attributed to these controls, and the phasing out of fuel oil combustion power plants in the case of Ni.

4.4. Source apportionment studies of PM_1 and sub-micron particle number concentrations

Long-term chemical speciation of PM_1 for regional background sites is relatively scarce across Europe, and a unique opportunity to perform source apportionment studies on the fine fraction presented itself. Following regular sampling of PM_1 between 24/09/2009 to11/01/2012 (182 valid cases in total), a source apportionment study, by means of Positive Matrix Factorisation, was applied to the dataset in order to identify the prevalent emission sources of PM_1 (Article 2). Furthermore, the simultaneous measurement of sub-micron particle number concentrations and size distribution

allowed for the identification of emission sources affecting particle number concentrations (Article 2). Simultaneous measurements of particle number concentration and PM_1 speciation was performed between 05/11/2010 to 18/12/2011 (with a hiatus in measurements between June and October), totalling 61 cases, and potential sources of particles were identified by Principal Component Analysis (PCA). Six sources of PM_1 were identified: secondary sulphate, secondary organic aerosol, fuel oil combustion, traffic + biomass burning, industrial and secondary nitrate. The sources affecting particle number concentration were similar, but some sources overlapped owing to the reduced dataset. The sources identified to contribute to particle number concentration were: Industrial + traffic + biomass burning, new particle formation + growth (NPF + G), secondary sulphate + fuel oil combustion, crustal material and nitrate. Thus, a source of particles (NPF + G) was identified that appears to be entirely separate to the sources affecting mass. Owing to the lack of summer measurements of particle number size distribution, a SOA source was not specifically identified as a source of particles. There is evidence to suggest that SOA is influential on the NPF + G source that will be discussed anon, and further measurements including summer months may clarify the relationship between the two. The secondary sulphate + fuel oil combustion source and industrial + traffic + biomass burning were merged owing to the reduced data set. Although OM was identified as the major component of PM_1, SOA was not found to explain the largest variance in PM_1, probably because OC levels were consistently high (and less variable) compared to other components.

The secondary sulphate source in PM_1 was mostly characterised by ammonium sulphate and was associated with pollution across the region, when atmospheric recirculation causes the accumulation and aging of pollutants, especially in summer. Thus, in summer concentrations are at a maximum as a result of regional pollution episodes and intensified solar radiation.

SOA was the second most important source affecting PM_1 concentrations and was mostly characterised by OC. The annual variation of this source was governed by two processes: 1) SOA produced from anthropogenic VOC and biomass burning emissions giving rise to elevated concentrations in winter, especially during intense pollution episodes, 2) an increasing trend during the summer months was related to increased biogenic emissions and enhanced photochemical reactions (Seco et al., 2012). Owing to the mix of anthropogenic and natural sources of SOA, this source did not undergo any discernable daily variation. Although a crustal source was not specifically identified by

PMF analysis, typical crustal elements were found in both the secondary sulphate and SOA sources. This was related to the seasonality of both these sources with elevated concentrations in summer, which is also when crustal material concentrations are at their highest (Pey et al., 2009a). The secondary sulphate source explained a significant amount of the variance of OC also, further highlighting the influence of seasonality on both these sources.

The third most influential source in terms of contribution to the PM_1 mass was the fuel oil combustion source which was characterised by typical tracers V, Ni and Sn (Pandolfi et al., 2011). Fuel oil combustion also accounted for some of the variance in ammonium and sulphate, indicating that the sulphate and fuel oil sources are not completely independent of each other which would be expected. The separation of fuel oil combustion and secondary sulphate may give an indication of the age of the aerosol, as SO_2 emitted alongside V and Ni during fuel oil combustion may not be oxidised to SO_4^{2-} before reaching MSY. On the other hand, secondary sulphate is typically more aged and represents emissions from across the region. The possibility of shipping emissions was indicated by the presence of marine aerosol tracers Na and Mg in the fuel oil combustion source. This source underwent a similar seasonal variation similar to that of secondary sulphate, which was related to enhanced sea breezes in summer, thus increasing the influence of shipping emissions. This source displayed gradually increasing concentrations during the week with a notable decrease at the weekend.

A traffic and biomass burning source was characterised by EC, OC, Sb, Sn and K (Amato et al., 2009; Minguillon et al., 2012), and explained the large majority of the variance of EC. Traffic emissions throughout the year should remain relatively constant, thus the observed variation must have been due to other variable factors such as winter pollution episodes and the influence of local meteorology (mountain breezes, thermal inversions), and also to some extent emissions from biomass burning. The peak observed in January may be directly related to local emissions from domestic heating systems. The peaks observed in April and October may be explained by controlled biomass burning from local agriculture, which is common during these months. The impact of this factor was reduced at the height of summer (July and August), when biomass burning is prohibited to minimise risk of uncontrolled forest fires and a reduction in traffic emissions occurred due to the vacation period in July/August and higher dilution processes owing to the increase in mixing layer height. A clear

increasing trend was recorded during the week followed by a reduction at weekends owing to reduced commuter traffic.

An industrial source was identified by the presence of typical industrial tracers Pb, As, Cd, Sn, Cu, Zn, Cr, Fe and Mn (Viana et al., 2006; Belis et al, 2013), but contributed little to the total PM_1 mass as it was mostly comprised of trace elements. Reflecting the typical working week, industrial emissions increased progressively during the week to Friday, followed by a decline in concentrations at weekends. Furthermore, on a monthly basis concentrations were relatively constant except for a reduction in emissions in July/August, as a consequence of the vacation period when industrial activity is lesser.

The final source with the least contribution to the PM_1 mass is the nitrate source. This factor was majorly characterised by nitrate, and also explained some of the variance in K and EC, possibly as a result of mixing with the traffic + biomass burning source. On a yearly basis, nitrate was observed to contribute little to the overall PM mass but this contribution increased substantially during the colder months when nitrate was more abundant.

The various sources affecting particle number concentrations were found to be mostly similar to those affecting particle mass. Particle number concentrations were calculated for a range of particle diameters, including the nucleation mode (9-30 nm), the lower Aitken mode (30-50 nm), the upper Aitken mode (50-100 nm) and finally the accumulation mode, which was divided into three ranges (100-300, 300-500 and 500-825 nm). The source which explained the largest variance in particle number concentration was the industrial + traffic + biomass burning source, with high factor loadings for variables typically associated with traffic emissions (EC, BC, OC, NO_2, Sn, Sb), industrial emissions (Pb, Zn, Cd, Mn, Cu) and biomass burning (OC, EC, BC, K). This component was closely associated with particles of 100-300 nm and 500-825 nm in diameter, suggesting this source mostly influences aerosol number concentrations in these two diameter ranges. Freshly emitted particles from these sources transported to MSY might be expected to be smaller ($N_{100\text{-}300}$). However, enduring regional pollution episodes, such as those that occur in winter, would promote the condensation of smaller particles onto the surface of larger particles within the aged air mass, and give rise to higher concentrations of larger particles ($N_{500\text{-}825}$).

The second most important component in terms of particle number concentration was NPF + G, which existed almost exclusively in the ultrafine mode (<100 nm). This

source was not associated with any specific pollutant gas or chemical component, but some relationship was observed with solar radiation stressing the importance of photochemical reactions for new particle formation. Secondary sulphate + fuel oil combustion was marked by high factor loadings for sulphate, ammonium, and V. PM_1 also had a high factor loading in this source showing how this source affects the mass and contributes less to the overall particle number concentration, although there was some factor loading for the largest particles (500-825 nm). The seasonality of this source, with maximum concentrations in warmer conditions, was highlighted by the presence of high factor loadings for solar radiation and temperature.

A crustal material source was identified, characterised by typical crustal elements and components Ce, La, Fe, Ni and Al_2O_3, but contributed little to the particle number concentration as it would mostly affect the particle mass. Finally, nitrate was characterised by high factor loadings for NO_3^-, K and to a lesser extent NH_4^+ in the range of 300-825 nm. The presence of K may suggest some influence of biomass burning in this factor. Temperature is negatively correlated with this source as expected, as a result of the predominance of nitrate in colder conditions owing to its thermal instability.

The mean daily contribution of each source to the particle number concentration for different size ranges was also investigated. Episodes of intense pollution occurring during winter resulted in relatively low particle number concentrations, especially in the ultrafine mode, as the majority of particles existed in the accumulation mode as a result of air mass stagnation. Under cold polluted conditions, the nitrate and industrial + traffic + biomass burning contributed most significantly to the particle number concentration. Conversely, under warm polluted conditions, the nitrate source was insignificant and the secondary sulphate was much more influential. The source NPF + G was observed to undergo a clear seasonality, with particle number concentrations from this source increasing as solar radiation intensity and temperatures increased. Sulphate and nitrate related particles were relatively scarce when NPF + G was most abundant, as they would scavenge the gaseous precursors necessary for new particle formation through condensation and coagulation processes.

Finally, the mean contribution of each component to the particle number concentration in various size ranges was performed. The source NPF + G contributed the majority of particles to the ultrafine mode. The industrial + traffic + biomass burning also contributed to the ultrafine mode and the influence of this source increased

with increasing particle diameter. The nitrate and secondary sulphate + fuel oil source existed almost exclusively in the accumulation mode and contributed little to the overall particle number concentration.

The combination of source apportionment studies on both sub-micron particles and the fine PM fraction highlights the dominating effect of anthropogenic emissions on both parameters. Although neither is currently controlled by air quality management protocols, there is strong evidence presented here to support measures to control both their emissions and their ambient concentrations. An inverse relationship between particle mass and particle number concentration has been observed (Rodríguez et al., 2007; Pey et al., 2008) and this indicates that a reduction in ambient PM, as highlighted in Article 1, might incur an increase in ambient particle number concentrations. When we consider that the source identified as NPF + G was not associated with any other source or chemical component, this appears to verify the inverse relationship. Moreover, this source also contributes the largest concentration of particles to the overall total number, which differs considerably to urban environments where vehicle exhaust is the dominant source (Pey et al., 2009). Thus, whereas anthropogenic emissions are the most important sources of PM and particles in certain environments, in rural and remote environments PM and ultrafine particles appear to have a very definite inverse relationship in winter. In summer, the two variables can both exist in elevated concentrations, although remain independent of each other, as will be discussed in the following section.

4.5. Variability of sub-micron particle number concentrations and size distribution

The daily and seasonal variability of particle number size distributions and concentrations were investigated (Article 3). As mentioned previously, a large increase in both nucleation and lower Aitken mode concentrations was recorded from the colder to warmer months. Similar studies on sub-micron particle number size distribution are few for the Mediterranean regional background, and none others exist for the WMB regional background as yet. Furthermore, the mid-altitude height of the MSY station makes it further unique in that the station resides both above and below the mixing layer depending on the season and prevailing meteorology. In Europe, many publications report a similar seasonality with increases in nucleation mode concentrations during the

summer months as a result of enhanced photochemical new particle formation (Venzac et al., 2009; Sorribas et al., 2011). The climate of the Mediterranean, with frequent clear sky conditions and intense solar radiation, provides ideal conditions for investigating sub-micron particle processes.

Based on the observation that particle number concentrations increased substantially during the warmer months, the dataset was initially divided into two periods based on temperature conditions; a cold and a warm period. These datasets were then subdivided into periods of polluted and clean air conditions (based on BC concentrations). Clean air conditions were associated with Atlantic advection episodes or occurred after periods of rainfall. Episodes of pollution were observed to be more varied than clean air episodes. The influence of the diurnal breeze system was the dominant process affecting variations in aerosol concentrations, especially during the colder season. Nocturnal concentrations were low when MSY resided above the mixing layer, but during the day mountain breezes carried pollution from the depressions below to the site giving rise to substantial increases in aerosol concentrations (Pérez et al., 2008). Long-range transport of particles occurred during African dust intrusions and transport of polluted air masses from mainland Europe to the region also occurred, although this was infrequent during the study period.

Particle number concentrations were elevated during the warmer period, especially for the ultrafine fraction. Higher levels of the upper Aitken and accumulation mode concentrations during the warmer period were attributed to the residence of MSY within the mixing layer for longer periods during the day in warmer months and lower precipitation. Higher number concentrations of nucleation and lower Aitken mode particles were believed to be a result of increased nucleation and growth of nucleating particles. As suggested in Article 2, new particle formation and growth processes are unrelated to other pollutant parameters and dominate the ultrafine mode. The modality of particle number size distributions for each period also showed significant differences. Almost all scenarios displayed a bi-modal size distribution except for polluted conditions during the colder season, which was distinctly uni-modal with a modal diameter in the upper Aitken mode. Under clean conditions in the colder period, two modes were recorded: one in the lower Aitken mode and a minor mode in the accumulation mode. Conversely, during the warmer months similar modality was observed for both clean and polluted conditions, although with largely different particle

number concentrations. In both cases, the dominant mode was in the upper Aitken mode with a minor mode in the nucleation mode.

Thus, the variability of particle number concentrations was investigated thoroughly for the scenarios outlined. Polluted conditions during the colder season were typically a consequence of the transport of polluted mixing layer air to the site. Aerosols, having accumulated in the populated valleys and depressions below MSY, were carried to the site by mountain breezes activated by insolation. The progression of the breeze during the day gave rise to a large increment in pollution, followed by a nocturnal drainage flow removing aerosols from the site. Nucleation mode concentrations were low under these conditions, owing to the elevated condensation sink which scavenged the necessary gaseous precursors. Similar concentrations of the lower and upper Aitken and the accumulation mode, and the uni-modal size distribution, highlighted the aged and mixed state of particles within the polluted mixing layer. Such conditions were also identified in Article 2, such as during WAE when ultrafine particle concentrations were low and accumulation mode particles dominated. These particles were associated with nitrate, traffic, biomass burning and industrial emissions, and elevated concentrations of PM_1 and gaseous pollutants.

On the contrary, under clean air conditions during the colder season, i.e. in the absence of the polluted breeze, little variation was detected for the upper Aitken and accumulation mode. The absence of a significant condensation sink therefore allowed new particle formation to take place, as was evidenced by the relatively elevated concentrations of both the nucleation mode and the lower Aitken mode (as a result of particle growth after formation). Nucleation processes were noted to occur when solar radiation was at its maximum strength, indicating the importance of photochemical reactions in initiating new particle formation. The influence of new particle formation on particle number concentrations and modality was evidenced by the size distribution, with a major modal diameter just outside the nucleation mode (35 nm).

The diurnal variation of particle number concentrations and other pollutant parameters under warm conditions was in considerable contrast to that observed for the colder season. The effect of the mountain breeze on the aerosol parameters was evident during this period also, but the duration of the peaks in pollutant concentrations was extended compared to the cold season, owing to the higher temperatures, increase in mixing layer height and the increase in wind speed during the warmer months. Unlike polluted conditions during the colder season, nucleation mode concentrations were

observed to be elevated irrespective of the high condensation sink. This suggested that under warmer conditions, nucleation processes could still take place even in the presence of a high background loading of particles. Freshly formed particles were evidently being produced and growing faster than they were being removed through coagulation and condensation processes. Similar behaviour has been observed under polluted conditions in the warmer season in a Northern Italy boundary layer site (Hamed et al., 2007). This was attributed to elevated concentrations of condensable organic vapours, such as biogenic emissions emitted by local vegetation, which are believed to contribute significantly to growth of nucleating particles. An abundance of such biogenic compounds in the atmosphere and intensified solar radiation typical of the climate might indeed have promoted the growth of nucleating clusters to a detectable size before the gaseous precursors are lost through removal processes. In Article 2, the SOA source exhibited elevated concentrations in summer when the new particle formation and growth source was most influential. A similar diurnal variability and modality was recorded for both clean and polluted conditions under warm conditions, indicating that nucleation processes are not controlled by the presence of pre-existing particles, but rather the abundance of gaseous precursors necessary for nucleation and subsequent growth.

4.6. Case studies of new particle formation and evaporation processes

Specific cases of sub-micron particle processes were chosen for in-depth investigation and to help identify the ideal atmospheric conditions for new particle formation (Article 4). Intense bursts of nucleation and growth were recorded during the winter when MSY resided above the polluted mixing layer with limited or no influence of the diurnal breeze system, as was evidenced in Article 3. Under these conditions, sulphuric acid, a low condensation sink and solar radiation were noted to be the most important factors for nucleation processes. Low growth rates were also a common feature, and it was hypothesised that less intense solar radiation and lower biogenic emissions typical of winter conditions were the reason for this. On one occasion, a nucleation event was recorded on the same day as the source apportionment analysis was performed as described in Article 2 (7/12/2010). On that specific day, PM_1 concentrations were low (4.4 µg m^{-3}) but was almost exclusively comprised of SOA,

with minimum contribution of the other sources identified, further highlighting the importance of condensable organic vapours.

Episodes of nucleation were also recorded even under polluted conditions during the colder season, albeit as an exception to the rule outlined in Article 3 (whereby nucleation typically only occurs during clean air conditions in winter). On one specific occasion, a clean air mass which had remained above MSY for days previously was abruptly replaced by a polluted air mass, resulting in a considerable increase in black carbon, NO_2 and condensation sink. A well defined tri-modal size distribution occurred on this day, with modal diameters in the upper and lower Aitken and the nucleation mode. Nucleation mode concentrations in this case were similar to the nucleation events recorded on the previous days (under clean air conditions) even though sulphuric acid concentrations were lower owing to the higher condensation sink, and solar radiation intensity was the same. Thus, it was suggested that such intense nucleation was a result of elevated concentrations of VOCs within the polluted air mass, allowing the freshly formed particles to grow before removal through coagulation and condensation. This was evidenced by the higher growth rate, which is typical of more polluted environments (Kulmala et al, 2005).

The effect of air mass mixing on sub-micron aerosol processes was also investigated. As is typical of mid-altitude sites, mixing between polluted and clean mixing layer air can result in the sampling of different parts of air masses undergoing different aerosol processes, such as a nucleation event at different phases of development. It was shown that new particle formation appeared to be occurring elsewhere but the growing particles were being transported to the site, suggesting that nucleation can be localised in the area. Furthermore, more than one burst of new particle formation was recorded within quick succession during the same day. In certain instances, it was observed that particles were observed to shrink or evaporate, causing a gradual and distinct decrease in the geometric mean diameter of the mode. In total, 10 episodes of particle shrinkage were recorded, 5 of which occurred on the same day as nucleation was recorded.

An example of particle shrinkage was investigated whereby the geometric mean diameter decreased from the upper Aitken (66 nm) mode to the lower Aitken mode to a minimum of 24 nm. As the shrinking mode decreased, the particle number concentration increased as larger particles were dissociating and producing greater concentrations of smaller particles. Before shrinkage occurred, solar radiation was

variable and indicated there may have been significant cloud cover. Afterwards, solar radiation increased and was less variable, suggesting the clouds had dispersed. At this moment, particle shrinkage commenced as the increase in temperature and solar radiation favoured the evaporation of volatile and semi-volatile particles from the surface of larger particles. Furthermore, an abrupt decrease in black carbon and NO_2 also occurred at the moment shrinkage commenced, indicating that aerosols were being diluted and may have produced a shift in the gas/particle partitioning. Similar behaviour under similar conditions has been observed in São Paulo (Backman et al., 2012), whereby shrinkage was observed to occur coinciding with an abrupt increase in solar radiation and temperatures. Yao et al. (2010) observed particle shrinkage in Hong Kong and they suggested that a change in atmospheric conditions, such as dilution in ambient concentrations of aerosols, allows for a shift in gas/particle partiontioning.

An example of an intense nucleation event was recorded when ideal conditions were present, with intensified solar radiation, elevated concentration of sulphuric acid, low background particle loading (condensation sink) and low relative humidity. These factors combined resulted in an extremely intense burst of new particle formation. The nucleating particles grew rapidly, with a very high growth rate. As the particles grew to the lower Aitken mode the geometric mean diameter was maintained while the condensation sink and black carbon reached a maximum. As seen in the previous case, once black carbon and the condensation sink began to decrease, particle shrinkage commenced, again maybe as a result of dilution processes, reversing gas-to-particle processes, and evaporation of the condensed semi-volatile species occurred. This process produced an arch-like profile for the particle size distribution contour plot, and concentrations of nucleation mode particles as a result of particle evaporation were almost equivalent as for those produced by new particle formation.

Comparisons of the two shrinkage events described suggested that the processes occurring may have been different. In the first case, particle shrinkage was not preceded by nucleation, i.e. particles appeared to be evaporating from larger particles, and the rate of evaporation was significantly lower than the second case. It was suggested that the evaporating species in each case may have been different. In the first case, it would appear that the evaporating species are volatilising from stable clusters that were transported to the site, and evaporation was initiated by an increase in solar radiation and temperature. However, in the second case, an intense burst of evaporation preceded particle evaporation, and no discernable change in solar radiation occurred during the

day. It was hypothesised that the evaporating species in the first case was a result of the volatilisation of NH_4NO_3 associated with its thermal instability. In the second case, the high growth rate observed which is most typical for polluted conditions, in the absence of an appreciable condensation sink indicated that the nucleating particles formed unstable larger particles, and the condensing species which contributed to particle growth were easily volatilised from the fresh particles, causing the shrinkage observed.

Chapter 5: Conclusions

Conclusions

Building upon previous knowledge accumulated through previous studies at MSY and expanding the monitoring station to incorporate a broad range of other measurement parameters since the beginning of this work has allowed for an unprecedented characterisation of atmospheric aerosols in the WMB regional background. Previous studies have shown the uniqueness of atmospheric aerosol characteristics in the WMB compared to the rest of Europe, but the majority of these studies have focused on the variability of PM and the chemical characterisation of PM_{10} and $PM_{2.5}$. This current work is the first time that sampling and chemical characterisation of PM_1 was performed. Furthermore, the inclusion of measurements of particle number concentration and size distribution and Black Carbon allowed for a greater understanding of aerosol phenomenology occurring in this region. The main conclusions that can be drawn from the work presented in this thesis are as follows:

- Concentrations of $PM_{2.5}$ in the WMB regional background fall within range of other regional background sites across Europe, and slightly higher than those recorded for sites across Spain. This surplus is attributed to the influence of anthropogenic emissions from across the region, which includes the Barcelona metropolitan area, dense industrialisation and road traffic. Continuous measurements and chemical characterisation of PM_1 are comparatively scarce across Spain and Europe, but levels at MSY are lower than levels reported in the literature for Central Europe. $PM_{2.5}$ and PM_1 is majorly characterised by organic matter, sulphate, nitrate and ammonia in both fractions, and crustal material in $PM_{1\text{-}2.5}$, which explains the seasonal variance. Higher PM in summer is related to elevated concentrations of organic matter and sulphate as a result of enhanced solar radiation, higher biogenic emissions, and regional recirculation episodes inducing the accumulation of pollutants across the region. Nitrate levels were negligible except during the colder months.

- The efficacy of Europe-wide pollution abatement strategies was evidenced through the gradual decline in $PM_{2.5}$ observed across the continent over the past decade. Reductions of 6 µg m^{-3} of $PM_{2.5}$ at MSY were recorded since 2002, and the mean reduction across Europe was in the region of 35%. Variations around this decreasing trend were attributed to large-scale meteorology affecting aerosol concentrations across Europe.

Maximum levels for Northern Europe coincided with anomalously hot summers in 2003 and 2006, and minimum concentrations coincided with mild winters in 2007, resulting in reduced emissions in domestic heating systems and greater dispersion of PM as a result of enhanced Atlantic advection. In contrast, warmer winters in Southern Europe gave rise to an opposing variation, with maximum concentrations recorded as a result of intensified winter pollution episodes. It is hypothesised that large-scale meteorology, namely the North Atlantic Oscillation, is influential on $PM_{2.5}$ concentrations, and this influence differs for Northern and Southern Europe. Positive phases of NAO produce milder, wetter weather across Northern Europe (reducing $PM_{2.5}$) and hotter, drier weather over Southern Europe with more frequent Saharan dust intrusions (increasing $PM_{2.5}$). When the NAO is extremely negative, as evidenced in the winter of 2010, the Atlantic weather fronts move on a more southerly trajectory bringing wetter, windier weather to Southern Europe, thus reducing pollutant levels. Furthermore, an accentuated decline in $PM_{2.5}$ coinciding with the beginning, and continuing, economic recession in the peripheral economic states of Europe was outlined, attributed to a reduction in industrial activity, commuter traffic and a deflated construction industry, i.e. activities associated with healthy economic activity. Taking advantage of the long time series of $PM_{2.5}$ and chemical composition data made available since the establishment of the MSY site, the temporal trends of the major and minor chemical components of $PM_{2.5}$ showed that the reduction in mass observed is a result of reducing anthropogenic organic matter and secondary inorganic aerosol concentrations. A gradual decline for organic matter and sulphate is likely a direct consequence of pollution abatement strategies. However, a distinct drop in nitrate since 2008 is probably due to reduced road traffic. Similarly, declining concentrations of trace elements verify the reducing trend, especially for trace elements associated with anthropogenic activities and those controlled by EU Directives.

- Six identifiable emission sources contribute to PM_1 in the WMB, which are: secondary sulphate, SOA, fuel oil combustion, traffic + biomass burning, industrial and secondary nitrate. Most of the sources are seasonal, such as secondary sulphate, SOA and nitrate, but all are prone to increased concentrations during winter pollution episodes. Furthermore, many of the sources undergo clear increasing weekly trends with diminished impact at the weekends. Two of the sources, specifically the industrial and traffic and biomass burning sources, have reduced concentrations coinciding with the

vacation period in summer. The influence of shipping emissions on the fuel oil combustion source is indicated by the presence of marine aerosols.

- Sources affecting sub-micron particles in the WMB regional background include: industrial + traffic + biomass burning, new particle formation + growth, secondary sulphate + fuel oil combustion, crustal material and nitrate. Thus, similar sources of PM and particle number concentration were identified, except for the new particle formation + growth which tended to have an inverse relationship with the other sources. The importance of photochemistry on this source was indicated by the factor loading observed for solar radiation. New particle formation + growth contributes the largest proportion of particles, mostly to the ultrafine faction, and its contribution to the particle number varied widely on a daily basis. The remaining sources mainly affect particles in the upper Aitken and accumulation mode, and the nitrate and secondary sulphate vary depending on the season.

- Particle number concentrations were observed to be in line with concentrations across Europe. Depending on the prevailing atmospheric dynamics at the MSY site, wintertime particle concentrations and size distribution reflected high altitude sites (clean conditions) or continental sites (polluted conditions), but bore little relation with concentrations and size distributions in Eastern Mediterranean sites. Springtime concentrations at MSY appeared elevated relative to winter, probably owing to higher biogenic emissions and active photochemistry. The majority of particles at MSY are in the Aitken mode, followed by the accumulation mode and the nucleation mode. During winter, local mountain breezes carrying pollutants to the site are the most influential processes affecting the diurnal variability of aerosols, especially affecting the Aitken and accumulation modes. Under such conditions, high background particle loadings prevent new particle formation processes. Conversely, low particle loadings under clean air conditions, with sufficient solar radiation and gaseous precursors, allow for new particle formation processes in winter. In the warmer months, particle number concentrations in all modes are elevated, especially in the nucleation and lower Aitken mode, indicating that new particle formation processes are still active and sufficiently rapid in order to avoid scavenging by the pre-existing particle population.

- Thirty episodes of new particle formation between October 2010 and June 2011 were identified (occurring on 14% of total days of measurements), and specific examples were chosen as case studies. Ideal atmospheric conditions for new particle formation depend on a number of variables, such as solar radiation, sulphuric acid for initial formation of clusters and sufficient condensable organic vapours. Nucleation processes occurring under clean air conditions are influenced by even small changes in condensation sink levels, and generally have low growth rates. Under polluted conditions, new particle formation can take place provided there are sufficient concentrations of condensable vapours and growth rates are more rapid, before the nucleating particles are removed by coagulation and condensation processes. Nucleation episodes can also be localised, with particles at different stages of formation and growth being carried to the site, or occurring at different stages within different air masses.

- Particle shrinkage is identified as an important process at the site, with 10 cases identified in total (5% of all measurement days), and is a process that is currently not well represented in literature. It is suggested that a reversal in the gas-particle partitioning of condensed species may be caused by dilution processes, which reduce the precursor vapour concentrations, allowing condensed species to evaporate. Warm temperatures, high solar radiation and low relative humidity are also common meteorological features present when particle evaporation occurs. Depending on the original species and atmospheric conditions preceding particle evaporation, it is hypothesised that different evaporating species may be involved, specifically by the volatilisation of ammonium nitrate and/or semi-volatile organic species.

Chapter 6: Future Research and Open Questions

Future Research and Open Questions

The research carried out in this study highlights the unusual physical and chemical processes affecting regional background aerosols in the Western Mediterranean Basin, and leads to further open questions and gaps in knowledge that future research will hopefully shed some light on.

The continuation of sampling of PM_{10}, $PM_{2.5}$ and PM_1 and chemical analysis will provide further information on the long-term trends of PM at the site, and will ascertain the causes for fluctuations in PM suggested in this study. Long term chemical speciation studies of PM are relatively scarce, especially for PM_1 which is most influenced by anthropogenic emissions, and thus it is essential to continue these measurements in order to fully characterise PM for the region. Furthermore, the continuous sampling of PM at the site is important for comparison with urban emissions in order to quantify the emissions that can be attributed to local emissions and identify the influence of long-range transport of pollution.

Results obtained during the DAURE intensive winter and summer campaigns are not included in this study, but they represent a unique opportunity to characterise organic aerosols, among other parameters, at the site to an unprecedented level. As indicated by this work, organic aerosols are very influential on PM concentrations at the site, as well as their involvement in growth of new particles after formation. The sources of organic carbon are varied, emitted from both anthropogenic and natural sources, and the data compiled during the DAURE campaign should hopefully close the knowledge gaps in this field. The information provided by the DAURE campaign should shed light on the sources and processes affecting organic aerosols at the site, and the subsequent continuous measurement of OC will determine the long-term variations.

Since the establishment of the site, the number of aerosol parameters measured has increased considerably. Measurements of aerosol optical properties such as scattering and absorption, BC, particle number concentration and size distribution have been on-going, and the continuation of these measurements will provide information on the long-term trends of these properties at the site and the climate forcing capabilities of aerosols at the site. Entire summer measurements for particle number concentration and size

distribution were unfortunately unavailable for this work, and evidence suggests that sub-micron particle processes during the summer are significantly different to those during the rest of the year, especially for the ultrafine fraction. Furthermore, source contribution studies on particle number concentrations with summer measurements should hopefully identify the importance of organic aerosols on the source identified in this study as new particle formation and growth.

As shown in this thesis, evaporation of ultrafine particles appears to be an important process affecting aerosols at the site. To date, there are very few publications and studies describing the process. The studies that do exist are still in their infancy, but judging by the information available, it appears that particle evaporation may be a common feature of hot climates. Continued study of these evaporation processes is essential to further understanding of what is occurring, what the evaporating species involved are and the thermodynamic processes allowing evaporation to occur. Real-time measurements of sulphate, nitrate, ammonia, chlorine and organics, as provided by aerosol chemical speciation monitors which has been deployed at the site recently, should hopefully indicate what the chemical species involved are.

The combination of continuous chemical characterisation of PM and aerosol optical measurements presents a unique opportunity to investigate the optical properties of specific chemical components. Such studies are important for determining the radiative forcing potential of specific components of PM, such as BC, sulphate, nitrate etc., and would thus provide essential information for long-term climate studies in the region.

Chapter 7: References

References

Amato, F., Pandolfi, M., Viana, M., Querol, X., Alastuey, A., Moreno, T.: Spatial and chemical patterns of PM10 in road dust deposited in urban environment, Atmos. Environ., 43, 1650-1659, 2009.

Amato, F.: Particulate Matter Resuspension from Urban Paved Roads: Impact on Air Quality and Abatement Strategies, PhD Thesis, Universitat Politécnica de Catalunya (UPC), 2010.

Anderson, J. O., Thundiyil, J. G. and Stolbach, A.: Clearing the air: a review of the effects of particulate matter air pollution on human health., Journal of medical toxicology : official journal of the American College of Medical Toxicology, 8(2), 166–75, doi:10.1007/s13181-011-0203-1, 2012.

Andrade, F., Orsini, C and Maenhaut, W.: Relation between aerosol sources and meteorological parameters for inhalable atmospheric particles in Sao Paulo, Brazil, Atmospheric Environment, 28, 2307-2315, 1994.

Andreae, M. O., Jones, C. D. and Cox, P. M.: Strong present-day aerosol cooling implies a hot future., Nature, 435(7046), 1187–90, doi:10.1038/nature03671, 2005.

Andreae, M. O. and Rosenfeld, D.: Aerosol–cloud–precipitation interactions. Part 1. The nature and sources of cloud-active aerosols, Earth-Science Reviews, 89(1-2), 13–41, doi:10.1016/j.earscirev.2008.03.001, 2008.

Anenberg, S. C., Horowitz, L. W., Tong, D. Q. and West, J. J.: An estimate of the global burden of anthropogenic ozone and fine particulate matter on premature human mortality using atmospheric modeling., Environmental health perspectives, 118(9), 1189–95, doi:10.1289/ehp.0901220, 2010.

Asmi, A., Wiedensohler, A., Laj, P., Fjaeraa, A.-M., Sellegri, K., Birmili, W., Weingartner, E., Baltensperger, U., Zdimal, V., Zikova, N., Putaud, J.-P., Marinoni, A., Tunved, P., Hansson, H.- C., Fiebig, M., Kivek¨as, N., Lihavainen, H., Asmi, E., Ulevicius, V., Aalto, P. P., Swietlicki, E., Kristensson, A., Mihalopoulos, N., Kalivitis, N., Kalapov, I., Kiss, G., de Leeuw, G., Henzing, B., Harrison, R. M., Beddows, D., O'Dowd, C., Jennings, S. G., Flentje, H., Weinhold, K., Meinhardt, F., Ries, L., and Kulmala, M.: Number size distributions and seasonality of submicron particles in Europe 2008–2009, Atmospheric Chemistry and Physics, 11, 5505–5538, 2011.

Backman, J., Rizzo, L.V., Hakala, J., Nieminen, T., Manninen, H.E., Morais, F., Aalto, P.P., Siivola, E., Carbone, E., Hillamo, R., Artaxo, P., Virkulla, A., Petäjä, T., Kulmala, M.: On the diurnal cycle of urban aerosols, black carbon and the occurrence of new particle formation events in springtime São Paulo, Brazil. Atmospheric Chemistry Physics 12, 11733-11751, 2012.

Barmpadimos, I., Keller, J., Oderbolz, D., Hueglin, C. and Prévôt, a. S. H.: One decade of parallel PM_{10} and $PM_{2.5}$ measurements in Europe: trends and variability, Atmospheric Chemistry and Physics Discussions, 12(1), 1–43, doi:10.5194/acpd-12-1-2012, 2012.

Belis, C.A., Karagulian, F., Larsen, B.R., Hopke, P.K.: Critical review and meta-analysis of ambient particulate matter source apportionment using receptor models in Europe, Atmos. Environ., 69, 94-108, 2013.

Bergametti, G., Gomes, L., Coudé-Gaussen, G., Rognon, P., Coustumer, M.N.L.: African dust observed over the Canaray Islands: Source regions identification and trasnport pattern for some summer situation, Journal of Geophysical Research, 94, 14855-14864, 1989.

Birch, M. E. and Cary, R. A.: Elemental carbon-based method for monitoring occupational exposures to particulate diesel exhaust, Aerosol Science and Technolody, 25, 221-241, 1996.

Birmili, W., Wiedensohler, A., Heintzenberg, J. and Lehmann, K.: Atmospheric particle number size distribution in central Europe: Statistical relations to air masses and meteorology, Journal of Geophysical Research D: Atmosphere, 106, 32005-32018, 2001.

Bond, T. C., Doherty, S. J., Fahey, D. W., Forster, P. M., Berntsen, T., DeAngelo, B. J., Flanner, M. G., Ghan, S., Kärcher, B., Koch, D., Kinne, S., Kondo, Y., Quinn, P. K., Sarofim, M. C., Schultz, M. G., Schulz, M., Venkataraman, C., Zhang, H., Zhang, S., Bellouin, N., Guttikunda, S. K., Hopke, P. K., Jacobson, M. Z., Kaiser, J. W., Klimont, Z., Lohmann, U., Schwarz, J. P., Shindell, D., Storelvmo, T., Warren, S. G., Zender, C. S.; Bounding the role of black carbon in the climate system: A scientific assessment, Journal of Geophysical Research, in press, doi: 10.1002/jgrd.50171, 2012.

Bougiatioti, A., Zarmpas, P., Koulouri, E., Antoniou, M., Theodosi, C., Kouvarakis, G., Saarikoski, S., Mäkelä, T., Hillamo, R. and Mihalopoulos, N.: Organic, elemental and water-soluble organic carbon in size segregated aerosols, in the marine boundary layer of the Eastern Mediterranean, Atmospheric Environment, 64, 251–262, doi:10.1016/j.atmosenv.2012.09.071, 2013.

Brook, R. D., Rajagopalan, S., Pope, C. A., Brook, J. R., Bhatnagar, A., Diez-Roux, A. V, Holguin, F., Hong, Y., Luepker, R. V, Mittleman, M. a, Peters, A., Siscovick, D., Smith, S. C., Whitsel, L. and Kaufman, J. D.: Particulate matter air pollution and cardiovascular disease: An update to the scientific statement from the American Heart Association., Circulation, 121(21), 2331–78, doi:10.1161/CIR.0b013e3181dbece1, 2010.

Bruno, J., Pon, J., Russi, D.: Report on Air Quality and Health: the cost of improvement of air quality (in Catalan). Generalitat de Catalunya, Departament de Medi Ambient i Habitatge, December, 2007.

Cappa, C. D., Onasch, T. B., Massoli, P., Worsnop, D. R., Bates, T. S., Cross, E. S., Davidovits, P., Hakala, J., Hayden, K. L., Jobson, B. T., Kolesar, K. R., Lack, D. a, Lerner, B. M., Li, S.-M., Mellon, D., Nuaaman, I., Olfert, J. S., Petäjä, T., Quinn, P. K., Song, C., Subramanian, R., Williams, E. J. and Zaveri, R. a: Radiative absorption enhancements due to the mixing state of atmospheric black carbon., Science (New York, N.Y.), 337(6098), 1078–81, doi:10.1126/science.1223447, 2012.

Casati, R., Scheer, V., Vogt, R. and Benter, T.: Measurement of nucleation and soot mode particle emission from a diesel passenger car in real world and laboratory in situ dilution, Atmospheric Environment, 41(10), 2125–2135, doi:10.1016/j.atmosenv.2006.10.078, 2007.

Castillo, S.: Impacto de las mases de aire africano sobre los niveles y composición del material particulado atmosférico en Canarias y el NE de la Península Ibérica, PhD Thesis, Universitat Politécnica de Catalunya (UPC), 2006.

Chan, C. K. and Yao, X.: Air pollution in mega cities in China, Atmospheric Environment, 42(1), 1–42, doi:10.1016/j.atmosenv.2007.09.003, 2008.

Chester, R., Nimmo, M. Keyse, S.; The influence of Saharan and Middle Eastern Desert-Derived dust on the Trace Metal Composition of Mediterranean Aerosols and Rainwater: an overview. In The Impact of Desert Dust across the Mediterranean, Vol. 11 (ed. S Guerzoni and R. Chester), 253-273, 2006.

Dall'Osto, M., Querol, X., Alastuey, A., O'Dowd, C., Harrison, R. M., Wenger, J. and Gómez-Moreno, F. J.: On the spatial distribution and evolution of ultrafine particles in Barcelona, Atmospheric Chemistry and Physics, 13(2), 741–759, doi:10.5194/acp-13-741-2013, 2013.

Dulac, F., Tanre, D., Bergametti, G., Buat-Menard, P., Desbois, M. And Sutton, D.: Assessment of the African airborne dust mass over the western Mediterranean Sea using Meteosat data, Journal of Geophysical Research, 101, 19, 515-531, 1992.

Durant, A. J., Bonadonna, C., Horwell, C. J.: Atmospheric and environmental impacts of volcanic particulates, Elements, 6, 235-240, 2010.

Eastern, R. C. and Peter, L. K.: Binary homogenous nucleation: temperature and relative humdity fluctuations, nonlinearity, and aspects of new particles production in the atmosphere, Journal of Applied Meteorology, 33, 775-784, 1994.

Escudero, M.: Wet and dry African dust episodes over eastern Spain, Journal of Geophysical Research, 110(D18), D18S08, doi:10.1029/2004JD004731, 2005.

Escudero, M., Querol, X., Pey, J., Alastuey, A., Pérez, N., Ferreira, F., Alonso, S., Rodríguez, S. and Cuevas, E.: A methodology for the quantification of the net African dust load in air quality monitoring networks, Atmospheric Environment, 41(26), 5516–5524, doi:10.1016/j.atmosenv.2007.04.047, 2007.

Fine, P. M. Cass, G. R., Simoneit, B. T.: Chemical characterization of fine particle emissions from the fireplace combustion of woods grown in the Southern United States. Environmental Science and Technology, 36, 1442-1451, 2002.

Fu, Q., Zhuang, G., Li, J., Huang, K., Wang, Q., Zhang, R., Fu, J., Lu, T., Chen, M., Wang, Q., Chen, Y., Xu, C. and Hou, B.: Source, long-range transport, and characteristics of a heavy dust pollution event in Shanghai, Journal of Geophysical Research, 115, D00K29, doi:10.1029/2009JD013208, 2010.

Giere, R. and Querol, X.: Solid Particulate Matter in the Atmosphere, Elements, 6(4), 215–222, doi:10.2113/gselements.6.4.215, 2010.

Gilbert, R. O., Statistical methods for environmental pollution monitoring. Van Nostrand Reinhold, New York, 1987.

Goldberg, E. D.: Black carbon in the environment: properties and distribution, John Wiley & Sons Inc., 1985.

Guenther, A., Geron, C., Pierce, T., Lamb, B., Harley, P. and Fall, R.: Natural emissions of non-methane volatile organic compounds , carbon monoxide , and oxides of nitrogen from North America, Atmospheric Environment, 2205-2230 , 34, 2000.

Hamed, A., Joutsensaari, J., Mikkonen, S., Sogacheva, L., Dal Maso, M., Kulmala, M., Cavalli, F., Fuzzi, S., Facchini, M. C., Decesari, S., Mircea, M., Lehtinen, K. E. J. and Laaksonen, A.: Nucleation and growth of new particles in Po valley, Italy, Atmospheric Chemistry and Physics, 7, 355-376. 2007.

Harris, J. S. and Maricq, M. M.: Signature size distributions for diesel and gasoline engine exhaust particulate matter, Journal of Aerosol Science, 32, 749-764, 2001.

Harrison, R. M. and Pio, C. a.: Size-differentiated composition of inorganic atmospheric aerosols of both marine and polluted continental origin, Atmospheric Environment (1967), 17(9), 1733–1738, doi:10.1016/0004-6981(83)90180-4, 1983.

Harrison, R. M. and Kito, A. M. N.: Field comparison of filter pack and denuder sampling methods for reactive gaseous and particulate pollutants, Atmospheric Environment, 24, 2633-2640, 1990.

Hidy, G. M.: Atmospheric sulfur and nitrogen oxides: Eastern North American source-receptor relationships. Academic Press, San Diego, pp. 447, 1994.

Hoek, G., Boogaard, H., Knol, A., De Hartog, J., Slottje, P., Ayres, J. G., Borm, P., Brunekreef, B., Donaldson, K., Forastiere, F., Holgate, S., Kreyling, W. G., Nemery, B., Pekkanen, J., Stone, V., Wichmann, H.-E. and Van der Sluijs, J.: Concentration response functions for ultrafine particles and all-cause mortality and hospital admissions: results of a European expert panel elicitation., Environmental science & technology, 44(1), 476–82, doi:10.1021/es9021393, 2010.

IPCC. Climate Change 2007: The Physical Science Basis. Contribution of Working Group I to the fourth Assessment Report of the IPCC (ISBN 978 0521 88009-1 Hardback; 9780521 070596-7 Paperback, 2007.

IUPAC 1995. International Union of Pure and Applied Chemistry. Nomenclature In Evaluation Of Analytical Methods Including Detection And Qualification Capabilities. Pure & Appl. Chem., Vol. 67, No. 10, Pp. 1699-1723, 1995.

Jiménez, P., Lelieveld, J. and Baldasano, J. M.: Multiscale modeling of air pollutants dynamics in the northwestern Mediterranean basin during a typical summertime episode, Journal of Geophysical Research, 111(D18), D18306, doi:10.1029/2005JD006516, 2006.

Jimenez, J. L., Canagaratna, M. R., Donahue, N. M., Prevot, a S. H., Zhang, Q., Kroll, J. H., DeCarlo, P. F., Allan, J. D., Coe, H., Ng, N. L., Aiken, a C., Docherty, K. S., Ulbrich, I. M., Grieshop, a P., Robinson, a L., Duplissy, J., Smith, J. D., Wilson, K. R., Lanz, V. a, Hueglin, C., Sun, Y. L., Tian, J., Laaksonen, a, Raatikainen, T., Rautiainen, J., Vaattovaara, P., Ehn, M., Kulmala, M., Tomlinson, J. M., Collins, D. R., Cubison, M. J., Dunlea, E. J., Huffman, J. a, Onasch, T. B., Alfarra, M. R., Williams, P. I., Bower, K., Kondo, Y., Schneider, J., Drewnick, F., Borrmann, S., Weimer, S., Demerjian, K., Salcedo, D., Cottrell, L., Griffin, R., Takami, a, Miyoshi, T., Hatakeyama, S., Shimono, a, Sun, J. Y., Zhang, Y. M., Dzepina, K., Kimmel, J. R., Sueper, D., Jayne, J. T., Herndon, S. C., Trimborn, a M., Williams, L. R., Wood, E. C., Middlebrook, a M., Kolb, C. E., Baltensperger, U. and Worsnop, D. R.: Evolution of organic aerosols in the atmosphere., Science (New York, N.Y.), 326(5959), 1525–9, doi:10.1126/science.1180353, 2009.

Jorba, O. and Baldasano, J. M.: Modelling the dynamics of air pollutants over the Iberian Peninsula under typical meteorological situations, , 6(07), 425–436, doi:10.1016/S1474-8177(07)06048-2, 2007.

Junge, C. E.: Air Chemistry and Radioactivity, Academic Press, 1963.

Kerminen, V.-M. and Worsnop, D. R.: Direct observations of atmospheric aerosol nucleation., Science (New York, N.Y.), 339(6122), 943–6, doi:10.1126/science.1227385, 2013.

Knibbs, L. D., Cole-Hunter, T. and Morawska, L.: A review of commuter exposure to ultrafine particles and its health effects, Atmospheric Environment, 45(16), 2611–2622, doi:10.1016/j.atmosenv.2011.02.065, 2011.

Knol, A. B., De Hartog, J. J., Boogaard, H., Slottje, P., Van der Sluijs, J. P., Lebret, E., Cassee, F. R., Wardekker, J. A., Ayres, J. G., Borm, P. J., Brunekreef, B., Donaldson, K., Forastiere, F., Holgate, S. T., Kreyling, W. G., Nemery, B., Pekkanen, J., Stone, V., Wichmann, H.-E. and Hoek, G.: Expert elicitation on ultrafine particles: likelihood of health effects and causal pathways., Particle and fibre toxicology, 6, 19, doi:10.1186/1743-8977-6-19, 2009.

Kulmala, M., Toivonen, A., Mäkelä, J. M. and Laaksonen, A.: Analysis of the growth of nucleation mode particles observed in Boreal forest, Tellus, 50B, 449-462, 1998.

Kulmala, M., Dal Maso, M., Mäkelä, J. M., Pirjola, L., Väkevä, M., Aalto, P., Miikkulainen, P., Hámeri, K., O´Dowd, C. D.: On the formation, growth and composition of nucleation mode particles, Tellus 53B, 479-490, 2001.

Kulmala, M. and Kerminen, V.-M.: On the formation and growth of atmospheric nanoparticles, Atmospheric Research, 90(2-4), 132–150, doi:10.1016/j.atmosres.2008.01.005, 2008.

Kulmala, M., Kontkanen, J., Junninen, H., Lehtipalo, K., Manninen, H. E., Nieminen, T., Petäjä, T., Sipilä, M., Schobesberger, S., Rantala, P., Franchin, A., Jokinen, T., Järvinen, E., Äijälä, M., Kangasluoma, J., Hakala, J., Aalto, P. P., Paasonen, P., Mikkilä, J., Vanhanen, J., Aalto, J., Hakola, H., Makkonen, U., Ruuskanen, T., Mauldin, R. L., Duplissy, J., Vehkamäki, H., Bäck, J., Kortelainen, A., Riipinen, I., Kurtén, T., Johnston, M. V, Smith, J. N., Ehn, M., Mentel, T. F., Lehtinen, K. E. J., Laaksonen, A., Kerminen, V.-M. and Worsnop, D. R.: Direct observations of atmospheric aerosol nucleation., Science (New York, N.Y.), 339(6122), 943–6, doi:10.1126/science.1227385, 2013.

Kumar, P., Robins, A., Vardoulakis, S. and Britter, R.: A review of the characteristics of nanoparticles in the urban atmosphere and the prospects for developing regulatory controls, Atmospheric Environment, 44(39), 5035–5052, doi:10.1016/j.atmosenv.2010.08.016, 2010.

Larssen, S., Sluyter, R. and Helmis, C.: Criteria for EUROAIRNET, the EEA air quality monitoring and information network. http://reports.eea.eu.int/TEC12/en. 1999.

Lenschow, P., Abraham, H. J., Kutzner, K., Lutz, M., Preuß, J. D., Reichenbächer, W.: Some ideas about the sources of PM_{10}, Atmospheric Environment, 42, 18, 4126-1437, 2001.

Lingard, J. J. N., Agus, E. L., Young, D. T., Andrews, G. E. and Tomlin, A. S.: Observations of urban airborne particle number concentrations during rush-hour conditions: analysis of the number based size distributions and modal parameters., Journal of environmental monitoring: JEM, 8(12), 1203–18, doi:10.1039/b611479b, 2006.

Llusia, J., Peñuelas, J., Seco, R. and Filella, I.: Seasonal changes in the daily emission rates of terpenes by Quercus ilex and the atmospheric concentrations of terpenes in the natural park of Montseny, NE Spain, Journal of Atmospheric Chemistry, 69(3), 215–230, doi:10.1007/s10874-012-9238-1, 2012.

Lopez-Bustins, J.-A., Martin-Vide, J. and Sanchez-Lorenzo, A.: Iberia winter rainfall trends based upon changes in teleconnection and circulation patterns, Global and Planetary Change, 63(2-3), 171–176, doi:10.1016/j.gloplacha.2007.09.002, 2008.

Lucas, D. D., Prinn, R. G.: Parametric sensitivity and uncertainty analysis of dimethylsulfide oxidation in the clear-sky remote marine boundary layer, Atmospheric Chemistry and Physics 5 (6), 1505–1525, doi:10.5194/acp-5-1505-2005, 2005.

Luterbacher, J., Liniger, M.A., Menzel, A., Estrella, N., Della-Marta, P.M., Pfister, C., Rutishauser, T., Xoplaki, E.: Exceptional European warmth of autumn 2006 and winter 2007: Historical context, the underlying dynamics and its phonological impacts, Geophysical Research Letters, 34, L12704, 2007.

Mamane, Y. and Mehler, M.: On the nature of nitrate particles in a coastal urban area, Atmospheric Environment, 21, 9, 1989-1994, 1987.

Mészáros, E.: Fundamentals of Atmospheric Aerosol Chemistry, Akadémiai Kiado, 1999.

Mildford, J. B. and Davidson, C. I.: The sizes of particulate sulphate and nitrate in the Atmosphere: A review., Journal of Air Pollution Control Association, 37, 2, 125-134, 1987.

Millán, M., Salvador, R., Mantilla, E. and Kallos, G.: Photo-oxidant dynamics in the Mediterranean basin in summer: results from European research projects, Journal of Geophysical Research, 102, 8811-8823, 1997.

Millán, M., Mantilla, E., Salvador, R., Carratalá, R., Sanz, M. J., Alonso, L., Gangoiti, G. and Navazo, M.: Ozone cycles in the Western Mediterranean Basin: Interpretation of monitoring data in complex coastal terrain, Journal of Applied Meteorology, 39, 487-508, 2000.

Minguillón, M. C., Perron, N., Querol, X., Szidat, S., Fahrni, S. M., Alastuey, a., Jimenez, J. L., Mohr, C., Ortega, a. M., Day, D. a., Lanz, V. a., Wacker, L., Reche, C., Cusack, M., Amato, F., Kiss, G., Hoffer, a., Decesari, S., Moretti, F., Hillamo, R., Teinilä, K., Seco, R., Peñuelas, J., Metzger, a., Schallhart, S., Müller, M., Hansel, a., Burkhart, J. F., Baltensperger, U. and Prévôt, a. S. H.: Fossil versus contemporary sources of fine elemental and organic carbonaceous particulate matter during the DAURE campaign in Northeast Spain, Atmospheric Chemistry and Physics, 11(23), 12067–12084, doi:10.5194/acp-11-12067-2011, 2011.

Molinaroli, E., Gerzoni, S. and Giacarlo, R.: Contribution of Saharan Dust to the Central Mediterranean Basin. In Processes Controlling the Composition of the Clastic Sediments, Vol. 284, Johnson N.J and Basu A. (Eds.), 303-312- Geological Society of Americ Special Paper, 1993.

Morawska, L., Bofinger, N. D., Kocis, L. and Nwankwoala, A.: Submicrometer and Supermicrometer Particles from Diesel Vehicle Emissions, Environmental Science & Technology, 32(14), 2033–2042, doi:10.1021/es970826+, 1998.

Morawska, L., Thomas, S., Gilbert, D., Greenaway, C. and Rijnders, E.: A study of the horizontal and vertical profile of submicrometer particles in relation to a busy road, Atmospheric Environment, 33(8), 1261–1274, doi:10.1016/S1352-2310(98)00266-0, 1999.

Morawska, L., Ristovski, Z., Jayaratne, E. R., Keogh, D. U. and Ling, X.: Ambient nano and ultrafine particles from motor vehicle emissions: Characteristics, ambient processing and implications on human exposure, Atmospheric Environment, 42(35), 8113–8138, doi:10.1016/j.atmosenv.2008.07.050, 2008.

Müller, T., Henzing, J. S., De Leeuw, G., Wiedensohler, a., Alastuey, a., Angelov, H., Bizjak, M., Collaud Coen, M., Engström, J. E., Gruening, C., Hillamo, R., Hoffer, a., Imre, K., Ivanow, P., Jennings, G., Sun, J. Y., Kalivitis, N., Karlsson, H., Komppula, M., Laj, P., Li, S.-M., Lunder, C., Marinoni, a., Martins dos Santos, S., Moerman, M., Nowak, a., Ogren, J. a., Petzold, a., Pichon, J. M., Rodriquez, S., Sharma, S., Sheridan, P. J., Teinilä, K., Tuch, T., Viana, M., Virkkula, a., Weingartner, E., Wilhelm, R. and Wang, Y. Q.: Characterization and intercomparison of aerosol absorption photometers: result of two intercomparison workshops, Atmospheric Measurement Techniques, 4(2), 245–268, doi:10.5194/amt-4-245-2011, 2011.

Murphy, D. M., Solomon, S., Portmann, R. W., Rosenlof, K. H., Forster, P. M. and Wong, T.: An observationally based energy balance for the Earth since 1950, Journal of Geophysical Research, 114(D17), D17107, doi:10.1029/2009JD012105, 2009.

Norris, G., Vedantham, R., Wade, K., Brown, S., Prouty, J., Foley, C.: EPA Positive Matrix Factorisation (PMF) 3.0 Fundamentals & User Guide, U.S. Environmental Protection Agency, 2008.

Oberdörster, G, Sharp, Z., Atudorei, V., Elder, A., Gelein, R., Kreyling, W., Cox, C.: Translocation of inhaled ultrafine particles to the brain, Inhalation Toxicology, 16, 437-445, 2004.

Oberdörster, G., Oberdörster, E. and Oberdörster, J.: Nanotoxicology: An Emerging Discipline Evolving from Studies of Ultrafine Particles, Environmental Health Perspectives, 113(7), 823–839, doi:10.1289/ehp.7339, 2005.

Ostro, B., Feng, W.-Y., Broadwin, R., Green, S. and Lipsett, M.: The Effects of Components of Fine Particulate Air Pollution on Mortality in California: Results from CALFINE, Environmental Health Perspectives, 115(1), 13–19, doi:10.1289/ehp.9281, 2006.

Ovrevik, J. and Schwarze, P. E.: Chemical composition and not only total surface area is important for the effects of ultrafine particles., Mutation research, 594(1-2), 201–2; author reply 199–200, doi:10.1016/j.mrfmmm.2005.10.002, 2006.

Patter, P. And Tapper, U.: Positive matrix factorisation: A non-negative factor model with optimal utilization of error estimates of data values, Environmetrics, 5, 111-126, 1994.

Paatero, P.: Least squares formulation of robust non-negative factor analysis, Chemometrics and Intelligent Laboratory Systems, 37, 23-35, 1997.

Pacyna, J. M.: Toxic metals in the atmosphere, Nriagu J. O. and Davidson C. I. (Eds.), Wiley, New York, 33-52, 1986.

Pandolfi, M., Cusack, M., Alastuey, A. and Querol, X.: Variability of aerosol optical properties in the Western Mediterranean Basin, Atmospheric Chemistry and Physics, 11(15), 8189–8203, doi:10.5194/acp-11-8189-2011, 2011.

Pandolfi, M., Amato, F., Reche, C., Alastuey, A., Otjes, R. P., Blom, M. J. and Querol, X.: Summer ammonia measurements in a densely populated Mediterranean city, Atmospheric Chemistry and Physics, 12(16), 7557–7575, doi:10.5194/acp-12-7557-2012, 2012.

Pérez, C., Sicard, M., Jorba, O., Comerón, A. and Baldasano, J. M.: Summertime re-circulations of air pollutants over the north-eastern Iberian coast observed from systematic EARLINET lidar measurements in Barcelona, Atmospheric Environment, 38(24), 3983–4000, doi:10.1016/j.atmosenv.2004.04.010, 2004.

Pérez, L., Tobías, A., Querol, X., Pey, J., Alastuey, A., Díaz, J. and Sunyer, J.: Saharan dust, particulate matter and cause-specific mortality: a case-crossover study in Barcelona (Spain)., Environment international, 48, 150–5, doi:10.1016/j.envint.2012.07.001, 2012.

Pérez, N., Pey, J., Querol, X., Alastuey, A., López, J. M. and Viana, M.: Partitioning of major and trace components in PM10–PM2.5–PM1 at an urban site in Southern Europe, Atmospheric Environment, 42(8), 1677–1691, doi:10.1016/j.atmosenv.2007.11.034, 2008.

Pérez, N.: Variability of atmospheric aersosols at urban, regional and continental backgrounds in the Western Mediterranean Basin, PhD Thesis, Universitat Autònoma de Catalunya (UAB), 2010.

Pey, J.: Caracterización físico-química de los aerosoles atmosféricos en el Mediterráneo Occidental, PhD Thesis, Universitat Politécnica de Catalunya (UPC), 2007.

Pey, J., Rodríguez, S., Querol, X., Alastuey, A., Moreno, T., Putaud, J. P. and Van Dingenen, R.: Variations of urban aerosols in the western Mediterranean, Atmospheric Environment, 42(40), 9052–9062, doi:10.1016/j.atmosenv.2008.09.049, 2008.

Pey, J., Pérez, N., Castillo, S., Viana, M., Moreno, T., Pandolfi, M., López-Sebastián, J. M., Alastuey, A. and Querol, X.: Geochemistry of regional background aerosols in the Western Mediterranean, Atmospheric Research, 94(3), 422–435, doi:10.1016/j.atmosres.2009.07.001, 2009a.

Pey, J., Querol, X., Alastuey, A., Rodríguez, S., Putaud, J. P. and Van Dingenen, R.: Source apportionment of urban fine and ultra-fine particle number concentration in a Western Mediterranean city, Atmospheric Environment, 43(29), 4407–4415, doi:10.1016/j.atmosenv.2009.05.024, 2009b.

Pey, J., Pérez, N., Querol, X., Alastuey, A., Cusack, M. and Reche, C.: Intense winter atmospheric pollution episodes affecting the Western Mediterranean., The Science of the total environment, 408(8), 1951–9, doi:10.1016/j.scitotenv.2010.01.052, 2010.

Pirjola, L., Kulmala, M., Wilck, M., Bischoff, A., Stratmann, F., Otto, E.: Formation of sulphuric acid aerosols and cloud condensation nuclei: an expression for significant nucleation and model comparison, Journal of Aerosol Science, 30(8), 1079–1094, 1999.

Pöschl, U.: Atmospheric aerosols: composition, transformation, climate and health effects., Angewandte Chemie International Edition, 44(46), 7520–40, doi:10.1002/anie.200501122, 2005.

Prospero, J. M.: Environmental characterization of global sources of atmospheric soil dust identified with the NIMBUS 7 Total Ozone Mapping Spectrometer (TOMS) absorbing aerosol product, Reviews of Geophysics, 40(1), 1002, doi:10.1029/2000RG000095, 2002.

Pruppacher, P. S. and Klett, J. D.: Microphysics of clouds and precipitation, Kluwer Academic, Dordrecht, The Netherlands, 1997.

Putaud, J.-P., Raes, F., Van Dingenen, R., Brüggemann, E., Facchini, M.-C., Decesari, S., Fuzzi, S., Gehrig, R., Hüglin, C., Laj, P., Lorbeer, G., Maenhaut, W., Mihalopoulos, N., Müller, K., Querol, X., Rodriguez, S., Schneider, J., Spindler, G., Brink, H. Ten, Tørseth, K. and Wiedensohler, A.: A European aerosol phenomenology—2: chemical characteristics of particulate matter at kerbside, urban, rural and background sites in Europe, Atmospheric Environment, 38(16), 2579–2595, doi:10.1016/j.atmosenv.2004.01.041, 2004.

Putaud, J.-P., Van Dingenen, R., Alastuey, a., Bauer, H., Birmili, W., Cyrys, J., Flentje, H., Fuzzi, S., Gehrig, R., Hansson, H. C., Harrison, R. M., Herrmann, H., Hitzenberger, R., Hüglin, C., Jones, a. M., Kasper-Giebl, a., Kiss, G., Kousa, a., Kuhlbusch, T. a. J., Löschau, G., Maenhaut, W., Molnar, a., Moreno, T., Pekkanen, J., Perrino, C., Pitz, M., Puxbaum, H., Querol, X., Rodriguez, S., Salma, I., Schwarz, J., Smolik, J., Schneider, J., Spindler, G., Ten Brink, H., Tursic, J., Viana, M., Wiedensohler, a. and Raes, F.: A European aerosol phenomenology – 3: Physical and chemical characteristics of particulate matter from 60 rural, urban, and kerbside sites across Europe, Atmospheric Environment, 44(10), 1308–1320, doi:10.1016/j.atmosenv.2009.12.011, 2010.

Querol, X., Alastuey, A. S., Puicercus, J. A., Mantilla, Ruiz, C.R., Lopez-soler, A. and Plana-, F, Juan, R.: Seasonal evolution of suspended particles around a large coal-fired power station: chemical characterization, Atmospheric Environment, 32(4), 719-731, 1998a.

Querol, X., Alastuey, A. S., Puicercus, J. A., Mantilla, E., Miro, J. V, Lopez-soler, A. and Plana-, F.: Seasonal evolution of suspended particles around a large coal-fired power station: particulate levels and sources, Atmospheric Environment, 32(11), 1963-1978, 1998b.

Querol, X., Alastuey, A., Rodriguez, S., Plana, F., Mantilla, E. and Ruiz, C. R.: Monitoring of PM10 and PM2.5 around primary particulate anthropogenic emission sources, Atmospheric Environment, 35(5), 845–858, doi:10.1016/S1352-2310(00)00387-3, 2001.

Querol, X., Alastuey, A., Rosa, J. D. La, Sánchez-de-la-Campa, A., Plana, F. and Ruiz, C. R.: Source apportionment analysis of atmospheric particulates in an industrialised urban site in southwestern Spain, Atmospheric Environment, 36(19), 3113–3125, doi:10.1016/S1352-2310(02)00257-1, 2002.

Querol, X., Alastuey, A., Viana, M. M., Rodríguez, S., Artiñano, B., Salvador, P., García do Santos, S., Fernandez Patier, R., Ruiz, C. R., De La Rosa, J., Sanchez de la Campa, A., Menéndez, M. and Gil, J. I.: Speciation and origin of PM10 and PM2.5 in Spain, Journal of Aerosol Science, 35, 1151-1172, 2004a.

Querol, X., Alastuey, A., Ruiz, C. R., Artiñano, B., Hansson, H. C., Harrison, R. M., Buringh, E., Ten Brink, H. M., Lutz, M., Bruckmann, P., Straehl, P. and Schneider, J.: Speciation and origin of PM10 and PM2.5 in selected European cities, Atmospheric Environment, 38(38), 6547–6555, doi:10.1016/j.atmosenv.2004.08.037, 2004b.

Querol, X., Alastuey, A, Rodríguez, S., Viana, M. M., Artíñano, B., Salvador, P., Mantilla, E., García do Santos, S., Fernandez Patier, R., De La Rosa, J., Sanchez de la Campa, A., Menéndez, M. and Gil, J. I.: Levels of particulate matter in rural, urban and industrial sites in Spain., Science of the total environment, 334-335(2004), 359–76, doi:10.1016/j.scitotenv.2004.04.036, 2004c.

Querol, X., Viana, M., Alastuey, A., Amato, F., Moreno, T., Castillo, S., Pey, J., De la Rosa, J., Sánchez de la Campa, A., Artíñano, B., Salvador, P., García Dos Santos, S., Fernández-Patier, R., Moreno-Grau, S., Negral, L., Minguillón, M. C., Monfort, E., Gil, J. I., Inza, a., Ortega, L. a., Santamaría, J. M. and Zabalza, J.: Source origin of trace elements in PM from regional background, urban and industrial sites of Spain, Atmospheric Environment, 41(34), 7219–7231, doi:10.1016/j.atmosenv.2007.05.022, 2007.

Querol, X., Alastuey, A., Pey, J., Cusack, M., Pérez, N., Mihalopoulos, N., Theodosi, C., Gerasopoulos, E., Kubilay, N. and Koçak, M.: Variability in regional background aerosols within the Mediterranean, Atmospheric Chemistry and Physics Discussions, 9(2), 10153–10192, doi:10.5194/acpd-9-10153-2009, 2009.

Raes, F., Liao, H., Chen, W.-T. and Seinfeld, J. H.: Atmospheric chemistry-climate feedbacks, Journal of Geophysical Research, 115(D12), D12121, doi:10.1029/2009JD013300, 2010.

Rebetz, M., Dupont, O., Giroud, M.: An analysis of the July heatwave extent in Europe compared to the record year of 2003, Theoretical and Applied Climatology, 95, 1-7, 2009.

Reche, C., Viana, M., Pandolfi, M., Alastuey, A., Moreno, T., Amato, F., Ripoll, A. and Querol, X.: Urban NH3 levels and sources in a Mediterranean environment, Atmospheric Environment, 57, 153–164, doi:10.1016/j.atmosenv.2012.04.021, 2012.

Robinson, A. L., Donahue, N. M., Shrivastava, M. K., Weitkamp, E. A, Sage, A. M., Grieshop, A. P., Lane, T. E., Pierce, J. R. and Pandis, S. N.: Rethinking organic aerosols: semivolatile emissions and photochemical aging., Science (New York, N.Y.), 315(5816), 1259–62, doi:10.1126/science.1133061, 2007.

Rodríguez, S., Querol, X., Alastuey, A., Kallos, G., Kakaliagou, O.: Saharan dust contributions to PM_{10} and TSP levels in Southern and Eastern Spain, Atmospheric Environment, 35, 2433-2447, 2001.

Rodríguez, S., Querol, X., Alastuey, A. and Plana, S.: Sources and processes affecting levels and composition of atmospheric aerosol in the western Mediterranean, Journal of Geophysical Research, 107(D24), 4777, doi:10.1029/2001JD001488, 2002.

Rodríguez, S., Querol, X., Alastuey, A., Viana, M.-M. and Mantilla, E.: Events affecting levels and seasonal evolution of airborne particulate matter concentrations in the Western Mediterranean., Environmental science & technology, 37(2), 216–22 [online] Available from: http://www.ncbi.nlm.nih.gov/pubmed/12564890, 2003.

Rodríguez, S., Van Dingenen, R., Putaud, J.-P., Martins-Dos Santos, S. and Roselli, D.: Nucleation and growth of new particles in the rural atmosphere of Northern Italy—relationship to air quality monitoring, Atmospheric Environment, 39(36), 6734–6746, doi:10.1016/j.atmosenv.2005.07.036, 2005.

Rose, D., Wehner, B., Ketzel, M., Engler, C. and Voigtl, J.: Atmospheric number size distributions of soot particles and estimation of emission factors, Atmospheric Chemistry and Physics, (6), 1021–1031, 2006.

Rückerl, R., Schneider, A., Breitner, S., Cyrys, J., and Peters, A.: Health effects of particulate air pollution: A review of epidemiological evidence, Inhalation Toxicology, 23, 555-592, doi: 10.3109/08958378.2011.593587, 2011.

Salmi, T., Määttä, A., Anttila, P., Ruoho-Airola, T., Amnell, T.: Detecting trends of annual values of atmospheric pollutants by the Mann-Kendall test and Sen´s slope estimates-the Excel template application MAKESENS. In publications on Air Quality No. 31 (ed. Finnish Meteorological Institute); 2002. p.35. Finnish Meteorological Institute.

Samet, J. M., Rappold, A., Graff, D., Cascio, W. E., Berntsen, J. H., Huang, Y.-C. T., Herbst, M., Bassett, M., Montilla, T., Hazucha, M. J., Bromberg, P. a and Devlin, R. B.: Concentrated ambient ultrafine particle exposure induces cardiac changes in young healthy volunteers., American journal of respiratory and critical care medicine, 179(11), 1034–42, doi:10.1164/rccm.200807-1043OC, 2009.

Sandradewi, J., Prevot, A. S. H., Szidat, S., Perron, N., Alfarra, M. R., Lanz, V.A., Weingartner, E., Baltensperger, U.: Using aerosol light absorption measurements for the quantitative determination of wood burning and traffic emission contributions to particulate matter, Environmental Science & Technology, 42, 3316-3323, 2008.

Schauer, J. J., Lough, G. C., Shafer, M. M., Christensen, W. F., Arndt, M. F., DeMinter, J. T. and Park J. S.: Characterization of metals emitted from motor vehicles, Health Effects Institute, Research report No. 133, 2006.

Seco, R., Peñuelas, J., Filella, I., Llusià, J., Molowny-Horas, R., Schallhart, S., Metzger, a., Müller, M. and Hansel, A.: Contrasting winter and summer VOC mixing ratios at a forest site in the Western Mediterranean Basin: the effect of local biogenic emissions, Atmospheric Chemistry and Physics, 11(24), 13161–13179, doi:10.5194/acp-11-13161-2011, 2011.

Seinfeld, J.H. & Pandis, S.N.; Atmospheric Chemistry and Physics: From air pollution to climate change. John Wiley and Sons, Inc., 1998.

Shindell, D., Kuylenstierna, J. C. I., Vignati, E., Van Dingenen, R., Amann, M., Klimont, Z., Anenberg, S. C., Muller, N., Janssens-Maenhout, G., Raes, F., Schwartz, J., Faluvegi, G., Pozzoli, L., Kupiainen, K., Höglund-Isaksson, L., Emberson, L., Streets, D., Ramanathan, V., Hicks, K., Oanh, N. T. K., Milly, G., Williams, M., Demkine, V. and Fowler, D.: Simultaneously mitigating near-term climate change and improving human health and food security., Science (New York, N.Y.), 335(6065), 183–9, doi:10.1126/science.1210026, 2012.

Sicard, M., Pérez, C., Rocadenbosch, F., Baldasano, J. M. and García-Vizcaino, D.: Mixed-Layer Depth Determination in the Barcelona Coastal Area From Regular Lidar Measurements: Methods, Results and Limitations, Boundary-Layer Meteorology, 119(1), 135–157, doi:10.1007/s10546-005-9005-9, 2005.

Simpson, D., Winiwarter, W., Börjesson, G., Cinderby, S., Ferreiro, A., Guenther, A., Hewitt, C. N., Janson, R., Khalil, M. A. K., Owen, S., Pierce, T. E., Puxbaum, H., Shearer, M., Skiba, U., Steinbrecher, R., Tarrasón, L., Öquist, M. G.: Inventorying emissions from nature in Europe, Journal of Geophysical Research, 104 (D7), 8113–8152, doi:10.1029/98JD02747, 1999.

Sorribas, M., de la Morena, B.A., Wehner, B., Lòpez, J.F., Prats, N., Mogo, S., Wiedensohler, A., and Cachorro, V.E.: On the sub-micron aerosol size distribution in a coastal - rural site at El Arenosillo Station (SW - Spain). Atmospheric Chemistry and Physics, 11, 11185-11206, 2011.

Soukup, J. M. and Becker, S.: Human alveolar macrophage responses to air pollution particulates are associated with insoluble components of coarse material, including particulate endotoxin., Toxicology and applied pharmacology, 171(1), 20–6, doi:10.1006/taap.2000.9096, 2001.

Spangl, W. and Nagl, C.: Jahresbericht der Luftgutemessungen in Osterrreich 2009, Umweltbundesamt, ViennaREP-0261, 2010.

Spindler, G., Brüggemann, E., Gnauk, T., Grüner, A., Müller, K., Herrmann, H.: A four-year size-segregated characterisation of particles PM_{10}, $PM_{2.5}$ and PM_1 depending on air mass origin at Melpitz, Atmos. Environ., 44, 164-173, 2010.

Szidat, S., Prevot, A. S. H., Sandradewi, J., Alfarra, M. R., Synal, H. –A., Wacker, L., Baltensperger, U.: Dominant impact of residential word burning on particulate matter in Alpine valleys during winter, Geophysical Research Letters, 34, L05820, 2007.

Thompson, M. and Howarth, R. J.: Duplicate analysis in geochemical practice. Part I. Theoretical approach and estimation of analyticla reproducibility, Analyst, 101, 690-698, 1976.

Thurston, G. D. and Spengler, J. D.: A quantative assessment of source contributions to inhalable particulate matter pollution in metropolitan Boston, Atmospheric Environment, 19, 1, 9-25, 1985.

Toll, I. and Baldasano, J. M.: Modeling of photochemical air pollution in the Barcelona area with highly disaggregated anthropogenic and biogenic emissions, Atmospheric Environment, 34(19), 3069–3084, doi:10.1016/S1352-2310(99)00498-7, 2000.

Turpin, B. J. and Lim, H. J.: Species Contributions to $PM_{2.5}$ Mass Concentrations: Revisiting Common Assumptions for Estimating Organic Mass, Aerosol Science and Technology, 35, 602-610, 2001.

Van Dingenen, R., Raes, F., Putaud, J.-P., Baltensperger, U., Charron, A., Facchini, M.-C., Decesari, S., Fuzzi, S., Gehrig, R., Hansson, H.-C., Harrison, R. M., Hüglin, C., Jones, A. M., Laj, P., Lorbeer, G., Maenhaut, W., Palmgren, F., Querol, X., Rodriguez, S., Schneider, J., Brink, H. Ten, Tunved, P., Tørseth, K., Wehner, B., Weingartner, E., Wiedensohler, A. and Wåhlin, P.: A European aerosol phenomenology—1: physical characteristics of particulate matter at kerbside, urban, rural and background sites in Europe, Atmospheric Environment, 38(16), 2561–2577, doi:10.1016/j.atmosenv.2004.01.040, 2004.

Venzac, H., Sellegri, K., Villani, P., Picard, D., and Laj, P.: Seasonal variation of aerosol size distributions in the free troposphere and residual layer at the puy de Dôme station, France, Atmospheric Chemistry Physics, 9, 1465–1478, 2009.

Viana, M., Querol, X., Alastuey, A., Cuevas, E. and Rodrírguez, S.: Influence of African dust on the levels of atmospheric particulates in the Canary Islands air quality network, Atmospheric Environment, 36(2002), 5861–5875, 2002.

Viana, M., PhD Thesis: Niveles, Composición y Origen del Material Particulado Atmosférico en los sectores Norte y Este de la Péninsula Ibérica y Canarias. Universtitat de Barcelona, 2003.

Viana, M., Pérez, C., Querol, X., Alastuey, A., Nickovic, S. and Baldasano, J. M.: Spatial and temporal variability of PM levels and composition in a complex summer atmospheric scenario in Barcelona (NE Spain), Atmospheric Environment, 39(29), 5343–5361, doi:10.1016/j.atmosenv.2005.05.039, 2005.

Viana, M., Querol, X., Alastuey, A., Gil, J.I., Menéndez, M.: Identifiaction of PM sources by principal component analysis (PCA) coupled with wind direction data, Chemosphere, 65, 2411-2418, 2006.

Vicente-Serrano, M. S., Trigo, M. R., López-Moreno, J. I., Liberato, M. L. R., Lorenzo-Lacruz, J., Beguería, S., Morán-Tejeda, E., El Kenawy., A.: Extreme winter precipitation in the Iberian Peninsula 2010: anomalies, driving mechanisms and future projections. Clim. Res., 46, 51-65, 2011.

Visbeck, M.H., Hurrell, J.W., Polvani, L., Cullen, H.M.: The North Atlantic Oscillation: past, present and future. PNAS 98, 12876-12877.

Volkamer, R., Jimenez, J. L., San Martini, F., Dzepina, K., Zhang, Q., Salcedo, D., Molina, L. T., Worsnop, D. R. and Molina, M. J.: Secondary organic aerosol formation from anthropogenic air pollution: Rapid and higher than expected, Geophysical Research Letters, 33(17), L17811, doi:10.1029/2006GL026899, 2006.

Wakamatsu, S., Utsunomiya, A., Mori, A., Uno, I. and Uehara, K.: Seasonal variation in atmospheric aerosols concentration covering northern Kyushu, Japan and Seoul, Korea, Atmospheric Environment, 30(13), 2343–2354, doi:10.1016/1352-2310(95)00421-1, 1996.

Wall, S. M., John, W. and Ondo, J. L.: Measurement of aerosol size distribution for nitrate and major ion species, Atmospheric Environment, 22, 8, 1649-1656, 1988.

Wang, K.-Y.: Long-range transport of the April 2001 dust clouds over the subtropical East Asia and the North Pacific and its impacts on ground-level air pollution: A Lagrangian simulation, Journal of Geophysical Research, 112(D9), D09203, doi:10.1029/2006JD007789, 2007.

Warneck, P.; Chemistry of the natural atmosphere, International Geophysics Series, Wiley & Sons, Vol. 41. Academy Press, pp. 757, 1988.

WHO. Health aspects of air pollution with particulate matter, ozone and nitrogen dioxide. World Health Organization, 2003.

WHO. Global Health Risks: Mortality and burden of disease attributable to selected major risks, World Health Organization, 2009.

WHO. Health effects of Black Carbon, Regional Office for Europe, World Health Organization, 2012.

WHO. Review on Evidence of Health Aspects of Air Pollution (REVIHAAP), Regional Office for Europe, World Health Organization, 2013.

Wiedensohler, A., Covert, D. S., Swietlicki, E., Aalto, P., Heintzenberg, J. and Leck, C.: Occurrence of an ultrafine particle mode less than 20 nm in diameter in the marine boundary layer during Arctic summer and autumn, Tellus, 48B, 213-222, 1996.

Wiedensohler, A., Birmili, W., Nowak, A., Sonntag, A., Weinhold, K., Merkel, M., Wehner, B., Tuch, T., Pfeifer, S., Fiebig, M., Fjäraa, A. M., Asmi, E., Sellegri, K., Depuy, R., Venzac, H., Villani, P., Laj, P., Aalto, P., Ogren, J. A., Swietlicki, E., Williams, P., Roldin, P., Quincey, P., Hüglin, C., Fierz-Schmidhauser, R., Gysel, M., Weingartner, E., Riccobono, F., Santos, S., Grüning, C., Faloon, K., Beddows, D., Harrison, R., Monahan, C., Jennings, S. G., O'Dowd, C. D., Marinoni, a., Horn, H.-G., Keck, L., Jiang, J., Scheckman, J., McMurry, P. H., Deng, Z., Zhao, C. S., Moerman, M., Henzing, B., De Leeuw, G., Löschau, G. and Bastian, S.: Mobility particle size spectrometers: harmonization of technical standards and data structure to facilitate high quality long-term observations of atmospheric particle number size

distributions, Atmospheric Measurement Techniques, 5(3), 657–685, doi:10.5194/amt-5-657-2012, 2012.

Yao, X., Choi, M.Y., Lau, N.T., Lau, A.P.S., Chan, C.K., Fang, M.: Growth and Shrinkage of New Particles in the Atmosphere in Hong Kong, Aerosol Science and Technology 44, 639-650, 2010.

Zhang, K. M. and Wexler, A. S.: Evolution of particle number distribution near roadways—Part I: analysis of aerosol dynamics and its implications for engine emission measurement, Atmospheric Environment, 38(38), 6643–6653, doi:10.1016/j.atmosenv.2004.06.043, 2004.

Annex: Dissemination of Results

Numerous publications have been produced from results obtained during this thesis.

Pandolfi, M., **Cusack, M.**, Alastuey, A., Querol, X.: Variability of aerosol optical properties in the Western Mediterranean Basin, Atmospheric Chemistry and Physics, 11, 8189-8203, 2011.

Van Drooge, B.L., **Cusack, M.**, Reche, C., Mohr, C., Alastuey, A., Querol, X., Prevot, A, Day, D.A., Jimenez, J., Grimalt, J.: Molecular marker characterisation of the organic composition of submicron aerosols from Mediterranean urban and rural environments under contrasting meteorological conditions, Atmospheric Environment, 61, 482-489, 2012.

Pérez, N., Pey, J., **Cusack, M.**, Reche, C., Querol, X., Alastuey, A., Viana, M.: Variability of particle number, black carbon and PM_{10}, $PM_{2.5}$ and PM_1 levels and speciation: Influence of road traffic emissions on urban air quality, Aerosol Science and Technology, 44, 487-499, 2010.

Querol, X., Alastuey, A., Pey, J., **Cusack, M**., Pérez, N., Mihalopoulos, N., Theodosi, C., Gerasopoulos, E., Kubilay, N., Koçak, M.: Variability in regional background aerosols within the Mediterranean. Atmospheric Chemistry and Physics, 2009
Moreno, T., Querol, X., Alastuey, A., Reche, C., **Cusack, M.**, Amato, F., Pandolfi, M., Pey, J., Richard, A., Prévôt, A.S.H., Furger, M., Gibbons, W.: Variations in time and space of trace metal aerosol concentrations in urban areas and their surroundings. Atmospheric Chemistry and Physics, 9, 4575-4591, 2011.

Querol, X., Pey, J., Pandolfi, M., Alastuey, A., **Cusack, M**., Pérez, N., Moreno, T., Viana, M., Mihalopoulos, N., Kallos, G., Kleanthous, S.: African dust contributions to mean ambient PM_{10} mass-levels across the Mediterranean Basin. Atmospheric Environment, 43, 4266-4277, 2009.

Pey, J., Pérez, N., Querol, X., Alastuey, A., **Cusack, M.**, Reche, C.: Intense winter atmospheric pollution episodes affecting the Western Mediterranean Basin. Science of the Total Environment, 408, 1951-1959, 2010.

Pey, J., Alastuey, A., Querol, X., Pérez, N., **Cusack, M**.: A simplified approach to the indirect evaluation of the chemical composition of atmospheric aerosols from PM mass concentrations. Atmospheric Environment, 44, 5112-5121, 2010.

Minguillón, M. C., Perron, N., Querol, X., Szidat, S., Fahrni, S. M., Alastuey, a., Jimenez, J. L., Mohr, C., Ortega, a. M., Day, D. a., Lanz, V. a., Wacker, L., Reche, C., **Cusack, M.**, Amato, F., Kiss, G., Hoffer, a., Decesari, S., Moretti, F., Hillamo, R., Teinilä, K., Seco, R., Peñuelas, J., Metzger, a., Schallhart, S., Müller, M., Hansel, a., Burkhart, J. F., Baltensperger, U. and Prévôt, a. S. H.: Fossil versus contemporary sources of fine elemental and organic carbonaceous particulate matter during the DAURE campaign in Northeast Spain, Atmospheric Chemistry and Physics, 11(23), 12067–12084, doi:10.5194/acp-11-12067-2011, 2011.

Moreno, T., Querol, X., Alastuey, A., Reche, C., **Cusack, M.**, Amato, F., Pandolfi, M., Pey, J., Richard, A., Prévôt, A.S.H., Furger, M., Gibbons, W.: Variations in time and space of trace aerosol metal concentrations in urban areas and their surroundings, Atmospheric Chemistry and Physics, 11, 9415-9430, 2011.

Querol, X., Alastuey, A., Viana, M., Moreno, T., Reche, C., Minguillón, M.C., Ripoll, A., Pandolfi, M., Amato, F., Karanasiou, A., Pérez, N., Pey, J., **Cusack, M.**, Vázquez, R., Plana, F., Dall'Osto, M., de la Rosa, J., de la Campa Sánchez, Fernández-Camacho, R., Rodríguez, S., Pío, C., Alados-Arboledas, L., Titos, G., Artíñano, B., Salvador, P., Dos Santos García, S., Patier Fernández, R.: Variability of carbonaceous aerosols in remote, rural, urban and industrial environments in Spain: implications for air quality policy, Atmospheric Chemistry and Physics Discussions, 13, 6971-7019, 2013.